Micro-Raman spectroscopic studies on the adhesive-dentine interface and the degree of conversion of dental adhesives

Vesna Miletic

Thesis presented for the degree of Doctor of Philosophy of

The University of Edinburgh

- 2010 -

DECLARATION

This thesis has been composed by the author and is author's own work, with the exception of the help and guidance from the individuals acknowledged in the text. The work presented in this thesis has not been submitted for any other degree or professional qualification.

Vesna Miletic

Signature: _____

Date: _____

ABSTRACT

A series of studies on monomer to polymer conversion in adhesive systems was undertaken using micro-Raman spectroscopy. A database of micro-Raman spectra was compiled for identification of tooth tissues and materials. The degree of conversion was assessed as a function of time and light source. Linear and two-dimensional micro-Raman characterisations of the adhesive-dentine and resin-based composite-adhesive-dentine interfaces were performed. The degree of monomer to polymer conversion of adhesive systems was correlated with the amount of eluted monomers obtained by high-performance liquid chromatography.

The degree of conversion varied significantly depending on adhesive chemical composition, curing time and light source. It was impossible to specify one curing time applicable to all adhesive systems, due to differences in conversion kinetics. In general, conventional halogen light-curing units at twenty seconds curing time produced similar or higher degree of conversion in adhesive systems compared to high-power LED units at ten seconds.

Significantly higher monomer conversion was found in the adhesive layer compared to the hybrid layer in both etch-and-rinse and self-etch systems. Etch-and-rinse adhesive systems formed thicker hybrid layers compared to self-etch systems. Micro-Raman spectroscopy gave a more precise indication of dentine demineralisation and adhesive penetration than scanning electron microscopy and indicated that the hybrid layer is a gradual transitional zone between the adhesive layer and un-affected dentine.

The absolute amount and weight percent of eluted monomers varied in all tested adhesive systems. In most adhesive systems, more than 90% of eluted monomers were detected within the first one hour of immersion. Overall, no correlation was found between the degree of conversion and the amount of eluted monomers.

TABLE OF CONTENTS

LIST OF FIGURES

LIST OF TABLES

LIST OF MATERIALS AND DEVICES

AdheSE One, Ivoclar Vivadent, Schaan, Liechtenstein, lot K15391
AdheSE, Ivoclar Vivadent, Schaan, Liechtenstein, lot H28512
Admira bond, Voco GmbH, Cuxhaven, Germany, lot 0802686
Admira, Voco GmbH, Cuxhaven, Germany, lot 76055
Adper Prompt L-Pop, 3M ESPE, St. Paul, MN, USA, lot 284081
Agilent 1100 Series HPLC system, Agilent Technologies, Santa Clara, CA, USA
Beta single wheel grinder-polisher, Buehler, Lake Bluff, IL, USA
BisEMA - Ethoxylated bisphenol A dimethacrylate, Ivoclar Vivadent, Schaan, Liechtenstein, lot H36622
BisGMA – 2,2-bis-[4-(2-hydroxy-3- methacryloyloxyprop-1-oxy)phenyl]propane or Bisphenol A glycol dimethacrylate, Ivoclar Vivadent, Schaan, Liechtenstein, lot J00415
Bluephase, Ivoclar Vivadent, Schaan, Liechtenstein
Camphorquinone, Sigma-Aldrich Chemie GmbH, Steinheim, Germany, lot S12442-216
Clearfil 3S Bond, Kuraray Europe GmbH, Frankfurt/Main, Germany, lot 00077A
Clearfil SE Bond, Kuraray Europe GmbH, Frankfurt/Main, Germany, lot 01054A
Collagen type I, Sigma-Aldrich Co. Ltd, Dorset, UK, lot 016K7043
Colloidal silica suspension, MasterMet, Buehler, Coventry, UK
Critical point drying machine, Polaron E3000 Series II, Watford, England
Diamond Wafering Blade ½″ (12.7mm), Buehler, Lake Bluff, IL, USA
Electronic digital calliper, Jade Products, Rugby, UK
Elipar Freelight2, 3M ESPE, St. Paul, MN, USA
Emscope SC500, Ashford, Kent, UK
Excite, Ivoclar Vivadent, Schaan, Liechtenstein, lot K12070
Fillers, Ivoclar Vivadent, Shaan, Liechtenstein
Filtek Silorane adhesive system, 3M ESPE, St. Paul, MN, USA, lot Primer 7AH, Bond 7AG
Filtek Silorane, 3M ESPE, St. Paul, MN, USA, lot 7AR
G Bond, GC Corp. Tokyo, Japan, lot 0609051
Gradia Direct, GC Corp. Tokyo, Japan, lot 0606142
HEMA, Sigma-Aldrich Co. Ltd, Dorset, UK, lot 06978-085
Hydroxyapatite, Sigma-Aldrich Co. Ltd, Dorset, UK, lot 015K53071
Isomet saw, Buehler, Lake Bluff, IL, USA
James-2, Saremco Dental AG, Rebstein, Switzerland, lot 7413
LABRAM 300, HORIBA Jobin Yvon, Stanmore, Middlesex, UK
LabSpec4.18, HORIBA Jobin Yvon, Stanmore, Middlesex, UK
Mat black coated, welled microscope slide, Erie Scientific Company, Portsmouth, UK

METTLER TOLEDO balance, AB104; d=0.1 mg; Mettler-Toledo Inc., Columbus, OH, USA

Minitab 15, Minitab Inc., State College, PA, USA

Mylar strip, DuPont Ltd, Stevenage, Herts, UK

One Coat Bond 1-step self-etch, Coltène Whaledent AG, Altstätten, Switzerland, lot 0130909

One Coat Bond 2-step self-etch, Coltène Whaledent AG, Altstätten, Switzerland, Primer lot 0111284, Bond lot 0115294

One-Coat Bond total-etch, Coltène Whaledent AG, Altstätten, Switzerland, lot 0116367

Optilux 500, Demetron/Kerr, Danbury, CT, USA

Phenomenex Prodigy 5 ODS 310CA HPLC column, Phenomenex, Torrance, CA, USA

Polishing cloths, TriDent, Buehler, Coventry, UK

Prismetics Lite, Dentsply DeTrey GmbH, Konstanz, Germany

Radiometer, SDS, Kerr, Danbury, CT, USA

Raman microscope, Olympus UK, London, UK

Saliveze™, LOT:20266-02, EXP: 2009.08, Wyvern Medical Ltd, Ledbury, UK

SEM, Philips XL30CP, Philips, Eindhoven, NL

Silicon carbide disc, Buehler, Lake Bluff, IL, USA

SiO_2 solution, Buehler, Lake Bluff, IL, USA

TEGDMA - Tetraethyleneglycol dimethacrylate, Ivoclar Vivadent, Shaan, Liechtenstein, lot F46757

Tetric EvoCeram, Ivoclar Vivadent, Schaan, Liechtenstein, lot H29487

UDMA – 1,6–bis-(methacryloyloxy-2-ethoxycarbonylamino)-2,4,4-trimethylhexane or Urethane dimethacrylate, Ivoclar Vivadent, Shaan, Liechtenstein, lot J02980

USB-502, temperature and humidity data logger, Measurement Computing Corp., Norton, MA, USA

Xeno III, Dentsply DeTrey GmbH, Konstanz, Germany, lot 0703002565

ABBREVIATIONS

10-MDP- 10- methacryloyloxydecyl dihydrogenphosphate
2D – two-dimensional
4-MET – 4-methacryloyloxyethyl trimellitic acid
4-META - 4-methacryloyloxyethyl trimellitate anhydride
BHT - 2,6-Di-tert-butyl-p hydroxyl toluene [butylated hydroxytoluene]
BisGMA - (2,2-bis[4-(2-hydroxy-3-methacryloylpropoxy)]-phenyl propane)
BPDM – biphenyl-dimethacrylate
BPO – benzoylperoxide
CCD - charged coupled device
CEMA - N,N-cyanoethyl methylaniline
CQ – camphorquinone
DABE- N,Ndimethyl-p-aminobenzoic acid ethyl ester
DC - degree of conversion
DCLS - direct classical least squares
DHEPT – 2,2'-dihydroxyethyl-para-toluidine
DMAEMA - dimethylaminoethyl methacrylate
DMOH - N,N-dimethylaminobenzyl alcohol
DMPOH – 4-(N,N-dimethylamino)phenethyl alcohol
DPIC - diphenyliodonium chloride
DPIHFP – diphenyliodonium hexafluorphosphate
DSC – differential scanning calorimetry
DTA – differential thermal analysis
EDMAB- ethyl-4-dimethylaminobenzoate
EPD - p-Dimethylamino ethyl benzoate
ESR – electron spin resonance
ETMA – 2,3-epithiopropyl methacrylate
GDMA - glycerol dimethacrylate
GMA – glycerol mono-methacrylate
HCl- hydrochloric acid
HEMA - 2-hydroxyethyl methacrylate
HL – hybrid layer
HPLC – high-performance liquid chromatography
HPMA – hydroxypropyl methacrylate
IPDM – (isopropylidene-diphenoxy)bis(phtalic) dimethacrylate
IR – infrared
LCU - light-curing unit
LED - light-emitting diode
MDPB – 12-methacryloyloxydodecylpyridinium bromide
MEAA - N-methylolacrylamide
MEHQ - monomethyl ether hydroquinone

NaOCl - sodium hypochlorite
NIR - near infrared
NPG - N-phenylglycine
ODPDM – oxydiphtalic-dimethacrylate
PAS-IR – infrared photoacoustic spectroscopy
PEM-F - Pentamethacryloxyethyl cyclophosphazen mono fluoride
PENTA – dipentaerythritol pentaacrylate monophosphate
PMDM – pyromellitic dimethacrylate
PMGDM - pyromellitic glycerol dimethacrylate
PPD – 1-phenyl-1,2- propanedione
Pyro-EMA – tetramethacryloyloxyethyl pyrophosphate
QTH- quartz tungsten halogen
RDB – ratio of double bonds
rpm – revolutions per minute
SEM – scanning electron microscopy
TBB - tri-n-butyl borane
TEGDMA - triethyleneglycol dimethacrylate
TMA – NN-3,5-tetramethylaniline
UDMA - Urethane dimethacrylate

CHAPTER 1

INTRODUCTION

1.1. TISSUES AND MATERIALS

1.1.1. Dentine

Dentine is a biologic composite of apatite crystals highly dispersed in a collagen matrix. It is a vital tissue containing approximately 55 vol% mineral, 30 vol% organic material and 15 vol% fluid (Marshall 1993). Anatomically, it consists of dentinal tubules containing odontoblast processes and tubular fluid, surrounded by hypermineralised peritubular dentine and interconnected with intertubular dentine (Marshall 1993). Most tubules contain multiple lateral branches, 2-6 μm in length (Nakabayashi 1998a).

Dentinal tubules run from the pulp chamber to the amelo-dentinal junction (ADJ) and resemble an inverted cone with the smallest diameter of approx. 0.8 μm at the ADJ and the largest diameter of approx. 3.0 μm at the pulpal surface (Eick 1997). The number of dentinal tubules varies depending on the position. At the ADJ, this number may be between 15,000 and 20,000 per mm^2, whereas, at the pulpal surface, it may be between 45,000 and 65,000 per mm^2 (Garberoglio & Brannstrom 1976). This is due to radial spread of the tubules from the pulp chamber to the ADJ. Furthermore, the amount of intertubular and peritubular dentine varies depending on the location within dentine. The percentage of intertubular dentine is approx. 12% at the predentine and increases up to 96% near the ADJ, while peritubular dentine decreases from 60% near the pulp to 3% at the ADJ (Pashley 1989).

Dentine is formed by odontoblast secretion of collagen matrix that subsequently mineralizes. The odontoblast processes extend into dentinal tubules, so dentine and pulp are considered a pulpo-dentinal complex (Pashley 1996). Dentinal tubules also contain a fluid which is a transudate of plasma and its movement along the tubular lumen is widely accepted as the basic mechanism for triggering painful stimuli (Walters 2005). The major water content of dentine is contained within the tubules, resulting in an increase in dentinal water from superficial towards deeper dentine (Pashley 1991).

As a vital, dynamic, biological structure, dentine undergoes changes as a result of physiological, aging and disease processes. It is possible to distinguish primary, secondary, tertiary, sclerotic, transparent, carious, demineralised, remineralised and hypermineralised dentine (Marshall 1997). These changes in dentine refer to the composition and anatomical arrangement of components.

Primary dentine is formed during tooth development. The other forms of dentine develop in the post-eruptive phases. Secondary dentine is a deposition of dentine after eruption and has a similar tubular structure as the primary dentine. However, it is deposited with slight irregularities as there are sites with lesser and greater deposition of secondary dentine (Marshall 1997). Tertiary dentine has several synonyms such as irregular secondary, reparative, reactionary, irritation or response and is deposited as a result of trauma, primarily caries, but also various clinical procedures. Its structure tends to be less regular with fewer dentinal tubules (Pashley 1996, Marshall 1997).

Carious dentine can be divided in two major layers, outer (infected) and inner (affected) (Kuboki 1977, Marshall 1997). Kuboki et al. found significant differences in the intermolecular cross links of collagen fibres between the inner and outer layer of carious dentine. The outer layer exhibited irreversible destruction of cross linkage between collagen fibres whereas the inner layer showed reversible cross linkage and lower numbers of collagen fibres. Only type I collagen is found in tertiary dentine while types I and III are found in carious dentine (Karjalainen 1986).

Transparent or sclerotic dentine is the term most often used to describe dentine associated with non-carious cervical lesions. Brännström & Garberoglio (1980) studied anatomical differences in dentinal tubules as a result of attrition and found that many tubules were occluded by a continuous growth of peritubular dentine. Furthermore, intratubular mineral deposits, or sclerotic casts, were found to occlude most dentinal tubules to some extent (Van Meerbeek 1994). This type of dentine is more resistant to treatment, particularly to demineralisation procedures (Heymann & Bayne 1993).

1.1.2. Adhesive systems

In an attempt to overcome the lack of adhesion between filling materials and dental tissues, Buonocore (1955) suggested four approaches:

"(1) the development of new resin materials with adhesive properties; (2) modification of present materials to make them adhesive; (3) the use of coatings as adhesive interface materials between filling and tooth and (4) the alteration of the tooth surface by chemical treatment to produce a new surface to which present materials might adhere".

The modern era of dental resin-based filling materials began with the synthesis of a new monomer, 2,2-bis-[4-(2-hydroxy-3-methacrylyl-oxypropoxy)phenyl]propane, commonly known as BisGMA Bowen (1956). The polymerisation of this monomer occurs through carbon-carbon double bonds of methacrylate groups. Since the introduction of the new BisGMA-based materials, the dental technology of both adhesive systems and resin-based composites (RBCs) has been changing rapidly.

Acid etching of enamel prior to the application of resins was introduced by Buonocore (Buonocore 1955). Although he originally used 85% phosphoric acid solution to etch enamel surfaces, subsequent studies showed that lower concentrations of phosphoric

acid produced less surface damage and comparable or higher bond strengths of resin polymers to enamel (Gwinnett & Buonocore 1965, Rock 1974, Dennison & Craig 1978). Phosphoric acid in the range of 30-40% is normally used with current etch-and-rinse adhesive systems.

Adhesion to dentine remains a current problem (Buonocore 1956, De Munck 2005, Breschi 2008).

In 1980s, there was an increase in the number of available dental adhesive systems. Traditionally, they were classified into 'generations' but this was driven mostly by manufacturers' marketing and was deficient in clinical and chemical information. Nevertheless, the following review is given for historical reasons.

The first generation adhesive systems were based on Buonocore's and Bowen's work on glycerophosphoric acid dimethacrylate-containing resin (Buonocore 1956) and N-phenylglycine and glycidyl methacrylate (Bowen 1965). The clinical results of these early systems were very poor because the bond strengths were only 1-3 MPa (Douglas 1989, Kugel & Ferrari 2000).

Second generation adhesive systems were developed about 1980 and were based on BisGMA and hydroxyethyl methacrylate, HEMA. Although they were an improvement, second generation systems bonded only to the smear layer, created on dentine surface by rotary instruments. Unlike enamel, dentine etching was not perceived as a desirable clinical procedure since it was believed that the smear layer would act as a protective barrier for the pulp (Pashley 1989). Dentine was not etched or conditioned leaving the smear layer virtually undisturbed resulting in resin penetration almost exclusively restricted to the smear layer. Bond strengths approached 10 MPa (Chan 1985).

Third generation adhesive systems were developed to promote resin adhesion to dentine by conditioning and priming the dentine surface. The difference between a primer and a

conditioner was that the former was applied and dried without being washed away whereas the latter was applied and subsequently washed away. Therefore, these systems partially removed and/or modified the smear layer. Acidic conditioners containing 3% ferric chloride in 10% citric solution removed the smear layer and demineralised the underlying dentine (Nakabayashi 1982). The priming solutions were based on hydrophilic resin monomers, such as hydroxyethyl trimellitate anhydride, 4-META, phosphate pentaacrylate, PENTA or biphenyl dimethacrylate, BPDM. Following primer application, an unfilled resin was applied and bonded to the primed dentine.

Fourth generation adhesive systems were characterised by the complete removal of the smear layer using the so-called "total-etch" technique. In these systems, enamel and dentine are etched simultaneously by phosphoric acid for 15-30 s which is then washed away. Acid etching results in the complete removal of the smear layer. Subsequent drying has been identified as a critical step for the successful adhesion of these systems since complete drying of dentine surface leads to the collapse of exposed collagen fibres (Han 2000). After acid etching, the primer and bond are applied as two separate steps which is why these adhesive systems are also known as three-step adhesive systems. In fourth generation systems, adhesion was promoted by monomer penetration into the dentinal tubules and the superficially demineralised dentine as a result of acid etching. Nakabayashi defined the so-called hybrid layer as "the structure formed in hard dental tissues by demineralisation of the surface and subsurface, followed by infiltration of monomers and subsequent polymerisation" (Nakabayashi 1982).

The fifth generation comprises two types of adhesives: (1) "one-bottle" systems which combined the primer and bond in one solution applied after acid etching of enamel and dentine. This generation is also known as the two-step adhesive systems because it consists of two clinical steps, acid etching and adhesive application; (2) self-etching primers. The development of self-etching primers, such as phenyl-P, allowed etching and priming to be combined (Watanabe 1993). These systems are also referred to as

two-step self-etch adhesive systems. The combination of etching and priming eliminated the need to wash away the acidic gel, reducing the risk of collagen collapse.

Sixth generation adhesive systems are also referred to as one-step self-etch or all-in-one adhesive systems. With these systems, the etching, priming and bonding steps are combined into one solution. Although this has significantly simplified the clinical procedure, initial studies have shown inferior bonding capabilities of these adhesive systems (Frankenberger 2001, Radovic 2006). However, due to the variety of chemical compositions in this group of adhesive systems, there is conflicting evidence of their effectiveness (Armstrong 2003, Sidhu 2007).

With increasing knowledge of the nature and properties of the smear layer (Pashley 1989, Watanabe 1993, Ferrari 1996, Van Meerbeek 1996), a classification was proposed, based on the interaction of adhesive systems with the smear layer (Van Meerbeek 1998). Accordingly, the adhesive systems were classified as: (1) one- and two-step smear layer modifying systems; (2) two- and three-step smear layer removing systems and (3) two-step smear layer dissolving systems. The modifying systems corresponded to the third generation, the removing systems to the fourth and fifth generations and the dissolving systems to the sixth generation.

Currently, adhesive systems are also classified according to the adhesion strategy and the number of clinical application steps but the present classification is modified compared to the previous one: 1) etch-and-rinse, 2) self-etch and 3) glass-ionomer adhesive systems (De Munck 2005).

Etch-and-rinse adhesive systems require the use of an acid (most commonly, phosphoric acid 30-40%) in order to remove the smear layer and demineralise enamel and dentine, thus, preparing them for inter-diffusion of resin monomers. After acid etching, the primer and bond are applied as separate phases in three-step adhesives or as a single step in two-step adhesives.

The principal mechanism of adhesion for these adhesive systems is currently considered to be the micromechanical interlocking of the adhesive resin and apatite crystallites in enamel and exposed collagen fibres in dentine (Nakabayashi 1982, Van Meerbeek 1993a). As previously stated, adhesion with dentine remains a challenge and further review is focused on the adhesive-dentine interaction. The HL in dentine is of variable thickness and is often covered by an amorphous phase which is attributed to denaturation and collapse of the residual smear layer collagen (Pashley 1993, Van Meerbeek 1993a). Wang & Spencer (2004) have shown that the depth of dentine demineralisation for clinically recommended times is about 5 to 8 μm (Wang & Spencer 2004a).

Primers promote adhesion since they contain hydrophilic moieties with an affinity for the dentine substrate as well as hydrophobic moieties which interact with the hydrophobic adhesive bond resin. Furthermore, it has been shown that primers may induce rapid re-expansion of the collapsed collagen network and enhance bonding (Eliades 1999).

Subsequent application of adhesive resins is intended to stabilise the formed resin-dentine hybrid layer and further enhance bonding by the formation of resin tags in open dentinal tubules (Van Meerbeek 1993a). These adhesive resins are then polymerised via the chemical, light or dual curing process. It is generally accepted that the disadvantage of chemically cured adhesive systems is an unacceptable polymerisation rate (Van Meerbeek 1998). Light-cured systems are cured prior to the application of RBCs which prevents the possibility of the displacement of adhesive resins. However, it has been shown that light curing in clinical conditions is associated with the formation of the so-called oxygen inhibition zone on the top of adhesive resin because oxygen inhibits polymerisation of methacrylate groups (Rueggeberg & Margeson 1990). It has been hypothesized that this layer offers sufficient carbon-carbon double bonds for co-polymerisation of adhesive with restorative resin (Van Meerbeek 1998).

The relatively complicated, technique-sensitive and time-consuming clinical application of etch-and-rinse adhesive systems resulted in an increasing demand for simplifying the procedure. A significant change in dental adhesive technology has been made with the development of self-etch adhesives. Self-etch adhesives contain acidic primers with the ability to demineralise the smear layer and the underlying dentine. According to the pH of these acidic primers, self-etch adhesive systems are classified as “mild” and “strong” (De Munck 2005). “Strong” self-etch adhesives produce a level of dentine demineralisation as etch-and-rinse systems, due to their very low pH (<1), while “mild” self-etch adhesives (pH~2) produce less aggressive demineralisation. Currently available self-etch systems are produced as two-step or one-step systems. Two-step systems consist of primers and bonding agents in separate bottles whereas one-step or all-in-one self-etch adhesives contain all components in a single bottle.

The intention with self-etch adhesives is to promote superficial dentine demineralisation with simultaneous penetration of resin monomers which are then polymerised in situ. This is of particular importance since it has been shown that a discrepancy occurs between the depth of dentine demineralisation and adhesive penetration with etch-and-rinse systems (Hashimoto 2002, Wang 2007). It has been hypothesized that with self-etch adhesives the depth of demineralisation should be equal to resin infiltration so that a continuum can be formed from the unaltered dentine to the adhesive resin. However, morphological studies have shown that even with self-etch adhesives there is a discrepancy between dentine demineralisation and adhesive penetration zones (Tay 2002, Wang & Spencer 2004b).

Glass-ionomers are still considered the only self-adhering materials to dental tissues (Yoshida 2000). The two-fold bonding mechanism of glass-ionomers is based on the principle of hybridisation (micro-mechanical bond) and the chemical interaction of calcium ions from hydroxyapatite with carboxyl groups of the polyalkenoic acid (chemical bond) (McLean 1988). However, the hybrid layer formed between glass-ionomers and the dental tissues is thinner than that of resin-based materials due to the

relatively high molecular weight of the self-etching polycarboxyl-based component. This limits the etching as well as infiltration capability of glass-ionomers which effectively influences bond strength (Inoue 2001a). Initial pre-treatment with polyalkenoic acid favours adhesion by removing the smear layer and exposing collagen fibres, but although this exposure in only up to 1 μm (Inoue 2001a), more aggressive conditioners are not recommended for use with glass-ionomers (De Munck 2004).

1.1.3. Resin-based composites

RBCs were introduced in mid-1960s following the synthesis of BisGMA and patenting the "dental filling material comprising vinyl silane treated fused silica and a binder consisting of the reaction product of Bis-phenol and glycidyl acrylate" (Bowen 1962). They were initially used as a filling material for anterior teeth. Improvements in RBC and adhesive system technology extended their use to posterior filling materials.

RBCs consist of three chemically different components: (1) the organic resin matrix; (2) the inorganic filler and (3) the organo-silane coupling agent. The organic resin matrix comprises a monomer system which is a backbone structure, an initiator system for polymerisation and additives, stabilisers and pigments for storage and chemical stability and aesthetic appearance. The inorganic filler consists of glass, quartz and/or fused silica particles to enhance the mechanical and physical properties. The organo-silane chemically bonds the filler particles to the resin matrix (Bowen & Marjenhoff 1992).

Filler technology expanded in the 1980s and 1990s in an attempt to overcome the disadvantages of the organic matrix such as wear, polymerisation shrinkage, strength, stiffness, thermal expansion and water absorption (Peutzfeldt 1997, Darvell 2002). Based on the filler content, RBCs are traditionally classified as macro-filled, micro-filled, hybrid, iso-filled and, more recently, nano-filled RBCs.

The first macro-fillers were made up by crushing or grinding pieces of quartz, glass, borosilicate or ceramic into splinter shaped particles, 5-30 μm in size. From this original diversity in size, production trend then changed towards smaller and rounded particles with an average size of 1 μm to 5 μm (Craig 1981). The first macro-filled RBCs exhibited low polishability, high surface roughness and low wear resistance (Lutz & Phillips 1983, Darvell 2002).

Micro-filled RBCs with filler particles of 0.04-0.2 μm allowed a significant increase in the filler content. Micro-filled RBCs achieved satisfactory surface qualities, good polishability and smoothness but, on the other hand, brought certain disadvantages. Due to the large surface area of the filler content, the viscosity of these RBCs was significantly increased resulting in increased polymerisation shrinkage and lower flexural strength than macro-filled RBCs (Lutz & Phillips 1983).

Containing a blend of both macro-fillers and micro-fillers, hybrid RBCs showed more favourable physical properties, good wear resistance and surface morphology compared to the previously mentioned RBCs. The mean particle size was about 1 μm. At the time they were brought into clinical practice, hybrid RBCs were considered an optimal combination of the well-tried traditional and new micro-filler technology (Lutz & Phillips 1983).

To maintain the favourable properties of micro-filled RBCs and overcome the problem of high polymerisation shrinkage and lower physical properties than macro-filled RBCs, a manufacturer has developed ‘iso-fillers’. Iso-fillers are milled micro-filled RBC to produce a grain size similar to that of macro-fillers. They are homogeneously dispersed into the organic matrix to promote favourable handling and physical properties.

More recently, with the introduction of nanotechnology, nano-filled RBCs have been produced. The primary particle size is in the range of 20-75 nm with particle clusters of 0.6-1.4 μm. Beun et al. have shown that these nano-filled RBCs have comparable or

better mechanical properties (elastic modulus, flexural strength, microhardness) than hybrid and micro-filled RBCs (Beun 2007). On the other hand, it has been reported that nano-filled RBCs have greater solubility and sorption than hybrid RBCs (da Silva 2008).

Apart from changes in the filler content, dental technology has progressed towards the development of new groups of resin monomers. Recently, a silorane-based RBC has been introduced on the market. Essentially, silorane is a microhybrid composite with a high amount of quartz particles coated with silane compatible with silorane resin. The manufacturer claims that the majority of filler particles are between 0.1 μm and 1 μm. The new silorane resin is a combination of two building blocks, siloxane and oxirane, and will be reviewed under 1.2.1.1. Monomers.

1.2. CHEMICAL COMPOSITION AND POLYMERISATION OF RESIN-BASED COMPOSITES AND ADHESIVE SYSTEMS

1.2.1. Chemical composition

The common ingredients of both RBCs and adhesive systems are resin monomers, filler particles, the initiator system and inhibitors. In addition, solvents are used in adhesive systems. Manufacturers also add other ingredients such as stabilisers, catalysts and/or pigments but specific information regarding the composition of these ingredients is most often not disclosed. This review concentrates on monomers, fillers, initiator systems, inhibitors and solvents.

1.2.1.1. Monomers

Resin monomers contained in both RBCs and adhesive systems are cross-linking monomers whose role is the formation of a three-dimensional polymer network.

Adhesive systems contain additional monomers, the so-called 'functional' monomers which allow the interaction of adhesive systems with dental tissues, especially dentine.

Monomer molecules consist of the following parts: polymerizable group(s), functional group and a spacer group. There are two types of monomers in RBCs: cross-linking and functional monomers. Cross-linking monomers contain at least two polymerizable groups grafted onto a spacer group whilst functional monomers contain a functional group and one or more polymerizable groups grafted onto a spacer group.

Cross-linking monomers: POLYMERIZABLE GROUP ----- SPACER ----- POLYMERIZABLE GROUP

Functional monomers: FUNCTIONAL GROUP ----- SPACER ----- POLYMERIZABLE GROUP

The most frequently used cross-linking monomers are dimethacrylates, BisGMA, UDMA and TEGDMA. The chemical properties and stability of the adhesive and RBC polymers depend on the quality of the cross-linked polymer network (Eliades 1995, Salz 2005b). The amount of BisGMA, UDMA and TEGDMA significantly affects the mechanical properties such as tensile strength, flexural strength and modulus of elasticity of the experimental resin composition (Asmussen & Peutzfeldt 1998). In RBCs, the effect of these cross-linking monomers on the strength and stability has been confirmed (Bagis & Rueggeberg 1997b, Feilzer & Dauvillier 2003, Lopez-Suevos & Dickens 2008) but this can be effectively modified by the filler content (Skrtic & Antonucci 2003, Musanje & Ferracane 2004, Turssi 2005, Beun 2007).

BisGMA is formed from epoxy resins by replacing epoxy groups with methacrylate groups. This so-called "Bowen-resin", after its inventor, is characterized by a large molecular size, high viscosity and low volatility and water solubility (Peutzfeldt 1997, Sideridou 2002). BisGMA provides lower polymerisation shrinkage and rapid hardening and the resulting polymer has good mechanical properties (Yamauchi 1979). However, the spacer part of this bi-functional molecule possesses two aromatic rings which make BisGMA rigid. The two polymerizable methacrylate groups interact more slowly with

the corresponding groups of other BisGMA molecules compared to dimethacrylates with no aromatic groups. This may have a negative effect on the conversion rate of the resulting polymer (Feilzer & Dauvillier 2003). These disadvantages can be overcome by diluting BisGMA with other cross-linking monomers, such as TEGDMA, UDMA or GDMA. With reduced monomer viscosity, the filler content can be increased. Diluting BisGMA with previously mentioned dimethacrylates increases water solubility and reduces phase separation in water-based adhesive systems. Although diluting BisGMA with more flexible dimethacrylates increases the conversion rate, this also leads to increased polymerisation shrinkage (Sideridou 2002, Feilzer & Dauvillier 2003).

TEGDMA (triethylene glycol dimethacrylate) is a low molecular weight component with no aromatic ring and only two aliphatic C=C bonds grafted on a spacer. This increase in the total number of C=C bonds per unit weight could result in a high conversion and a high degree of cross-linking during polymerisation (Sideridou 2002). Furthermore, it has been found that increasing the distance between methacrylate groups in mono-, di-, tri- and tetraethyleneglycol methacrylates increases their reactivity (Ruyter & Svendsen 1978). It has also been shown that TEGDMA increases tensile but reduces flexural strength of the resulting polymer (Asmussen & Peutzfeldt 1998).

UDMA (urethane dimethacrylate) is similar to TEGDMA in that it contains two aliphatic and no aromatic bonds. Unlike TEGDMA, UDMA has an N-H bond and more carbonyl C=O bonds which results in a higher molecular weight and fewer C=C bonds per unit weight. The viscosity of UDMA is greater than TEGDMA but substantially lower than BisGMA (Dickens 2003). UDMA is more flexible than BisGMA because the two ether groups allow easier rotation than the two bulky aromatic moieties in BisGMA. Homopolymerisation of UDMA reaches the degree of conversion (DC) of 43% compared to only 7% of the BisGMA homopolymer (Dickens 2003). Furthermore, UDMA significantly increases polymerisation rate in UDMA-based resins compared to BisGMA-based resins (Dickens 2003). Studies have shown that UDMA-based resins have better mechanical properties than BisGMA-based when all other components are

constant (Asmussen & Peutzfeldt 1990, Peutzfeldt & Asmussen 1992, Indrani 1995). In contrast to TEGDMA, UDMA helps reduce shrinkage, aging and sensitivity to moisture (Peutzfeldt 1997). In both RBCs and adhesive systems, UDMA is often used alone or in combination with TEGDMA and/or BisGMA.

Polymerisation shrinkage is an inherent property of dimethacrylate-based materials mainly because monomer molecules are maintained at van der Waals distances, while in the corresponding polymer the monomeric units are covalently bonded. This equates to the reduction of intermolecular distances and has been suggested to be the cause of RBC polymerisation shrinkage (Davidson & Feilzer 1997). Attempts have been made to develop systems that would contain non-shrinking or even expanding monomers known as bicyclic monomers. The most extensively studied class of bicyclic monomers are the spiro-orthocarbonates (Stansbury 1992, Millich 1998, Vodak 2002). In these monomers, for every van der Waals distance converted to a covalent distance, at least two rings open during polymerisation. Eick et al. reported that the expansion of spiro-orthocarbonate homopolymers was 3.5%, experimental spiro-orthocarbonate-epoxy resin mixtures 0.1-0.8%, whereas the epoxy resin control showed 0.3% shrinkage (Eick 1993). However, the shrinkage reducing ability of spiro-orthocarbonates was found to be minimal with BisGMA/TEGDMA monomers (Peutzfeldt 1997).

More recent advances in polymer technology have led to the development of siloranes, monomers based on the combination of siloxanes and oxiranes. The polymerisation of these monomers is based on the cationic ring-opening reaction during which the oxirane rings open and compensate for the loss of volume caused by the formation of covalent bonds. In the commercially available silorane RBC, polymerisation shrinkage has not been completely eliminated but is significantly lower than that of dimethacrylate-based RBCs (Weinmann 2005). Other studies with experimental silorane formulations have shown satisfactory stability and insolubility in aqueous enzymatic solutions (Eick 2006) as well as the potential to reduce polymerisation stress but maintain mechanical properties comparable to commercially available RBCs (Eick 2007). However, Palin et

al. (2005) have shown reduced cuspal deflection but higher microleakage of the two experimental silorane and oxirane resins compared to the well-established Z100 and Filtek Z250 RBCs (Palin 2005). Other mechanical properties, such as Vickers hardness, modulus of elasticity, and creep resistance, appear to be comparable with those of methacrylate-based RBCs (Ilie & Hickel 2006). These findings suggest that the non-shrinking ideal has not yet been achieved and that further studies are necessary to optimise the silorane formulation.

In adhesive systems there are three types of monomers: cross-linking, functional and intermediary. Cross-linking monomers form 3D polymer chains as they contain two or more polymerizable groups. Functional monomers form linear polymeric chains since they contain only one polymerizable group and one functional group. Intermediary monomers contain several polymerizable and functional groups.

Dimethacrylates are the most commonly used cross-linking monomers in adhesive systems. Ester groups [R_1-CO-OR_2] in dimethacrylate-based monomers are prone to water hydrolysis especially in low pH solutions. Methacrylamides, which contain more water resistant amide groups [R_1-CO-NH-R_2], have been designed to overcome this problem (Salz 2005a, Salz 2005b).

Methacrylamide monomers have been developed specifically for self-etch adhesive systems to overcome the problem of hydrolytic instability of methacrylates in acidic aqueous solutions. Apart from this, amide groups in these monomers are similar to amines which are constituents of collagen so it is expected that methacrylamides may form hydrogen bonds with collagen (Nishiyama 2001). It has been shown that methacrylamides have significantly higher hydrolytic stability than methacrylates (Salz 2005b) though their effect on other properties of adhesive systems is still unclear.

Spacer groups separate polymerizable and functional groups. These are usually alkyl chains, but can also contain ester, amide or aromatic groups and affect properties such as

solubility, water uptake, viscosity, flexibility are affected by the chemical characteristics of spacer groups (Van Landuyt 2007).

Functional groups in functional monomers are responsible for properties such as wetting and demineralisation of the dentine substrate, fluoride release or antibacterial activity (Van Landuyt 2007). Phosphates and carboxyl acid are the most common functional groups, though sulfonic acid and alcohol groups are also used. In aqueous solutions, these groups act as proton-donors for acid-base reactions with the dentine substrate resulting in superficial dentine demineralisation. Etching effectiveness depends on the acidity of these groups and is ranked as follows: sulfonic acid > phosphonic > phosphoric > carboxylic acid >> alcohol (Moszner 2005). Dihydrogen acids are always more acidic than their monohydrogen counterparts, as they release more protons upon dissociation. In addition to the hydrolytic potential of methacrylate polymerizable monomers in acidic aqueous solutions, phosphate and carboxyl groups may also undergo hydrolysis in water (Moszner 2005, Van Landuyt 2007).

HEMA, a monomethacrylate, is the most commonly used functional monomer. It is a small molecule which dissolves well in all solvents, such as water, ethanol and acetone. HEMA is known for its hydrophilicity which makes it an excellent adhesion-promoting monomer and ensures good wetting of the dentine substrate (Van Landuyt 2007). Furthermore, it prevents collagen collapse and partly rewets the collapsed collagen network (Hitmi 2002). Increased dentine wetting has been shown to improve bond strength (Nakaoki 2000, Perdigao & Frankenberger 2001). After polymerisation, HEMA maintains its hydrophilic properties within the polymer chain which may lead to increased water uptake and swelling of the polymer (Burrow 1999). It is known to lower the vapour pressure of water and probably ethanol which may result in higher solvent content remaining in the adhesive system. The low molecular weight and flexibility of HEMA result in poorer mechanical properties of resins (Tay & Pashley 2001). More recent studies have indicated that phase separation occurs between HEMA and BisGMA within the hybrid layer resulting in a heterogeneous distribution of the hydrophobic

adhesive component (Spencer 2002). Water seems to be an additional factor contributing to HEMA/BisGMA phase separation (Ye 2008).

Other frequently used functional monomers, which differ in chemical composition from HEMA, are 4-MET, 10-MDP, PENTA and pyro-EMA. 4-MET is also available as the anhydride 4-META, which hydrolyzes in water to form 4-MET. Aqueous solutions of 4-MET have a pH<2 due to two carboxylic groups attached to an aromatic ring which ensures the demineralising effect on both enamel and dentine (Monticelli 2007). On the other hand, the aromatic group increases hydrophobicity and reduces reactivity of this monomer and, therefore, moderates its acidity (Unemori 2003). 4-MET dissolves in acetone, to a less extent in ethanol and not in water. Acetone is the most appropriate solvent for this monomer because esterification of carboxylic groups with alcohol hydroxyl groups may occur in acidic conditions (Van Landuyt 2005).

10-MDP contains a dihydrogenphosphate group which is primarily responsible for the etching ability of this monomer since it dissociates in water to form two protons. The dihydrogenphosphate group is attached to a long carbonyl chain which increases hydrophobicity. Because of its hydrophobic properties, more appropriate solvents than water are ethanol and acetone (Van Landuyt 2007). Phase separation may occur in water and it has been shown that aqueous solutions of 10-MDP are not stable at room temperatures (Salz 2005b).

PENTA belongs to the group of intermediary functional monomers since it contains five polymerizable methacrylate groups but also a functional phosphate group. It is capable of etching enamel and dentine and promoting adhesion due to its high hydrophilicity (Moszner 2005). On its own, PENTA does not etch dentine sufficiently for adequate adhesion and additional acid conditioning may be required to increase the thickness of the HL (Sunico 2002). Due to the presence of multiple methacrylate groups, PENTA may from cross-linked rather than linear polymer chains. However, any possible effect

of such feature of PENTA on adhesive bond strength has not been confirmed in the literature.

Pyro-EMA is known as a "masked acid" since it forms free phosphoric acid groups in contact with water. According to the manufacturer, upon contact with dental tissues, the free phosphoric acid groups of the hydrolyzed Pyro-EMA demineralise hydroxyapatite. Ca^{2+} ions are released from the hydroxyapatite resulting in neutralisation of phosphoric acid groups via ionic interaction of the Ca^{2+} ions with the phosphoric acid. Since the initial Pyro-EMA molecule breaks down into two, after hydrolysis, two methacrylate groups remain instead of the initial four which is still sufficient to form cross-linked polymers. The etching potential of pyro-EMA is enhanced in some adhesive systems by another monomer PEM-F. Fluoride ions from PEM-F and phosphoric acid groups from Pyro-EMA compete for hydroxyapatite Ca^{2+} ions. The former have a stronger affinity for Ca^{2+} ions leaving phosphoric acid groups more available for demineralisation of enamel and dentine.

1.2.1.2. Fillers

RBCs contain filler particles responsible for improving mechanical and physical properties of the resulting polymer (Bowen & Marjenhoff 1992). Adhesive systems initially did not contain fillers. Subsequently, filler particles have been added to improve mechanical properties and increase film thickness (Perdigao 1999, Van Landuyt 2007).

There are different types, sizes, shapes and amounts of filler particles in both adhesive systems and RBCs. The main filler of both RBCs and adhesive systems is silicon dioxide in the form of glass, quartz and/or fused silica particles but boron silicates and lithium aluminium silicates are also common. Frequently, quartz is partially replaced by heavy metal particles such as barium, strontium, zinc, aluminium or zirconium to

increase radio-opacity. The surface of filler particles is silanized to allow chemical bonding between the filler and the resin matrix.

The size of filler particles has changed considerably over the years, being constantly reduced, from macro-fillers (0.1-100 μm) and micro-fillers (0.04-0.2 μm) (Lutz & Phillips 1983) to most recent nano-fillers (25 nm) and nano-aggregates (75 nm) (Puckett 2007). It has been reported that the amount of fillers in hybrid RBCs is between 70-80%, micro-filled 50-55% and nano-filled RBCs 70-85% (Beun 2007). Though spherical and irregular shaped filler particles are incorporated in different RBCs (Beun 2007), spherical particles allow higher filler content (Bayne 1994) and increased fracture strength since stresses tend to concentrate around sharp edges of irregular shaped particles (Suzuki 1995).

In adhesive systems, the filler content and particle size differ compared to RBCs. Low amounts of fillers are desirable in adhesive systems because otherwise they may impair wetting ability of adhesives due to high viscosity. The filler size is defined by the interfibrillar spaces of the exposed collagen network which has been shown to be about 20 nm (Van Meerbeek 1993a). According to manufacturers' data, pure silicon dioxide particles, up to 7 nm in diameter, are added to contemporary adhesive formulations to allow the flow of resin monomers into the collagen network. However, it has been shown that nanofillers fail to do so and agglomerate around tubular orifices (Tay 1999). Although pure silicon dioxide is the most common type of adhesive filler, systems with silicate glass and heavy metals have been developed to achieve radio-opacity. Fluoride-containing filler particles have also been employed in some adhesive systems for their anti-cariogenic potential but literature lacks data to support this hypothesis. It has been shown that fluoride-containing adhesive systems maintain bond strength after 6 months in water in contrast to non-fluoride-containing systems (Nakajima 2003).

Fillers are added to adhesive systems to increase tensile and flexural strength since the adhesive-tooth interface is considered a weak link of the restored tooth under stress (Bae

2005). Also, fillers are added to optimize viscosity of adhesive resins as well as to increase the thickness of the formed layer. In very thin adhesive layers, oxygen inhibits free radical polymerisation and this may result in incomplete polymerisation. It is postulated that thicker adhesive layers may allow relief of contraction stresses of RBCs (Van Landuyt 2007). Moreover, it has been shown that the addition of up to 3 wt% of nanofillers increases flexural and microtensile bond strength of adhesive mixtures (Kim 2005). It is not known to what extent adhesive bond strength is affected by adhesive filler concentration levels (Nunes 2001).

Both hydrophilic and hydrophobic particles can be used as fillers and this may influence the overall hydrophilicity of adhesive systems. The hydrophilic silicon dioxide contains silanol [-Si-OH] groups whereas the hydrophobic one contains di- and tri-methylsilyl groups [-Si-$(CH_3)_2$-] and [-Si-$(CH_3)_3$-] (Van Landuyt 2007).

1.2.1.3. Initiator system

Polymerisation of adhesive systems and RBCs is triggered by small amounts of initiator molecules, which contain bonds with low dissociation energy and form radicals under certain conditions. There are two types of initiators: (1) redox initiators are incorporated in 'two-component systems' which allow polymerisation to start on mixing; (2) photo-initiators initiate polymerisation on absorbing energy from a light source (Odian 2004).

The amount of initiators in adhesive systems and RBCs is in the range of 0.1-1%. Though it has been previously reported that a positive correlation exists between the amount of initiators and the mechanical strength of the cured resin (Kalliyana K & Yamuna 1998), more recent studies have indicated a more complex effect of the initiator system on the mechanical and chemical properties of resin-based materials (Guo 2008b, Schneider 2008). Schneider et al. (2008) found that a higher amount of photo-initiators increases the absorbed power density as well as the rate of polymerisation and micro

hardness. However, the DC was not directly correlated to the amount of photo-initiators and was less affected than the rate of polymerisation by the initiator/co-initiator composition (Schneider 2008).

Guo et al. have shown that the hydrophobic/hydrophilic nature of the initiator system is affected by its chemical composition. Consequently, this has an adverse affect on the DC and rate of polymerisation of experimental BisGMA/HEMA resin mixtures in the presence of water (Guo 2008b). The hydrophobic/hydrophilic nature of the initiator system is much more important in adhesive systems than RBCs. The incompatibility between the initiators and hydrophilic monomers as well as the increased water content may result in incomplete polymerisation (Guo 2008b).

It should be noted that initiators generally reduce biocompatibility of adhesive systems and RBCs due to high reactivity and the formation of free radicals (Datar 2004). Initiators have been identified among other leachable components from adhesive systems (Geurtsen 1999) as well as RBCs, compomers and glass-ionomer cements (Michelsen 2003).

The absorption spectrum and, particularly, the peak absorption wavelength of photo-initiators are considered to be among the main characteristics affecting polymerisation. It is often stated that the spectral emission range of the light source should match the absorption characteristics of the initiator system (Caughman 1995, Van Landuyt 2007). It should be kept in mind that the absorption range of photo-initiators may change depending on the solvent polarity (Sun 2000). This is especially important in self-etch systems with high solvent content when cured with LED LCUs which typically exhibit a narrower spectral emission range than conventional halogen LCUs (Mills 2002, Warnock 2004, Owens & Rodriguez 2007).

On absorption of light energy, photo-initiators initiate the formation of free radicals in two ways depending on their chemical structure: (1) decomposition or photolysis of the

initiator molecule (benzoyl esters, benzophenone, acylphosphine oxides, PPD); (2) bimolecular interaction of the excited initiator molecule with a co-initiator molecule (Odian 2004). Aliphatic and aromatic amines are often used as hydrogen donors.

The combination of CQ, a diketone, with a tertiary amine as the co-initiator is the most commonly used initiator system in contemporary adhesive systems and RBCs. At room temperature, CQ is a crystalline powder that is fully soluble in water. Its intensive yellow colour is considered a disadvantage especially in RBCs and to a less extent in adhesive systems. For this, but also for the reason of slow polymerisation kinetics (Schroeder 2008), CQ is mixed with co-initiators which reduce the amount of CQ in the initiator system. CQ has a relatively broad absorption range between 360-510 nm and its peak absorbance wavelength is around 468 nm (Schroeder 2008). This falls into the emission range of blue light, so filters in the conventional halogen LCUs or the appropriate light-emitting diodes in LED LCUs are used to achieve blue light emission.

CQ is predominantly used with the tertiary amine DMAEMA as the co-initiator. Not only is this molecule an efficient hydrogen donor but its polymerizable methacrylate group may be incorporated into the polymer network. It has been hypothesized that, due to this reason, leaching out of any remaining co-initiators may be prevented (Darvell 2002). However, it has been shown, by the use of gas chromatography-mass spectrometry, that not only CQ but also DMAEMA are capable of leaching out of RBCs, compomers and glass-ionomer cements (Michelsen 2003). Besides DMAEMA, other co-initiators have been developed to match the hydrophilic nature and the high water content of adhesive systems. Initial studies have shown that co-initiators as NPG and DPIC are also compatible with HEMA and may enhance polymerisation even in the presence of water (Wang 2006c)

In chemically cured adhesive systems and RBCs, two chemical initiators are most often used: benzoylperoxide, BPO, and tri-n-butyl borane, TBB. BPO is a colourless crystalline solid which requires the use of a co-initiator (tertiary amine) to yield the free

radical formation. It is recommended that it is stored in darkness and refrigerated as slow photolysis occurs when exposed to light and radicalization may be initiated at high temperatures (Darvell 2002, Odian 2004). In adhesive systems, ethanol or acetone are recommended solvents since rapid hydrolysis occurs when dissolved in water (Van Landuyt 2007). TBB does not require the use of a co-initiator since it interacts with oxygen to produce free radicals. This initiator is very unstable in water, air and acid which limits its use, especially in adhesive systems (Van Landuyt 2007).

Although the ketone/amine or peroxide/amine initiator systems are widely used in RBCs and etch-and-rinse adhesive systems, their use in self-etch adhesive systems has been questioned since an acid-base reaction between acidic monomers and amines is an intrinsic property of these adhesive systems (Moszner 2005). This interaction would reduce the amount of available amines for initiating the polymerisation reaction resulting in incomplete polymerisation. One suggestion is to exactly match the amount of amines and acidic monomers in the adhesive system so that the equilibrium of the acid-base reaction can be reached at levels of protonized amines which would not impair polymerisation. Another possible solution could be the development of new co-initiator compounds that could overcome this problem (Moszner 2005).

1.2.1.4. Solvents

Solvents are added to adhesive formulations to reduce viscosity of resin monomers, increase hydrophilicity and wetting potential for optimal bonding to dental tissues (Van Landuyt 2007). The most commonly used solvents are water, ethanol and acetone.

The solubility potential depends on the polarity of the substances. Non-polar or weakly polar compounds dissolve in non-polar or weakly polar solvents and highly polar compounds dissolve in highly polar solvents. Though solvents in adhesive systems are all polar, the polarity of water and ethanol is determined by hydroxyl groups that form

hydrogen bonds whereas the polarity of acetone derives from its large dipole moment (Ghosh 2005). Another important characteristic of solvents is vapour pressure which is responsible for solvent evaporation after application to dental tissues. It has been shown that complete evaporation of solvents from adhesive systems is hard to achieve in clinical conditions and the remaining solvent has an adverse effect on the bond strength (Ikeda 2005). Solvents that have a hydrogen-bonding potential (water and ethanol) are expected to re-expand collapsed fibres after dehydration because of the potential to break the hydrogen bonds between collagen fibres. The bond strengths of water and, to a less extent ethanol-based adhesive systems, have shown to be higher than those of acetone-based systems when applied to dry dentine (Perdigao & Frankenberger 2001).

Water is a poor solvent of organic compounds such as resin monomers and the use of a co-solvent such as ethanol or acetone is usually required. It is an important ingredient in self-etch adhesive systems, added to ensure ionization of acidic monomers (Moszner 2005). However, high residual water content in the adhesive system or in dentine impairs polymerisation and results in low DC values of HEMA-based adhesive systems (Wang 2006c). Several studies have reported that water-based adhesives exhibited inferior adhesive-dentine interface quality compared to other systems (Gwinnett & Kanca 1992, Jacobsen & Soderholm 1995). Furthermore, adhesive phase separation has been observed in the form of BisGMA-rich particles in HEMA-rich matrix (Spencer 2002). Even though water-based adhesive systems are supposed to be less-technique sensitive than acetone-based, the adhesive itself must be properly dried in order to remove excess water, as this may have a significant effect on adhesive performance (De Munck 2005).

Ethanol has a higher vapour pressure than water which allows better solvent evaporation in clinical conditions. It is either used alone or in combination with water. The water-ethanol mixture is “azeotropic” meaning that the two solvents will form hydrogen bonds and join into aggregates which have a higher evaporation potential than pure water (Moszner 2005). Ethanol is not recommended with monomers that contain carboxylic

acid groups because an esterification reaction occurs and inactivates the acidic function of the monomer (Van Landuyt 2007). De Munck et al. stated that three-step ethanol-water based etch-and-rinse adhesives were the "gold standard" in terms of bond durability. Three-step etch-and-rinse adhesives exhibited no changes in adhesion stability after different aging methods, water storage, thermo-cycling and mechanical loading (De Munck 2003b, Frankenberger 2003). However, their simplified two-step counterparts have shown less satisfactory bonding effectiveness with significantly lower bond strengths after long-term storage (Meiers & Young 2001, De Munck 2003b, Giannini 2003),

Acetone is recommended as a solvent for adhesive systems that have both hydrophobic and hydrophilic components because of its ability to dissolve both polar and apolar compounds. Like ethanol, acetone can be used as a solely solvent or as a co-solvent with water. It, too, forms an azeotropic mixture with water, increases vapour pressure and evaporation and reduces the amount of water in the system (Chaudhry 1980). However, because acetone evaporates more readily than water, the ratio of acetone and water may change in the acetone-water-based systems. This may lead to phase separation and precipitation of other components in the adhesive systems (Moszner 2005). Since acetone has a low potential to form hydrogen bonds, it cannot re-expand collapsed collagen fibres. Therefore, when using acetone-based adhesive systems, dentine must be kept wet and this high sensitivity has led to the development of the so-called "wet" bonding technique (Gwinnett & Kanca 1992). Acetone-based adhesives have shown satisfactory in vitro adhesion (Frankenberger 2001, Meiers & Young 2001, Perdigao & Frankenberger 2001, Rosales-Leal 2001), but the results are less satisfactory in clinical trials. The reason for this could be the inability to apply these adhesive systems in strict accordance with the manufacturers' recommendations in often complex in vivo conditions (Burrow & Tyas 1999, Baratieri 2003).

Solvent-free adhesives have been developed for the use with acid etching. These are basically polyalkenoate mixtures of different methacrylates and dimethacrylates. There

is less information on these adhesive systems compared to solvent-based ones. Clinically, they have exhibited very good retention rate of 93% after 12 months (Aw 2004) and 90% after 36 months (Aw 2005). Good adaptation of solvent-free adhesives to dentine with resin tags penetrating dentinal tubules has been reported (Breschi 2003).

1.2.1.5. Other ingredients

Inhibitors (stabilizers) are added to dental adhesives and RBCs in order to prevent spontaneous polymerisation which may occur in certain conditions, such as high temperature, when premature initiator decomposition may set off polymerisation. According to their chemical composition, inhibitors are antioxidants with high affinity towards free radicals. On the other hand, the effect of inhibitors during the actual polymerisation is insignificant because the amount and rate of free radical formation by far outweigh the amount of inhibitors (Odian 2004). The most frequently used inhibitors are butylated hydroxytoluene, BHT, and monomethyl ether hydroquinone (MEHQ). BHT is hydrophobic and, therefore, used in RBCs and hydrophobic adhesive systems whereas MEHQ is used in hydrophilic systems.

Antibacterial agents are sometimes added to adhesive systems and RBCs in order to prevent recurrent caries but also to reduce dental plaque growth on the surface of RBC restorations (Imazato 2003a). These agents may be in the form of monomers with antibacterial properties, such as MDPB (Imazato 1997), fluoride attached to the fillers or as fluorine compounds, parabenes, or in the form of glutaraldehyde, which is also known to be a fixating agent (Perdigao 1996). Because MDPB is incorporated into the polymer matrix, it only exhibits antibacterial properties before polymerisation and may act as a contact antimicrobial agent afterwards (Imazato 1998, Imazato 2003a). The in vivo antibacterial effect of glutaraldehyde has not been confirmed (Imazato 2003a, Van Landuyt 2007).

RBCs contain various pigments but their chemical composition is seldom revealed by the manufacturers. After extensive review of manufacturers' technical data, it has been noted that only one manufacturer has listed iron oxide, titanium oxide and aluminium sulfo-silicate as pigments. In the literature, there is no data on the effect of pigments on the mechanical and physical properties of RBCs.

In adhesive systems, dyes are sometimes used to allow better visual control during the mixing procedure of two-component systems (Van Landuyt 2007). The colour of these dyes fades after polymerisation.

1.2.2. The chemistry of polymerisation

1.2.2.1. Polymerisation of methacrylates and methacrylamides

Methacrylate- and methacrylamide-based adhesive systems and RBCs polymerise via a free radical addition polymerisation chain reaction. This process comprises three distinct phases: initiation, propagation and termination (Darvell 2002, Odian 2004, Van Landuyt 2007).

Radicalization (excitation) of initiators, for example CQ/BPO and tertiary amine, precedes the initiation phase of free radical polymerisation, during which the free radicals form. CQ, as a photo-sensitive molecule is excited by blue light irradiation. BPO, on the other hand, breaks down into free radical at temperatures just above the room temperature. CQ and BPO interact with the tertiary amine involving electron and hydrogen transfer which results in their break down to highly reactive free radicals. These free radicals have an affinity for carbon-carbon double bonds in the methacrylate groups (Figure 1).

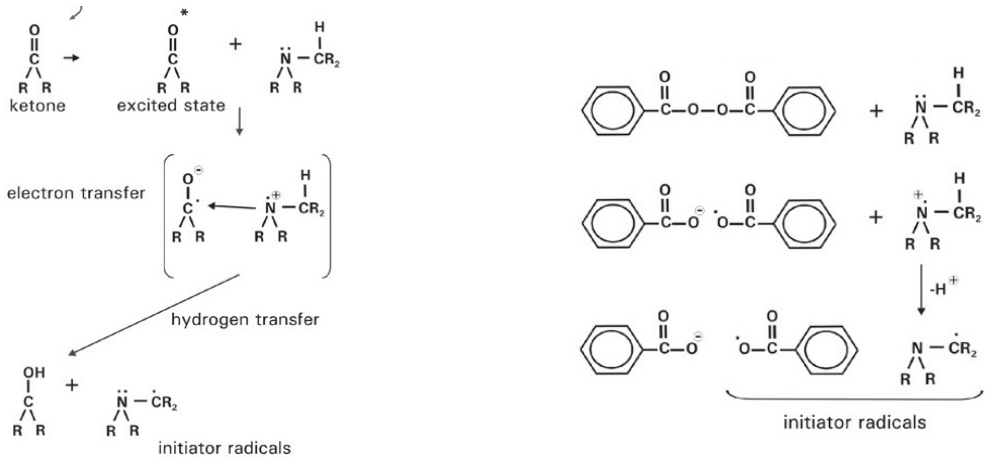

Figure 1. Radicalization of the camphorquinone (left) and benzoyl-peroxide (right).

Free radicals initiate the opening of carbon-carbon double bonds in the methacrylate groups during the initiation phase of monomer polymerisation. This results in the formation of another set of free radicals (Figure 2). One carbon atom forms a single bond with the free radical saturating it, but an unpaired electron remains on the central carbon atom of the methacrylate group. This selective affinity of the free radical towards the more exposed carbon atom is a result of the steric hindrance of the methacrylate groups. Nevertheless, the interaction of free radicals with centrally positioned carbon atoms cannot be ruled out but is, rather, an exception in the polymerisation chain reaction.

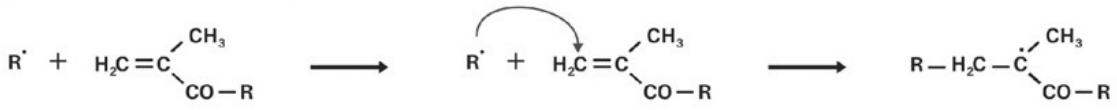

Figure 2. Initiation reaction. Interaction between free radical and methacrylate groups. New free radicals are formed.

In the propagation phase, the new free radicals are equally able to interact with carbon-carbon double bonds in unreacted monomers resulting in the growth of the polymer chains. This reaction repeats between newly formed unpaired electrons on carbon atoms of methacrylate groups in a cascade effect. The complexity of the polymer chains increases the steric hindrance effects and it may be expected that all new bonds will be created with the more exposed carbon atoms of the methacrylate groups via methylene [-CH_2-] bridges (Figure 3).

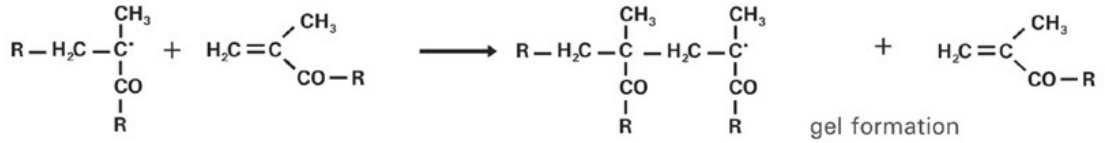

Figure 3. Propagation reaction.

The termination phase can occur at any time during polymerisation and depends on the concentration of free radicals and not the length of polymer chains. Chain termination occurs when two free radicals come close enough to interact with each other. Radicals in this case can be both the initiators radicals as well as 'growing' polymer chains. This type of chain termination is also known as combination. Chain transfer or disproportionation is another way of self-limiting polymerisation. It occurs through hydrogen abstraction when hydrogen from virtually any site within the growing chain interacts with a free radical which then becomes a branch of the polymer chain. This reaction terminates the propagation of one chain but may start another (Figure 4).

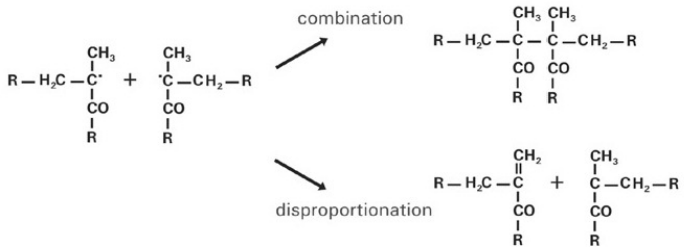

Figure 4. Termination reaction. Chain termination occurs when any two free radicals interact. Chain transfer is another possibility to terminate chain propagation.

1.2.2.2. Polymerisation of siloranes

Silorane-based RBCs polymerise through cationic polymerisation in which the active end of the growing polymer molecule is a positive ion (Crivello 1984). The initiator system of the only commercially available silorane RBC at the moment (Filtek Silorane) is the combination of CQ, an iodonium salt and an electron donor, not disclosed by the manufacturer. During the initial radicalization of the initiator system, the excitation of CQ by the electromagnetic energy of the light source and subsequent interaction with the iodonium salt and the electron donor produce reactive cations. Cations initiate polymerisation in much the same way as free radicals in the free radical polymerisation. In cationic polymerisation, a negatively charged pair of electrons from the carbon-carbon double bond is attracted by this cation resulting in the formation of a single bond with the initiator in the initiation phase. However, one of the carbon atoms, usually the more centrally positioned one, is now left with a positive charge due to the loss of electrons. This newly formed cation interacts with another monomer molecule in the same manner as the initiator reacted with the first monomer molecule in the propagation phase. Following molecular rearrangement, the positively charged species propagate in three dimensions to form a tightly cross-linked network (Crivello 1984). The termination phase occurs in the same way as with free radical polymerisation (Faust 1997).

In Filtek Silorane, the functional group of the oxirane is the centre of polymerisation. Unlike free radical polymerisation, more time is required to generate a sufficient amount of cations for polymerisation. Therefore, the manufacturer recommends a minimum curing time of 20 s which cannot be compensated by increasing light intensity.

1.2.3. Light-curing units (LCUs)

LCUs are used to initiate polymerisation in adhesive systems and RBCs containing photo-initiators in the initiator system. The first light curing RBCs used externally applied long wavelength, UV radiation (Buonocore 1970, Lee 1976). To overcome the

low curing efficiency of the UV LCUs and potential health hazards, RBCs cured with visible light were developed in late 1970s (Bassiouny & Grant 1978).

The properties of LCUs which are considered to affect polymerisation are the LCU type, light intensity and wavelength, curing mode and time and the distance from the material (Caughman 1995). The most commonly used types of LCUs in modern dental practice are halogen and LED LCUs. However, other types (plasma arc and laser LCUs) have been developed over the past years, but have not been so widely accepted in the dental community.

Wavelength is one of the main characteristics of the LCUs that affects polymerisation of light curing RBCs and the most efficient wavelength is around 470 nm (Nomoto 1997). Apart from the wavelength, light intensity is another internal characteristic of LCUs that also significantly influences the quality of resin polymerisation (Davidson & de Gee 2000) and is defined as radiation flux density or light irradiance (mW/cm^2).

Light intensity of early halogen LCUs was between 200-400 mW/cm^2 and LEDs around 100 mW/cm^2 and then, during 1990s, increased to between 500-700 mW/cm^2. Currently available LCUs have a wide variety of light intensities from 100 mW/cm^2 to more than 2000 mW/cm^2. ISO standard 4049 states that the minimum light intensity of LCUs for curing RBCs, adhesive systems and luting materials should be 300 mW/cm^2 (ISO 4049:2000). It has been reported that higher light intensities correspond to better DC and mechanical properties of RBCs (Mills 2002, Soares 2004, Ye 2007). However, other studies offered contrasting evidence, as different types of LCUs with different intensities gave comparable or, even lower, values for certain mechanical properties (St-Georges 2003) or DC values (Soh 2004, Silva Soares 2005). Furthermore, plasma arc LCUs have not induced higher DC values compared to halogen and LED LCUs despite significantly higher light intensities (Knezevic 2002, Tarle 2002, Ye 2007).

In a recent study, Emami & Söderholm hypothesized that light energy per unit area (J/cm^2) rather than light intensity was a more important curing property for optimal polymerisation. The authors concluded that the same DC in RBCs could be achieved as long as a material receives a fixed amount of energy irrespective of light intensity (Emami & Soderholm 2003). Witzel et al. confirmed this conclusion and also found that mechanical properties of RBCs, such as flexural strength, flexural modulus, hardness and contraction stress, were not affected by different curing methods as long as the same energy density was delivered (Witzel 2005).

Polymerisation shrinkage and shrinkage stress have been associated with rapid light curing with high energy levels (Davidson & Feilzer 1997). Calheiros et al. and Braga & Ferracane found that higher energy outputs in LCUs resulted in increased contraction stress and volumetric shrinkage in RBCs (Braga 2002, Calheiros 2004). Therefore, soft-start and pulse curing modes have been introduced. At the beginning of the curing process, significantly lower energy density or light intensities are used with a gradual increase to high power. This allows composite to flow during the pre-gel phase which relieves the stress within the restoration (Davidson & Feilzer 1997).

All LCUs are associated with temperature rise during photopolymerisation of adhesives and RBCs (Hannig & Bott 1999, Knezevic 2001, Knezevic 2002, Tarle 2002, Ozturk 2004, Tarle 2006, Millen 2007, Durey 2008). This temperature rise has been associated with the exothermic nature of the polymerisation process as well as the heat output from light sources. It can be considered as a drawback of all LCUs. Nevertheless, temperature can be controlled to a certain extent because it is affected by other factors, which can be classified as LCU, material and tooth-related. Some studies have shown that conventional and high power halogen LCUs produce significantly higher temperatures than LED or plasma arc LCUs (Knezevic 2001, Knezevic 2002, Tarle 2002). It is often stated that LEDs induce lower temperature changes due to their narrower spectrum. However, the extent of temperature changes reported in the literature is somewhat contrasting. Hannig & Bott have suggested that light intensity and not the type of light

source is more important for temperature rise. Halogen and LED LCUs of similar intensities gave comparable results in this respect. These findings were confirmed by Vandewalle et al. who also reported there was no significant difference in RBC hardness after polymerisation with LED or high power halogen with similar energy densities (Vandewalle 2005). It has been shown that temperature rise in the pulp chamber is always higher during curing of adhesives than RBCs (Millen 2007, Durey 2008) irrespective of the LCU type. The temperature rise in the pulp chamber is lower during RBC curing possibly because of the thermo-insulation capacity of the bulk of the RBC (Durey 2008). Therefore, clinicians are advised to be aware of the potential risk to the pulp arising from light curing of adhesives and RBCs. It is recommended that adhesives are cured with lower energy modes, e.g. soft-start or pulse, and that maximum power is exclusively used for bulk RBC curing (Millen 2007).

CHAPTER 2

LITERATURE REVIEW

2.1. CONVERSION OF MONOMERS TO POLYMERS

2.1.1. Review of terminology

Conversion of monomers to polymers has been identified as an important determinant of the quality of RBCs since the mid-1970s (Ruyter & Svendsen 1978). A number of methods to determine monomer conversion to polymers in light curing RBCs and, to a less extent, adhesive systems, have been used since then (Cook 1980, Newman 1983, DeWald & Ferracane 1987, Eliades 1987, Baharav 1988, Rueggeberg 1988, Fowler 1994, Davidson-Kaban 1997, Bouschlicher 2004, Cadenaro 2005, Emami & Soderholm 2005, Rode 2007, Santos 2007, Tomlins 2007). This has led to a number of different terms used to describe monomer conversion to polymers.

The term 'remaining methacrylate groups' has been suggested and calculated as a ratio between the IR absorbance bands of aliphatic and aromatic C=C double bonds before and after polymerisation (Ruyter & Svendsen 1978).

The term 'remaining carbon-carbon double bonds (RDB)' was used in one of the earliest studies (Eliades 1987) using infrared spectroscopy and the RDB was calculated as previously mentioned by Ruyter & Svendsen (1978).

The term 'depth of cure' was used in studies which indirectly assessed monomer conversion to polymers based on the hardness method (Cook 1980, DeWald &

Ferracane 1987, Baharav 1988, Rueggeberg 1988, Fowler 1994, Davidson-Kaban 1997), optical changes (Newman 1983, DeWald & Ferracane 1987, Baharav 1988), penetration and scrapping tests (ISO 4049, Cook 1980, DeWald & Ferracane 1987, Baharav 1988).

The term 'degree of conversion (DC)' has been used to indicate the amount of monomer conversion in studies which used the following methods: calorimetry (Cadenaro 2005, Emami & Soderholm 2005, Tanimoto 2005, Cadenaro 2006, Cadenaro 2008), spectroscopy (DeWald & Ferracane 1987, Rueggeberg 1988, Lundin & Koch 1992, Shin 1993, Knezevic 2001, Sideridou 2002, Tarle 2002, Calheiros 2004, Tarle 2006), electron spin resonance (Hotta 1998) and interferometry (Tomlins 2007).

In the study by Eliades et al. (1987) four different terms were used, degree of double bond conversion, degree of cure, degree of saturation and remaining carbon-carbon double bonds, probably as synonyms to refer to monomer conversion to polymers. Such terminological inconsistencies are found in other papers (Rueggeberg & Tamareselvy 1995, Nomoto 1997, Emami & Soderholm 2003, Cadenaro 2005, Tanimoto 2005, Ilie & Hickel 2006, D'Alpino 2007, Atai & Motevasselian 2008) and this may result in confusion as to what the authors actually refer.

In previously quoted studies using the term DC, monomer conversion to polymers is calculated as the ratio of a certain feature of carbon-carbon double bonds such as absorbance, scattering, heat emission or electron spin resonance in cured and uncured material related to an internal standard. An internal standard is a particular bond within the monomer molecule which does not take part in polymerisation and whose feature of interest does not change in uncured and cured states.

The DC should represent only the conversion of double bonds involved in the process of polymerisation. It should not be used to describe the double bonds remaining after certain processes which may result in an overall change in the number of C=C double bonds, such as post-polymerisation cure ('dark' cure) (Lopez-Suevos & Dickens 2008,

Sadek 2008), hydrolysis (Santerre 2001), elution (Ferracane 1994, Yap 2004b) or heating (Bagis & Rueggeberg 1997a). This calls into question the often used term 'degree of conversion' but also 'remaining methacrylate groups' and 'remaining carbon-carbon double bonds'. The latter two suggest a measurement of unreacted groups which is not what is calculated in the formula frequently used in this type of study. [vide infra. Page 41]

Miletic et al. considered the term "ratio of C=C double bonds" (RDB) to be more appropriate than DC, since it refers to the ratio of carbon-carbon double bonds that take part in polymerisation irrespective of the processes that may affect the initial monomer to polymer conversion (Miletic 2009b). However, it is accepted that this term may be ambiguous in certain cases, and it is suggested that, for clarity, the 'double bonds' are specifically defined in every case. Furthermore, the term 'C=C double bonds' may be inappropriate in resin-based materials, such as Filtek Silorane, which have a different chemical composition and whose polymerisation is based on the opening of C-O-C rings and not C=C double bonds.

Despite these limitations, the most commonly used term 'degree of conversion' (DC) will be used throughout this thesis.

2.1.2. Methods of determination

2.1.2.1. Spectroscopy

Currently, spectroscopy is one of more frequently used methods to determine monomer to polymer conversion and will be described in much greater detail than previous methods. In general, it is the use of light, sound or particle emission to study the properties of matter. Of particular interest for dental material science is vibrational spectroscopy based on the interaction between light and molecules of matter. The

interaction between light and the molecule is mutual, one influences another and vice versa (Steele 1971).

Vibrational spectroscopy is based on the fact that atoms in molecules are in constant state of vibrations. There are two main types of vibrations: (1) stretching and (2) bending. Stretching is a change in the inter-atomic distance along the bond axis (length of the bond). Stretching vibrations can be symmetric and asymmetric depending on the direction of inter-atomic vibrations for two or more bonds. Bending is a change in the angle between the atomic bonds and can be further classified as rocking, scissoring, wagging and twisting. Rocking is a change in the angle between a group of atoms and the rest of the molecule when the atoms bend in the same direction. Scissoring is similar to rocking but the atoms bend in opposite directions. During rocking and scissoring, atoms remain in the same plane as the rest of the molecule. Wagging is a change in the angle between the plane of a group of atoms and the plane of the rest of the molecule. Twisting is a change in the angle between the planes of two atoms or two groups of atoms within the molecule. Wagging and twisting are also known as out-of-plane vibrations (Steele 1971, Schrader 1995).

Vibrations of atomic groups within molecules are important because they affect the electromagnetic radiation (light) upon interaction. When light interacts with a molecule, it excites certain types of vibrations which result in light absorption, reflection or scattering. Infrared (IR) spectroscopy is based on light absorption, Raman spectroscopy on light scattering and both are used in dental materials studies (Steele 1971, Schrader 1995).

2.1.2.1.1. Theoretical review of infrared spectroscopy

The main goal of IR spectroscopy is to determine the chemical functional groups in the sample which allow identification and structural characterization of gas, liquid or solid substances. Different functional groups absorb characteristic frequencies of IR radiation (Schrader 1995, Hsu 1997).

Chemical analysis of many organic compounds is done using IR spectroscopy since the energy of molecular vibrations occurs in the infrared spectrum, in many cases in a very narrow range. The infrared spectrum covers all functional groups as their vibration frequencies are within the mid-IR range between 4000 cm^{-1} and 625 cm^{-1} (Hsu 1997). IR spectra of pure compounds are generally so unique that they are often called a molecular “fingerprint" (Williams 1995). While organic compounds have very rich, detailed spectra, inorganic compounds are usually much simpler. Each functional group is identified by its characteristic vibration frequency which corresponds to well-defined regions of the infrared spectrum. These regions are also known as “fingerprint regions”. Not only can IR spectroscopy detect vibrational modes of the whole molecule, it may also detect localized vibrations. These are the vibrations of individual bonds and functional groups within a complex molecule (Schrader 1995, Williams 1995). Stretching and bending are the most common vibrations detected in molecules of dental resins (Williams 1995).

The basic principle of the IR spectrometer is that, after calibration using known materials, examined samples are subjected to the infrared light. The light is split into two beams of the same intensity and one of those beams irradiates the sample. The other passes through a reference which is often the substance in which the sample is dissolved. Both light beams are reflected, dispersed by a monochromator into component frequencies and collected on the detector and an electrical signal is generated. The IR spectrum is a result of the comparison of the two beams, the one that does not interact with the sample and the one that passes through it. The resulting spectrum is in the form

of downward peaks which correspond to energy absorption (Schrader 1995, Williams 1995).

Traditional IR spectroscopy has been substantially improved with the development of Fourier-transform infrared (FTIR) spectrometers. In FTIR spectrometers, a monochromator is replaced by an interferometer. Not only has this significantly reduced the cost of equipment but also increased the speed by allowing simultaneous analysis of the outgoing frequencies. Improved optics and internal laser reference for automatic calibration have increased the sensitivity and accuracy of FTIR spectrometers (Schrader 1995). This is of particular importance in dentistry because it can be used for scanning small samples. The two IR beams are recombined after the interaction with the sample in order to produce repetitive interference signals (interferograms) measured by a detector as a function of wavelength. A mathematical operation known as Fourier transformation is applied to the interferogram converting it to the final IR spectrum, which plots absorption intensity against wavenumber (Schrader 1995, Hsu 1997).

2.1.2.1.2. Theoretical review of Raman spectroscopy

In Raman spectroscopy, an incident beam of light is directed at a sample and the reflected light is scattered in two ways. These are known as Rayleigh and Raman scattering (Schrader 1995). Raman scattering can be subdivided into Stokes and Anti Stokes Raman scattering. Rayleigh scattering occurs when there is no change in the amount of energy exchanged between the incident photons and the sample molecules. Thus, the scattered light has the same wavelength as the incident light. Raman scattering occurs when sample molecules exchange energy with light photons. Usually, the molecule gains energy from the incident photon and is excited from the ground state to the so-called first vibrational excited state. Since the resulting energy of the scattered photons is smaller, their wavelength is longer. This phenomenon is known as Stokes Raman scattering. On the other hand, if the molecule is at the first vibrational excited

state and interacts with the incident photon, it loses energy and returns to the ground state. The scattered light photons have gained energy and, therefore, have a shorter wavelength. This is known as Anti-Stokes Raman scattering. The change in the energy and wavelength of the scattered light is known as the Raman shift.

Rayleigh scattering forms the dominant part of the scattered light and Raman is only about 10^{-7} of the initial light source power. Stokes Raman is much stronger than Anti Stokes because at room temperature the major state of most molecules is the ground state and only a small number of molecules are in a higher vibrational excited state. The ratio of Anti Stokes to Stokes increases with temperature as more molecules appear in the first vibrational excited state (Schrader 1995).

FT-Raman spectroscopy has brought certain advantages to Raman spectroscopy, as did FTIR to IR spectroscopy. Interferometers have replaced monochromators to record excited Raman spectra and Fourier transformation is applied to interferograms converting them into Raman spectra. Furthermore, near-IR source of radiation prevents fluorescence which is the most common problem in traditional Raman spectroscopy (Schrader 1995).

Though IR and Raman spectroscopy are considered to be complementary and not substitute techniques for chemical analysis (Schrader 1995), seldom are they jointly used. Advantages of Raman over IR spectroscopy, concerning dental application, is that Raman bands of double and triple bonds tend to be much stronger than those of the IR. In some cases, these bonds maybe totally inactive in the IR. Also, Raman signals can be observed from all directions whereas IR signals have a co-linear optical arrangement. Raman signals are independent of excitation light and its frequency. Intensities of Raman bands linearly correlate to chemical concentrations of components (Schrader 1995). Furthermore, IR analysis of aqueous solutions is difficult because of solvent opacity, whereas the Raman spectrum of water is very weak providing an ideal solvent. Raman spectroscopy requires no or very little sample preparation and a rapid, non-

destructive optical spectrum is easily achieved (Williams 1995). Inorganic fillers, particularly silica and glass, are poor Raman scatterers, appearing as weak and broad features in the Raman spectrum and do not spectrally interfere with the peaks used to calculate monomer conversion (Shin 1993). IR is a more powerful qualitative than quantitative analytical tool and is predominantly used for identification of substances in unknown samples. Because the strength of the absorption is proportional to the concentration, IR can be used for some quantitative but rather simple analyses. However, sample preparation techniques, especially for solid substances, may affect absorption characteristics resulting in altered quantitative data (Williams 1995).

Both IR and Raman spectroscopic methods have been increasingly used in studying monomer conversion into polymer of RBCs (Ruyter & Svendsen 1978, Eliades 1987, Chung & Greener 1988, Caughman 1991, Oooka 2004, Soares 2004, Soh 2004, Silikas 2005, Santos 2007, Cassoni 2008), adhesive systems (Imazato 1997, Yamada 2004, Kanehira 2006, Kim 2006, Xu 2006, Arrais 2007, D'Alpino 2007, Ye 2007, Sadek 2008) as well as experimental resin mixtures (Rueggeberg & Margeson 1990, Shin 1993, Jacobsen & Soderholm 1995, Venhoven 1996, Sideridou 2002, Skrtic 2003, Bae 2005, Dickens & Cho 2005, Gauthier 2005a, Turssi 2005, Atai & Watts 2006, Ogliari 2006, Wang 2006c, Ogliari 2007, Guo 2008a, Lopez-Suevos & Dickens 2008).

Possible reasons for increasing popularity of these methods are:

(1) The signal for aliphatic and aromatic C=C bonds is constant in IR and Raman spectroscopy. The position of the aliphatic bond peak is at 1639 cm^{-1} and the aromatic bond peak is at 1609 cm^{-1}.

(2) The method for calculating DC is straightforward:

$$DC=[1-R_{cured} / R_{uncured}] * 100$$

where R_{cured} represents the ratio of intensities of IR or Raman peaks associated with aliphatic and aromatic bonds (1639/1609 cm^{-1}) in the cured sample and $R_{uncured}$ represents the same ratio in the uncured material.

(3) Relative simplicity in sample preparation and the non-destructive nature of the method.

The principle of these measurements is based on the fact that polymerisation normally occurs by breaking the carbon-carbon double bond of one monomer and linking the second monomer via the free electrons. Because these bonds generate very distinctive peaks in the IR and Raman spectra, the change in their intensity is monitored as the polymerisation takes place (Schrader 1995). The extent of the curing reaction is assessed by following the intensity of the peaks associated with the C=C vibrations and comparing them to bands associated with bonds that remain unchanged during polymerisation. The latter are known as an internal standard (Schrader 1995, Williams 1995). The review of previously quoted papers on monomer conversion in RBCs, adhesive systems and experimental resin mixtures revealed that C=C bonds in aromatic moieties were used as the internal standard in BisGMA-based materials and C=O bonds in non BisGMA-based materials.

The calculated DC does not indicate the actual amount of monomer converted into polymer but the percentage of converted aliphatic C=C double bonds in the resulting polymer (Emami & Soderholm 2003). The DC of 60% means that 60% of C=C bonds are converted leaving 40% of C=C bonds and not 40% of the monomer unreacted.

2.1.2.1.3. Commercial resin-based composites

Ruyter & Svendsen quantified the number of remaining methacrylate groups in six chemically cured, two-paste RBCs using multiple internal reflection spectroscopy. They also used molar ratios of 0.2-1.8 of Bisphenol A-TEGDMA and BisGMA-TEGDMA to produce calibration curves and confirm the linear relationship between the concentration of C=C double bonds and absorbance. The percentage of the remaining methacrylate groups in RBCs was in the range of 20-30% after 24 h storage at 37°C (Ruyter &

Svendsen 1978). However, the storage media was not mentioned so the effect of possible elution could not have been assessed.

Eliades et al. evaluated the degree of double bond conversion in five light cured RBCs and the effect of post-cure heating on the ratio of C=C double bonds using micro-attenuated total reflection (micro-ATR) IR spectroscopy. A smaller depth of cure and greater number of unreacted C=C double bonds were found in micro-filled RBCs as a function of distance and curing time. It was concluded that IR spectroscopy was more sensitive than KHN in detecting the changes in the number of unreacted C=C double bonds. Heat-induced post-cure after 24 h storage at 37°C resulted in less than 10% reduction in the initial number of uncured C=C double bonds. The authors attributed these results to the decay of free radicals and chain termination (Eliades 1987).

Chung & Greener used FTIR spectroscopy to compare monomer conversion of seven commercial RBCs and reported that the DC values were in the range of 43-73 %. Comparable DC was found for RBCs with different chemical composition. It was suggested that DC was affected by various factors such as initiator and diluent concentrations and, to a less extent, filler concentration (Chung & Greener 1988).

Rueggeberg et al. emphasized the necessity to establish a precise relationship between the concentration and absorption of C=C double bonds which may be either linear or non-linear. Using BisGMA/TEGDMA mixtures of different concentrations, a regression calibration plot was produced and five baseline methods for determining monomer conversion were tested. Then, the molar ratio of aliphatic and aromatic double bonds was determined in nine commercially available RBCs. It was found that different baseline methods may have a significant effect on the calculated values for monomer conversion. Aliphatic-to-aromatic molar ratios of up to 6 to 1 should be used for calibration purposes in order to include differences in commercial RBCs (Rueggeberg 1990).

Caughman et al. correlated the filler content and cytotoxicity with the degree of monomer conversion in three commercial RBCs containing between 45% and 85% of fillers. The degree of monomer conversion was determined using ATR-FTIR spectroscopy. Significant differences in monomer conversion were reported for top and bottom surfaces of 1 mm thick samples of each RBC. Monomer conversion increased with increased curing times but no significant differences were observed among the three RBCs. Cytotoxicity was measured as a function of cellular protein synthesis of primary human gingival fibroblasts. A negative correlation was observed between cytotoxicity and the degree of monomer conversion for all three RBCs. Based on the results of this in vitro study, the authors suggested incremental polymerisation and prolonged curing times during clinical placement of RBCs in order to minimise potential in vivo cytotoxic effects (Caughman 1991).

Bagis & Rueggeberg examined the effect of different post-cure heating temperatures and time intervals on monomer conversion in a commercial hybrid RBC. The DC values were in the range of 50% to 70%. The authors found that both temperature and heating time resulted in increased DC but at a given temperature no obvious trend was observed for different heating times (Bagis & Rueggeberg 1997a).

Oooka et al. calculated the DC in chemically and dual-cured RBCs. FTIR spectra were taken after 24 h storage in distilled water at 37°C. Significantly higher DC values were found for dual-cured RBCs compared to chemically-cured RBCs. Furthermore, a UDMA-based RBC showed higher DC values than a BisGMA-based one irrespective of the curing mode (Oooka 2004).

Silikas et al. used a series of physico-chemical methods to analyse the surface characteristics of three micro-hybrid and one nano-filled RBC. Micro-multiple internal reflectance (micro-MIR) FTIR spectroscopy was used to determine the DC immediately after polymerisation. The DC was calculated as the ratio of peak absorbance areas of ‘analytical’ and ‘reference frequencies’ of cured and uncured materials. Significant

differences in DC values for one micro-hybrid and the nano-filled RBC compared to the two micro-hybrid RBCs were attributed to the differences in monomer composition and not the filler content (Silikas 2005).

The effect of LCUs on monomer conversion in a single RBC material was studied using both Raman (Soares 2004, Soh 2004, Silva Soares 2005, Santos 2007, Cassoni 2008) and FTIR spectroscopy (Lohbauer 2005).

Soares et al. calculated the DC, using NIR FT-Raman spectroscopy, in Z100 RBC cured by either an argon laser or a conventional halogen LCU and correlated this DC with Vickers hardness at the top and bottom surfaces. They found comparable or insignificantly higher DC values when samples were cured with argon laser on both surfaces. The DC was in the range of 57-66% for both LCUs. The DC increased with increasing curing times and an exponential relationship between the DC and Vickers hardness was established using correlation analysis (Soares 2004).

Using NIR-FT-Raman spectroscopy, Silva Soares et al. investigated the DC in Z100 RBC cured with either an LED or a conventional halogen LCU. Raman measurements were done immediately after curing. The DC values were comparable or higher at the top compared to the bottom surface irrespective of the LCU. The DC increased significantly between 20 s and 40 s but not between 40 s and 60 s curing time (Silva Soares 2005).

Soh et al. investigated the effect of different LCUs (two LED, two high power halogen and a conventional halogen) operating at different curing modes (standard, exponential, pulse, turbo, soft-start and high power) on the DC of Z100 RBC, using micro-Raman spectroscopy. Comparable results were found for all LCUs and all curing times and the DC values were in the range of 56-59% for top and 52-57% for bottom surfaces (Soh 2004).

Santos et al. studied the depth of cure curing RBC samples with a quartz-tungsten halogen (QTH) or an LED LCU. QTH produced higher DC values than the LED LCU and for both LCUs, a decrease in DC was found as a function of depth (Santos 2007).

Rode et al. studied the DC in an RBC cured with an LED, an argon laser or a conventional halogen LCU at distances of 0 mm, 3 mm, 6 mm and 9 mm. The DC values decreased for all LCUs with increasing RBC thickness and curing distances. The LCUs produced comparable DC in samples 1 mm thick and cured from the maximum distance of 3 mm (Rode 2007).

Cassoni et al. studied DC, using NIR FT-Raman spectroscopy, and KHN of Z350 RBC cured with an argon laser operating at two power levels or a conventional halogen LCU. After 24 h storage in deionised water at 37°C, the DC was only calculated for the non-irradiated bottom surface and was between 44% and 49%. No significant differences were observed between the two types of LCUs or the two operating modes of the argon laser LCU (Cassoni 2008).

Lohbauer et al. studied the DC, using FTIR spectroscopy, and mechanical properties of Tetric Ceram RBC after light curing with plasma, an LED or a conventional halogen LCU. The DC was measured after 14 days of dark storage in air at 37°C. A positive correlation was found between the light energy density and DC and the light energy density and cyclic fatigue strength. No correlation was found between the flexural fatigue limit and DC at 2.5 mm within the RBC. The results were explained in terms of light energy density, internal stresses, polymer structure and specific monomer cross-linkage (Lohbauer 2005).

The effect of LCUs and curing modes on monomer conversion in different RBCs has been studied using FTIR spectroscopy (Knezevic 2001, Knezevic 2002, Tarle 2002, Bala 2005, Ilie & Hickel 2006, Tarle 2006, Atai & Motevasselian 2008) and Raman

spectroscopy (Leloup 2002, Emami & Soderholm 2003, Emami 2003, Witzel 2005, Beun 2007, da Silva 2008).

Knezevic et al. measured the DC and temperature rise in three hybrid RBCs cured with either plasma or a high power halogen LCU on soft-start mode. The FTIR measurements were performed on the top and bottom surfaces. The high power halogen LCU produced comparable or higher DC values for all three RBCs irrespective of the depth. The DC values were in the range of 56-76% (top) and 52-67% (bottom) and decreased as a function of depth in all cases. Significant differences in DC but comparable values for temperature rise were observed for the three RBCs cured with the same LCU. When different LCUs were compared, the high power halogen LCU produced a significantly higher temperature rise than the plasma LCU in all three RBCs (Knezevic 2002).

Knezevic et al. measured the DC and temperature rise in hybrid RBCs after curing with an experimental blue LED, a high power halogen, on soft-start mode, or a conventional halogen LCU. Using FTIR spectroscopy and the standard baseline method, the authors found that the DC values were in the range of 45-76%. Significantly lower DC values were found for the experimental LED LCU compared to halogen LCUs but the experimental LED LCU induced significantly lower temperature rise than the halogen LCUs (Knezevic 2001).

In a similar study, Tarle et al. measured the DC and temperature rise in hybrid RBCs after curing with an experimental blue LED, a plasma arc or a conventional halogen LCU. The conventional halogen LCU produced significantly higher DC values than plasma whereas the high power halogen LCU, at exponential mode, produced similar DC values as plasma. The experimental LED LCU induced significantly lower temperature rise in RBC samples than the halogen LCUs but comparable with the plasma arc LCU (Tarle 2002).

Tarle et al. also compared the DC, temperature rise and polymerisation shrinkage of a hybrid and a micro-hybrid RBC cured with an experimental blue LED or a high power halogen LCU, operating at three curing modes (high power, low power and pulse/soft-start). The conventional halogen LCU produced higher DC values than soft-start high power halogen and experimental LED LCUs with no differences at top and bottom surfaces. Lower polymerisation shrinkage was found after light curing with the experimental LED compared to halogen LCUs (Tarle 2006).

Bala et al. compared the effect of an LED and a conventional halogen LCU on the DC of two hybrid and four packable RBCs and one ormocer-based RBC. FTIR measurements were done immediately after light curing and the standard baseline technique was used for post-processing of data. The DC values were between 47% and 61%. The LED LCU produced comparable or higher DC values than the conventional halogen LCU despite the lower light energy density. Significant differences were observed among several RBCs irrespective of their type (Bala 2005).

Ilie & Hickel investigated the DC and mechanical properties of a silorane-based RBC (Hermes, 3M ESPE) light cured with one of three LED LCUs, operating at different modes, or a high power halogen LCU. 'Real time' FTIR measurements were performed from the bottom surface of the RBC samples for the duration of light curing and up to 20 min thereafter. The DC was calculated as the peak height ratio of the C-O-C bond at 883 cm^{-1} and the C-H bond at 1257 cm^{-1} which was used as the internal standard. The DC values measured at the bottom of the 2 mm and 6 mm thick samples were in the range of 57-66%. The curing time, and not the irradiance, was held responsible for the high DC values. The mechanical properties of the silorane-based RBC were similar to methacrylate-based RBCs (Ilie & Hickel 2006).

Atai & Motevasselian compared the DC and temperature rise in a nano-filled and a hybrid RBC cured with an LED, a high power halogen, at standard or ramp mode, or a conventional halogen LCU. The DC values were 42-44% for the nano-filled RBC and

44-59% for the hybrid RBC. The DC was significantly higher for the high power halogen LCU at the ramp mode compared to the standard mode or the other two LCUs. The conventional halogen and LED LCUs produced similar DC values and temperature rise (Atai & Motevasselian 2008).

Using Raman spectroscopy Leloup et al. studied the effect of shade, translucency and thickness as well as the type and distance of LCUs on the DC of four RBCs. A non-linear relationship was found between the DC and material thickness. Higher DC values were associated with more translucent shades and higher light energy density of the LCUs. No differences were found in the DC of samples cured from tip-to-sample distances of 10 mm or less (Leloup 2002).

Emami & Soderholm suggested that light energy and not light irradiance has a more profound effect on composite resin polymerisation. Using FT-Raman spectroscopy, they generated calibration curves for a series of differently hydrogenated solutions of BisGMA (50 wt%) / TEGDMA (50 wt%). The DC of two RBCs (Z100 and Filtek Z250) of similar BisGMA/TEGDMA ratios as the calibration mixtures was determined after light curing with a halogen LCU operating at different curing modes and times. Light energy per unit area (light energy density, J/cm^2) was calculated as light irradiance multiplied by the curing time. Different curing modes with the same light energy density produced comparable DC values. Light energy density greater than 30 J/cm^2 is required to produce similar DC at the bottom surface of 2-6 mm thick samples (Emami & Soderholm 2003).

Emami et al. also studied the effect of light intensity and curing times on the DC and polymerisation shrinkage of two RBCs. Immediately after light curing, FT-Raman measurements were performed on the top and bottom surfaces. The DC was calculated according to the conventional formula and shrinkage was measured using strain-gauges. Though the results for DC confirmed the previous findings, polymerisation shrinkage

was independent of the light energy density. The DC was significantly higher on top than bottom surfaces of the 4 mm thick samples of both RBCs (Emami 2003).

Witzel et al. compared the effect of different curing modes with similar light energy densities on the DC of an RBC and an unfilled resin. FT-Raman spectroscopy was performed after storage in air at 37°C for 24 h. The DC of the RBC was about 65% whereas the DC of the unfilled resin was 73-79%. The authors concluded that the curing modes of similar light energy densities did not affect the DC of the RBC. A high intensity curing mode induced significantly higher DC in the unfilled resin than a low intensity or pulse mode (Witzel 2005).

Beun et al. measured the DC and mechanical properties of two micro-filled, three nano-filled and four universal hybrid RBCs cured with either a halogen or an LED LCU. The DC was measured at 0.5 mm steps within the 6 mm thick samples, immediately after light curing. The DC was significantly lower for the LED LCU in all RBCs and more rapidly decreased with depth. Though the LED LCU was a high power one (Elipar Freelight2), the authors used the low light intensity of 450 mW/cm^2 and 10 s curing time. The delivered light energy density was substantially lower than that of the halogen LCU for the light intensity of 650 mW/cm^2 and 40 s curing time (Beun 2007).

Da Silva et al. correlated the DC, solubility and salivary sorption of a hybrid and a nano-filled RBC light cured with a high power halogen LCU operating at either standard or soft-start mode, but with the same light energy density. FT-Raman measurements were done after dry storage at 37°C for 24 h. Significantly higher DC was found for the hybrid than the nano-filled RBC as well as the standard compared to the soft-start curing mode. A different set of samples was used to determine solubility and salivary sorption. A negative correlation was found between the DC and solubility but no correlation was found between the DC and salivary sorption (da Silva 2008).

Lohbauer et al. assessed DC, polymerisation shrinkage and intra-cavity temperatures of a nano-filled RBC after different pre-heating procedures and storage intervals. The RBC was stored and polymerised at 10°C, 23°C, 39°C, 54°C and 68°C and the DC was measured after 5 min and 24 h of dry-heat oven storage at 37°C. A positive correlation was found between the DC on the top surface and pre-polymerisation temperatures and storage intervals. The same trend was observed for the bottom surface DC. For clinical use, the authors recommended that RBCs should be used at room or body temperatures. Pre-heating of RBCs is potentially beneficial but specific heat capacity and thermal diffusivity should be taken into account due to possible pulp damage (Lohbauer 2009).

To the best of my knowledge, only one study compared the DC of RBCs placed in vivo and in vitro. Posterior RBC restorations were placed in MOD cavities in contra-lateral premolars, one in vivo and the other in vitro after tooth extraction. Point Raman spectra were taken from proximal surfaces and the DC calculation was performed solely as the ratio of 1610/1640 cm^{-1} peak intensities. A higher ratio was found in vivo (Lundin & Koch 1992). However, the results are questionable since the authors made an error assigning Raman peaks to the actual vibrational groups. They assigned 1610 cm^{-1} peak to the aliphatic and 1640 cm^{-1} to the aromatic C=C bonds, instead vice versa. Furthermore, they failed to apply the correct formula for calculating DC and used only the ratio of 1610/1640 cm^{-1} of the cured material.

2.1.2.1.4. Experimental resin-based composites

The aim of studies on experimental resin mixtures is to determine the effect of specific ingredients of resin-based materials or curing characteristics on monomer conversion.

Asmussen measured the number of remaining unreacted double bonds in light-cured and chemically-cured BisGMA-based mixtures using IR spectroscopy. The number of remaining unreacted double bonds was found to be between 23% and 43%. For a fixed

amount of amine, peroxide, and inhibitor, the number of remaining double bonds decreased with increasing content of diluting monomer (Asmussen 1982).

Rueggeberg & Margeson studied the effect of oxygen inhibition on monomer conversion in a commercial unfilled adhesive resin and an RBC using FTIR spectroscopy. The adhesive was cured in three atmospheric conditions: (1) air, (2) air combined with the stream of argon or (3) pure argon. FTIR spectra were taken immediately after polymerisation of adhesive alone and after RBC placement. The DC of the RBC was significantly higher than that of the adhesive resin in all three atmospheres. For both materials, the DC increased in the order: air<air+argon<argon. It was suggested that, in clinical conditions, light curing under a continuous stream of argon could result in higher DC of RBCs (Rueggeberg & Margeson 1990).

Shin et al. compared the DC, obtained by Raman and FT-Raman spectroscopy, of various molar mixtures of BisGMA/TEGDMA, Bisphenol A/TEGDMA and EGDMA/EGDA. The combined Gaussian-Lorentzian function was used for band fitting and determination of accurate peak shape and the authors stated that no particular peak shape should be a priori expected. The DC values were comparable for both Raman and FT-Raman which proved that both methods could be used to determine monomer conversion in dental resin-based materials (Shin 1993).

Jacobsen & Soderholm studied the effect of water on monomer conversion in BisGMA/HEMA mixtures using FTIR spectroscopy. The results indicated that water had an adverse effect on DC. The DC decreased with increasing amounts of water up to a saturation point beyond which no significant difference in DC was observed (Jacobsen & Soderholm 1995).

Imazato et al. studied the relationship between the DC and internal discoloration of experimental RBCs with different amounts of BisGMA and TEGDMA. FTIR and colour measurements were done after 1, 2, 3 and 4 weeks of immersion in water at 60°C.

Annealed RBCs showed higher DC values and less discoloration than their non-annealed counterparts. Increasing amounts of TEGDMA resulted in higher DC and less discoloration in non-annealed RBCs (Imazato 1995).

Venhoven et al. studied the effect of different initiator concentrations on the curing rate of a BisGMA/TEGDMA mixture using FTIR spectroscopy and linear contraction measurement. FTIR spectra were taken continuously during curing and for 2 h thereafter and the standard baseline method was used in data analysis. Both FTIR and linear contraction measurements gave a DC value of about 64% after 20 s and 60 s of curing. Significantly lower DC values were found for lower initiator concentrations and 10 s curing time (Venhoven 1996).

Sideridou et al. studied the DC in different mixtures of BisGMA, TEGDMA, BisEMA and UDMA using FTIR spectroscopy. FTIR spectra were taken immediately after curing resin mixtures using a high power halogen LCU for times ranging from 10s to 240 s. Initial polymerisation rates of UDMA and BisGMA were significantly higher than those of TEGDMA and BisEMA. The polymerisation rates of UDMA and BisGMA then rapidly decreased whereas those of BisEMA and TEGDMA continued to increase and reached their maximum values about 8 and 9 s after the start of polymerisation. The final DC was in the increasing order: BisGMA<BisEMA<UDMA<TEGDMA and was not affected by the reactivity of monomers. The DC of BisGMA mixed with other dimethacrylates showed a linear relationship with the mole fraction of BisGMA. The differences in polymerisation rates for the four resins were attributed to the different chemical structures of the spacer groups. The polymerisation rates of BisGMA/BisEMA and BisGMA/UDMA mixtures were similar to those of neat resins whereas BisGMA/TEGDMA showed a faster polymerisation rate than the two neat resins (Sideridou 2002).

Dickens et al. studied the effect of TEGDMA on polymerisation kinetics and the extent of polymerisation of BisGMA, UDMA and EBADMA-based mixtures. Initial resin

viscosity and molecular structure were concluded to be the main factors for optimum reactivity of resin mixtures. Though low viscosity resin mixtures may have a high extent of polymerisation, other material properties such as shrinkage, toughness, wear and strength may be compromised (Dickens 2003).

Skrtic et al. studied the effect of unhybridised, silica or zirconia-hybridised amorphous calcium phosphate fillers on the DC and volumetric contraction of a series of experimental resin-based mixtures. Monomer conversion was independent of the type of fillers but dependent on the monomer matrix. Volumetric contraction depended on both the type of fillers and monomers, particularly in UDMA and HEMA-based mixtures (Skrtic 2003).

Musanje & Ferracane studied the effect of resin viscosity and silanization of colloidal silica fillers on the DC and mechanical properties of TEDGMA/UDMA/BisGMA mixtures. The resin mixtures contained a fixed amount of UDMA and the viscosity was varied by reducing TEGDMA and increasing BisGMA. Following light curing, FTIR spectra were taken after 24 h storage in deionised water at 37°C. The DC decreased with increasing viscosity of resin mixtures with silanized silica fillers. Conversely, the DC increased with increasing viscosity of resin mixtures with unsilanized fillers. No relationship was found between the DC and the filler surface treatment. Furthermore, the addition of untreated nanofillers did not affect the long-term mechanical properties of resin mixtures (Musanje & Ferracane 2004).

Turssi et al. investigated the effect of filler size and shape on the DC and wear of BisGMA/UDMA/TEGDMA mixtures. Spherical silica and irregular barium-aluminium-boron-silicate glass fillers were used in mono, bi or tri-modal formulations and the total amount of fillers was always 56.7%. FTIR measurements were done 24 h after storage in deionised water at 37°C. Though wear could be reduced by adding larger filler particles, irrespective of their shape, this may compromise the DC. It was suggested that hybrid

combinations of larger and smaller particles, irrespective of the shape, could maintain high wear resistance and DC values (Turssi 2005).

Gauthier et al. investigated the effect of viscosity, filler content and temperature on DC and oxygen inhibition in unfilled and filled BisGMA/TEGDMA mixtures using confocal micro-Raman spectroscopy. The unfilled mixtures contained various amounts of BisGMA whereas the filled ones contained various amounts of silica fillers in a fixed BisGMA/TEGDMA ratio. The micro-Raman measurement was done within the oxygen inhibited layer. A higher DC was found within the top 15 μm of the oxygen inhibition layer in more viscous samples. However, the correlation between viscosity and DC was not confirmed in the bulk polymer. A filler content exceeding 30 wt% resulted in increased DC within the top 15 μm and the reduced thickness of the oxygen inhibited layer but also decreased DC in the bulk polymer. Oxygen inhibition was eliminated when samples were cured at temperature above 110°C (Gauthier 2005b).

Atai & Watts developed a new kinetic model for studying the shrinkage-strain behaviour in RBCs but also evaluated the effect of filler content on the DC of an experimental BisGMA/TEGDMA mixture. Silanized barium-aluminium-silicate glass fillers were added in 31-57 vol% and the FTIR spectra were taken immediately after light curing. No significant differences were observed in the DC and polymerisation rates of different RBC mixtures and it was concluded that monomer conversion was not affected by the filler fraction (Atai & Watts 2006).

Palin et al. studied monomer conversion and flexural strength of an experimental oxirane-based RBC compared to hybrid and micro-hybrid commercial RBCs (Z100 and Filtek Z250). The oxirane-based RBC showed lower DC values and lower flexural strength than the control RBCs (Palin 2003).

In a subsequent study Palin et al. studied the DC, cuspal deflection and microleakage of an experimental silorane-based, an oxirane-based RBC and two commercial RBCs. The

lower DC and an inadequate marginal seal at the tooth-restoration interface were found for the oxirane-based RBC compared to other materials. Lower DC values but comparable or better marginal seal were found for the silorane-based RBC compared to the control RBCs (Palin 2005).

Lopez-Suevos & Dickens evaluated the effect of acidic monomers and storage conditions on the DC and mechanical properties of an experimental BisGMA/TEGDMA-based RBC. The newly developed monomers PMDM, BPDM, ODPDM and IPDM contain one or more aromatic groups, two or three carboxylic acid groups and polymerizable C=C double bonds. FTIR spectra were taken 15 min after light curing, 24 h after dry storage at 37°C or 24 h after storage in distilled water at 37°C. Increased DC values were found after 24 h storage compared to those obtained 15 min after polymerisation, confirming the 'dark' cure phenomenon. BPDM and IPDM resulted in lower DC than ODPDM and the control RBC irrespective of the storage conditions. The results for wet conditions were associated with a higher hydrogen-bonding potential of BPDM and IPDM which may have increased water absorption and subsequently impaired post-polymerisation. The authors also reported a positive correlation between the DC and mechanical properties of the experimental RBCs (Lopez-Suevos & Dickens 2008).

Schroeder & Vallo studied the effect of amine co-initiators on monomer conversion in an experimental BisGMA/TEGDMA-based RBC (Schroeder & Vallo 2007) as well as the effect of N,N-dimethylaminobenzyl alcohol (DMOH) as a novel amine co-initiator with CQ and PPD (Schroeder 2008). In the former study, either low (0.5 wt%) or high concentration (1.5 wt%) of the initiator system containing CQ and DMAEMA, EDMAB, DMPOH or TMA was added to the experimental RBC and cured using an LED LCU for 2 s, 10 s, 20 s or 40 s. FTIR spectra were taken immediately after polymerisation. The highest DC was found for CQ/EDMAB and lowest for the CQ/DMAEMA system. RBCs with high initiator concentrations showed higher DC than those with low initiator concentrations irrespective of the type of co-initiators. No

differences were observed in DC after light curing for 10 s, 20 s or 40 s (Schroeder & Vallo 2007).

In the other study, the efficiency of DMOH co-initiator in various CQ and PPD formulations was compared to DMAEMA. Comparable reactivity of BHO/DMOH and BHO/DMAEMA systems was confirmed by DSC. Higher DC was found for CQ/DMOH than CQ/DMAEMA systems using FTIR. The DC increased with increasing CQ concentrations. The PPD/DMOH system showed lower reactivity and lower DC than the CQ/DMOH system. The authors concluded that the CQ/DMOH may be a suitable initiator system for the polymerisation of light cured RBCs (Schroeder 2008).

Schneider et al. investigated the effect of the type and concentration of the initiator system on the DC, polymerisation rate, hardness and the "yellowing effect" of an experimental BisGMA/TEGDMA-based RBC. Low (0.5 wt%), intermediate (1 wt%) and high (1.5 wt%) concentrations of CQ/EDMAB, PPD/EDMAB and CQ/PPD/EDMAB was used as the initiator system. FTIR results indicated an increase in DC with increasing concentrations of initiators irrespective of their type. A positive correlation was found between the absorbed power density and DC, polymerisation rate and hardness. However, the reduced "yellowing effect" was found only with the low concentration of PPD, but the use of PPD alone resulted in lower hardness values (Schneider 2008).

2.1.2.1.5. Commercial adhesive systems

The first paper on commercial adhesive systems was published by Yamada et al. who studied the effect of mixing self-etching primers and bonding agents from different manufacturers on DC and bond strength. FTIR measurements and microtensile bond strength (μTBS) were performed 24 h after water storage at 37°C. The highest DC values were observed when self-etching primers and bonding agents from the same

manufacturer were used. When self-etching primers and bonding agents from different manufacturers were used consecutively, μTBS and DC decreased in some cases (Yamada 2004).

Kanehira et al. correlated the DC of seven all-in-one adhesive systems with their shear bond strength (SBS). SBS of human enamel samples restored with an adhesive and a hybrid RBC was measured. The DC was calculated from a different set of samples which were prepared by applying the adhesive and RBC to the ATR accessory crystal. FTIR spectra were taken immediately after polymerisation and 10 min, 1 h, 2 h and 24 h thereafter. The DC increased with time after polymerisation in all adhesive systems. This confirmed that the post-polymerisation phenomenon occurs in adhesive systems as well as in RBCs (Lohbauer 2009). The DC values varied significantly from 50% to 75% immediately after polymerisation and from 66% to 94% after 24 h. No definite conclusion regarding the differences in DC among adhesive systems could be made due to large variations in adhesive chemical composition. A linear relationship between DC and SBS was found for all adhesive systems (Kanehira 2006).

Kim et al. investigated the effect of curing time on the DC of two adhesive systems, the thickness of the oxygen inhibition layer (OIL) and the μTBS. Acetone-based three-step (All Bond 2, Bisco) and two-step (One Step, Bisco) etch-and-rinse adhesive systems were placed on a glass slide and cured using a conventional halogen LCU for 10 s, 20 s, 30 s or 60 s. The DC was calculated as a ratio between the absorbance peaks for C=C double bonds and the CH internal standard in cured and uncured samples. The DC values were in the range of 72-87% and increased with longer curing times. A negative correlation was observed between the DC and the thickness of the OIL. μTBS obtained after adhesive and RBC application to dentine discs decreased with longer curing times. The lowest bond strength values were observed in the group with no OIL i.e. where the adhesive systems were cured through a Mylar strip. The authors concluded that an OIL with an adequate thickness is necessary for satisfactory μTBS and that manufacturers' recommended times should be followed (Kim 2006).

Xu et al. correlated the DC and SBS of a two-step etch-and-rinse adhesive system (Single Bond, 3M ESPE) cured for 20 s, 40 s or 60 s from tip-to-surface distances of 0 mm, 2.3 mm, 4.6 mm and 6.9 mm. The adhesive system was placed on a glass slide, covered with a Mylar strip, cured and FTIR were taken immediately after curing. The DC values were between 65% and 85% and a negative correlation was observed between the curing distance and DC. SBS was measured on a different set of samples, which were prepared by applying the adhesive and a hybrid RBC to dentine discs. The same relationship was observed between the curing distance and SBS as it was observed for the curing distance and DC. It was concluded that a decrease in radiant exposure, due to the increasing distance, could be compensated by longer curing times. Curing times of 40-60 s were proposed for curing adhesives in deep and proximal cavities (Xu 2006).

Arrais et al. studied the effect of LCU types on the DC of a two-step etch-and-rinse (Single Bond, 3M ESPE) and a two-step self-etch (Clearfil SE Bond, Kuraray) adhesive systems. A halogen at 600 mW/cm^2 and an LED LCU at 400 mW/cm^2 were used for 10 s. FTIR spectra were taken immediately after light curing of the adhesive applied to potassium bromide pellet with no Mylar strip and after a week of storage in distilled water. The halogen LCU produced higher DC values in both adhesive systems, immediately after curing and after one week of storage. The initial DC values were around 27-35% and after storage increased to 50-56%. Though the self-etch adhesive showed initially lower DC, the DC of both systems was comparable after storage (Arrais 2007).

D'Alpino et al. also studied the effect of LCUs on polymerisation kinetics and the DC of a two-step etch-and-rinse adhesive system containing nanofiller particles (Adper Single Bond, 3M ESPE) using FTIR spectroscopy. The adhesive was applied to the ATR accessory crystal and cured for 10 s using a conventional halogen, an LED or a plasma arc LCU. The LED LCU produced the highest and the plasma arc the lowest DC values and polymerisation rates (D'Alpino 2007).

Ye et al. studied the effect of LCU types and irradiance on the polymerisation kinetics and the DC of a two-step etch-and-rinse (Single Bond, 3M ESPE) and two all-in-one self-etch adhesive systems (One-Up Bond F, Tokuyama; Adper Prompt, 3M ESPE) using ATR-FTIR with a real-time spectrum collector. The samples were placed on ATR accessory crystals and cured with either a halogen and or an LED LCU for 10 s, 20 s or 40 s. The real-time spectrum collector allowed continuous collection of IR spectra during polymerisation. The highest initial polymerisation rate and highest DC were found in the etch-and-rinse system with least solvent. Higher light irradiance accelerated curing kinetics and the resulting DC in all three systems. Adper Prompt showed the lowest DC values for all curing times, 11-20% after 10 s and 35-63% after 40 s (Ye 2007).

Sadek et al. correlated early and 24 h bond strength and DC of three-step etch-and-rinse (Adper Scotchbond MP, 3M ESPE), two-step etch-and-rinse (Adper Scotchbond 2, 3M ESPE), two-step self-etch (Clearfil SE Bond, Kuraray) and one-step self-etch adhesive systems (Adper Prompt L-Pop, 3M ESPE). The adhesive systems were placed in 0.5 mm thick iron moulds, covered with Mylar strips and cured with a halogen LCU. FT-Raman spectra were taken immediately after curing, then after 1 h and 24 h dark storage in air at 37°C. μTBS was measured on a different set of samples, prepared by applying the adhesive and a micro-filled RBC to human dentine discs. No correlation was found between the DC and μTBS. The DC was in the following order: Clearfil SE Bond (81-87%) > Scotchbond Multipurpose (77-81%) > Scotchbond 2 (60-65%) > Adper Prompt L-Pop (37-42%). The authors concluded that very limited ‘dark’ cure occurred within 24 h in the studied adhesive systems (Sadek 2008).

Faria e Silva et al. studied the DC of a dual-cured resin cement (RelyX ARC, 3M ESPE) related to the fiber post translucency (Faria e Silva 2007). In another study, the DC of light-cured, dual-cured and chemically-cured adhesive systems ScotchBond Multipurpose and Prime&Bond NT (Dentsply De Trey) were compared (Faria-e-Silva

2008). In the former study, micro-Raman spectra were taken from the top, middle and apical areas in a simulated root canal after 24 h of storage. In the latter study, a real-time spectrum collector was used to obtain FTIR spectra from adhesives applied to ATR accessory crystals. Spectra were taken continuously up to 5 min after the start of polymerisation. The translucent fiber post produced higher DC values at all depths than the non-translucent one. The DC decreased with increasing depth in the root canal irrespective of the type of fiber posts (Faria e Silva 2007). In the second study, light-cured and dual-cured adhesive systems showed rapid polymerisation during the first 30 s. After 5 min, the DC was around 60% for Scotchbond Multipurpose and 50% for Prime&Bond NT. Chemically-cured Scotchbond Multipurpose showed very slow polymerisation reaction and the DC of around 40% after 5 min, whereas chemically-cured Prime&Bond NT showed no reaction for the entire observation period (Faria-e-Silva 2008).

Monomer conversion was also studied using FTIR in orthodontic adhesive resins (Eliades 2000, Bang 2004, Lim & Lee 2007) and orthodontic lingual retainer adhesives (Usumez 2005). Eliades et al. reported the highest DC values for a dual-cured adhesive, followed by a light-cured one whereas a chemically-cured adhesive showed the lowest DC (Eliades 2000). Bang et al. reported a positive correlation between the DC and polymerisation shrinkage in three orthodontic adhesives cured with a conventional halogen LCU but not with a plasma arc LCU. The conventional halogen LCU produced higher DC values in all adhesives than the plasma arc LCU (Bang 2004). Lim & Lee showed that the DC of orthodontic adhesives was affected by the reflectance of the background teeth and not the diffuse light transmittance of orthodontic brackets. The DC was affected by the types of adhesives, brackets, LCUs and curing protocols (Lim & Lee 2007). Usumez et al. showed that plasma arc, high power halogen and LED LCUs produce comparable or higher DC in orthodontic lingual retainer adhesives compared to a conventional halogen LCU. The DC of the lingual retainer adhesives was also affected by their chemical composition but the authors offered no conclusive statement as to what caused the differences in the two tested materials (Usumez 2005).

2.1.2.1.6. Experimental adhesive systems

Imazato et al. studied the effect of an antibacterial monomer, MDPB, on the antibacterial activity, DC and tensile bond strength of an experimental adhesive mixture (Imazato 1997, Imazato 2003b). MDPB was added in 2%, 4% or 10% concentrations to the primer of the two-step self-etch adhesive system (LB Bond, Kuraray) and the final concentrations after mixing of primer and bond were 1%, 2% or 5%. Spectra were taken immediately after curing of the primer-bond mixture placed on a potassium bromide disc of the FTIR spectrometer. Antibacterial activity against Streptococcus mutans was shown to be significantly higher in the system containing MDPB than in the control system without MDPB. The DC values were 66-69% (Imazato 1997) and 61-65% (Imazato 2003b) and no significant differences were observed between the groups with various amounts of MDPB and the controls. Bond strength values were comparable between experimental resin mixtures and controls in both studies. The authors suggested that MDPB could increase the antibacterial potential of dentine primers without an adverse effect on DC and bond strength (Imazato 1997, Imazato 2003b).

Bae et al. studied the effect of BisGMA on the DC and mechanical properties of an experimental adhesive system. A series of adhesive mixtures were prepared containing 20/80 to 80/20 wt% of BisGMA and TEGDMA, placed on a potassium bromide disc, covered with a Mylar strip and cured for 20 s. Scotchbond Multipurpose was used as a control. FTIR spectra were taken immediately after curing and after 48 h of dark storage in air at an unstated temperature. The highest DC was found in the mixtures containing 30-50 wt% of BisGMA and was comparable to the commercial adhesive. The DC of all mixtures increased after storage. The authors suggested that high DC associated with better mechanical properties was due to the high molecular weight and cross-linking potential of BisGMA. However, extreme amounts of BisGMA may restrict monomer reactivity due to high viscosity resulting in lower DC and inferior mechanical properties (Bae 2005).

Dickens & Cho investigated the DC, mechanical properties and residual acetone content of experimental adhesive systems containing various amounts of PMGDM and HEMA. The adhesive was placed in three increments in 1 mm deep moulds and in one increment in 0.52 mm deep moulds held between two glass slides and cured through the top slide. FTIR spectra were taken immediately after light curing and after 48 h of dark storage. No differences in the DC were observed in bulk adhesives with different initial acetone content. Significantly higher DC was found for 60 s curing time and 48 h of dark storage. The DC decreased significantly with increasing initial acetone content in thin films. Computer simulation showed that residual acetone content depended on sample thickness. In thin films, the adhesive with the highest initial acetone concentration gave the least residual acetone content after drying, whereas the opposite was observed for bulk adhesives. The authors concluded that solvent removal from adhesive systems is a diffusion-controlled process dependent on solvent nature and amount as well as the thickness of the adhesive layer (Dickens & Cho 2005).

Kim et al. investigated the effect of hydrophilic nanofillers on the DC and mechanical properties of ethanol-based experimental adhesive mixtures containing BisGMA, HEMA and 4-META. The nanofillers were added up to 3 wt% and FTIR spectra were taken immediately after curing on potassium bromide discs. Though DC values were comparable for all groups irrespective of the presence of nanofillers, mechanical properties showed inconsistent values so it was concluded that hydrophilic nanofillers did not improve the adhesive formulation (Kim 2005).

Ogliari et al. studied the effect of a new co-monomer ETMA on the DC and bond strength (Ogliari 2006) as well as the effect of an onium salt as a co-initiator on polymerisation kinetics of adhesive resins (Ogliari 2007). In the former study, 0.1 wt%, 1 wt% and 10 wt% of ETMA was added to a BisGMA/HEMA adhesive system (Scotchbond Multipurpose, 3M ESPE). FTIR measurement was done after 24 h of dark, dry storage. μTBS was evaluated on a different set of samples, prepared by applying the adhesive and a micro-hybrid RBC to human dentine discs. ETMA resulted in

comparable DC but significantly higher μTBS than the control (Ogliari 2006). In the latter study, real-time FTIR spectra were taken during curing of a series of experimental adhesives containing CQ as the initiator and various amounts of EDAB and an onium salt (DPIHFP) as the co-initiators. The effect of co-initiators increased the reactivity of the initiator system. Comparable DC values were obtained with the two co-initiators irrespective of their concentration. The fastest rate of polymerisation was observed in the system containing both co-initiators confirming the hypothesis that an onium salt improves the polymerisation kinetics in an experimental dental adhesive resin (Ogliari 2007).

The effect of water and initiator systems on the polymerisation kinetics was studied in HEMA-based (Wang 2006c) and BisGMA/HEMA-based experimental adhesive systems (Guo 2008b). In the former study, co-initiators DHEPT, DMAEMA, NPG or DPIC were added to water-based HEMA/CQ mixtures. The adhesive was placed on a glass slide, covered with a Mylar strip and cured for 40 s using a halogen LCU and micro-Raman spectra were taken immediately after curing. The differences in polymerisation and reactivity of HEMA were observed for different co-initiators. Unlike DHEPT, NPG and DMAEMA were compatible with HEMA. DPIC had an accelerating effect on the polymerisation rate. Though CQ/DHEPT is used commonly in adhesive systems, this combination did not initiate HEMA polymerisation. Water had an adverse effect on polymerisation (Wang 2006c). In the latter study, DMAEMA, EDMAB or DPIHFP were added as co-initiators in water-based BisGMA/HEMA/CQ mixtures. Real-time FTIR measurements were used to monitor polymerisation. The results were in agreement with the study of Ogliari et al. (2007) and confirmed that the onium salt significantly improves polymerisation kinetics and DC. Guo et al. confirmed that water significantly reduces polymerisation but suggested that this may be compensated by the addition of onium salts (Guo 2008b).

2.1.2.2. Hardness

Hardness studies reviewed in this section refer to hardness as a function of the depth of cure of RBCs and should not be confused with studies on hardness as a mechanical property. The first traced paper on the use of hardness as a function of the depth of cure dates back to the time when the UV LCUs were used for light curing of RBCs and adhesive systems (Cook 1980).

Knoop (KHN) is the most commonly used hardness test (DeWald & Ferracane 1987, Eliades 1987, Baharav 1988, Rueggeberg 1988, Bouschlicher 2004, Santos 2007), but Vickers (Rode 2007), Brinell (Davidson-Kaban 1997) and Barcol (Fowler 1994) have also been employed. Hardness testing was used as the sole method to determine the depth of cure by Fowler et al. who found that clinicians failed to detect slight changes in top and bottom hardness of light cured RBCs (Fowler 1994).

In earlier studies, hardness was correlated with other methods of determining the depth of cure, such as optical (DeWald & Ferracane 1987, Baharav 1988) and scrapping (Newman 1983, DeWald & Ferracane 1987) but also FTIR spectroscopy (DeWald & Ferracane 1987, Eliades 1987, Rueggeberg 1988). These studies have suggested that hardness is more accurate in determining the depth of cure than the optical or scrapping methods and that hardness gives results in accordance with FTIR findings. Though Eliades et al. (1987) did not perform correlation analysis, they reported the same pattern of decreasing KHN and remaining double bonds with increasing depth.

Hardness is usually measured on the top and/or bottom surfaces of the sample. The ratio of hardness change is calculated when both top and bottom measurements are performed. Alternatively, hardness is measured longitudinally after sample sectioning along the irradiation axis. The results of the latter approach give a more precise insight into the hardness changes within the sample and a point of abrupt decrease may be distinguished (Rueggeberg 1988, Santos 2007).

Rueggeberg & Craig (1988) tested KHN, water sorption and elution of RBCs as predictors of monomer conversion and correlated these methods with FTIR. They concluded that KHN was the best conversion predictor, elution the next best whereas water sorption was the worst.

In more recent studies, hardness has been correlated with Raman or IR spectroscopy in order to estimate more accurately the depth of cure and the DC in RBCs (Bouschlicher 2004, Rode 2007, Santos 2007). All three studies have reported decreasing hardness and DC values with increasing depth. Furthermore, they all established a direct linear relationship between hardness and DC though different hardness (KHN or Vickers) and spectroscopic methods (micro-Raman, FT-Raman or FTIR) were used.

Bouschlicher et al. (2004) reported that as a measure of conversion, bottom-top ratio of KHN was approximately 2.5 times more sensitive than the bottom-top DC ratio. They stated that KHN alone cannot indicate the differences in monomer conversion in different RBCs due to variables, such as filler content. However, they concluded that the relationship between the bottom-top ratios of KHN and DC is independent of the filler content.

Santos et al. (2004) reported that the depth of cure was greater after light curing RBC samples with a QTH compared to an LED LCU. They identified a relatively uniform and slow decrease in hardness and DC with a sudden drop for both characteristics at 4 mm for the QTH and 3 mm for the LED LCU.

Rode et al. (2007) studied the DC and Vickers microhardness in an RBC cured with an LED, an argon laser or a conventional halogen LCU at various distances (0, 3, 6 and 9 mm). Both DC and microhardness decreased for all LCUs with increasing RBC thickness and curing distances. The LCUs produced comparable DC and microhardness values in samples 1 mm thick and irradiated from the maximum distance of 3 mm.

2.1.2.2.1. ISO 4049:2000

The International Organization for Standardization (ISO) has proposed a standard ISO 4049:2000 for measuring the "depth of cure" of polymer-based filling materials. Briefly, stainless steel moulds, 6 mm high and 4 mm in diameter, are placed on a glass slide covered with a Mylar strip, filled with the RBC covered with another Mylar strip, pressed to remove excess material and light cured with the light tip in contact with the top Mylar strip. Immediately after irradiation, the RBC sample is removed from the mould and the soft, uncured material at the bottom is scrapped away manually with a plastic spatula. The length of the cured portion is then measured with a micrometer to the nearest of 0.01 mm. The depth of cure is calculated as 50% of this length. The minimum required depth of cure for RBCs is 1.5 mm when the material is light cured according to manufacturer's recommended time at a minimum light intensity of 300 mW/cm^2. A pass/fail criterion is used to determine if the material meets the standard.

This standard has been widely accepted and used by the manufacturers as well as material scientists. The importance of this standard is its universal use which allows material comparison. Moreover, its simplicity and minimal required instrumentation enable the use of this method in dental practices to periodically verify the depth of cure of RBCs as well as the efficiency of LCUs.

Other researchers have used less conservative approach and identified the depth of cure as the total of the remaining length (Cook 1980, DeWald & Ferracane 1987, Baharav 1988, Dunne 1996) or 55% of the remaining length after scrapping away the uncured material (Hansen & Asmussen 1993). However, DeWald & Ferracane (1987) concluded that optical and scrapping tests, when the total remaining length was used, overestimated the depth of cure in comparison to more sensitive hardness and spectroscopic measurements.

2.1.2.3. Other methods

Other methods that have been used to determine the DC in RBCs and adhesive systems include polymerisation contraction/shrinkage (Venhoven 1993, Rueggeberg & Tamareselvy 1995), electron spin resonance (ESR) (Hotta 1998), infrared photoacoustic spectroscopy (PAS-IR) (Calheiros 2004), differential scanning calorimetry (DSC) (Cadenaro 2005, Emami & Soderholm 2005, Tanimoto 2005, Cadenaro 2006, Cadenaro 2008) and differential thermal analysis (DTA) (Imazato 2001).

Polymerisation contraction, as a method to determine DC, is based on the fact that the number of converted methacrylate groups is the main factor determining contraction (Loshaek & Fox 1953). It measures the vertical displacement of an aluminium disc due to the polymerisation contraction of the resin sample in a linometer device. The linear displacement is then converted to volumetric contraction based on the assumption that the contractions are isotropical. Subsequently, the "conversion of methacrylates" is calculated using the molar volume of complete conversion and the molar volume of the sample. This method was used to study the effect of diluting monomers (TEGDMA, MMA and HPMA) on the polymerisation contraction and monomer conversion of BisGMA-based resin mixtures. The results showed that the conversion of methacrylates increased with the increasing amount of diluents, irrespective of their type (Venhoven 1993).

In one study, the "extent of cure" of dental resins was measured by polymerisation shrinkage and compared to that obtained by FTIR spectroscopy (Rueggeberg & Tamareselvy 1995). MMA/TEGDMA mixtures with increasing amounts of TEGDMA and a commercial adhesive system were prepared as either thin films or 1 mm thick bar-shaped specimens. The polymerisation shrinkage was determined based on the differences in volumes of cured and uncured samples. The molar volume contraction was calculated based on the number of moles of C=C double bonds in the calibration curve. The subsequent extent of cure was calculated as a ratio of the observed shrinkage

and a total shrinkage in the case of complete conversion. The results showed no significant differences between the conversion values obtained by shrinkage and FTIR methods. The authors suggested that if manufacturers disclosed the molar C=C content and resin density of their products, researchers would only need to determine weight differences between dry and water-immersed cured material in order to calculate the DC. Additionally, the results of this study showed no correlation between the amount of TEGDMA and DC in thin samples whereas the amount of TEGDMA in excess of 5 mol% resulted in significant decrease in DC in bar-shaped samples.

ESR is a technique for chemical analysis of substances, such as free radicals, with one or more unpaired electrons which is associated with molecular paramagnetism. Electron transitions can be induced between spin states by applying a magnetic field and then supplying electromagnetic energy, usually in the microwave range of frequencies. The resulting absorption spectra are based on the principle that resonant frequencies for a particular substance are directly proportional to the strength of the applied magnetic field (Wertz 1972). ESR was used to indirectly measure monomer conversion by measuring the amount of free radicals after irradiation of adhesive mixtures with increasing amounts of monomers. The amount of propagating radicals gradually increased with irradiation time but decreased with the addition of primers (Hotta 1998).

In PAS-IR, part of the IR incident light is absorbed by the sample and converted to thermal energy which diffuses towards the sample surface. Sound pressure waves are generated at the surface and captured by a high-sensitivity microphone. The detected signal is converted into a conventional IR spectrum (McClelland 1998). This method was used by Calheiros et al. to determine the DC of two hybrid and two micro-filled RBCs. The DC values were between 15% and 45% for both RBCs irrespective of the applied light energy density. The authors attributed the lower DC values in this study compared to other studies to lower sensitivity of PAS-IR compared to other spectroscopic methods, particularly FTIR and Raman (Calheiros 2004).

DSC is a calorimetric technique based on the assumption that heat generated during resin polymerisation is proportional to the percentage or concentration of reacted monomers (Wunderlich 2005). After light curing of resin-based materials, the temperature is measured using thermocouples attached to a differential scanning calorimeter. The heat of polymerisation is calculated from the area under the peak of the differential temperature curve and the extent of polymerisation (Ep) is calculated as the ratio of the obtained heat related to the reference values for 100% conversion. This is the theoretical amount of heat evolved during complete polymerisation of the material and is calculated using the molar heat of polymerisation of lauryl methacrylate (Imazato 2001, Tanimoto 2005). Using this method, it was shown that the Ep increases with increasing amounts of TEGDMA in UDMA/TEGDMA mixtures. The Ep of experimental mixtures decreased with increasing filler content between 0-60% but then significantly increased at 70% of the filler content.

DSC was also used to study adhesive DC and permeability (Cadenaro 2005), the effect of dentine bleaching on DC in commercial adhesive systems (Cadenaro 2006) as well as the effect of hydrophilicity and solvent content on the Ep of experimental adhesive systems (Cadenaro 2008). Comparing a three-step and two-step etch-and-rinse and two-step and one-step self-etch commercial adhesive systems, lower DC and higher permeability values were found in two-step etch-and-rinse and one-step self-etch adhesives. Curing times, beyond manufacturers' recommended times, improved polymerisation and reduced permeability of these adhesive systems (Cadenaro 2005). Hydrogen peroxide, as a bleaching agent, had an adverse effect on the DC whilst storage in 100% humidity at 37°C resulted in increased DC (Cadenaro 2006). Low DC values were found in experimental adhesive systems with the solvent in excess of 50 wt%. Although the authors claimed that resin hydrophilicity had an influence on the DC (Cadenaro 2008), this remains unclear since the adhesive systems contained different monomer compositions rather than different percentages of the same hydrophobic/hydrophilic components.

Breschi et al. correlated the permeability and polymerisation kinetics of adhesives after exposure to different LED LCUs. DSC measurements showed that the rate of polymerisation increased with longer curing times in all adhesives. An inverse correlation was reported between the rate of polymerisation and permeability of adhesives (Breschi 2007).

DSC was also used to study the effect of curing modes and initiators on the DC of BisGMA (50wt%)/TEGDMA (50wt%) mixtures. A high power halogen LCU operating at standard and soft-start modes and an LED LCU at standard mode were used. The initiators, CQ or PPD, were combined with one of three co-initiators, DABE, CEMA or DMAEMA. Standard modes of both halogen and LED LCUs resulted in higher DC values than soft-start after 10 s of light curing. Soft-start resulted in comparable DC values as the standard halogen and higher than the LED LCU after 40 s of light curing. CQ-based initiator systems produced higher DC values than PPD-based systems after 10 s of light curing irrespective of the LCU and curing mode. However, all systems showed comparable DC values after 40 s of light curing (Emami & Soderholm 2005).

DTA was used to calculate the DC of experimental RBCs containing various amounts of TEGDMA and fillers and compare these values with those obtained by FTIR spectroscopy. Essentially, this method is the same as previously reviewed DSC. DTA resulted in slightly greater DC values (3-10%) compared to FTIR values. The authors attributed these differences to the method of DC calculation as well as to the theoretical assumption that the heat of conversion of C=C double bonds is the same for all methacrylate monomers. Furthermore, they suggested that possible reflection of the incident light at the bottom of the thermal chamber could result in an augmenting effect (Imazato 2001).

2.2. INTERACTION OF MATERIALS AND TISSUES

2.2.1. The mechanisms of adhesion

Micromechanical adhesion was proposed by Buonocore who suggested that acid pre-treatment significantly increases the surface area in enamel and dentine and exposes dentine collagen network facilitating the materials with dental tissues (Buonocore 1955, 1956). This micromechanical interlocking was further explained by Nakabayashi who introduced the term "hybridisation" (Nakabayashi 1982, Nakabayashi 1985). Hybridisation is generally referred to as the formation of the hybrid layer between adhesive and dentine, but similar interdiffusion occurs in enamel. Acid etching produces rough and porous surface of enamel due to dissolving more inter-prismatic than prismatic crystallites. The penetration of adhesive resins into the demineralised zone of enamel and subsequent polymerisation create a strong interlocking or resin-enamel hybrid layer (Nakabayashi 1998b). Not only does this promote retention but also increases enamel resistance to acids due to the entanglement of hydroxyapatite crystals with polymerised resin (Gwinnett & Buonocore 1965, Hotta 1992). During dentine treatment, phosphoric acid or acidic monomers in self-etch adhesives, open dentinal tubules and dissolve hydroxyapatite in the intertubular dentine exposing collagen fibres. After demineralisation, collagen fibres are supported by water in interfibrillar spaces 15-20 μm wide (Van Meerbeek 1996). Subsequently, resin monomers diffuse into dentinal tubules and through permeable tubular walls into the intertubular dentine, infiltrating the interfibrillar spaces, to create the dentine-adhesive hybrid layer. The penetration and polymerisation of adhesive monomers in dentinal tubules result in the formation of resin tags which were considered contributory to the overall retention (Nakabayashi 1998a).

Glass-polyalkenoate cements have been described as having the unique properties of chemical adhesion to hard dental tissues (Yoshida 2000). These authors suggested a mechanism in which carboxylic groups from the polyalkenoic acid replace PO_4^{3-} ions

from hydroxyapatite and form ionic bonds with Ca^{2+} ions. Furthermore, it was shown that carboxylic acids such as maleic, citric, lactic, polyacrylic and oxalic, may also form ionic bonds with Ca^{2+} from hydroxyapatite, though their affinity to Ca^{2+} may differ significantly (Yoshida 2001). In the proposed "Adhesion/Decalcification (AD) concept", acidic carboxyl groups form ionic bonds with Ca^{2+} whilst PO_4^{3-} and OH^- are extracted by H_3O^+ from the hydroxyapatite surface. Afterwards, the acids remain attached to hydroxyapatite or de-bond having a significant decalcification potential. Whether the acid adheres to or decalcifies hydroxyapatite depends on the dissolution rate of the Ca^{2+} salts and not the acidity of the solution. The stability of acid-hydroxyapatite bond is inversely related to the solubility of the Ca^{2+} salts (Yoshida 2001). In another study, it was shown that the AD concept may be applied to organic and inorganic acids as well as human hard tissues irrespective of their hydroxyapatite crystallinity (Yoshioka 2002).

Hydrophilic monomers in both etch-and-rinse and self-etch adhesive systems may interact with the exposed collagen fibres to form covalent or metallic bonds (Duke & Lindemuth 1990, Nakabayashi 1998b) as well as secondary intermolecular bonds such as van der Waals, London dispersion forces or hydrogen intermolecular bonds (Eick 1997, Nishiyama 1998). Highly charged glycosaminoglycans and noncollagenous proteins such as phosphoryn and dentine sialoprotein, are distributed along the collagen fibres with the potential for hydrogen bonding (Cribb 1995). Primary chemical bonding, ionic, covalent or metallic, is considered chemical adhesion whereas secondary intermolecular bonds are considered physical adhesion (Eick 1997).

Physical adhesion, based on hydrogen bonding, may occur between the amide or carboxylic acid groups of adhesive primers and amino acids of the collagen peptides (Nishiyama 1998, Nishiyama 2001). It was suggested that this type of interaction was probably due to the triple helix structure of the dentinal collagen macromolecule (Nishiyama 2001). The triple helix in the collagen structure is typically made up of three helical α chains of amino acids whose surface characteristics are favourable for binding ligands (Brodsky 1995). Most recent attempts to explain physical adhesion to dentine

include computer simulation and modelling of self-etch primer 'docking' to amino acid residues in type 1 collagen triple helix (Vaidyanathan 2007). This approach provides valuable information on hydrogen, van der Waals and electrostatic bonding between adhesive ligands and collagen (Vaidyanathan & Vaidyanathan 2009). However, such computer simulations must be viewed in light of their limitations, since many clinical variables cannot be taken into account.

2.2.2. Dentine-adhesive interface

2.2.2.1. Morphology

The hybrid layer (HL) consists of two different materials and is considered a three-dimensional interphase at the dentine – adhesive interface (Nakabayashi 1998b). Because chemical alterations occur in dentine with subsequent diffusion of adhesive resins, the resulting HL has unique physical and chemical properties. Numerous studies of surface characterization employed electron microscopy such as SEM and TEM (Nakabayashi 1982, Hotta 1992, Van Meerbeek 1993a, Shimada 1995, Carvalho 1996a, Carvalho 1996b, Ferrari 1996, Raspanti 1996, Van Meerbeek 1996, Cagidiaco 1997, Ferrari 1997, Kwong 2000, Santini 2001, Agee 2003, Breschi 2003, Wang & Spencer 2004b, Santini & Miletic 2008). These morphological investigations are conducted to measure the thickness of the HL and study the appearance, length and continuity of resin tags, the quality of entanglement within the interdiffusion zone, the extent of resin penetration and the quality of collagen network.

It has been shown that the thickness of the HL varies between 1 μm and 19 μm (Nakabayashi 1982, Van Meerbeek 1996, Yoshiyama 2002, Wang & Spencer 2004b, Wang 2006a). Resin infiltration within the HL varies due to many factors, which may be classified as dentine-related (Cagidiaco 1997, Kwong 2000, Yoshiyama 2000, Yoshiyama 2002, Wang 2006a), adhesive-related (Shimada 1995, Ferrari 1996, Spencer

2000, Abdalla & Garcia-Godoy 2002, Yoshiyama 2002, Breschi 2003) and technique-related (Ferrari 1996, Ferrari 1997, Santini 2001, Hashimoto 2002, Wang & Spencer 2004a).

Cagidiaco et al. have reported reduced HL thickness in root dentine below the cementum-enamel junction with less predictable morphology compared to more occlusal regions (Cagidiaco 1997). Yoshiyama et al. have suggested that the increase in HL thickness in carious-affected dentine is due to caries-induced dentine demineralisation. However, increased porosity and structural irregularities within the formed HL were also reported (Yoshiyama 2000, Yoshiyama 2002). A hypermineralised layer, which reduced resin penetration into the HL, was found on the surface of acid-etched sclerotic dentine. This was associated with the inability of acidic monomers as well as phosphoric acid to effectively dissolve sclerotic plugs that occluded the dentinal tubules. Furthermore, sporadic absence of the HL in sclerotic dentine was observed (Kwong 2000). Wang et al. have shown that HL thickness is greater in deep dentine at the CEJ than superficial dentine at ADJ. Apart from the HL thickness and different orientation of resin tags, no other differences were reported regarding the quality of the HL at the CEJ and ADJ (Wang 2006a).

Shimada et al. found that the HL thickness depended on the conditioner or primer used in the adhesive system. The thicker HL was associated with longer conditioning and higher conditioner acidity (Shimada 1995). Similar finding of deeper resin penetration due to better etching or conditioning was reported by other authors (Abdalla & Garcia-Godoy 2002). Ferrari et al. found that self-etch adhesives produced thinner HL than etch-and-rinse adhesive systems with morphological differences in resin tags. Etch-and-rinse adhesives formed cone shaped resin tags with substantial lateral branching whereas self-etch adhesives formed narrow tags with less lateral branching (Ferrari 1996, Santini 2001). Yoshiyama et al. have shown that etch-and-rinse systems produced thicker HL than self-etch ones irrespective of the quality of dentine substrate (Yoshiyama 2002). The depth of dentine demineralisation and adhesive penetration varied with different

one-step self-etch adhesives, but were always less than those obtained with etch-and-rinse systems (Sato & Miyazaki 2005). Micro-Raman spectroscopy has revealed adhesive phase separation within the HL indicating that the differences in adhesive penetration may be due to chemical composition (Spencer 2000).

Ferrari et al. studied the effect of conditioning time on the HL thickness of a self-etching adhesive. A thicker HL was found after conditioning for 60 s compared to 30 s. Rough and long resin tags with numerous lateral branches were associated with longer conditioning. Shorter conditioning resulted in smooth resin tags with only sporadic and thin lateral branches (Ferrari 1997). Hashimoto et al. reported significantly deeper resin penetration of acetone-based adhesives for "wet" than "dry" bonding technique (Hashimoto 2002). In another study, deeper resin infiltration was associated with agitated etching due to the deeper zone of demineralisation (Wang & Spencer 2004a).

A detailed analysis of the HL ultrastructure of a three-step etch-and-rinse adhesive system was carried out by Van Meerbeek et al. using comparative SEM and TEM (Van Meerbeek 1993a). A zone of filler particles was identified as the demarcating zone between the adhesive layer and the HL. Within the HL, three layers were distinguished: (1) the top layer or 'resin-impregnation base' appeared as a dark, amorphous zone with no ultrastructural arrangement at the decalcified dentine surface. This layer contained resin-impregnated, denatured collagen arising from dentine or smear layer; (2) the elastic resin-impregnated collagen layer contained closely packed collagen fibres parallel to the dentine surface and with small interfibrillar spaces. Within this layer, interfibrillar funnel-shaped, densified structures were observed as well as resin encapsulated hydroxyapatite crystals, which were associated with electron dense lines between collagen fibres; (3) the electron-dense base layer abruptly demarcated decalcified from unaltered dentine and contained hydroxyapatite crystals incompletely dissolved by the acid treatment. This layer of hydroxyapatite crystals was more resistant to EDTA pre-treatment for TEM and was associated with protective resin encapsulation. The authors suggested that the elastic resin-impregnated collagen layer could act as a

buffering mechanism to compensate for RBC polymerisation contraction (Van Meerbeek 1993a).

Using TEM, Milia & Santini studied the ultrastructure of the HL formed by one-bottle etch-and-rinse and self-etch systems. Irregularities in the HL and dense resin tags were observed for both adhesive systems (Milia & Santini 2003). The ultrastructural findings for the one-bottle etch-and-rinse system were in agreement with the previous study on etch-and-rinse systems with separate prime and bond steps (Van Meerbeek 1993a). For the self-etch system, densely compacted collagen fibres were observed within the adhesive resin with hydroxyapatite crystals occurring between collagen bundles toward the base of the HL (Milia & Santini 2003).

SEM and TEM offer a useful insight into the HL with spatial resolutions below 1 μm, but the limitations of these techniques should be mentioned as they may significantly affect the results (Van Meerbeek 2000). Both techniques require subtle specimen preparation to expose the HL and resin tags. Prior to SEM, samples are treated with hydrochloric acid, sodium hypochlorite or sodium hydroxide to expose resin tags. However, these treatments as well as high vacuum drying may introduce morphological artefacts in that part of the HL that is only partially infiltrated by adhesive resin (Carvalho 1996a, Carvalho 1996b, Raspanti 1996, Agee 2003). In TEM, the preparation of ultra thin sections may result in samples being distorted, ripped or torn by shear forces and tissue or material displaced resulting in micrographs which do not mirror the actual interdiffusion zone characteristics (Nakabayashi 1998a).

2.2.2.2. Chemical aspects

Chemical degradation of the tooth tissue-restoration bond may occur when this is exposed to oral fluids and bacterial by-products. One aspect of this is the uptake of fluids and its subsequent effect on the resin matrix and another is elution of unreacted

monomers and other products from the restoration (Santerre 2001). It has been shown that water uptake by RBCs occurs as soon as the material is exposed to water and the amount of water uptake is material dependent and increases with time (Ferracane & Condon 1990, Ortengren 2001).

Water affects the tooth tissue-restoration bond through oxidation, hydrolysis and plasticization (Oysaed 1988, Ortengren 2001, De Munck 2005). The primary oxidation of unsaturated methacrylate groups may occur within the polymer network due to the presence of unreacted monomers and pendant C=C double bonds. Another possibility is the formation of oxygen-methyl methacrylate during polymerisation due to the presence of atmospheric oxygen. Both mechanisms of oxidation are enhanced in water and result in the formation and elution of formaldehyde (Oysaed 1988).

Hydrolysis is an inherent weakness of resin-based materials due to the presence of ester groups –COO that link the methacrylate group to the central part of the monomer molecule. Apart from ester, other condensation-type bonds may undergo hydrolysis by reaction with water (Santerre 2001). Oxidation and hydrolysis can break covalent bonds not only in the polymer matrix, but also between the resin and collagen fibres (Hashimoto 2000).

Plasticization occurs as a result of polymer chain swelling due to reduced frictional forces between polymer chains, water penetration into the matrix and expansion of the intermolecular spaces (Finer & Santerre 2004, De Munck 2005, Sideridou & Achilias 2005). Plasticization reduces saturation of water per unit volume and enhances water uptake, but also enables elution of any leachable products that may be trapped in the polymer network (Finer & Santerre 2004, Sideridou & Achilias 2005).

Enzymes originating from either bacterial activity or local tissue inflammatory cells may enhance the effect of water (Santerre 2001). It has been shown that salivary enzymes, such as cholesterol esterase, may affect RBC degradation due to the hydrolysis of ester

bonds within the polymer (Finer & Santerre 2004). Bacterial enzymes, such as collagenase or chondroitinase, have the potential to degrade collagen fibres (Ho 2005). However, the minimal level of such enzymes required to induce biodegradation in clinical conditions remains unclear (Santerre 2001).

2.2.2.2.1. Elution of monomers and by-products

Elution of unreacted monomers and by-products has been studied using high-performance liquid and gas chromatography and mass spectrometry. The majority of studies have been done on RBCs (Munksgaard 2000, Ortengren 2001, Michelsen 2003, Moon 2004, Michelsen 2008, Uzunova 2008) and resin mixtures (Kim & Chung 2005, Sideridou & Achilias 2005, Zhang & Xu 2008) with a few studies on fissure sealants (Moon 2000) and orthodontic adhesives (Eliades 1995, Eliades 2007). HPLC was used to identify components from adhesive systems (Silikas & Watts 2000), compare hydrolytic stability of different monomers (Salz 2005b) and, most recently, quantify the amount of HEMA eluted from two different adhesive systems (Altintas & Usumez 2009).

Gerzina & Hume used reversed phase HPLC to measure the amount of monomers eluted into the pulp chamber from RBC restorations placed with dentine bonding agents. Three simulated pulpal pressures were used. Distilled water was used as a solvent and 2 mm deep cavities were restored with Scotchbond Multipurpose and Z100. Intrapulpal pressure did not prevent an inward movement of both HEMA and TEGDMA and a higher diffusion coefficient was reported for HEMA (Gerzina & Hume 1995).

Munksgaard et al. reported 7 and 4 times higher monomer elution from a commercial RBC (Z100) and an experimental BisGMA/TEGDMA mixture, respectively, after curing with a plasma arc compared to a conventional halogen LCU. Resin mixture cured

under the same conditions as the commercial RBC showed 8 times higher monomer elution due to the absence of fillers (Munksgaard 2000).

Ortengren et al. compared elution from various resin-based materials stored in distilled water for 4 h to 180 days. TEGDMA eluted after 4 h with the maximum concentration after 7 days. BisGMA was found in detectable but not quantifiable amounts whereas UDMA and bisphenol-A were not detected (Ortengren 2001).

Michelsen et al. identified 32 substances eluted from light-cured RBCs (Z250, Tetric Ceram), a compomer (Dyract AP) and a GIC (Fuji II) after immersion in ethanol for 24 h and Ringer's solution for 7 days. BisGMA and UDMA were indirectly confirmed based on their by-products. Significantly higher elution was seen in ethanol than Ringer's solution. Certain substances were eluted from cured but not from uncured samples indicating that polymerisation may be responsible for such structural modifications (Michelsen 2003).

More recently, Michelsen et al. studied HEMA and TEGDMA elution from two RBCs (Z250 and Tetric EvoCeram) cured with a conventional LCU into human non-stimulated saliva after 24 h. HEMA was found for both RBCs and was stated to be a by-product of UDMA breakdown. TEGDMA was eluted from Z250 but not from Tetric EvoCeram, possibly because of the nanofillers present in the latter RBC (Michelsen 2008).

Moon et al. studied monomer elution from a commercial RBC (Z250) cured with plasma, an LED or a halogen LCU. For the same light energy density, plasma showed similar or lower leachability than halogen and LED LCUs. After 7 days, greater elution was observed for the pulse than two-step and one-step curing modes. With increased curing time and light energy density, no differences between LCUs were found (Moon 2004).

Kim & Chung found significantly lower monomer elution from a trimethacrylate-based resin mixture than a dimethacrylate-based mixture, though the DC values obtained by FTIR spectroscopy were similar. The differences in elution were associated with less residual monomers in trimethacrylate-based resin, its greater functionality, larger molecular size and lower solubility. It was confirmed that higher elution occurred into ethanol than water (Kim & Chung 2005).

Sideridou & Achilias studied the effect of monomers in BisGMA, TEGDMA, UDMA and BisEMA-based mixtures on elution in 75% ethanol at intervals ranging from 3 h to 7 days. The results showed that increased curing time reduced monomer elution (Sideridou & Achilias 2005).

Zhang & Xu studied the effect of solvents such as distilled water, artificial saliva and 75% ethanol on monomer elution from two experimental RBCs. The highest amount of eluted monomers was seen in ethanol, followed by distilled water and artificial saliva. In the latter two solvents, no detectable monomers were found after 7 days. More monomers eluted from materials where TEGDMA was partially substituted by UDMA. For both materials, greater elution of TEGDMA was found in water and saliva than ethanol, whereas BisGMA was predominant in ethanol, probably due to lower solubility in water and saliva (Zhang & Xu 2008).

Uzunova et al. found the eluted concentration of monomers in deionised water to be twice as high from Charisma as Solitaire RBC. TEGDMA showed the greatest elution, due to smaller and more mobile molecules and higher water solubility. In the same study, nine in vivo placed restorations were milled and immersed in ethanol for 24 h at room temperature after extraction. The chromatogram showed the presence of BisGMA, BisGA (bisphenol-A acrylate) and BisDMA (bisphenol-A dimethacrylate), which could act as potential irritants (Uzunova 2008).

Moon et al. studied the elution of leachable components from pit and fissure sealants into artificial saliva and 75% ethanol solution over 28 days. The majority of monomers, BisGMA, TEGDMA and UDMA and their by-products were eluted within the first few days. Greater elution was found in ethanol than artificial saliva for all components, possibly due to a slight matrix plasticization by artificial saliva, high solubility of BisGMA and UDMA in ethanol and almost none in water and the higher ability of ethanol compared to water, to penetrate the cross-linked resin matrix (Moon 2000).

Eliades et al. found that higher amounts of TEGDMA and BisGMA were eluted from chemically cured compared to light cured orthodontic adhesives. There was no difference in the effect of direct and indirect irradiation of light cured orthodontic adhesive on monomer elution (Eliades 1995). In a recent study, Eliades et al. reported that no traces of eluted Bisphenol-A at 0.1 ppm levels could be found for chemically and light-cured orthodontic adhesives after accelerated aging in absolute alcohol for periods ranging from 24 h to 5 weeks (Eliades 2007).

Silikas & Watts analysed the composition of dentine primers and bonding agents using reversed phase HPLC after primer and bond samples were dissolved in methanol. Dimethacrylates, BisGMA, UDMA and TEGDMA, and monomethacrylates, HEMA, HPMA and MMMA as well as an acidic monomer, 4-META, were eluted from the investigated dentine primers and bonding agents. A positive correlation between chromatographic retention time and partition coefficient was reported (Silikas & Watts 2000).

Salz et al. compared the hydrolytical stability of conventional dimethacrylates with a new bisacrylamide cross-linking monomer in acidic aqueous conditions. At pH 1.5, 90% of TEGDMA and GDMA were hydrolyzed after 16 weeks of storage at 42°C and about one third after storage at 23°C. The new bisacrylamide monomer was stable for the duration of the study at both temperatures (Salz 2005b).

Altintas & Usumez quantified in vitro elution of HEMA from Single Bond (3M ESPE) and Optibond Solo Plus (Kerr) which were used with dual-cured resin cements (RelyX ARC, 3M ESPE or Nexus 2; Kerr) for cementation of ceramic inlays. HPLC was used to measure the amount of HEMA in the 75% ethanol solution after 10 min, 1 h, 24 h, 3, 7, 14, and 21 days of storage. The amount of HEMA eluted from Optibond Solo Plus was significantly higher compared to Single Bond. The total amount of eluted monomers was the highest after 21 days.

2.2.2.3. Physical aspects

Polymerisation shrinkage of RBCs and functional stresses such as mastication and thermal expansion and contraction are major physical factors affecting the long-term durability of the tooth tissue-material interface and the subsequent longevity of the resin-based restorations in clinical conditions (Davidson & Feilzer 1997, Breschi 2008).

It is widely accepted that polymerisation shrinkage of RBCs results in stresses of circa 15 MPa (Eick 1997) due to the shift from intermolecular van der Waals to intramolecular covalent bonds between monomer units in the polymer. It has been shown that polymerisation shrinkage is proportional to the volume fraction of the resin matrix (de Gee 1993). The addition of fillers significantly reduces polymerisation shrinkage due to the lower unfilled resin content (Darvell 2002). It has been suggested that this shrinkage is dependent on the cavity configuration factor, the 'C' factor, which is defined as the ratio of the bonded to unbonded surfaces of a resin-based restoration. Restorations with a higher 'C' factor show lower capacity to allow stress-relieving flow (Davidson 1984, Feilzer 1987). A more recent study has shown that this effect may not be clinically significant as the loss of marginal seal and subsequent microleakage were observed in etch-and-rinse and self-etch adhesives irrespective of the 'C' factor (Santini 2004). One study suggested that placement techniques could minimise polymerisation shrinkage by minimizing the mass of in situ-cured RBC and altering the shrinkage

vectors (Lutz 1991). However, another study indicated that placement techniques may not reduce microleakage with either etch-and-rinse or self-etch adhesive systems (Santini 2001).

Functional and non-functional occlusal loading, as well as the differences in the coefficient of thermal expansion and contraction of RBCs and dental tissues, impose stresses at the tooth tissue-material interface (Versluis 1996, Breschi 2008). Fracture, loss of compliance or wear may result in restoration failure over time as a result of stress or strain-induced material fatigue (Baran 2001).

2.2.2.3.1. Bond strength

The literature contains a great number of studies using different bond strength tests to measure adhesive performance. A search of the Pubmed database using the keywords "dentine", "adhesive" and "bond strength" in February 2009 revealed more than 1500 scientific articles and 29 review papers. However, data from different studies are frequently incomparable since bond strength measurements are significantly affected by the testing conditions. Test geometry, loading modes and material properties may result in variations in nominal bond strengths and a standardised testing protocol is advocated (Van Noort 1989). Nevertheless, a meta-analysis conducted by Leloup et al. more than 10 years later, showed wide variations in bond strength data as well as the lack of a standardised approach by different researchers. This meta-analysis identified that dentine, material type and bonding area, storage conditions and testing mode were major factors affecting bond strength (Leloup 2001).

Absolute test values should not be interpreted as an inherent material property and only relative study outcomes, such as 'A is better than B' may be used as a basis for further study (Eick 1997, De Munck 2005). Though in vitro conditions, even in well-controlled studies, cannot take into account all clinical variables, bond strength tests are still

frequently used to screen adhesive systems. Currently, SBS and μTBS tests are most commonly used (Inoue 2001b, Uno 2001, Kwong 2002, Perdigao 2002, Yoshiyama 2002, De Munck 2003a, Sadek 2008).

Short-term adhesion studies have shown values for adhesive-dentine bond strength in excess of 30 MPa for contemporary etch-and-rinse and self-etch adhesive systems (Inoue 2001b). Three-step etch-and-rinse systems produced the highest bond strength values followed by two-step etch-and-rinse and self-etch systems, which were comparable, and the lowest values were observed for one-step self-etch systems. Significantly lower values for two-step etch-and-rinse and one-step self-etch systems compared to three-step etch-and-rinse and two-step self-etch systems, respectively, were confirmed in another study (De Munck 2003a). The predominant type of failure reported for one-step self-etch adhesives occurred between dentine and adhesive layer in contrast to mixed adhesive-cohesive failures in two- and three-step adhesive systems (De Munck 2003a). However, another study has shown comparable bond strength values between two-step and one-step self-etch systems and predominantly a mixed mode of failure (Sidhu 2007). In a recent study, two-step etch-and-rinse and self-etch systems had higher bond strength values than three-step etch-and-rinse and one-step self-etch systems (Sadek 2008).

A possible role of fillers, in increasing short-term bond strength, has not been confirmed and there are contrasting results for different adhesive formulations (Frankenberger 2001, Nunes 2001, Kim 2005). Comparable or higher bond strength values were observed in systems with functional monomers MDPB (Imazato 1997) or ETMA compared to controls (Ogliari 2006).

Significant differences in bond strength values were found for an adhesive system used with different surface treatments or restorative materials (Sunico 2002). Short-term bond strength was found to be higher for acetone-based adhesive systems when bonded to wet than dry dentine (Gwinnett & Kanca 1992, Kanca 1992b, Kanca 1992a, Kanca 1996,

Perdigao & Frankenberger 2001), but rewetting potential of the solvent may result in bond strengths similar to those on moist dentine (Perdigao & Frankenberger 2001, Rosales-Leal 2001). Furthermore, the orientation of dentinal tubules was suggested to be a significant factor for bond strength as higher μTBS was observed in coronal than apical dentine (Uno 2001). Bonding to sound dentine yields higher strength values than bonding to sclerotic (Kwong 2002) or carious dentine (Yoshiyama 2002). Significantly lower SBS values were found when adhesive was bonded to dentine immediately after bleaching compared to a 2-week delay (Bulucu & Ozsezer 2007).

The type of LCUs seems to be insignificant for short term SBS (Bulucu & Ozsezer 2007, Korkmaz & Attar 2007) or μTBS (Camilotti 2008). A linear correlation between short-term SBS and irradiation exposure during light curing was reported (Xu 2006) but another study showed that increased exposure may result in reduced μTBS, possibly due to the reduction in thickness of the oxygen inhibition layer (Kim 2006).

Long-term adhesion in bond strength studies is evaluated after introducing an aging factor. Different artificial aging techniques, such as chemical, thermal and mechanical, allow specific types of bond degradation to be studied.

Water storage is the most commonly used method for in vitro aging. The duration of water storage at 37ºC may vary from 3-4 weeks (Frankenberger 2003, Wang & Spencer 2005), several months (Shono 1999, Armstrong 2003, Giannini 2003, Nakajima 2003, Spencer 2006) to several years (Burrow 1996, Kato & Nakabayashi 1998, Fukushima 2001, Meiers & Young 2001, De Munck 2003b). In order to prevent bacterial growth, antimicrobial agents are usually added, such as sodium azide (Burrow 1996), chloramines (Armstrong 2003, De Munck 2003b) and antibiotics (Shono 1999). Artificial saliva or 75% ethanol/water solution are used to simulate more clinically relevant conditions (Lee 1994, Lee & Lin 1997, Eckert & Platt 2007, Garcia-Godoy 2007). Recently, a buffered solution containing bacterial enzyme collagenase was used as the storage medium (Toledano 2007).

It has been shown that indirect contact of adhesive systems with the storage medium does not necessarily affect bond strength unlike direct exposure which reduced bond strength values in two-step etch-and-rinse adhesives after 4 weeks (De Munck 2003b). Dentine priming seems to increase bond strength only in the short period since comparable bond strength values were obtained for primed and non-primed dentine after 3 years of storage (Burrow 1996). Significantly lower bond strength values were observed in deep than superficial dentine after 3 months of storage (Shono 1999) which is in agreement with short-term findings (Uno 2001).

When different adhesive systems were tested, three-step etch-and-rinse and two-step self-etch systems produced higher bond strength values than a two-step etch-and-rinse system after one and six months of storage but all systems produced comparable values after 15 months of storage. A one-step self-etch system, included in this study, could not be evaluated since the majority of samples did not withstand the preparation procedure indicating inferior bond strength compared to other systems (Armstrong 2003). Higher bond strength values were obtained when fluoride-containing varnish was applied to bonded surfaces (Nakajima 2003). Other hydrophilic functional monomers, potential HEMA substitutes, such as MEAA, may improve long-term bond strength regardless of the type of etchant (Fukushima 2001).

Thermo-cycling is another widely used aging method with a two-fold effect on dentine bonding: (1) water uptake and subsequent hydrolysis and elution of breakdown products or unreacted monomers and (2) repetitive hot and cold baths induce interfacial thermal stresses due to the differences in coefficients of thermal expansion and contraction between teeth and restorative materials (De Munck 2005). The ISO TR 11450 standard suggests that 500 cycles between water baths held at 5°C and 55°C should be used (ISO TR 11450;1994). It has been shown that an increasing number of cycles, up to 4000, does not affect bond strength significantly (Burger 1992). However, 500 cycles may be insufficient to induce detectable changes in dentine-adhesive bonding since this

corresponds to about 18 days in vivo whereas 10,000 cycles correspond to 1 year (Gale & Darvell 1999).

Thermo-cycling may be used on its own (Burger 1992, Xie 2002, Bonilla 2003) or in combination with storage (Meiers & Young 2001, Giannini 2003), mechanical loading (Bedran-de-Castro 2004) or both (Nikaido 2002a, Nikaido 2002b, Frankenberger 2003). Differences in bond strength were found associated with the type of adhesive system or the application techniques (Bonilla 2003) in both short-term (Xie 2002, Bonilla 2003) and long-term studies (Meiers & Young 2001, Giannini 2003). Thermo-cycling and mechanical loading had a synergistic adverse effect on bond strength resulting in significantly lower values than each aging method applied alone (Bedran-de-Castro 2004). Short-term aging combined with thermal and mechanical aging resulted in significant differences among different adhesive systems (Nikaido 2002b, Frankenberger 2003). It was also shown that surface preparation, C-factor, cavity depth, dentine substrate and smear layer characteristics affected bond strength (Nikaido 2002a).

In an in vivo study on monkeys, after one year, higher bond strength was found for a self-etch than an etch-and-rinse adhesive system (Koshiro 2005). Another study, using the same animal model, showed that bond strength for two self-etch systems decreased after one year of in vivo degradation but with no statistical significance (Takahashi 2002). Self-etch adhesives showed different resistance to degradation after one year of in vivo aging in human teeth and in vitro aging in artificial saliva for the same period, but bond strength values in adhesive systems were independent of the type of aging (Donmez 2005). A study on human premolars, scheduled for extraction for orthodontic reasons, showed that μTBS of three two-step etch-and-rinse adhesive systems was comparable for clinically moist dentine and dentine air-dried for 5 s. The authors concluded that residual dentine moisture, during clinically recommended procedure, may not have such an effect on bond strength as suggested by in vitro studies (Perdigao 2002).

2.2.2.3.2. Leakage

One of the most important functions of dental restorations is to seal exposed dentine and prevent vital pulp from being adversely affected by exogeneous factors. However, poor marginal seal and leakage around resin-based restorations have been identified from the inception of RBCs and adhesive systems in the clinical practice (Kidd 1976, Chohayeb 1988). Clinically unidentifiable passage of fluids, bacteria, molecules and ions through voids between the restoration and cavity walls can be classified as microleakage or nanoleakage, depending on the size of the voids (De Munck 2005).

Microleakage tests are used to study the marginal integrity of dental restorations by assessing the penetration between the restoration and cavity walls of dyes, such as basic fuchsine, procion red, silver nitrate or methylene blue or radioactive isotopes and bacteria. Most studies use a dye penetration method involving a nominal scale measurement. This approach makes dye penetration evaluation semi-quantitative and of low sensitivity (De Munck 2005). In order to overcome this, other methods have been used such as linear and dye volume measurements (Veis 1996). In most studies, a limited number of sections through restorations are used for dye penetration measurement further limiting experimental robustness. In attempts to overcome this problem, techniques such as sequential grinding followed by 3D models generated from photographs (Gale 1994, Tay 1995) or area metric analysis (Veis 1996) have been used. However, due to its simplicity, microleakage tests are still the most commonly used to assess marginal integrity with over 1500 articles in the MEDLINE database, found in August 2009 using the keyword “microleakage” and limiting the search to dental journals. Studies have shown that current etch-and-rinse and self-etch adhesive systems result in no or significantly lower microleakage at enamel-restoration compared to dentine-restoration interface (Santini 2001, Santini 2004, Rosales-Leal 2007). Several studies compared in vitro with in vivo microleakage test results with contradictory conclusions (Abdalla & Davidson 1993, Barnes 1993, Ferrari 1994). In a recent systematic review, no correlation between microleakage tests and clinical outcomes of

Class V restorations in terms of hypersensitivity, discoloration and secondary caries has been found, indicating that microleakage is a poor predictor of clinical performance of RBCs (Heintze 2007). This is in agreement with a previous view that microleakage tests should be considered only as an indication of a theoretic level of maximum leakage (Pashley 1990, Santini 2004). However, Heintze has expressed a more strident view that microleakage tests "should be eliminated from laboratory test portfolios" (Heintze 2007).

Nanoleakage was first described by Sano et al. who reported the presence of silver ions within the hybrid layer around the collagen fibres which were not completely infiltrated by adhesive resin (Sano 1994). Studies have shown that nanoleakage occurs in both etch-and-rinse (Sano 1995) and self-etch systems though they are designed to etch and infiltrate dentine simultaneously (Tay 2002). Though these nanometer-sized spaces are too small for bacterial penetration, they make the HL more susceptible to hydrolytic and enzymatic degradation by fluids and bacterial by-products (Paul 1999). However, the clinical significance of nanoleakage still remains unclear in light of contrasting results of in vitro studies regarding micro- and nanoleakage. It has been shown that water storage and thermocycling have little effect on microleakage unlike mechanical loading alone or in combination with thermocycling. On the other hand, water storage, mechanical loading and thermocycling were found to increase nanoleakage (De Munck 2005).

CHAPTER 3

STATEMENT OF THE PROBLEM

The clinical use of resin-based composites and adhesive systems involves the chemical or light-induced polymerisation of monomers. The quality of the final polymer network of resin-based composites and adhesive systems has a significant effect on the properties of these restorations and their clinical performance. The overall effect of incomplete polymerisation may result in materials with less than optimal clinical performance as well as the elution of components which may have an adverse effect on local and systemic functions. In addition, the adhesive-dentine interface is recognised as important in maintaining the integrity of resin-based composite restorations.

The current investigations were undertaken to assess monomer to polymer conversion, mainly in adhesive systems, using micro-Raman spectroscopy. The restoration-dentine interface was quantified in terms of dentine demineralisation, adhesive penetration and the degree of monomer to polymer conversion using micro-Raman spectroscopy. High-performance liquid chromatography was used to determine the type and amount of eluted monomers from the cured adhesive systems.

CHAPTER 4

AIMS AND OBJECTIVES

4.1. OVERALL AIM

Determine monomer to polymer conversion in adhesive systems using micro-Raman spectroscopy.

4.2. AIMS

4.2.1. Characterise tissues and materials used in the study.

4.2.2. Investigate the effect of sample preparation and storage conditions on monomer conversion in RBCs and adhesive systems.

4.2.3. Determine monomer conversion in adhesive systems as a function of time and light source.

4.2.4. Analyse the qualitative and quantitative aspects of the adhesive-dentine and RBC-adhesive-dentine interface.

4.2.5. Correlate monomer elution with monomer conversion in adhesive systems.

4.3. OVERALL OBJECTIVE

Quantify the degree of conversion (DC) in adhesive systems using micro-Raman spectroscopy.

4.4. OBJECTIVES

4.3.1. Make a database of micro-Raman spectra of tissues and materials used in the study.

4.3.2. Quantify the DC of RBCs and adhesive systems as affected by different sample preparation procedures and storing conditions.

4.3.3. Quantify the DC of adhesive systems as a function of curing times and types of LCUs.

4.3.4. Quantify the depth of dentine demineralisation, the hybrid layer and DC of adhesives across the adhesive-dentine interface.

4.3.5. Quantify the DC of RBCs and adhesive systems using micro-Raman spectroscopy and evaluate the RBC-adhesive interface using scanning electron microscopy.

4.3.6. Quantify the DC of adhesive systems using micro-Raman spectroscopy and correlate this with monomer elution obtained by high-performance liquid chromatography.

4.4. NULL HYPOTHESES

4.4.1. There is no significant difference in the DC of RBCs or adhesive systems regarding sample preparation and storage conditions.

4.4.2. Increasing curing times have no effect on the DC of adhesive systems.

4.4.3. There is no significant difference in the DC of different adhesive systems after the maximum curing time of 20 s.

4.4.4. There is no significant difference in the DC of adhesive systems with respect to different types and intensities of LCUs.

4.4.5. There are no significant differences in dentine demineralisation, adhesive penetration and DC of different adhesive systems.

4.4.6. There are no significant differences in the DC of different RBCs or adhesive systems.

4.4.7. There are no significant differences in the amount of monomer elution or the DC of different adhesive systems.

4.4.8. There is no correlation between monomer elution and the DC of adhesive systems.

CHAPTER 5

GENERAL MATERIALS AND METHODS

These are general materials and methods used throughout the studies and are listed here to avoid duplication. Specific materials and methods are given for each experiment in a designated chapter.

5.1. SAMPLE PREPARATION

Non-carious, human third molars, extracted for orthodontic reasons were used in Chapters 6, 7.2, 10, 11 and 12. Informed consent was obtained from patients for the use of these teeth for research purposes. Ethical approval was granted by the Ethics Committee, Lothian NHS Board (Edinburgh, UK) to use such teeth in this study. The teeth were cleaned of organic debris and stored in 0.02% thymol in a refrigerator set at 4ºC for no longer than 3 months before the start of experiments. Rubber moulds 1.5 x 1.5 x 3 cm^3 were used to embed teeth in cold acrylic up to the amelo-cemental junction. The acrylic was allowed to set for 24 h at 55°C and 3 bar pressure. Each tooth was then mounted on an Isomet saw (Buehler, Lake Bluff, IL, USA) and the occlusal one-third of the crown was sectioned perpendicular to the long axis of the tooth using a water-cooled, low-speed diamond wafering blade at 800 rpm (Figure 5). A smear layer was produced on flat dentine surface by grinding the surface with a 600-grit silicon carbide (SiC) disc (Buehler, Lake Bluff, IL, USA) under water for 30 s.

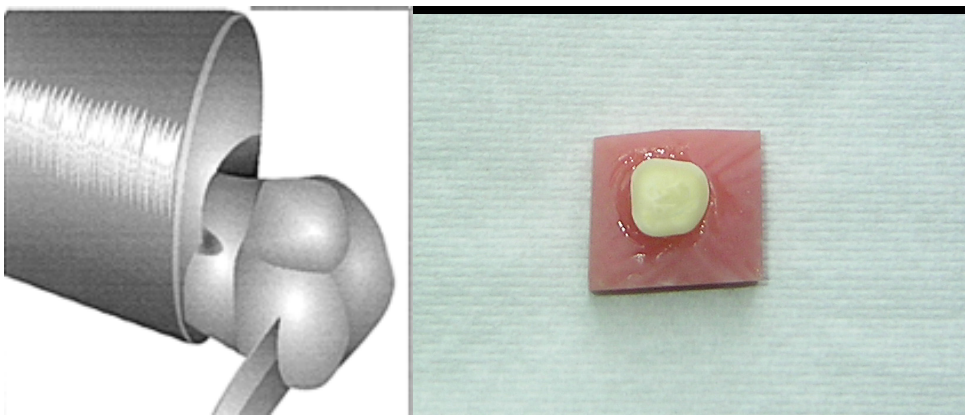

Figure 5. Sectioning the occlusal one-third of the tooth crown perpendicular to the long axis to expose flat dentine surface.

Acrylic moulds for RBC samples were used in the pilot study under 7.1. Acrylic moulds were prepared by pouring freshly mixed acrylic in rubber moulds 1.5 x 1.5 x 6 cm^3 around vertically placed precision metal rods 5 mm in diameter. After setting of the acrylic for 24 h at 55ºC and 3 bar pressure, the metal rod was removed, leaving an acrylic block with a 5 mm diameter internal cylinder. From these acrylic blocks, using the Isomet saw, 20 standardised acrylic moulds 1 mm thick and 70 moulds 2 mm thick were sectioned (Figure 6).

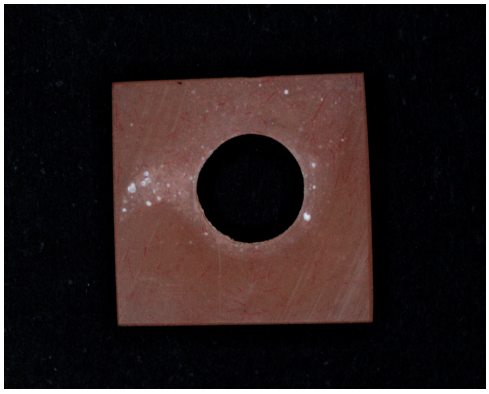

Figure 6. A 2 mm thick acrylic mould with a 5 mm diameter hole.

The dimensions of acrylic moulds were verified using an electronic digital calliper (Jade Products, Rugby, UK) and, where necessary, adjustments to the thickness were made by

polishing. The acrylic mould was placed on a glass-mixing slab, and filled with the RBC. In order to standardise the amount of material in the mould, a constant load was applied by first placing a Mylar strip on top of the material followed by a metal sheet. A 1 kg weight was used to compress the material into the mould.

Samples of adhesive systems were prepared for micro-Raman analysis in the following manner. Samples of one-bottle etch-and-rinse and one-step self–etch systems were prepared by spreading one drop of adhesive over an area of approximately 2 mm^2 on mat black coated microscopic slides. Samples of two-step self-etch systems were prepared by using either bond alone or mixed with the primer. One drop of primer and one drop of bond were mixed and applied to the microscopic slide over an area of approximately 2 mm^2 as was one drop of the bond alone. In all cases, the adhesive was gently mixed on the slide for 10 s and gently blow-dried for 5 s. These were, then, covered with a Mylar strip and cured according to the protocol for each experiment.

Custom-made light guides were prepared to standardise the curing distance at 1 mm, 2 mm and 4 mm during curing of RBC and adhesive samples in all experiments. This was done by cutting discs from plastic sheets 1 mm, 2 mm and 4 mm thick. A hole, just smaller than the diameter of the LCUs was drilled in each disc. In order to steady the LCU tip, another disc was cut with a hole slightly larger than the LCU tip was glued to the top of the light guide. The tip of the LCU rested on this internal rim and was kept at the desired curing distance from the material surface during curing (Figure 7).

Figure 7. Custom-made light guides.

5.2. MICRO-RAMAN SPECTROSCOPY

5.2.1. Principles of micro-Raman spectroscopy

Raman hardware consists of a monochromatic source of laser light such as HeNe, Ar/ion, diode or Kr/ion, a standard optical microscope with focusing and collecting objective, a series of mirrors which direct the laser beam towards the sample and collect the returning Raman signal, the spectrometer itself consists of a "triple-grating" monochromator system that disperses Raman scattered light into its component wavelengths which are detected by a charged couple device (CCD) detector and a cryostat containing liquid nitrogen or helium keeps the CCD detector at the appropriate temperature.

The Raman signal passes through the microscope collecting objective and an entrance slit and is focused on the first grating. It separates different wavelengths and the reflected light passes through another slit whose width is adjustable in order to eliminate unnecessary Rayleigh scattering wavelengths. The passing light is refocused on the second grating which acts as a mirror to the first grating and directs the passing light to the spectrometer. A third grating is used to separate the incoming light into a series of signals of different wavelengths, each with a distinctive and unique position. A multi-channel CCD array detects and reads simultaneously the incoming different wavelengths as a function of position. The CCD detector assigns each wavelength to the corresponding intensity. The wavelength/intensity information is then converted by the complementary software into a wavenumber/intensity plot which is a typical Raman spectrum.

For microscopic samples, confocal Raman spectroscopy is used to increase the spatial resolution. The incident laser is focused on a point in the sample using the microscope objective. The Raman signal from that point is sent back through the same microscope

objective and focused on a pinhole aperture. Raman scattered light from out-of-focus points is refracted by the microscope objective to be out of focus at the pinhole aperture. This light is blocked and prevented from being transmitted to the detector. The intensity of the Raman signal from locations outside of the focal point decreases to 50% at only 0.7 μm (Schrader 1995). Therefore, the resulting Raman spectrum contains Raman signal almost exclusively from the focal point of the laser from the sub-surface area of the sample. Not only does the confocal Raman affect the spatial resolution of microscopic samples, it also reduces fluorescence that may occur in biologic samples. With confocal Raman spectroscopy, laser is focused on such a small point that the laser flux in the sample is high enough to quench fluorescence in a fraction of time. Also, fluorescent photons are likely to miss the pinhole aperture and be blocked from passing to the detector. Fluorescence occurs in samples with 'impurities', which are found in most biologic samples, when excited sample molecules reach electronic instead of virtual energy states and the subsequent slow release of energy initiates fluorescence. If the incident light is visible or UV, fluorescence is much stronger than Raman scattered light and, therefore, most current spectrometers use NIR light source (Schrader 1995).

5.2.2. Micro-Raman spectroscopy as used in the present study

Prior to each session, the micro-Raman spectrometer (LabRam 300, Horiba JobinYvon, Stanmore, Middlesex, UK), shown in Figure 8, was calibrated internally for zero and then, using a Si sample, calibrated for coefficient values. These two parameters are important for an accurate determination of the position and intensity of subsequently obtained Raman peaks. The 520.8 cm^{-1} wavenumber was used as the known position of the Si peak. Standard micro-Raman parameters used in all experiments were: 20 mW HeNe laser with 632.817 nm wavelength, spatial resolution ~1.5 μm, spectral resolution ~2.5 cm^{-1}, and magnification x10, x50 and x100. Samples were placed on the computerised XYZ stage and focused under x10 and x50 magnification using an integrated microscope (Olympus UK, London, UK).

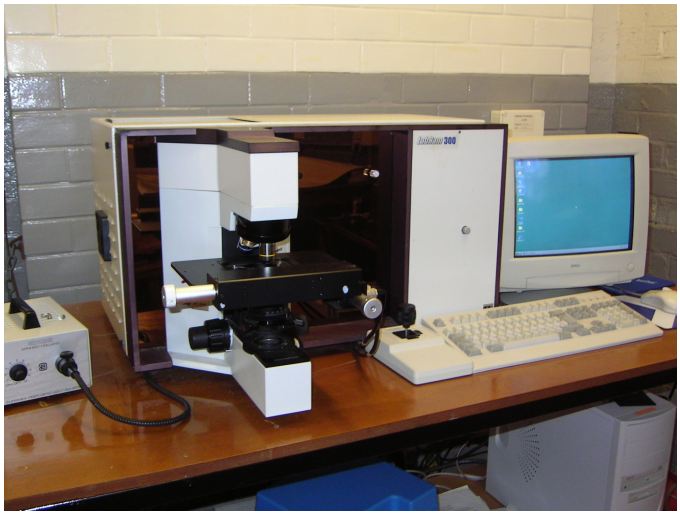

Figure 8. Micro-Raman spectrometer used in the present study.

Specific locations for taking micro-Raman spectra were selected depending on the aim of each experiment and are explained in specific materials and methods for each experiment. Then, x100 magnification was selected and micro-Raman obtained. Point spectra were taken with the XYZ stage in a stationary position whereas linear and two-dimensional mappings were done at 1 μm intervals along X axis only or both X and Y axes, respectively. Acquisition time and the number of accumulations were pre-determined for each experiment and are given in specific materials and methods for each experiment. These two parameters are used to reduce spectral noise which is influenced by the chemical composition of a given material.

Post-processing of micro-Raman spectra was performed by the dedicated software LabSpec4.18 (Horiba JobinYvon, Stanmore, Middlesex, UK). For point spectra, this included band fitting of characteristic peaks as a combined Gaussian / Lorentzian function with 1000 iterations to determine the exact position and peak intensities. The band fitting procedure, using the Levenberg-Marquardt method of non-linear peak fitting, provided the best fit over the entire peak. Post-processing of linear and two-dimensional maps was also performed by LabSpec4.18 and consisted of analysis with modelling which allowed distinguishing spectral components of different materials. The

modelling algorithms were based on correlation fitting of known reference spectra with raw data. Low level noise in the spectrum does not cause major deviation of the fitting routine, since by nature it is a random effect over the peak.

5.3. SCANNING ELECTRON MICROSCOPY

The same samples used for micro-Raman spectroscopy in experiments in Chapters 10 and 11 were subsequently prepared and analysed by SEM thereafter. Samples were polished on a Beta single wheel grinder-polisher machine (Buehler, Lake Bluff, IL, USA) using 600-grit and 1000-grit SiC discs under water and finished with polishing cloths with 3 μm diamond particles in a colloidal silica suspension. After rinsing under tap water, the samples were etched with 5M HCl for 30 s and rinsed with tap water for 5 min. They were then deproteinized in 1% NaOCl solution and rinsed under tap water for 5 min. The samples were critically point dried, mounted on aluminium stubs and sputter coated with 15 to 20 nm gold particles in an Emscope SC500 coating unit (Ashford, Kent, UK). Areas of interest were examined at appropriate magnifications, specified for each experiment, using an SEM (Philips XL30CP, Philips, Eindhoven, NL) with a secondary electron detector giving the resolution of the microscope of 3.5 nm at 30 kV (Figure 9).

Figure 9. Scanning electron microscope used in the present study.

5.4. STATISTICAL ANALYSIS

Data were analysed in Minitab 15 (Minitab Inc, State College, PA, USA). Power and sample size calculations at the alpha value of 0.05 showed that:

(1) For one-way ANOVA, 5 teeth per group would give 80% power of detecting as statistically significant a difference of 4 μm for the depth of dentine demineralisation based on the expected standard deviation of 1. 6 μm.

(2) For one-way ANOVA, 5 teeth per group would give 80% power of detecting as statistically significant a difference of 2.5 μm for adhesive penetration or the HL thickness based on the expected standard deviation of 1 μm.

(3) For t-tests, 5 teeth per group would give 80% power of detecting as statistically significant a difference of 2 μm for the HL thickness based on the expected standard deviation of 0.9 μm. For t-tests with Bonferroni correction required for the comparison of data obtained by micro-Raman spectroscopy and SEM ($p<0.008$), 7 teeth per group would give 80% power of detecting as statistically significant a difference of 2 μm for the HL thickness based on the expected standard deviation of 0.9 μm. Using the same tests, 5 teeth per group would give 80% power of detecting as statistically significant a difference of 2.5 μm for the HL thickness.

(4) For one-way ANOVA, 5 teeth per group would give 80% power of detecting as statistically significant a difference of 10% for the DC based on the expected standard deviation of 4%.

(5) For one-way ANOVA, 5 teeth per group would give 80% power of detecting as statistically significant a difference of 10 ppm for eluted monomers based on the expected SD of 4 ppm.

The variables were summarized and described using the classical measures of the "average" and "spread" of the observations, minimum, maximum, mean, standard deviation, median, interquartile range. The values of the descriptive statistics were presented in tables and figures.

Hypotheses were tested using parametric tests, t-test and ANOVA or non-parametric Mann-Whitney and Kruskal-Wallis test. The two assumptions for parametric tests were first checked. Kolmogorov-Smirnov test was used to assess whether the data followed normal Gaussian distribution and Bartlett's test for equal variances, to assess the assumption of equal variances. If both assumptions were met, the data were analysed using parametric tests. If either or both assumptions were not met, the data were first transformed according to Box Cox transformation lambda values using y^2, 1/y, ln y, $\sqrt{y}$, $1/\sqrt{y}$ transformation options. If the assumptions were not met with the transformed data, the non-parametric tests were used. The null hypothesis for these tests was that all population means in parametric testing or medians in non-parametric testing were the same. The alternative hypothesis was that one or more population means/medians differ from the others.

The level of significance was set at $\alpha=0.05$ in all experiments. However, adjustments were made for multiple comparisons in order to avoid one or more type I errors, i.e. concluding that there is a significant difference when there is none, for an entire set of comparisons. These included the use of post-tests, Tukey's for ANOVA and Dunn's for Kruskal-Wallis which controlled the rate of type I error using a family error rate of 0.05 for Tukey's and 0.20 for Dunn's post-test. Based on the family error rate or family α value, Tukey's post-test automatically adjusted individual confidence level, which is the probability of not making a type I error, i.e. concluding that there is a difference when there is none, for that individual comparison. Based on the family α value, Dunn's post-test automatically adjusted individual α values (Bonferroni correction) for each individual comparison.

CHAPTER 6

DATABASE OF MICRO-RAMAN SPECTRA

Prior to the beginning of the experimental work, I attended a basic course in micro-Raman spectroscopy, given by Dr Simon Fitzgerald of HORIBA Jobin Yvon, Stanmore, Middlesex in February 2007.

Prior to commencing the studies, a list of known and accepted characteristic Raman bands for molecular vibrations, occurring in materials likely to be used in the subsequent studies, was compiled from texts and various publications.

The aim of this pilot study was to acquire the knowledge of micro-Raman spectroscopy, characterise tissues and materials and define sample preparation and micro-Raman parameters to be applied in the main studies. The objective was to collect a micro-Raman point spectra database of tissues and materials and perform linear scans across enamel-dentine junctions, dentinal tubules, to include peritubular and intertubular dentine, and adhesive-dentine interfaces and 2D scans across the adhesive-dentine interface.

6.1. Materials and Methods

Table 1 lists tissues and materials used in main studies and from which micro-Raman spectra were obtained. Adhesive systems used in this pilot study are listed in Table 2. For simplicity, manufacturers' details for each material are omitted from Table 2 and are to be found in the comprehensive list of materials and devices on page XIII. RBCs used in the present study are listed in Table 3.

Table 1. Tissues and materials.

Tissues	**Materials**
hydroxyapatite	resin monomers
	camphorquinone
collagen (type I)	fillers
enamel	adhesive systems
dentine	RBCs

Table 2. Adhesive systems.

Type	Adhesive system	Composition
etch-and-rinse, 1-bottle	Excite	Phosphonic acid acrylate, HEMA, BisGMA, dimethacrylates, silica, ethanol, catalysts, stabilizers
	James-2	HEMA, UDMA, HPMA, GDMA, methacrylized polyalkenoate, catalysts, inhibitors. Solvent-free
	One-Coat Bond	HEMA, HPMA, GDMA, UDMA, methacrylized polyalkenoate, amorphous silica. Solvent-free
	Admira bond	HEMA, HPMA, BisGMA, ormocers, acetone, catalysts, additives
2-step self-etch, 2-bottle	AdheSE	Primer: Phosphonic acid acrylate, bis-acrylamide, water, initiators, stabilizers Bond: HEMA, BisGMA, dimethacrylates, Si-dioxide, initiators, stabilizers
	Clearfil SE Bond	Primer: MDP, HEMA, dimethacrylate hydrophilic, camphorquinone, N,N-diethanol p-toluidine, water. Adhesive: MDP, BisGMA, HEMA, dimethacrylate hydrophobic, camphorquinone, N,N-diethanol p-toluidine, silica
	One Coat Bond	Primer: water, acrylamidosulfonic acid, HEMA, GMA, GDMA, methacrylized polyalkenoate Bond: HEMA, GMA, GDMA, UDMA, methacrylized polyalkenoate
	Filtek Silorane adhesive system	Primer: phosphorylated methacrylates, Vitrebond copolymer, BisGMA, HEMA, water, ethanol, silane-treated silica filler, initiators, stabilizers. Bond: hydrophobic dimethacrylate, phosphorylated methacrylates, TEGDMA, silane-treated silica filler, initiators, stabilizers
1-step self-etch, 1-bottle	AdheSE One	Bis-acrylamide, water, bis-methacrylamide dihydrogen phosphate, amino acid acrylamide, hydroxyl alkyl methacrylamide, highly dispersed silicon dioxide, catalysts, stabilizers
	Clearfil 3S Bond	MDP, BisGMA, HEMA, initiator, stabilizer, ethanol, water, filler
	One Coat Bond	Methacrylates, photoinitiators, ethanol
	Adper Prompt L-Pop	Methacrylated phosphoric esters, BisGMA, HEMA, CQ-based initiator, stabilizer, polyalkenoic acid, water
	G Bond	4-MET, UDMA, acetone, water, sillanated colloidal silica, initiator
	Xeno III	Part A: HEMA, water, ethanol, BHT, nanofiller Part B: Pyro-EMA, PEM-F, UDMA, BHT, CQ, EPD

Table 3. Resin-based composites.

RBC	Manufacturer	Type	Composition
Tetric EvoCeram	Ivoclar Vivadent, Schaan, Lichtenstein, lot H29487	dimethacrylate-based, nanohybrid	Dimethacrylates, prepolymers, barium glass, ytterbium trifluoride, mixed oxide fillers, additives, catalysts, stabilizers, pigments
Gradia Direct	GC Corp., Tokyo, Japan, lot 0606142	dimethacrylate-based, microhybrid	UDMA, silica powder, alumino-silicate glass, organic filler
Filtek Silorane	3M ESPE, St. Paul, MN, USA, lot 7AR	silorane-based, microhybrid	Silorane resin, CQ, iodonium salt, quartz filler, yttrium fluoride, stabilizers, pigments
Admira	Voco GmbH, Cuxhaven, Germany, lot 76055	ormocer-based, microhybrid	BisGMA, UDMA, ormocer, silicate filler, catalysts, additives

6.1.1. Sample preparation for micro-Raman point spectra

A small amount of hydroxyapatite (Sigma-Aldrich Co. Ltd, Dorset, UK) was placed on a microscopic slide and flattened with a plastic instrument. A small amount of collagen type I (Sigma-Aldrich Co. Ltd, Dorset, UK) was placed on a microscopic slide and covered with a drop of water. After the water evaporated, the collagen sample was homogenized and flattened. One drop of each of the following resin monomers, BisGMA, BisEMA, UDMA, TEGDMA (Ivoclar Vivadent, Schaan, Liechtenstein) and HEMA (Sigma-Aldrich Co. Ltd, Dorset, UK), was placed on a microscopic slide and flattened using a metal spatula. Small amounts of CQ (Sigma-Aldrich Chemie GmbH, Steinheim, Germany) or a filler mixture, containing silicon oxide, barium glass, ytterbium trifluoride and mixed oxides (Ivoclar Vivadent, Schaan, Liechtenstein) were placed on microscopic slides, homogenised with a metal spatula and flattened using Mylar strips which were discarded prior to taking spectra.

Samples of adhesive systems were prepared by placing one drop each of an etch-and-rinse, two-step self-etch [bond only] or one-step self-etch adhesives on mat black coated welled microscopic slides. For primer and bond mixture of two-step self-etch adhesives, one drop of both primer and bond were mixed in a small, plastic cup for 10 s and then placed on a welled microscopic slide. These samples were used to obtain micro-Raman spectra of uncured materials. A new set of samples was prepared in a similar fashion, covered with a Mylar strip and cured for 20 s with a conventional halogen LCU (Prismetics Lite, Dentsply DeTrey GmbH, Konstanz, Germany) at an intensity of 400 mW/cm^2 from a standardised 1 mm distance. The Mylar strip was discarded immediately after curing and these samples were used to obtain micro-Raman spectra of cured materials.

Samples of RBCs were prepared in acrylic moulds as detailed in 5.1. First, micro-Raman spectra of uncured materials were obtained. Afterwards, a new set of samples was prepared in the same fashion, covered with a Mylar strip and cured for 40 s with a Prismetics Lite at an intensity of 400 mW/cm^2 from a standardised 1 mm distance. The Mylar strip was discarded immediately after curing and micro-Raman spectra obtained from cured materials.

A non-carious, human third molar was embedded in cold acrylic and a flat dentine surface exposed as detailed in 5.1. A 1 mm thick section of mid-coronal tooth tissue was cut using the Isomet saw. The section contained dentine surrounded circumferentially by enamel. An area of enamel, halfway between the enamel-dentine junction and enamel periphery, was selected randomly for micro-Raman analysis. This section was used to obtain point spectra of enamel, dentine and linear maps of the enamel-dentine junction. After micro-Raman analysis of un-treated dentine, the same dentine sample was etched with 35% phosphoric acid for 15 s, rinsed and excess water removed with a mild stream of air and micro-Raman point spectra of acid-etched dentine were obtained.

Micro-Raman point spectra of all tissues and materials were taken according to the protocol described in 5.2. For hydroxyapatite, collagen type I, enamel, dentine, resin monomers, adhesive systems and RBCs, the acquisition time was 10 s and each spectrum consisted of 10 accumulations. For CQ and fillers, the acquisition time was 5 s and each spectrum consisted of 5 accumulations. Spectra were taken over a range of wavenumbers, 0-2100 cm^{-1}. No form of data post processing was done at this stage. Additional spectra in the range of 2700-3300 cm^{-1} were taken for collagen type I and dentine.

6.1.2. Sample preparation for micro-Raman linear and 2D maps

The same tooth section used to obtain micro-Raman point spectra of enamel and dentine was used for linear mapping across the enamel-dentine junction. The enamel-dentine junction was inspected under x10 magnification using the Raman microscope and a location was randomly selected for micro-Raman analysis. After capturing the image using LabSpec4.18, dentine was aligned left and enamel right and the "linear imaging" option was selected. The computerized XYZ stage was programmed using the feature "acquisition data parameters". A horizontal line scan was obtained across the enamel-dentine junction using 40 points at 1 µm intervals. The acquisition time was 10 s with 10 accumulations per point and the spectral range was set at 800-1800 cm^{-1}.

For micro-Raman linear maps across dentinal tubules, a new sample was prepared from a second non-carious, human third molar. This was embedded in cold acrylic and a flat dentine surface exposed as detailed in 5.1. A 1 mm thick section was cut parallel to the long axis in order to expose vertically oriented dentinal tubules. A location for micro-Raman linear mapping was chosen randomly, to include tubular lumen, peritubular and intertubular dentine. After capturing the image at x100 magnification, the "linear imaging" option was selected. A linear scan was obtained as 30 points at 1 µm intervals. After obtaining spectra of this untreated dentine, the sample was polished using 600-grit,

1000-grit and 1200-grit SiC discs under water for 30 s each. It was then rinsed under tap water and blot-dried. Linear spectra were taken from locations randomly selected in the same fashion as detailed above. After obtaining spectra of polished dentine, the sample was treated with 35% phosphoric acid for 15 s to remove the smear layer, rinsed and then treated with 1% NaOCl for 1 min to remove any organic debris. The sample was rinsed under tap water and blot-dried. Linear spectra were taken from locations randomly selected in the same fashion as detailed above.

For micro-Raman linear maps across adhesive-dentine interfaces, two further non-carious, human third molars were prepared as detailed in 5.1. Admira bond and Adhese were used. Prior to the application of Admira bond, dentine was etched with 37% phosphoric acid for 15 s. The acid was then washed away and dentine was dried according to the wet bonding technique. Admira bond was applied according to the manufacturer's recommendations. Adhese was applied according to manufacturer's recommendations for self-etch adhesives. Both adhesive systems were cured for 20 s with a Prismetics Lite at an intensity of 400 mW/cm^2. The samples were left for 24 h in distilled water in light-proof containers in a water bath at 37ºC. Samples for micro-Raman analysis were prepared by mounting on the Isomet saw in such a way that, in the first instance, four cuts were made parallel to the long axis at 1 mm intervals. The tooth was then rotated for 90º and re-mounted on the Isomet. A final cut was made perpendicular to the long axis, thus, producing three 1 mm thick sections. A location for micro-Raman linear mapping was chosen randomly. After capturing the image at x100 magnification, the image was aligned so that adhesive was to the top and dentine to the bottom and the "linear imaging" option was selected. Lines of different length, 20 μm, 25 μm and 30 μm were obtained at 1 μm intervals across the adhesive-dentine interface.

The same samples used for linear mapping were used for 2D mapping across the adhesive-dentine interface. After capturing the image at x100 magnification, the "square imaging" option was selected. The computerized XYZ stage was programmed using the

feature “acquisition data parameters”. Two-dimensional maps were taken over areas of 15x15, 15x20 or 20x20 points at 1 μm intervals.

Micro-Raman analysis was done according to the parameters detailed in 5.2. The spectral range was 800-1800 cm^{-1} and the acquisition time was 10 s for all linear and 2D maps. Ten accumulations per point were made for linear maps and 2 accumulations per point for 2D maps.

6.2. Results

6.2.1. Micro-Raman point spectra

6.2.1.1. Tissues

Figure 10 shows the micro-Raman spectrum of hydroxyapatite and the identified bands are summarised in Table 4. The "fingerprint" region was identified between 400 cm^{-1} and 1100 cm^{-1}.

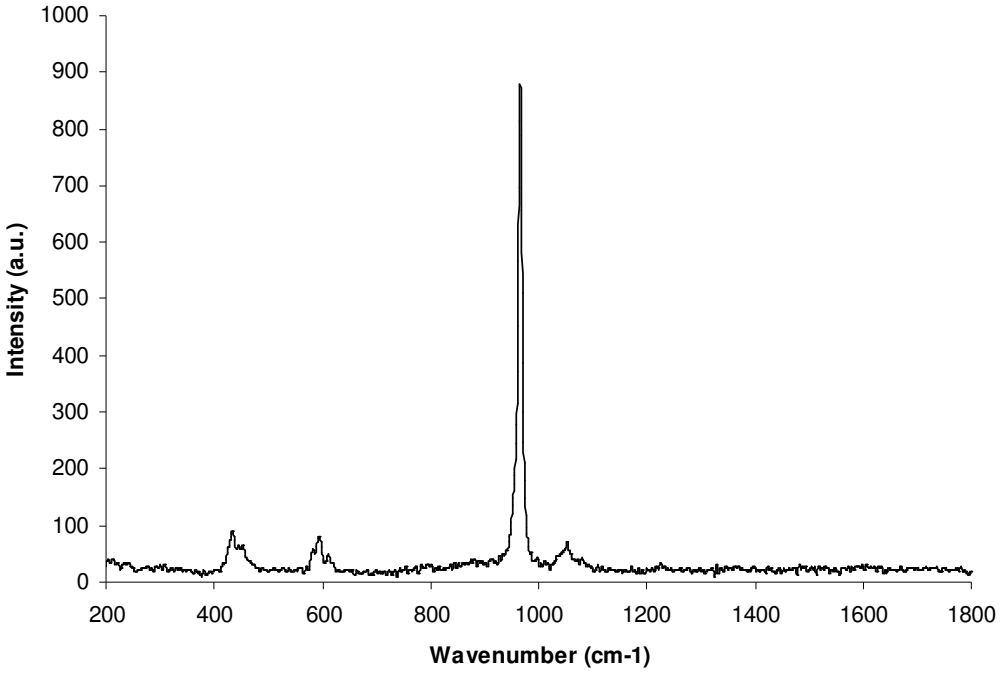

Figure 10. Micro-Raman point spectrum of hydroxyapatite.

Table 4. Characteristic bands for hydroxyapatite.

wavenumber (cm^{-1})	430 cm^{-1}	590 cm^{-1}	960 cm^{-1}	1070 cm^{-1}
band	PO_4 ν_2 (O-P-O bending)	PO_4 ν_4 (O-P-O bending)	PO_4 ν_1 (P-O symmetrical stretching)	CO_2

Figure 11 illustrates the micro-Raman spectrum of collagen type I and the identified bands are summarised in Table 5. The "fingerprint" region was identified between 0 cm^{-1} and 1800 cm^{-1} and 2800-3100 cm^{-1}.

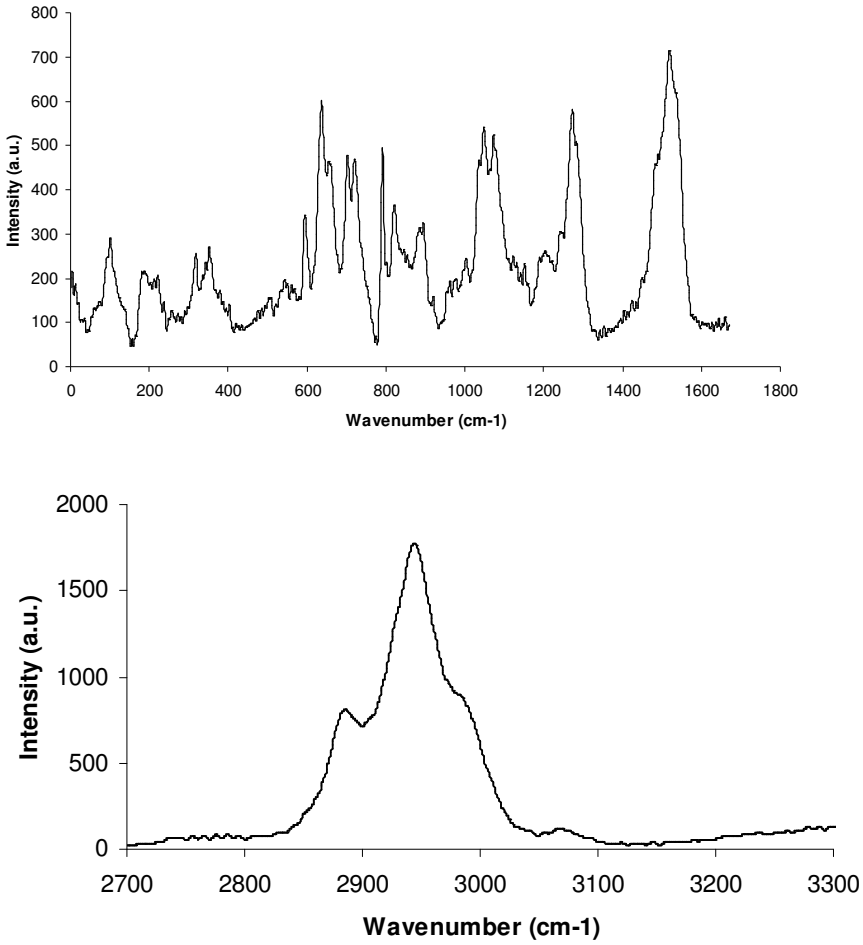

Figure 11. Micro-Raman point spectrum of collagen type I.

Table 5. Characteristic bands for collagen type I.

wavenumber (cm^{-1})	820	855	940	1247	1275	1455	1667	2943
band	CCH, aliphatic, bending	CCH, aromatic, olefinic, bending	CC, praline, valine, stretching	Amide III, NH bending	Amide III, NH bending	Amide II, CH_2, CH_3 , bending	Amide I, C=O stretching	C-H stretching

Figure 12 shows the micro-Raman spectrum of enamel and the identified bands are summarised in Table 6. All identified bands in the enamel spectrum correspond to the hydroxyapatite spectrum. The "fingerprint" region for enamel was between 400 cm^{-1} and 1100 cm^{-1}.

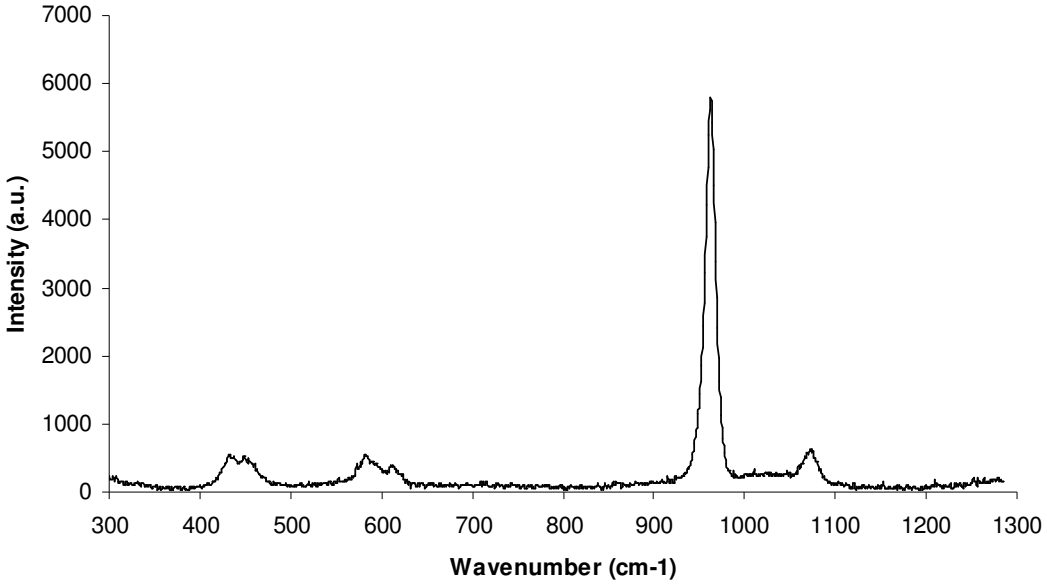

Figure 12. Micro-Raman point spectrum of enamel.

Table 6. Characteristic bands for enamel.

wavenumber (cm^{-1})	430 cm^{-1}	590 cm^{-1}	960 cm^{-1}	1070 cm^{-1}
band	PO_4 ν_2 (O-P-O bending)	PO_4 ν_4 (O-P-O bending)	PO_4 ν_1 (P-O symmetrical stretching)	CO_2

Figure 13 shows the micro-Raman spectrum of dentine and the identified bands are summarised in Table 7. Bands identified in the dentine spectrum show a combination of hydroxyapatite and collagen bands. Collagen bands around 900 cm^{-1} associated with aliphatic, aromatic, olefinic, praline and valine are masked in the dentine spectrum by the intensive 960 cm^{-1} phosphate band of hydroxyapatite. The "fingerprint" region for dentine was between 400-1800 cm^{-1} and 2800-3100 cm^{-1}.

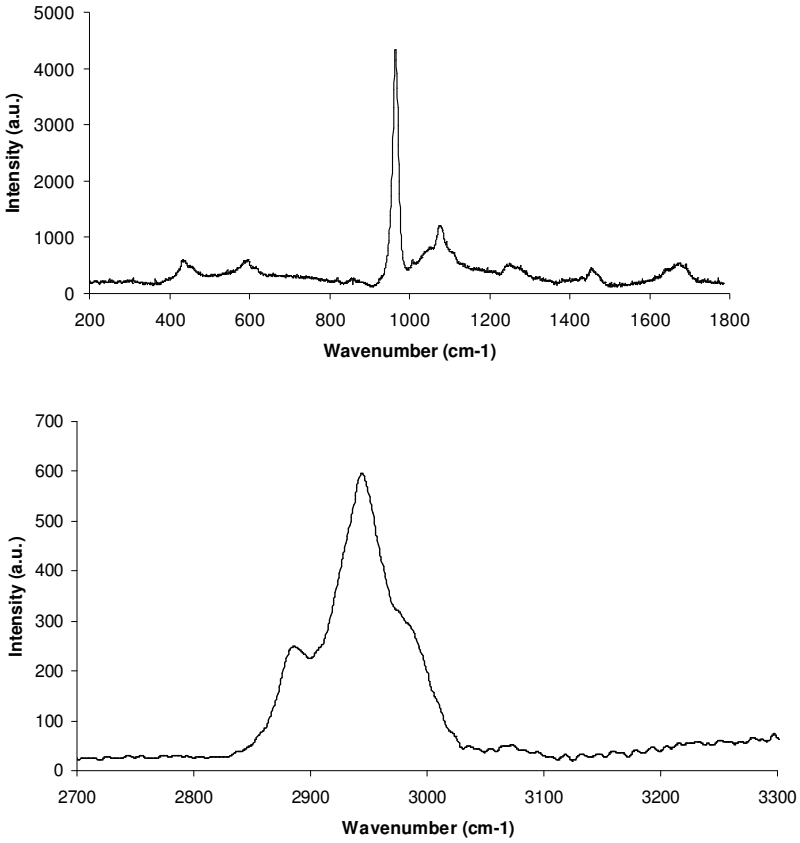

Figure 13. Micro-Raman point spectrum of dentine.

Table 7. Characteristic bands for dentine.

wavenumber (cm^{-1})	430	590	960	1070	1247-1275	1457	1667	2943
band	PO_4 ν_2	PO_4 ν_4	PO_4 ν_1	CO_2	Amide III	Amide II & CH_2	Amide I	C-H

Figure 14 shows spectra of dentine before and after etching. Band fitting procedures were used to calculate the intensity of the phosphate band of hydroxyapatite (960 cm^{-1}). The ratio of these bands before and after etching was 6.9:1.

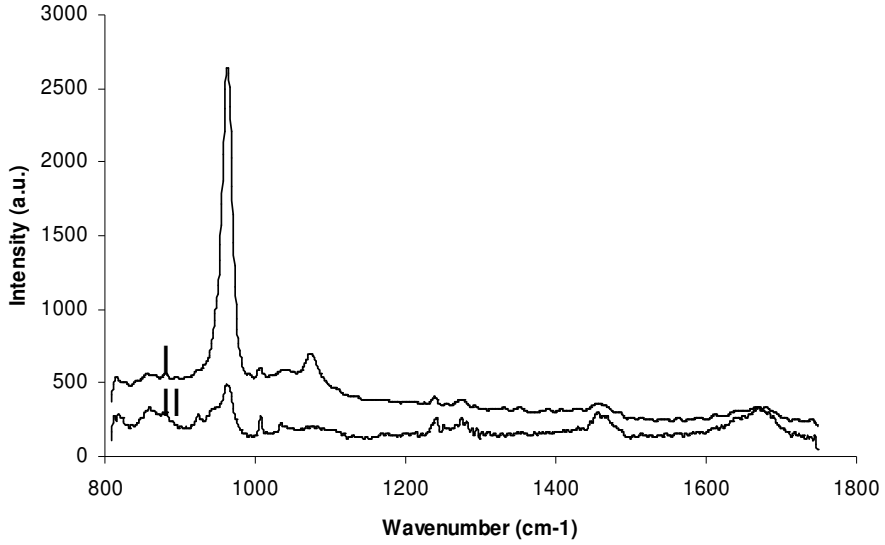

Figure 14. Micro-Raman point spectra of dentine before and after acid etching; I – Dentine before etching; II – Dentine after etching.

6.2.1.2. Resin monomers

Figures 15-19 illustrate the spectra of resin monomers and the identified bands are summarised in Tables 8-12. The "fingerprint" region for all monomers was identified between 300 cm^{-1} and 1800 cm^{-1}.

In both BisGMA and BisEMA, the 1639 cm^{-1} band is associated with the aliphatic C=C double bonds in the methacrylate groups of resin monomers which take part in polymerisation and convert to C-C single bonds connecting two monomer units. The 1609 cm^{-1} band is associated with the aromatic C=C double bonds in the aromatic ring which is not involved in polymerisation.

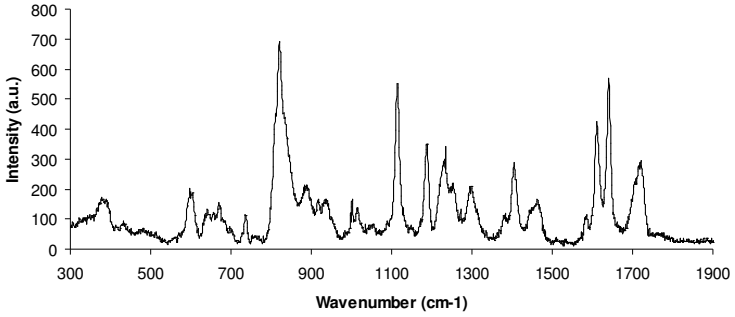

Figure 15. Micro-Raman point spectrum of BisGMA.

Table 8. Characteristic bands for BisGMA.

384	604-640	800-900	1113	1195	1230	1300	1410-1460	1609	1639	1720
C-C, aliphatic, bending	C=O carbonyl	>C=CH_2	C-O-C	CH_3-C-CH_3	CH-OH	=CH_2 rocking, C-O stretch	CH_2, CH_3 asym. bend.	C=C aromatic	C=C aliphatic	C=O carbonyl

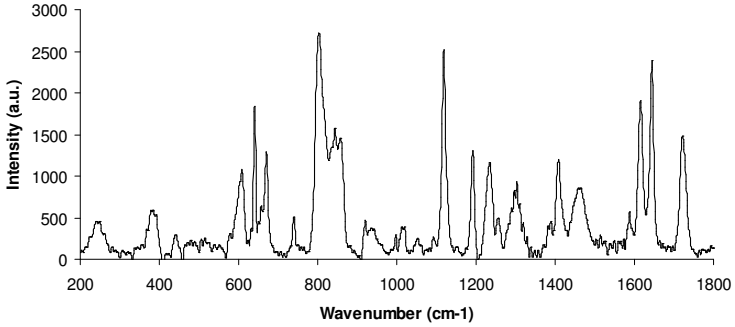

Figure 16. Micro-Raman point spectrum of BisEMA.

Table 9. Characteristic bands for BisEMA.

384-450	604-640	800-900	1113	1195	1236-	1300	1410-1460	1609	1639	1720
C-C, aliphatic, bending	C=O carbonyl	>C=CH_2	C-O-C	CH_3-C-CH_3	CH-OH	=CH_2 rocking, C-O stretch	CH_2, CH_3 asym. bend.	C=C aromatic	C=C aliphatic	C=O carbonyl

The absence of aromatic ring(s) in UDMA resulted in the absence of the aromatic C=C band at 1609 cm^{-1}. Vibrations of the N-H functional group occur in the 1490-1580 cm^{-1} range but are often too weak to be recorded.

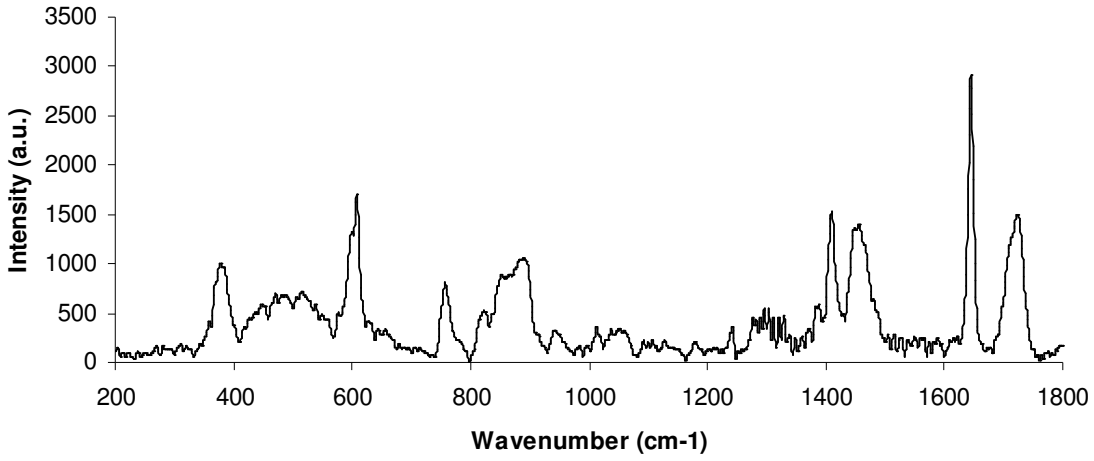

Figure 17. Micro-Raman point spectrum of UDMA.

Table 10. Characteristic bands for UDMA.

wavenumber (cm^{-1})	384	604	760	800-900	1300	1410-1460	1639	1720
band	C-C, aliphatic, bending	C=O carbonyl	CH_2	$>C=CH_2$	$=CH_2$ rocking, C-O stretch	CH_2, CH_3 asym. bend.	C=C aliphatic	C=O carbonyl

The absence of aromatic ring(s) in TEGDMA and HEMA resulted in the absence of the aromatic C=C band at 1609 cm^{-1} the micro-Raman spectra of these resin monomers.

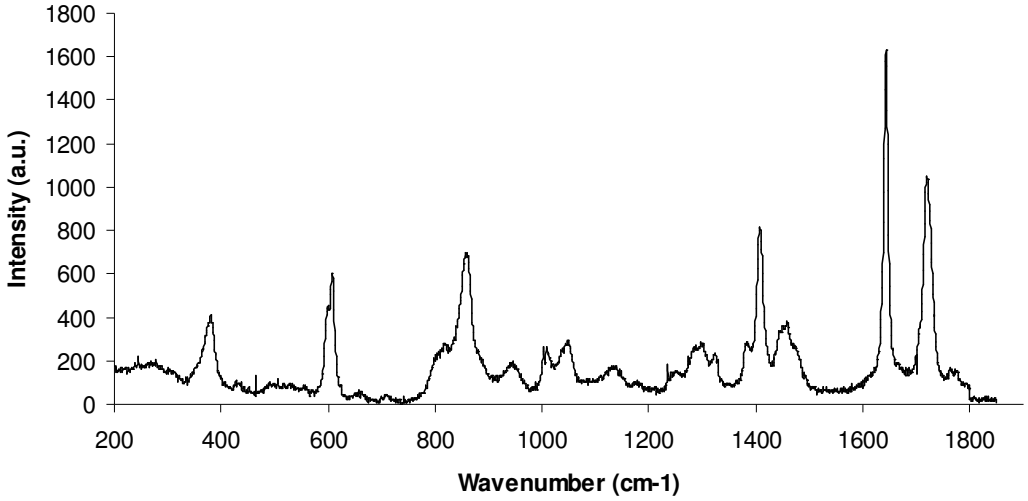

Figure 18. Micro-Raman point spectrum of TEGDMA.

Table 11. Characteristic bands for TEGDMA.

wavenumber (cm^{-1})	384	604	760	800-900	1300	1410-1460	1639	1720
band	C-C, aliphatic, bending	C=O carbonyl	CH_2	>C=CH_2	=CH_2 rocking, C-O stretch	CH_2, CH_3 asym. bend.	C=C aliphatic	C=O carbonyl

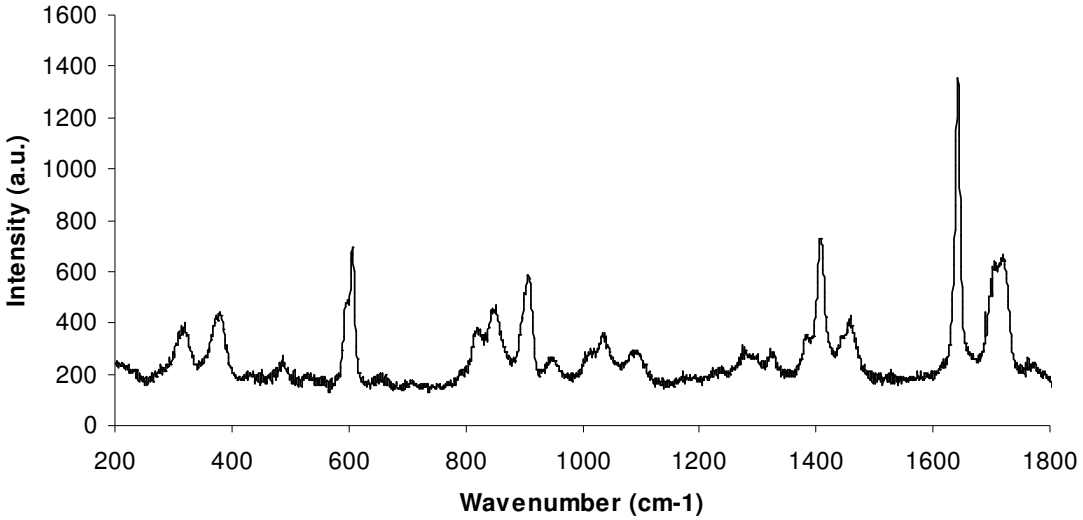

Figure 19. Micro-Raman point spectrum of HEMA.

Table 12. Characteristic bands for HEMA.

wavenumber (cm^{-1})	322	384	607	800-900	1300	1410-1460	1639	1720
band	C-C aliphatic, bending	C-C, aliphatic, bending (horiba)	C=O	>C=CH_2	=CH_2 rocking, C-O stretch	CH_2, CH_3 asym. bend.	C=C aliphatic	C=O carbonyl

6.2.1.3. Camphorquinone

Figure 20 shows the CQ spectrum and the identified bands are summarised in Table 13. The "fingerprint" region for was identified between 200 cm^{-1} and 1800 cm^{-1}.

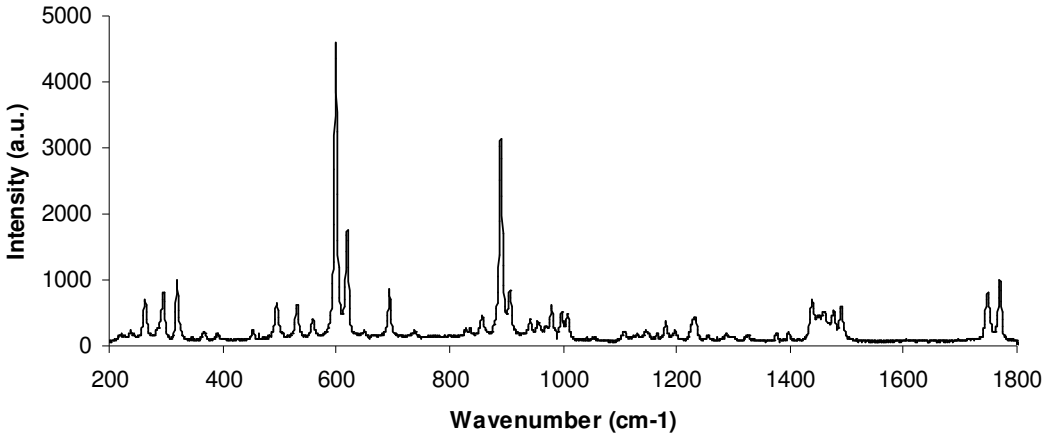

Figure 20. Micro-Raman point spectrum of camphorquinone.

Table 13. Characteristic bands for camphorquinone.

wavenumber (cm^{-1})	260 - 320	600	1437-1491	1720
band	C-C	C=O carbonyl	CH_2, CH_3 asym. bending	C=O carbonyl

6.2.1.4. Fillers

Figure 21 illustrates the filler spectrum and the identified bands are summarised in Table 14. The "fingerprint" region for the mixture was identified between 400 cm^{-1} and 1200 cm^{-1}.

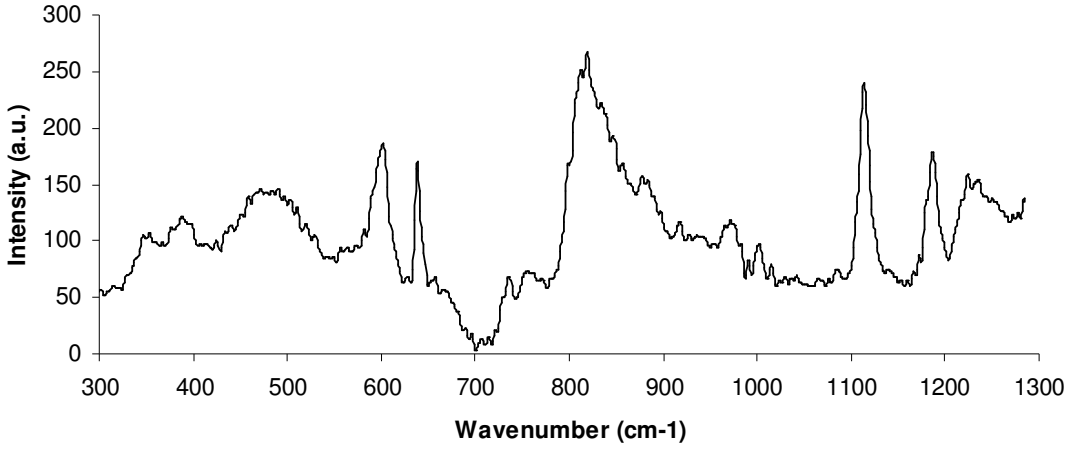

Figure 21. Micro-Raman point spectrum of fillers.

Table 14. Characteristic bands for fillers.

wavenumber (cm^{-1})	460	600	800	1100
band	O-Si-O bending	C=O carbonyl	Si-O-Si bending	Si-O stretching

6.2.1.5. Adhesive systems

Figures 22-24 show representative micro-Raman point spectra of uncured and cured BisGMA-based, non-BisGMA-based and acrylamide-based adhesive systems, respectively. The "fingerprint" region for all adhesive systems, uncured and cured, was identified between 200 cm^{-1} and 1800 cm^{-1}. A complete list of all obtained micro-Raman spectra from each adhesive system, uncured and cured, is given in the Appendix.

BisGMA-based adhesive systems

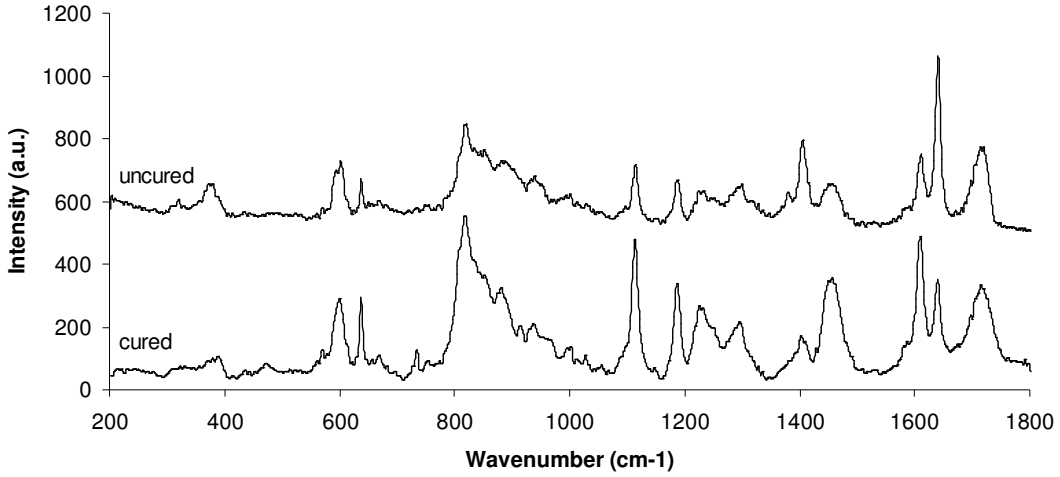

Figure 22. Micro-Raman point spectra of uncured and cured BisGMA-based adhesive system (Excite).

The spectrum of Excite is shown as representative of BisGMA-based systems. Almost identical micro-Raman spectra of other BisGMA-based systems were obtained and are listed in the Appendix. The 1639 cm^{-1} and 1609 cm^{-1} bands are associated with the aliphatic and aromatic C=C groups of BisGMA, respectively. Other major bands characteristic for BisGMA (Table 6) are also found in BisGMA-based adhesive systems.

Non-BisGMA-based adhesive systems

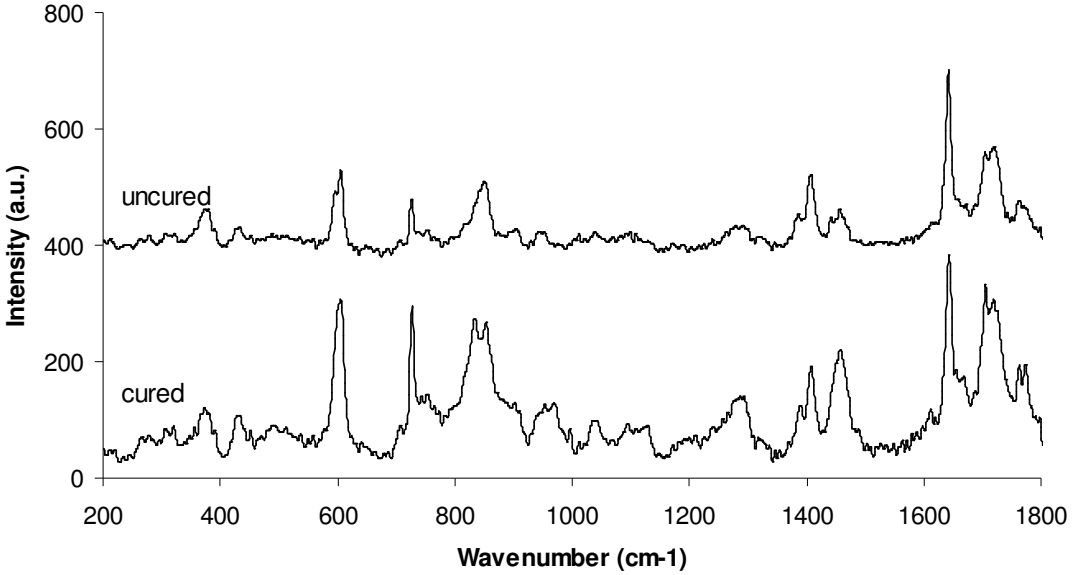

Figure 23. Micro-Raman point spectra of uncured and cured non-BisGMA-based adhesive system (Xeno III).

The spectrum of Xeno III is shown as representative of non-BisGMA-based systems. Almost identical micro-Raman spectra of other non-BisGMA-based systems were obtained and are listed in the Appendix. The absence of the aromatic ring(s) in non-BisGMA-based adhesive is reflected in the absence of the 1609 cm^{-1} band. The spectrum of a non-BisGMA-based adhesive system is dominated by the bands associated with its resin monomer(s), such as UDMA in the case of Xeno III.

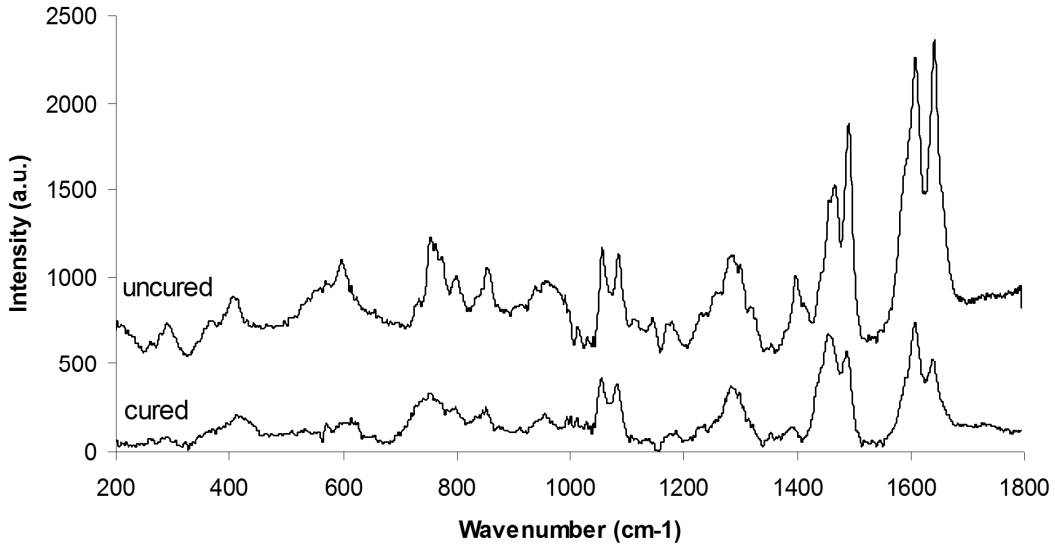

Figure 24. Micro-Raman point spectra of uncured and cured acrylamide-based adhesive system (Adhese One).

In the case of Adhese One, the only acrylamide-based adhesive system in the present study, the 1609 cm^{-1} band indicates the presence of the aromatic ring in the spacer group. The 1639 cm^{-1} band is associated with the aliphatic C=C double bonds which take part in the polymerisation process similar to methacrylate-based adhesives. Vibrations of the N-H group occur in the 1490-1580 cm^{-1} range.

6.2.1.6. Resin-based composites

The "fingerprint" region for all materials was identified between 200 cm^{-1} and 1800 cm^{-1}. Figures 25 and 26 show micro-Raman point spectra of uncured and cured dimethacrylate - based RBCs. Aliphatic and aromatic bands at 1639 cm^{-1} and 1609 cm^{-1}, respectively, were identified in the micro-Raman spectrum of Tetric EvoCeram, a typical BisGMA-based RBC. In a non-BisGMA-based RBC, Gradia Direct, the aliphatic band at 1639 cm^{-1} was identified. Though Gradia Direct contains UDMA with no

aromatic moieties, the presence of an aromatic band at 1609 cm^{-1} may be associated with other components of the RBC, undisclosed by the manufacturer.

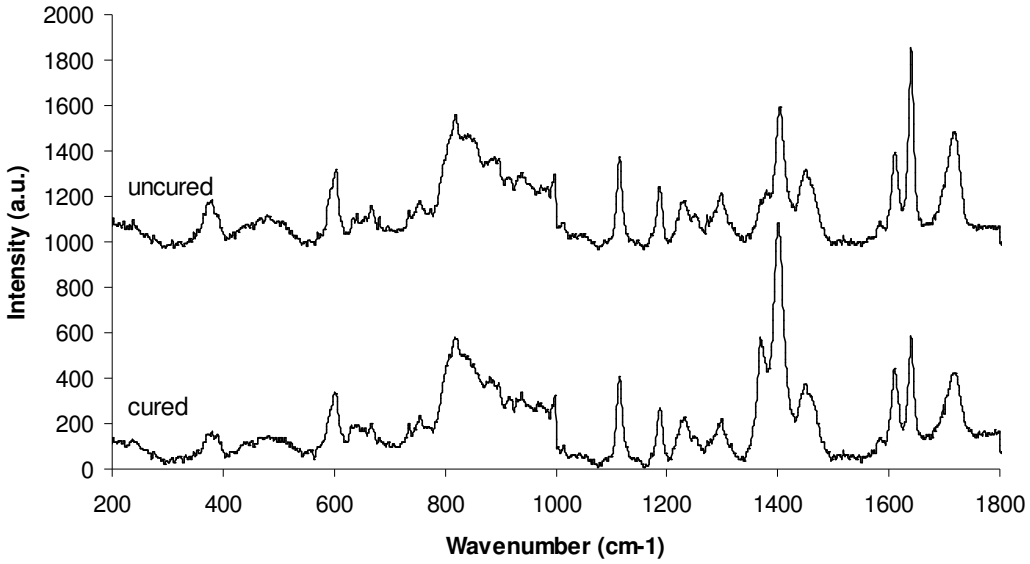

Figure 25. Micro-Raman point spectra of uncured and cured BisGMA-based composite (Tetric EvoCeram).

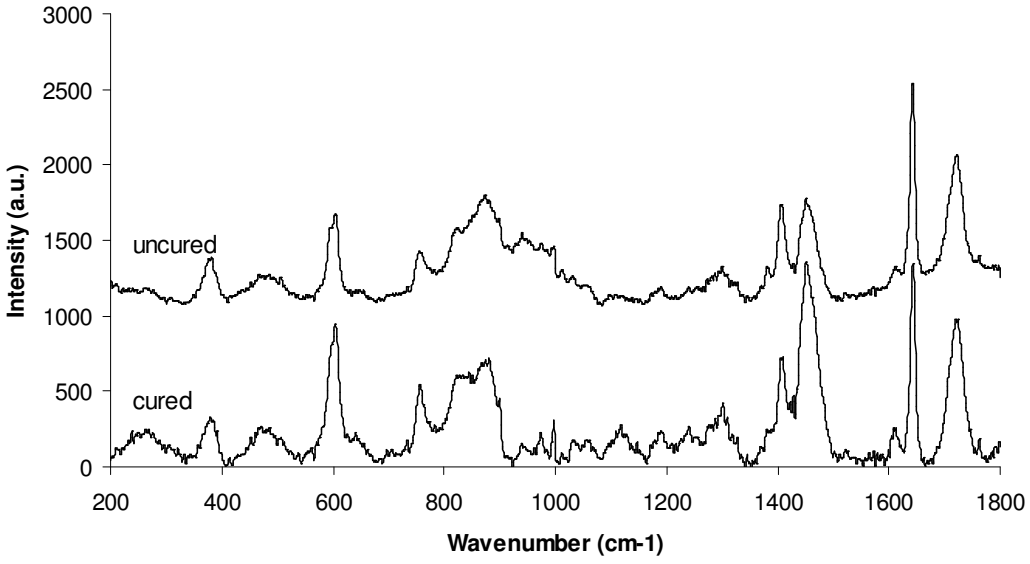

Figure 26. Micro-Raman point spectra of uncured and cured UDMA-based composite (Gradia Direct).

Figure 27 shows representative spectra of uncured and cured Filtek Silorane RBC, a silorane-based RBC. Both spectra are dominated by sharp peaks at 470 cm^{-1} (υSi-O-Si) and 1005 cm^{-1} but bands at 755 cm^{-1}, 796 cm^{-1}, 850 cm^{-1}, 890 cm^{-1} (υC-O-C), 1036 cm^{-1}, 1267 cm^{-1} and 1450 cm^{-1} are also identifiable.

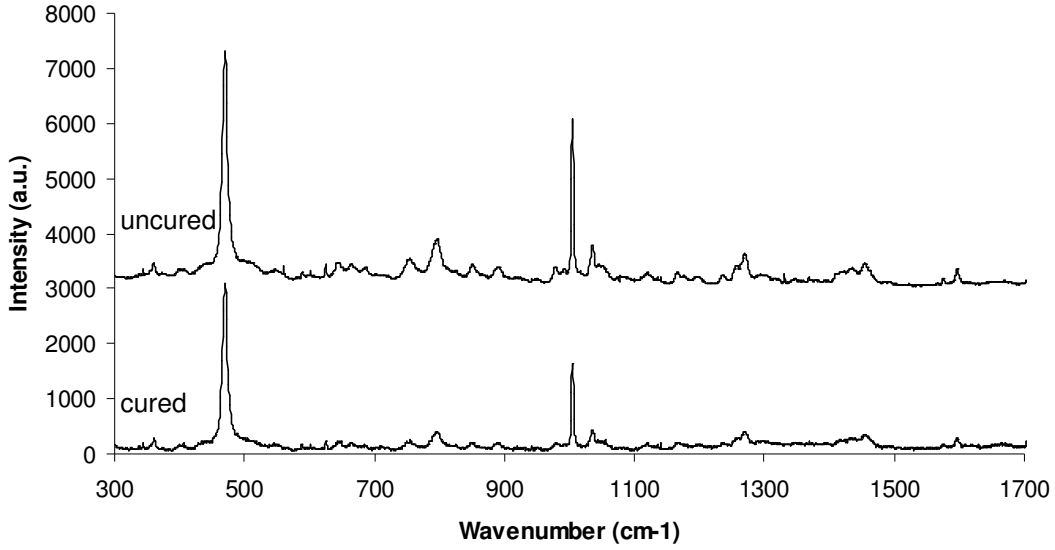

Figure 27. Micro-Raman point spectra of uncured and cured silorane-based composite (Filtek Silorane).

Figure 28 shows spectra of uncured and cured Admira, the ormocer-based RBC. Because it contains dimethacrylate monomer units attached to the ormocer, as well as a small amount of free dimethacrylates, 1639 cm^{-1} and 1609 cm^{-1} bands were identified in spectra of both uncured and cured Admira. The sharp peak at 1400 cm^{-1} could be associated with the ormocer groups as a peak of such intensity was not identified in any of the other tested RBCs. However, this can only be assumed because the exact formula of the ormocer was not disclosed or pure samples provided by the manufacturer.

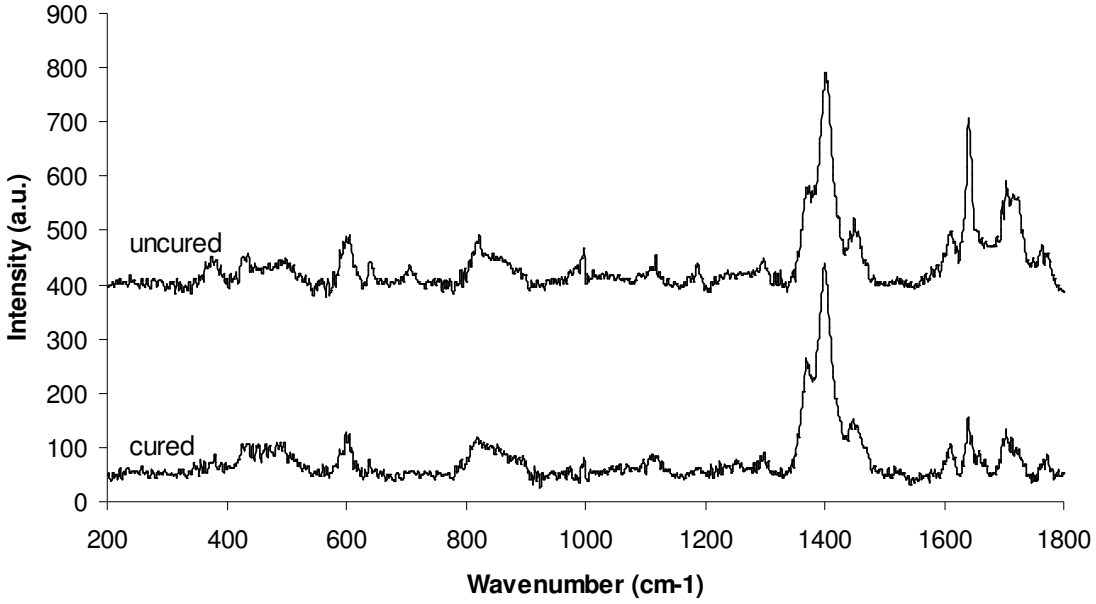

Figure 28. Micro-Raman point spectra of uncured and cured ormocer-based composite (Admira).

6.2.2. Micro-Raman linear spectra

6.2.2.1. Enamel-dentine junction

Figure 29 shows the enamel-dentine junction and Figure 30 shows the reference spectra of enamel and dentine and the distribution of mineral content across the enamel-dentine junction. The enamel-dentine junction presents as a zone of gradual rather than abrupt change in mineral content.

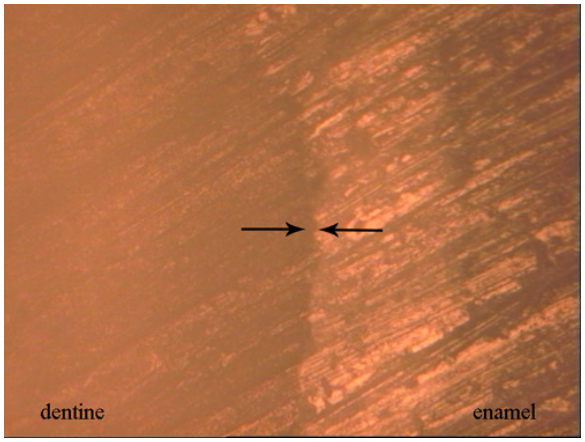

Figure 29. Enamel-dentine junction indicated by black arrows at x10 magnification.

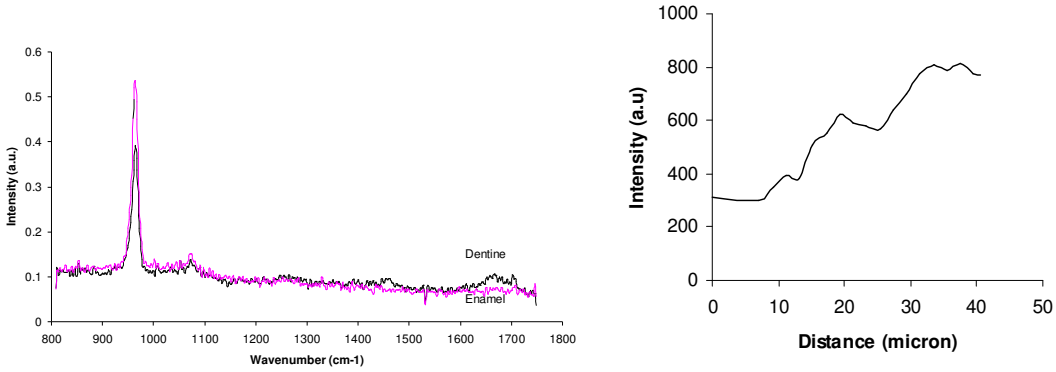

A. B.

Figure 30. A. Reference spectra of enamel and dentine and B. The distribution of mineral content across the enamel-dentine junction as a function of the 960 cm^{-1} peak intensity at each point of the linear scan.

6.2.2.2. Dentinal tubules

Figure 31 illustrates untreated, polished and treated dentine at x100 magnification.

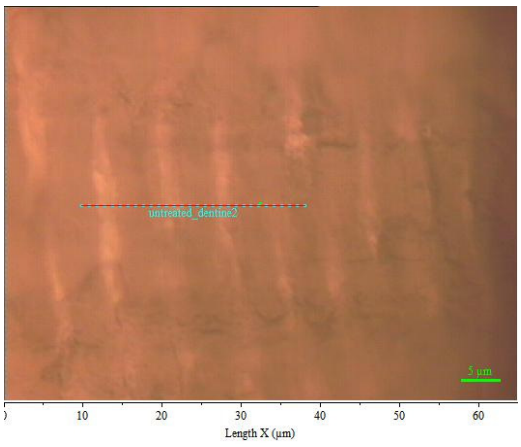

A.

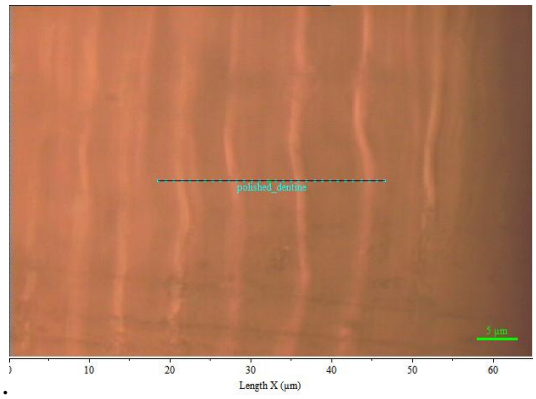

B.

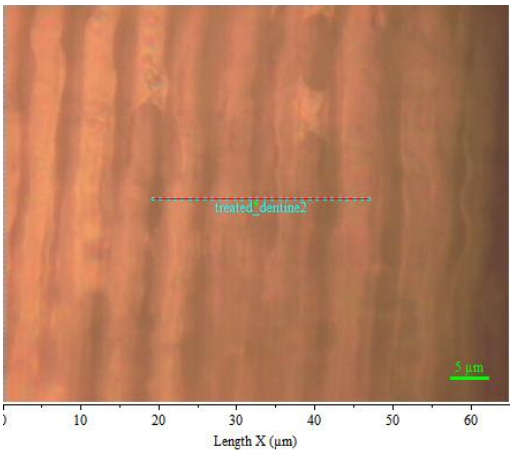

C.

Figure 31. Dentinal tubules. A. Untreated dentine, B. Polished dentine and C. Polished and acid-base treated dentine. The line of scanning is indicated by blue dots.

Figure 32 shows the distribution of mineral content across dentinal tubules in untreated, polished and treated dentine. Each line corresponds to the intensity of the 960 cm^{-1} peak at a given point of the linear scan. Higher intensities correspond to peritubular and lower intensities to intertubular dentine.

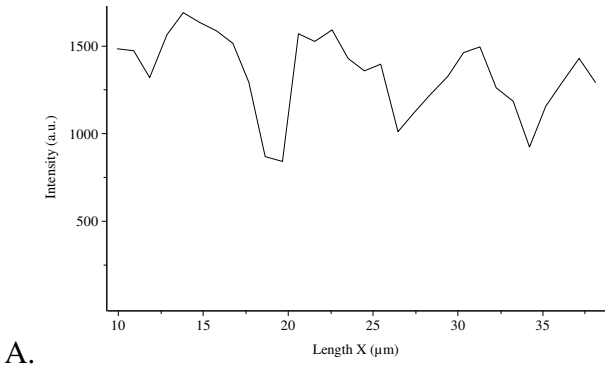

A.

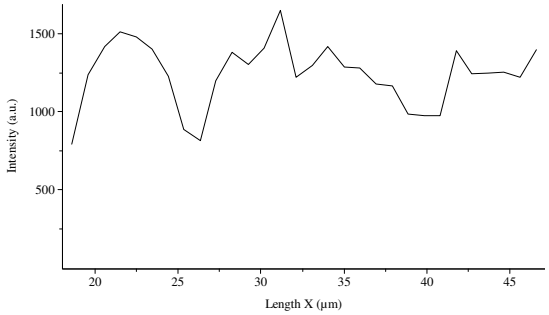

B.

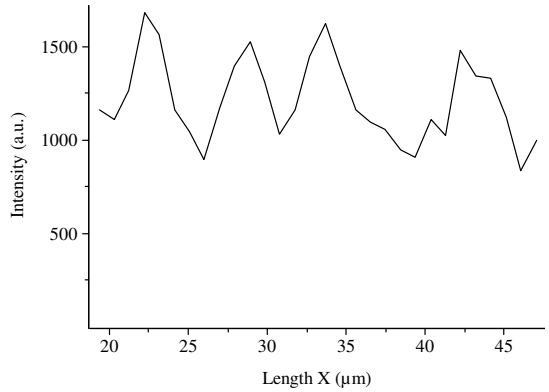

C.

Figure 32. The distribution of mineral content across dentinal tubules. A. Untreated dentine, B. Polished dentine and C. Polished and acid-base treated dentine.

6.2.2.3. Adhesive-dentine interface

Figure 33 shows the adhesive-dentine interface of Admira bond and Adhese at x100 magnification. Figure 34 shows the distribution of adhesive and dentine across the adhesive-dentine interface. The hybrid layer is the zone between the pure adhesive layer and mineralised dentine with spectral features associated with both adhesive and dentine. This zone is characterised by a gradual decrease of spectral features of adhesive and increase of those associated with dentine as the scan progresses apically from pure resin to un-affected dentine. This zone is wider in the etch-and-rinse than the self-etch adhesive.

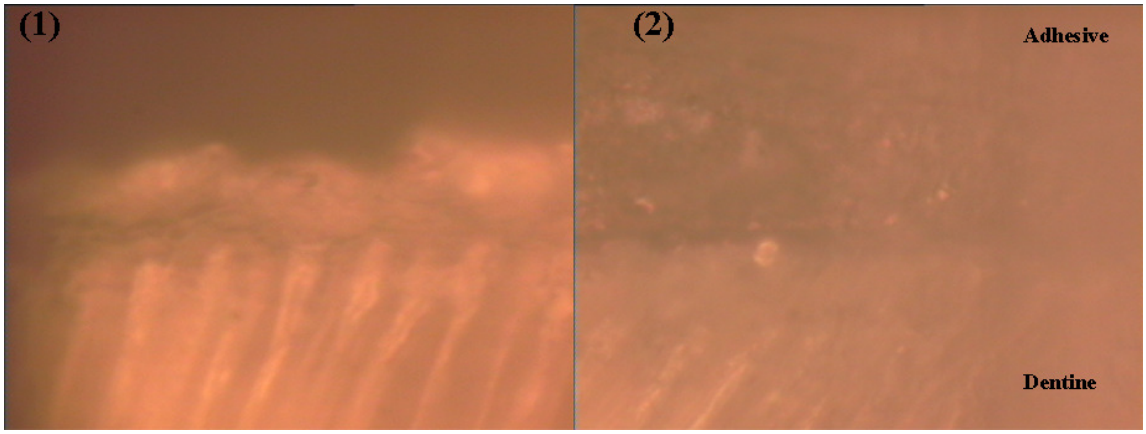

Figure 33. Adhesive-dentine interface at x100 magnification. (1) Admira bond; (2) Adhese.

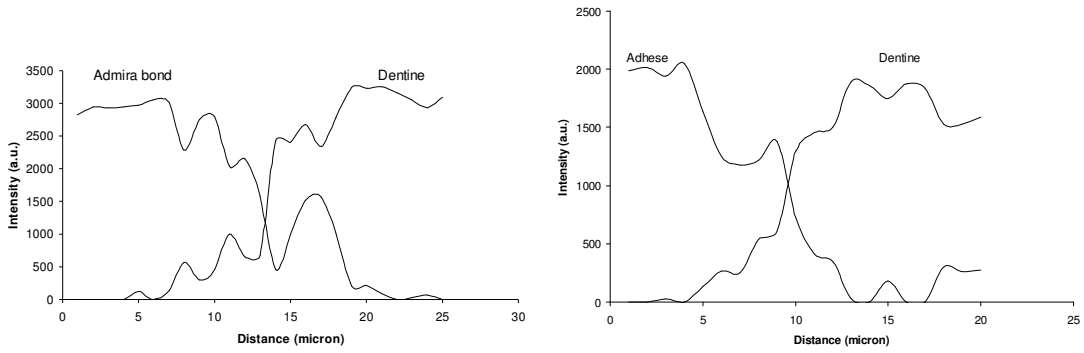

Figure 34. The distribution of adhesive and dentine across the adhesive-dentine interface of an etch-and-rinse adhesive, Admira bond, and a self-etch adhesive, Adhese.

6.2.3. Two-dimensional mapping of adhesive-dentine interface

Figures 35 and 36 illustrate the distribution of adhesive and dentine across the mapped area. Figures 35(1) and 36(1) show the gradual decrease in the intensity of spectral features associated with adhesive systems. Figures 35(2) and 36(2) show the gradual increase in the intensity of spectral features associated with dentine. The vertical scales indicate the intensity of spectral features and are given in arbitrary units, as are micro-Raman point spectra, with red being the most and purple the least intensive. In Figures 35 and 36, the upper black arrows indicate the beginning of the hybrid layer (adhesive aspect) and the lower black arrows indicate the end of the hybrid layer (dentinal aspect).

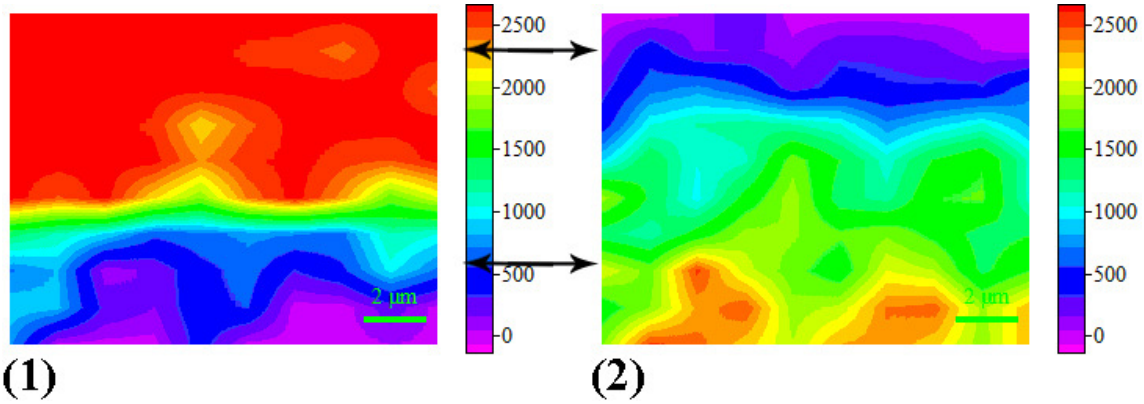

Figure 35. Two-dimensional map of the adhesive-dentine interface for Admira bond. (1) The distribution of Admira bond; (2) The distribution of dentine.

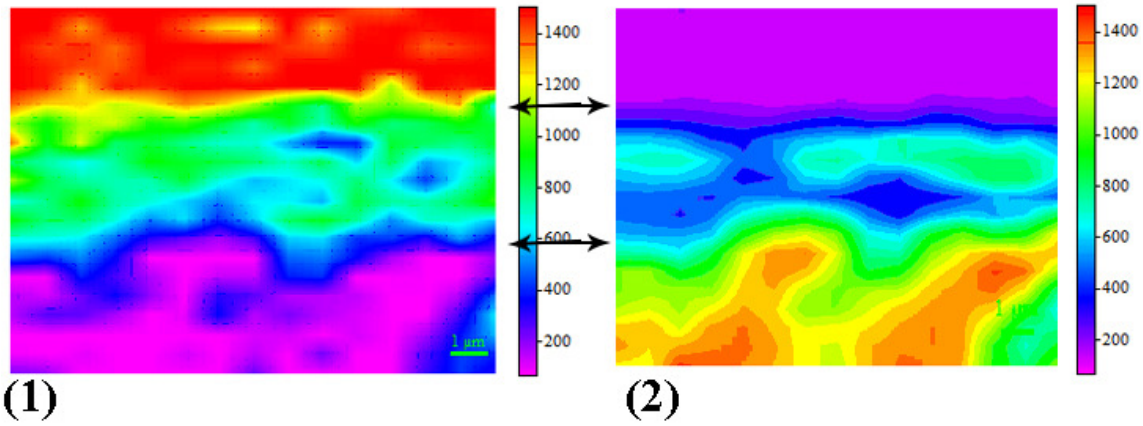

Figure 36. Two-dimensional map of the adhesive-dentine interface for Adhese. (1) The distribution of Adhese; (2) The distribution of dentine.

6.3. Discussion

Micro-Raman point spectra were obtained from all tissues and materials. Linear maps were taken across enamel-dentine junctions, dentinal tubules to include peritubular and intertubular dentine, and adhesive-dentine interfaces. Two-dimensional adhesive-dentine maps were obtained for an etch-and-rinse and a self-etch adhesive system.

The database of point spectra has shown that the "fingerprint" regions for all tissues and materials occur in a spectral range of 200-1800 cm^{-1}. This complements previous statements that, in IR spectroscopy, all functional groups show vibrational frequencies between 625 cm^{-1} and 4000 cm^{-1} (Hsu 1997). It was also shown that micro-Raman spectra of organic compounds, such as resin monomers, adhesive systems and RBCs have more detailed spectra than inorganic compounds, such as fillers or hydroxyapatite, as suggested previously for other organic and inorganic substances (Schrader 1995, Williams 1995). Micro-Raman spectra of enamel and dentine have shown characteristics of their main "building" blocks, hydroxyapatite in the spectrum of enamel and hydroxyapatite and collagen in dentine.

Within spectra of each tissue or material in this pilot study, characteristic molecular vibrations were identified which allow identification but also quantification of chemical changes, such as demineralisation of enamel and dentine or monomer to polymer conversion of adhesives and RBCs.

The peak at 960 cm^{-1}, associated with P-O symmetrical stretching within the phosphate groups of hydroxyapatite, has been used to determine the amount of mineral content of enamel and dentine (O'Shea DC 1974, Casciani FS 1979, Nishino 1981, Tsuda & Arends 1993, Tsuda 1993, Tsuda & Arends 1994, Tsuda 1996a, Tsuda 1996b, Tramini 2000, Tramini 2001, Arvidsson 2002, Camerlingo 2004, Sakoolnamarka 2005, Gilchrist 2007). More recently, this peak has been used to determine the changes in dentine demineralisation as a result of adhesive application (Sato & Miyazaki 2005, Wang &

Spencer 2005, Wang 2006b, Wang 2007, Santini & Miletic 2008). Additionally, amide peaks in dentine at 1247-1275 cm^{-1}, 1457 cm^{-1} and 1667 cm^{-1} or the C-H peak at 2943 cm^{-1}, associated with collagen, have been used to monitor structural changes in dentine (Camerlingo 2004) or dentine demineralisation which is then shown as a ratio between the phosphate and any of the collagen peaks (Wang & Spencer 2004b).

The peak at 1639 cm^{-1}, associated with the methacrylate (aliphatic) group, has been identified in all dimethacrylate-based monomers, adhesive systems and RBCs. The 1609 cm^{-1} peak, associated with the aromatic group, has been identified in BisGMA and BisEMA and adhesive systems and RBCs based on these monomers. The change in the ratio of these two peaks has been used to determine the ratio of double bonds after monomer to polymer conversion in adhesives and RBCs (Silva Soares 2005, Rode 2007, Santos 2007, Sadek 2008). In non-BisGMA-based materials, the aromatic 1609 cm^{-1} peak is most often absent due to the absence of aromatic moieties in cross-linking monomers. However, in some cases, such as G Bond and Gradia Direct, which are UDMA-based materials, the presence of the 1609 cm^{-1} peak may be associated with either functional monomers in the adhesive or additional cross-linking monomers in the RBC. In spite of this, in materials whose main cross-linking monomers do not contain aromatic moieties, it is common to use other groups as the internal standard in DC calculations, such as the C=O group, associated with 1710 cm^{-1}, or the CH_2 group, associated with 1453 cm^{-1}, or the COO group, associated with 605 cm^{-1} (Wang & Spencer 2005, Spencer 2006, Navarra 2009).

Linear micro-Raman mapping across enamel-dentine junction in the present study has confirmed previous findings that this is a zone of gradual rather than an abrupt change in mineral content (Schulze 2004). Micro-Raman analysis in this pilot study showed that chemical identification of enamel and dentine is easily obtained and can be further verified using an optical microscope within the Raman set-up. This is of particular importance for the main studies which are to be conducted on dentine. Raman characterisation eliminates any ambiguity as to the type of substrate which is being

analysed and possible misinterpretation during the subsequent analysis of the adhesive-dentine interface.

In the present study, linear micro-Raman mapping across dentinal tubules revealed less variation in intensities of the phosphate-associated peak at 960 cm^{-1} compared to those obtained with linear scans across the enamel-dentine junction. The observed differences across dentinal tubules may be associated with the differences in mineralization of peritubular and intertubular dentine. Based on the previous knowledge of dentine anatomy, somewhat greater differentiation in mineral content was expected between intertubular and peritubular dentine but was not confirmed on the linear scans performed in this pilot study. This could be associated with the fact that micro-Raman spectra for both types of dentine contained the same spectral features, the 960 cm^{-1} peak associated with hydroxyapatite and amide peaks associated with collagen. LabSpec4.18 software was only used to follow the distribution of spectral features on the linear scan. No form of post-processing of data was done at this stage, thus, the true degree of mineralisation of intertubular and peritubular dentine was neither calculated by the software nor indicated by Figure 32.

Though micro-Raman scans were performed across dentinal tubules, the linear map showed no discontinuity that would indicate the presence of the tubular lumen. Instead, spectral features associated with dentine were continuously detected. This could be explained by the technical properties of the used micro-Raman spectrometer. It has been previously shown that the diameter of dentinal tubules is 0.8 µm in the area close to the enamel-dentine junction compared to 3.0 µm at the pulpal surface (Eick 1997). The section for this pilot study was made mid-coronally presenting narrower dentinal tubules than those at the pulpal surface. The surface of the scanned area contained zones of flat intertubular and concave peritubular dentine at the bottom of the tubular lumen. Though micro-Raman spectra were obtained from subsurface areas, it is impossible to determine the exact position of the Raman laser spot which could be on the peritubular dentine at the bottom or slightly above it, within the tubular lumen. However, the Raman signal

may detect slightly out-of-focus points and allow the signal from the adjacent peritubular dentine to be collected, especially when air is the medium between the true focal and out-of-focus point (Schrader 1995).

In the present study, linear micro-Raman mapping across the adhesive-dentine interface showed a zone of gradual transition between adhesive and dentine for both etch-and-rinse and self-etch systems. Lines of different length were selected in order to determine the most appropriate length for linear mapping in the main studies. For both adhesive systems, 30 µm lines were found sufficient to include part of the adhesive layer, HL, partially demineralised, un-infiltrated dentine and un-affected dentine. Previous studies have shown that linear scans across the adhesive-dentine interface of various length, from 10-22 µm, may be required to completely include the aforementioned zones (Wieliczka 1996, Wang 2005, Wang 2006b). In the present study, the 30 µm linear scans were found to be sufficient also in etch-and-rinse systems where deeper zone of dentine demineralisation is expected. Therefore, it was decided to use linear scans of 30 µm for both etch-and-rinse and self-etch systems in the main studies.

Two-dimensional micro-Raman mapping across the adhesive-dentine interface was also performed in the present study to determine the optimal area for 2D mapping in the main studies. Areas of 15x15 µm, 15x20 µm or 20x20 µm were found sufficient to include part of the adhesive layer, HL, partially demineralised, un-infiltrated dentine and un-affected dentine. Smaller areas reduce the time required to obtain 2D maps which is substantially longer than that of linear scanning and also reduce the risk of thermal damage of samples. Therefore, it was decided to use these maps in the main studies, since the size of the maps has no effect on the results as long as the entire area of interest is included. Smaller areas may be applied in self-etch adhesive systems which have thinner HL thickness and shallower zone of dentine demineralisation.

6.4. Conclusions

All tissues and materials, to be used in the main studies, were characterised using micro-Raman spectroscopy. In micro-Raman point spectra, characteristic bands were identified which are to be used in the main studies to identify tissues and materials and quantify chemical changes, such as dentine demineralisation and monomer conversion. Linear scans of 30 µm allow the entire adhesive-dentine interface to be scanned, including part of the adhesive layer, HL, partially demineralised, un-infiltrated dentine and un-affected dentine, in both etch-and-rinse and self-etch systems. 2D maps of 20x20 µm allow scanning across the adhesive-dentine interface in both types of adhesive systems, but smaller maps, 15x15 µm and 15x20 µm, may also be used if they allow the entire area to be included. This does not affect the results and significantly reduces the time required to obtain 2D maps as well as the risk of thermal damage of samples.

Samples of viscous liquid substances, such as resin monomers and adhesive systems, should be placed on a microscopic slide using an applicator brush and spread thinly so that x100 objective can be focused. Otherwise, it was found that micro-Raman spectra were very difficult, if not impossible, to obtain.

Samples of solid substances in the form of powder, such as CQ or filler mixtures, should be dispensed on a microscopic slide with a spatula and then homogenized so that a flat surface is obtained without empty spaces between sample particles.

Samples of solid substances in the form of paste, such as hydroxyapatite or RBCs, should be dispensed on a microscopic slide with a spatula and flattened prior to focusing x100 objective.

Samples of tooth tissues, enamel and dentine, should be sectioned using the Isomet saw, in such a way that both top and bottom surfaces are flat. A flat bottom surface ensures stability of the sample on the microscope slide. A flat top surface facing the Raman laser

allows optimal focusing using x100 objective for the maximum spectral and spatial resolution for the given micro-Raman set-up. For linear and 2D mapping across adhesive-dentine junctions, sections parallel to the long axis of the tooth should be made mid-coronally. In this way, their positioning on a microscopic slide, as explained above, allows the junctions to be facing the Raman laser.

CHAPTER 7

SAMPLE PREPARATION AND STORAGE AND THEIR EFFECT ON THE DEGREE OF CONVERSION IN MATERIALS

The aim of this study was to investigate the effect of sample preparation and storage conditions on monomer conversion in RBCs and adhesive systems. The objective was to quantify the DC values of an RBC and adhesive system as affected by different sample preparation procedures and storage conditions. The null hypothesis is that there is no significant difference in the DC of RBCs or adhesive systems regarding sample preparation and storage conditions.

7.1. Resin-based composite

7.1.1. Material and Methods

As explained in 5.1., 70 samples of Tetric EvoCeram were prepared in acrylic moulds 5 mm in diameter and 2 mm thick and 20 samples of the same RBC in moulds 5 mm in diameter and 1 mm thick. The 2 mm thick samples were cured with an LED LCU (bluephase, Ivoclar Vivadent, Schaan, Liechtenstein) at an intensity of 1100 mW/cm^2 for 20 s at 1 mm curing distance. Two 1 mm thick samples, one on top of the other and separated by a Mylar strip, were cured simultaneously using the same curing parameters, giving ten 2 mm thick "split" samples.

Mylar strips were discarded immediately after light curing. Seventy 2 mm thick samples were allocated randomly to 7 groups (10 samples per group) and the 10 "split" samples were allocated to the 8^{th} group.

Micro-Raman analysis was done according to the protocol for point spectra, detailed in 5.2. The acquisition time was 10 s with 10 accumulations per spectrum. During each session, spectra from uncured material were taken under the same instrumentation parameters and served as reference.

Effect of polishing

Group 1 consisted of ten 2 mm thick samples. The top and bottom surfaces were polished according to the following protocol: 240-grit, 600-grit and 1000-grit SiC discs in wet conditions, for 30 s each and finished with a soft cloth with SiO_2 solution for 30 s. Group 2 (ten 2 mm thick samples) was not polished.

Three micro-Raman measurements were obtained from random locations on top and bottom surfaces of each sample.

Effect of sectioning

Group 3: ten 2 mm thick samples were used. Each sample was sectioned vertically on the Isomet saw through its greatest diameter. Three micro-Raman spectra were taken randomly at three locations on top and bottom surfaces, and in the middle of the section.
Group 4: ten "split" samples were used. Three micro-Raman spectra were taken on the top and bottom surfaces of both parts of the 'split' sample.

Values from corresponding regions in both 'sectioned' and 'split' samples were statistically analyzed, top with top, bottom with bottom and spectra from the middle of the sectioned with bottom of the upper 'split' sample.

Effect of storage conditions

Groups 5-8 consisted of ten 2 mm thick samples each.

Group 5 was stored at room temperature (22±2ºC) and humidity (45±3%) for 24 h.
Group 6 was stored at body temperature (37±1ºC) and humidity (90±2%) for 24 h.

Group 7 was stored in distilled water at body temperature (37±1ºC) for 24 h.

Group 8 was stored in a buffered incubation medium (BIM) at body temperature (37±1ºC) for 24 h. The pH of BIM was measured before storage of RBC samples. The composition of BIM is given in Table 15.

Table 15. The composition of the buffered incubation medium (per ml).

Calcium Chloride	0.15 mg
Magnesium Chloride	15 mg
Sodium Chloride	0.05 mg
Potassium Chloride	1.2 mg
Dibasic Sodium Phosphate	0.28 mg
Sorbitol	30 mg

Micro-Raman spectra were obtained from three randomly chosen locations on the top and bottom surface of each sample, after they had been air-dried with a mild stream of air from a dental syringe. The DC was calculated according to the formula:

$$DC=[1-Rcured / Runcured] * 100$$

where R is the ratio of peak heights at 1639 cm^{-1} and 1609 cm^{-1} in cured and uncured material.

Data for polished versus unpolished samples were analyzed using an unpaired t-test since the data showed a normal distribution and the F-test showed equal variances ($p=0.124$).

Data for sectioned versus 'split' samples were analyzed using the two-way analysis of variance (ANOVA) since the data showed a normal distribution and Bartlett's test confirmed equal variances ($p=0.370$). The data were fitted in the two-way model for DC in terms of "preparation type" and "surface" and "preparation type" x "surface" interaction. The latter term tested whether the differences in position were consistent between the two groups. Since the two-way ANOVA showed that the interaction term was not significant ($p=0.843$), the individual effects of either factor were interpreted separately.

Data for storage conditions showed a normal distribution but significantly different variances in spite of data transformation ($p<0.001$; Bartlett's test). Therefore, the differences for storage conditions at top and bottom surfaces were tested using the non-parametric Kruskal-Wallis test with Dunn's multiple comparisons post-test.

7.1.2. Results

The mean DC of polished RBC samples was 63.6%(3.2%SD) whereas mean DC of unpolished material was found to be 54.7%(5.2%). There was a statistically significant difference between DC of polished and unpolished samples ($p<0.001$; unpaired t-test).

Figure 37 shows mean (SD) values for the DC of sectioned vs. 'split' samples. The effect of sectioning was not significant i.e. both sectioned and 'split' samples showed similar DC values with mean values of 59.1% for sectioned and 58.1% for 'split' samples. Individual 95% confidence intervals for mean based on pooled SD were 57.6-60.1% for sectioned and 56.4-59.7% for 'split' samples ($p=0.396$; two-way ANOVA).

On the other hand, the effect of surface was significant i.e. the DC values were significantly different for top, middle and bottom surfaces ($p<0.001$; two-way ANOVA). The mean values were: top 63.6%, middle 58.2% and bottom 54.0%. Individual 95% confidence intervals for mean based on pooled SD were 61.6-65.1% for top, 56.2-60.8% for middle and 52.5-55.9% for bottom surfaces.

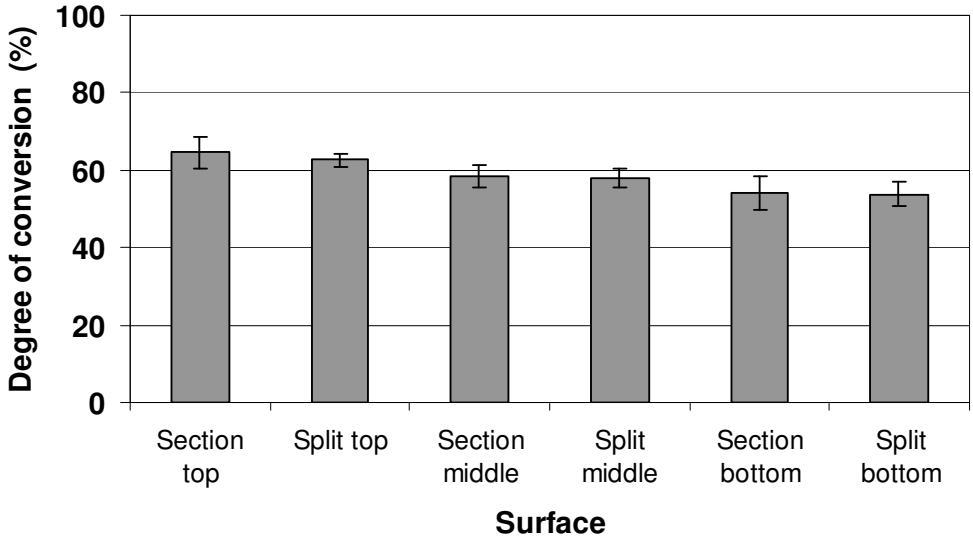

Figure 37. Mean and standard deviation of the degree of conversion of sectioned versus 'split' samples of Tetric EvoCeram.

Figure 38 presents mean and SD values of the DC of samples kept in different storage conditions. Significantly higher DC values were found in Group 8 in BIM at 37ºC compared to all other storage conditions at both top and bottom surfaces ($p<0.001$; Kruskal-Wallis test). There were no significant differences in DC values for Groups 5-7 at both top and bottom surfaces ($p>0.05$).

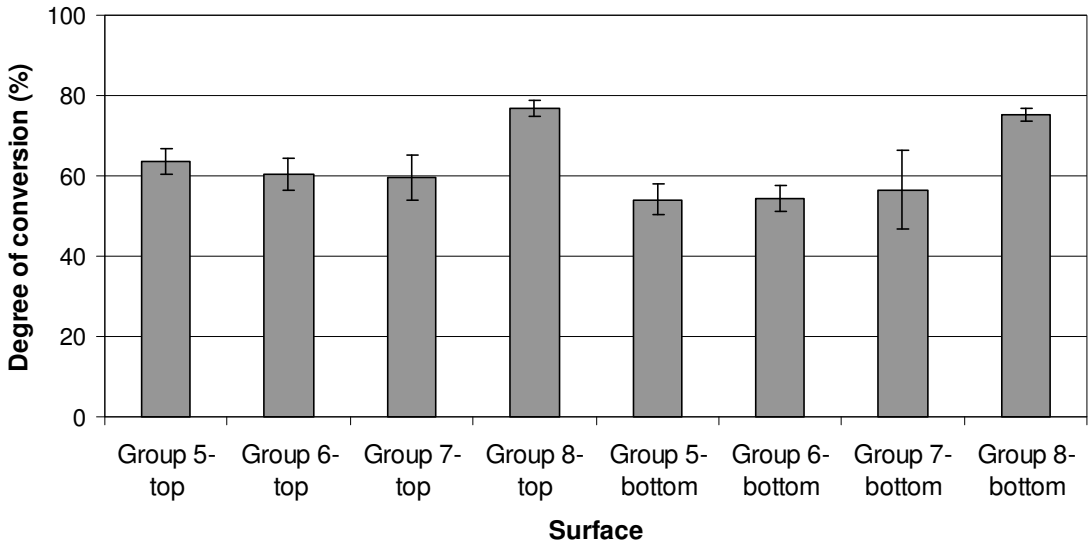

Figure 38. Mean and standard deviation of the degree of conversion of Tetric EvoCeram samples stored in different storage conditions.

7.1.3. Discussion

Tetric EvoCeram was used since it was the most recent marketed material of the Tetric "family" at the time of this study, combining the technology of previously developed materials and, therefore, reflecting the properties of a wide range of available RBCs.

Variations in sample preparation and storage conditions have been observed in previous studies on the DC of RBCs which may influence results and make data comparison difficult if not impossible. These differences are related to sample polishing after curing as well as the time, temperature, medium and humidity in which the samples are kept between curing and spectroscopic analysis (Ferracane & Greener 1984, Wentrup-Byrne 1997, Tramini 2000, Finer & Santerre 2004, Yap 2004a, Gauthier 2005a, Finer & Santerre 2007, Ye 2007, Lopez-Suevos & Dickens 2008).

Polishing directly affects the resin-rich layer which forms on top of an RBC after polymerisation due to textural features of the material, such as filler loading, size and distribution (Okazaki & Douglas 1984, Mair 1989). It is believed that filler particles have a tendency to compress together, thus exuding resin towards the surface layer. The results of the present study showed that the DC was significantly lower prior to polishing when the resin-rich layer was intact. This could be due to the inhibitory effect of the atmospheric oxygen on the polymerisation process and the lower filler content in this layer. The removal of the resin-rich layer by polishing exposed much better cured RBC material and resulted in significantly higher DC values.

Consideration was also given to whether or not sectioning of RBC samples on an Isomet type machine, influenced DC values. It has been shown that post-polymerisation heating of RBCs may result in weight loss of monomers and that the loss of volatile monomers and the "extent of cure" correlate with the temperature and duration of heat (Bagis & Rueggeberg 1997a, Bagis & Rueggeberg 1997b). In the present study, micro-Raman spectra were acquired from the middle of the sectioned samples and compared with data from the corresponding 'middle' section of the 'split' samples. According to the present study, sectioning, when performed under cooling, does not appear to be a source of material overheating, which significantly alters the DC. Although theoretically, water coolant may cause the washout of soluble unreacted monomers, the present study showed no difference in DC in samples stored in water and air (45% humidity), suggesting that there was no washing out of unreacted monomers under these conditions. Therefore, it was assumed that there was, also, no washing out of unreacted monomers during the 10 s of sectioning with water coolant.

Storage conditions may affect the 'dark' cure as well as the elution of unreacted monomers and result in different DC values. Therefore, four different storing conditions were used in the present study. BIM solutions similar to the one used in the present study are often referred to and marketed as "artificial saliva". Human saliva is no longer recommended for in vitro studies to comply with UK Health and Safety policies. To

replicate clinical conditions as closely as possible, artificial saliva, more properly designated as buffered incubation medium (BIM), is used. However, there is no standard BIM formula and it is, therefore, difficult to compare results from different studies. In the present study, results suggested that storing material samples in BIM at 37±1°C had a substantial effect on the measured DC. The DC values for both top and bottom surfaces of these samples reached 76.8% and 75.2%, respectively, being significantly higher than in samples stored at 37±1°C and humidity 90±2%, at 22±2°C and humidity 45±3% and in distilled water at 37±1°C. BIM may have resulted in greater elution of unreacted monomers due to its higher ionic strength than distilled water. The monomers contain the -COOH carboxylic acid group that will dissociate to some extent, as the anion CO^{2-} and cation $H3O^{+}$. The solubility of this carboxylic acid will increase with increasing ionic strength and it would be expected that the monomers will be more soluble in BIM than in distilled water, and so would be leached out to a greater extent. Neither high nor low humidity seem to induce the evaporation of unreacted monomers. Both conditions resulted in significantly lower DC values compared with BIM.

In addition, it was also observed that DC values decreased with depth for 2 mm thick Tetric EvoCeram samples. A tendency of decreasing DC with depth was shown in previous studies (Knezevic 2001, Bouschlicher 2004) although this was not the case in others (Bala 2005, Ilie & Hickel 2006). These findings indicate that monomer conversion in RBCs, expressed as the DC values at top and bottom surfaces, depends on material composition and the properties of the light source.

7.1.4. Conclusions

The null hypothesis was rejected since significant differences in the DC of RBC were found regarding sample preparation and storage conditions. Polishing and storage of samples in BIM at 37±1ºC for 24 h had a significant effect on the DC. Water-cooled sectioning and humidity had little effect on the DC.

7.2. Adhesive system

7.2.1. Material and Methods

Sixty samples of Excite were prepared on glass slides as explained in 5.1. and were randomly allocated to six groups (n=10). Furthermore, two groups were randomly allocated to study sample preparation methods (Groups I and II) and four groups to study storage conditions (Groups III-VI).

Thirty non-carious, human third molars were prepared as detailed in 5.1. One dentine disc was cut perpendicular to the long axis in the mid-coronal portion of each tooth using an Isomet saw with water coolant at 800 rpm. The dentine discs were randomly allocated to six groups (n=5). Groups A and B were used to determine the effect of sample preparation methods and Groups C-F to determine the effect of storage conditions on the DC of the adhesive. Prior to the application of Excite, each dentine disc was etched with 37% phosphoric acid for 15 s, rinsed with water for 10 s and blot-dried in accordance with the conventional wet bonding technique. Excite was applied to the dentine surface, gently agitated for 10 s and immediately dried by a mild stream of air.

Effect of sample preparation

In Group I on glass slides and Group A on dentine discs, each sample was covered with a Mylar strip and cured for 10 s with the bluephase LCU operating at an intensity of 650 mW/cm^2 at 1 mm tip-to-surface distance. The intensity of the LCU was monitored using the Bluephase meter (Ivoclar Vivadent, Schaan, Liechtenstein) before and after curing. The Mylar strip was discarded immediately after use. In Group II on glass slides and Group B on dentine discs, samples were cured without the Mylar strip.

In Groups I, II, A and B, micro-Raman measurements were done within 5 min after curing according to the protocol explained in 5.2. Three point spectra were taken from randomly chosen locations on the top surface of each sample whether on glass slides or dentine discs. In groups in which Excite was cured without a Mylar strip, additional spectra were taken after each sample was brushed with a disposable applicator brush to remove the oxygen inhibition layer.

Effect of storage conditions

All samples on glass slides (Groups III-VI) and dentine discs (Groups C-F) were covered with Mylar strips and cured for 10 s with the bluephase LCU operating at an intensity of 650 mW/cm^2 at 1 mm tip-to-surface distance. Mylar strips were discarded immediately after use. All groups were stored for 24 h in different storage conditions:
Groups III and C were stored at 22±2ºC and 45±3% humidity.
Groups IV and D were stored at 37±1ºC and 90±2% humidity.
Groups V and E were stored in distilled water at 37±1ºC.
Groups VI and F were stored in BIM at 37±1ºC. The pH of BIM was measured before storage of adhesive samples. The composition of BIM is given in Table 15.
Groups IV-VI and D-F were kept in light-proof containers in a water bath set at 37ºC. The temperature and humidity were monitored using a USB-502 logger (Measurement Computing Corp., Norton, MA, USA).

The samples of Excite on glass slides in Groups IV, V and VI were deformed after storage. In order to obtain micro-Raman spectra from these samples, milling into fine particles was required to homogeneously disperse them on the microscopic slide. It was, therefore, impossible to obtain spectra from top surfaces as was initially done, so groups IV, V and VI were not included in the final experiment. Only DC values for Group III were analysed statistically and taken into account.

All samples of Excite on dentine discs in Groups C-F were intact after storage and were included in the study. The samples stored in distilled water and BIM were taken out of the storage medium and blot-dried prior to micro-Raman analysis.

Micro-Raman measurements were done after 5 min and 24 h post-curing according to the protocol detailed in 5.2. Data post-processing for both sample preparation and storage conditions was done as detailed in 5.2. The DC was calculated using the same formula as used in 7.1.1.

The data for Groups I and II on glass slides and A-F on dentine discs showed a normal (Gaussian) distribution, but significantly different variances in spite of several transformation attempts ($p<0.001$). Therefore, the non-parametric Kruskal-Wallis test was used to assess the differences between the medians for samples prepared either on glass slides or dentine discs.

Since the assumptions for parametric testing were met for the corresponding groups on glass slides and dentine discs, unpaired t-tests were used to evaluate the differences between the means for the following groups: Group I vs. Group A; Group II vs. Group B (before brushing) and Group II vs. Group B (after brushing). The Bonferroni correction was applied so the p value for each t-test was set at 0.017. The data for Group III on glass slides before and after storage showed a normal distribution with equal variances and were analysed using a paired t-test. Because only one group on glass slides was tested, the p value was 0.05. Since the assumptions for parametric testing were met for samples on dentine discs before and after storage, paired t-tests were also used to evaluate the differences between the means, but the p value of each test was adjusted to 0.0125 (Bonferroni correction). The power and sample size calculation showed that even with these p values, both the unpaired and paired t-tests would have at least 80% power of detecting as statistically significant the difference in DC of 5% between the groups.

7.2.2. Results

Figure 39 shows mean and SD values for the DC of Excite with respect to different sample preparation methods.

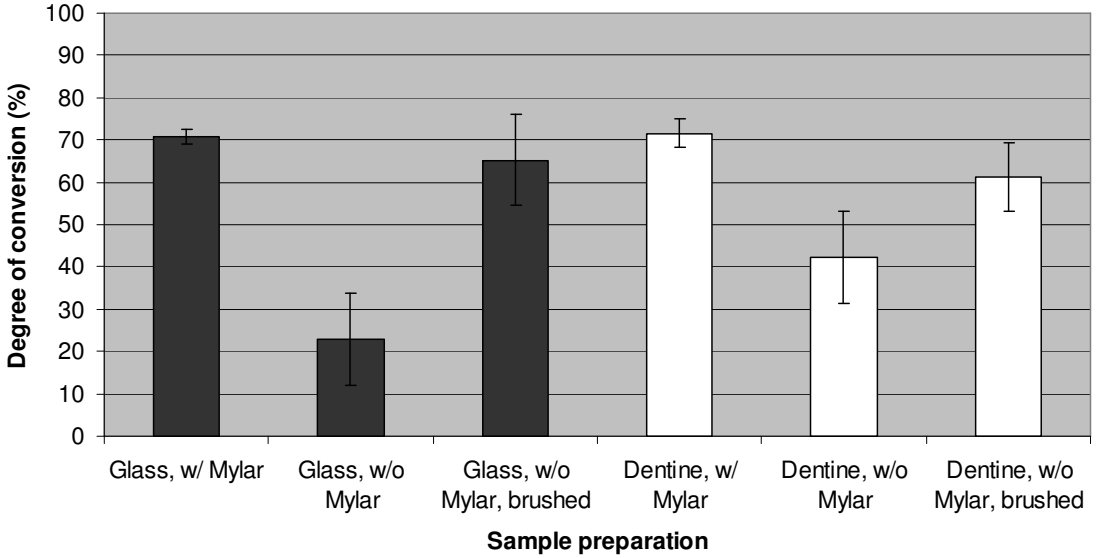

Figure 39. Mean and standard deviation of the degree of conversion of Excite with respect to different sample preparation methods.

For glass slides, the mean (SD) values were 69.4%(3.2%) for Group I, 22.8%(10.7%) for Group II initially and 65.1%(10.3%) after brushing. The median DC values for Excite in Group II before brushing were significantly lower than Group II after brushing and Group I ($p<0.001$; Kruskal-Wallis test). There was no significant difference between Group I and Group II after brushing ($p>0.05$).

For dentine discs, the mean (SD) values were 71.6%(3.45%) for Group A and 42.2%(10.9%) for Group B initially and 61.2%(8.2%) after brushing. The median DC values in Groups A and B initially and after brushing were significantly different ($p<0.05$; Kruskal-Wallis test).

Significantly lower DC values were observed after curing with a Mylar strip on glass slides than dentine discs ($p=0.024$; unpaired t-test). Significantly lower DC values were observed after curing without a Mylar strip on glass slides compared to dentine discs ($p<0.001$). Brushing resulted in comparable DC values for glass slides and dentine discs ($p=0.07$).

The mean (SD) values in Group III before and after storage for 24 h at 22±2ºC and 45±3% humidity were 69.9%(3.3%) and 73.1%(3.2%), respectively. The mean DC values after 24 h storage were significantly higher than those obtained 5 min post-curing ($p<0.001$; paired t-test).

Figure 40 shows the mean and SD values for Excite on dentine discs before and after storage in different conditions. The mean DC values were between 70.4% and 72.3% before storage and increased to values between 73.4% in air at 22±2ºC and 45±3% humidity and 90.2% in BIM at 37±1ºC. No significant difference was observed in the DC medians for all groups before storage ($p=0.179$). After storage, significant differences were observed in the DC medians for all groups ($p<0.05$), except for Groups C and D, stored in air at 22±2ºC and 45±3% humidity and air at 37±1ºC and 90±2% humidity ($p>0.05$; Kruskal-Wallis test).

When groups before and after storage were compared, significantly higher mean DC values were found in all groups after storage compared to those obtained before storage (Group C, $p=0.002$; Group D, $p=0.007$; Group E, $p<0.001$; Group F, $p<0.001$; paired t-test).

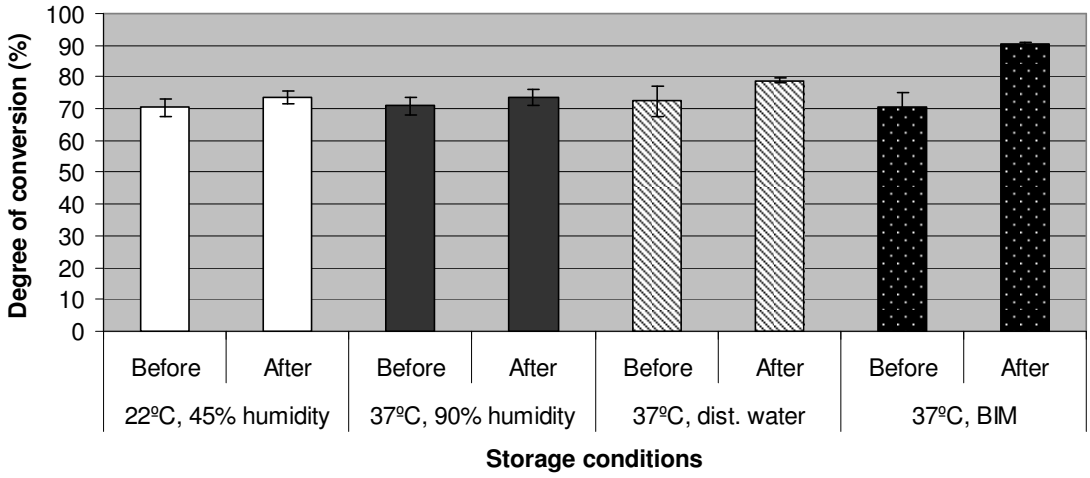

Figure 40. Mean and standard deviation of the degree of conversion of Excite cured on dentine discs before and after storage in different conditions.

7.2.3. Discussion

The results of this study showed that sample preparation methods and storage conditions had a significant effect on the DC of the etch-and-rinse adhesive, Excite. Therefore, the null hypothesis was rejected.

Significantly lower DC values were obtained when Excite was cured on glass slides or dentine discs without a Mylar strip covering compared to the values obtained after curing the material with a Mylar strip covering. Brushing the surface layer resulted in significantly higher DC in all samples. This confirms that atmospheric oxygen impairs polymerisation in the superficial zones of the adhesive resulting in the formation of the oxygen inhibition layer, as was previously reported for etch-and-rinse systems using FTIR and SEM (Kim 2006) and self-etch systems using NMR (Nunes 2005). The same effect of oxygen was reported for RBCs (Okazaki & Douglas 1984, Mair 1989, Rueggeberg & Margeson 1990) and was found in the previous study in 7.1.

Lower DC values for Excite were found after curing on glass slides compared to dentine discs irrespective of whether the Mylar strips were used. Though Excite is an etch-and-rinse adhesive applied after dentine is etched with phosphoric acid, it contains a certain amount of acidic monomers, phosphonic acid acrylate, as well as the hydrophilic monomer, HEMA. Glass is an inert substrate which does not allow the diffusion of adhesive components. On the other hand, interaction of acidic monomers and HEMA with dentine may result in the change in monomer distribution and phase separation when dentine is used as the substrate (Spencer 2002). This could alter the polymerisation kinetics and result in different DC values on glass slides compared to dentine discs. Therefore, care should be taken when extrapolating to clinical conditions the DC values obtained on glass slides.

Glass slides proved to be inadequate for measuring the DC under different storage conditions. Adhesive samples were deformed after 24 h storage at 37ºC in distilled water, BIM or high humidity air. It was not possible to obtain micro-Raman spectra from the top surfaces of such samples and further processing of samples could result in spectra acquisition from locations other than the top surface, invalidating any comparisons. Only samples cured on glass slides and stored in air at 22ºC and 45% humidity were undeformed and suitable for post-storage analysis. The present results confirmed that a 'dark' cure occurred in Excite under these conditions, resulting in significantly higher DC compared to values obtained 5 min after curing. This is in accordance with a previous study which reported significantly higher DC values for 6 self-etch and one experimental adhesive system after 24 h of storage in "ambient laboratory conditions". The adhesives were applied to an ATR accessory crystal and analysed using FTIR but the temperature and humidity conditions were not stated (Kanehira 2006). Conversely, using FT-Raman spectroscopy, no significant difference in the DC was found for etch-and-rinse and self-etch adhesives after 24 h storage in dark bottles at 37ºC (Sadek 2008). However, the humidity was not stated. In another study using FTIR spectroscopy, different BisGMA/TEGDMA-based experimental adhesives cured on KBr discs showed higher DC values after 48 h of storage compared to values

obtained immediately after curing (Bae 2005). Neither the medium nor temperature and humidity were stated. In another study, storage of experimental TEGDMA-based RBCs for 24 h in air or distilled water at 37ºC resulted in significantly higher DC values compared to those obtained 15 min after curing. Similar DC values for the BisGMA/TEGDMA mixture were found irrespective of the storage conditions. TEGDMA-based mixtures containing acidic monomers resulted in comparable of higher DC in dry compared to wet storage conditions (Lopez-Suevos & Dickens 2008).

In the present study, 24 h storage of Excite samples applied to dentine discs resulted in significantly higher DC values irrespective of the storage conditions, though the extent of this increase varied. The highest increase in DC was observed after storage at 37ºC in BIM, similar to the findings of the study in 7.1. on Tetric EvoCeram. Unlike the results for Tetric EvoCeram, Excite DC showed significantly higher values after storage in distilled water at 37ºC compared to air at 37ºC and 90% humidity and 22ºC and 45% humidity. Storage in air resulted in the smallest increase in DC irrespective of the temperature and humidity.

The present results showed that a 'dark' cure occurred in Excite on dentine discs. This was the same as was found when Excite was cured on glass slides and stored in air at 22ºC and 45% humidity. The DC was further increased when samples were stored in distilled water or BIM. This could be attributed to the elution of unreacted and poorly reacted monomers and oligomers from the adhesive surface. Previous studies have reported monomer elution from RBCs (Munksgaard 2000, Ortengren 2001, Michelsen 2003, Moon 2004, Michelsen 2008, Uzunova 2008), resin mixtures (Kim & Chung 2005, Sideridou & Achilias 2005, Zhang & Xu 2008), fissure sealants (Moon 2000), orthodontic adhesives (Eliades 1995, Eliades 2007) and, most recently, adhesive systems (Altintas & Usumez 2009). It has been previously shown that the presence of an oxygen inhibition layer can be completely prevented only by curing resin-based materials in an atmosphere devoid of oxygen (Rueggeberg & Margeson 1990, Endo 2007). The use of Mylar strips in the present study reduced the inhibitory effect of atmospheric oxygen on

the polymerisation kinetics but may not have fully prevented the formation of an oxygen inhibition layer on the adhesive surface.

The higher increase in DC in Excite, after storage in BIM compared to distilled water, may be explained by the higher ionic strength of BIM. This could bring about an increased dissociation of the COOH group in the monomer and additionally increase monomer solubility. This was also suggested as an explanation for the same findings for Tetric EvoCeram in 7.1.

After storage in distilled water at 37ºC for 24 h, there was a significant increase of the adhesive DC (Excite). This was different to the results obtained for the resin-based composite (Tetric EvoCeram), under the same conditions, when it was found that the DC remained virtually unchanged. This may indicate that leachable monomers from adhesives may be more readily available for elution than those from RBCs. Future studies should investigate whether this phenomenon applies to a wider range of adhesives and RBCs. If it is found that most cured adhesives have a greater pool of leachable monomers compared to RBCs, this could have clinical implications as it is the adhesive and not the RBC which is in direct contact with the vital tooth tissues.

7.2.4. Conclusions

The effect of oxygen inhibition on polymerisation was confirmed irrespective of the substrate to which the etch-and-rinse adhesive was applied. The effect of the atmospheric oxygen on the DC was significantly reduced by the use of Mylar strips during adhesive curing.

When the etch-and-rinse adhesive was applied to glass slides and stored in air at 22±2ºC and 45±3% humidity, a significantly higher DC was found after 24 h, confirming a ‘dark’ cure phenomenon. Similarly, a significantly higher DC was found under all stated

storage conditions when the adhesive was applied to dentine discs. In addition to this 'dark' cure phenomenon, storage of the adhesive on dentine discs in liquid media resulted in a further increase in the DC, suggesting that monomer elution had occurred.

Glass slides may be used for determining the DC of one-bottle etch-and-rinse systems immediately after curing but they are not adequate for storing samples as deformation may occur in liquid media and high humidity air. For determining the DC by micro-Raman spectroscopy, when samples are required to be stored, dentine discs are more appropriate than glass slides as sample deformation does not occur on dentine discs.

CHAPTER 8

THE DEGREE OF CONVERSION IN ADHESIVE SYSTEMS AS A FUNCTION OF TIME

The aim of this study was to determine the DC of adhesive systems as a function of time. The objective was to quantify the DC of adhesive systems on glass slides related to increasing curing times. The null hypotheses were:
(1) Increasing curing times have no effect on the DC of adhesive systems and
(2) There is no significant difference in the DC of different adhesive systems cured for the maximum curing time of 20 s.

8.1. Materials and Methods

Table 16 lists the adhesive systems used in this study. Forty samples of each material were prepared as explained in 5.1. and allocated to one of four groups (n=10) according to curing times.

Each sample was cured using an LED LCU (Elipar Freelight2, 3M ESPE, St. Paul, MN, USA) for 5 s, 10 s or 20 s at an intensity of 1000 mW/cm^2. In addition, the Elipar Freelight2 soft-start mode, at an initial intensity of 380 mW/cm^2 rising to the maximum of 1000 mW/cm^2 over 5 s, was used for 10 s. The tip-to-surface curing distance was 1 mm, maintained with a standardised light guide. The intensity of the LCU was monitored before and after polymerisation of adhesives using a Bluephase meter.

Table 16. Adhesive systems used in the present study.

Type	Adhesive system	Composition
etch-and-rinse, 1-bottle	Excite	Phosphonic acid acrylate, HEMA, BisGMA, dimethacrylates, silica, ethanol, catalysts, stabilizers
	James-2	HEMA, UDMA, HPMA, GDMA, methacrylized polyalkenoate, catalysts, inhibitors. Solvent-free
	One-Coat Bond	HEMA, HPMA, GDMA, UDMA, methacrylized polyalkenoate, amorphous silica. Solvent-free
2-step self-etch, 2-bottle	AdheSE	Primer: Phosphonic acid acrylate, bis-acrylamide, water, initiators, stabilizers Bond: HEMA, BisGMA, dimethacrylates, Si-dioxide, initiators, stabilizers
	Clearfil SE Bond	Primer: MDP, HEMA, dimethacrylate hydrophilic, camphorquinone, N,N-diethanol p-toluidine, water. Adhesive: MDP, BisGMA, HEMA, dimethacrylate hydrophobic, camphorquinone, N,N-diethanol p-toluidine, silica
	One Coat Bond	Primer: water, acrylamidosulfonic acid, HEMA, GMA, GDMA, methacrylized polyalkenoate Bond: HEMA, GMA, GDMA, UDMA, methacrylized polyalkenoate
1-step self-etch, 1-bottle	AdheSE One	Bis-acrylamide, water, bis-methacrylamide dihydrogen phosphate, amino acid acrylamide, hydroxyl alkyl methacrylamide, highly dispersed silicon dioxide, catalysts, stabilizers
	Clearfil 3S Bond	MDP, BisGMA, HEMA, initiator, stabilizer, ethanol, water, filler
	One Coat Bond	Methacrylates, photoinitiators, ethanol
	Adper Prompt L-Pop	Methacrylated phosphoric esters, BisGMA, HEMA, CQ-based initiator, stabilizer, polyalkenoic acid, water
	G Bond	4-MET, UDMA, acetone, water, sillanated colloidal silica, initiator
	Xeno III	Part A: HEMA, water, ethanol, BHT, nanofiller Part B: Pyro-EMA, PEM-F, UDMA, BHT, CQ, EPD

Micro-Raman analysis was done within 5 min post-curing according to the protocol detailed in 5.2. Spectra of the uncured materials were obtained during the same session and used as references for DC calculation. Point spectra were taken from three randomly chosen locations. Post-processing of data was performed in LabSpec4.18 according to the principles detailed in 5.2. The DC of the adhesive was calculated according to the following formula:

$$\mathbf{DC = (1 - R_{cured} / R_{uncured}) \; X \; 100}$$

where R is the ratio of aliphatic and aromatic peak intensities at 1639 cm^{-1} and 1609 cm^{-1} in cured and uncured BisGMA-based systems, or the ratio of aliphatic and carbonyl peak intensities at 1639 cm^{-1} and 1720 cm^{-1} in non-BisGMA-based systems. The internal standards in BisGMA-based and non-BisGMA-based systems were the aromatic peak at 1609 cm^{-1} and the carbonyl peak at 1720 cm^{-1}, respectively.

Although data exhibited Gaussian distribution (Kolmogorov-Smirnov test, $p>0.15$), Bartlett's test for equal variances showed significant differences ($p<0.001$) despite several attempts to transform data. Therefore, a non-parametric test, the Kruskal-Wallis test with Dunn's multiple comparisons post-test, was used to evaluate the differences in DC at each curing time for each adhesive system. The same test was used to evaluate the differences between all the adhesive systems after the maximum curing time of 20 s. No inter-group comparison was done for the intermediate curing times of 5 s and 10 s at 1000 mW/cm^2 and 10 s in the soft-start mode.

8.2. Results

The mean and SD values for each adhesive system and each curing time are presented in Figures 41-44. The summary of statistical analysis is presented in Tables 17-19.

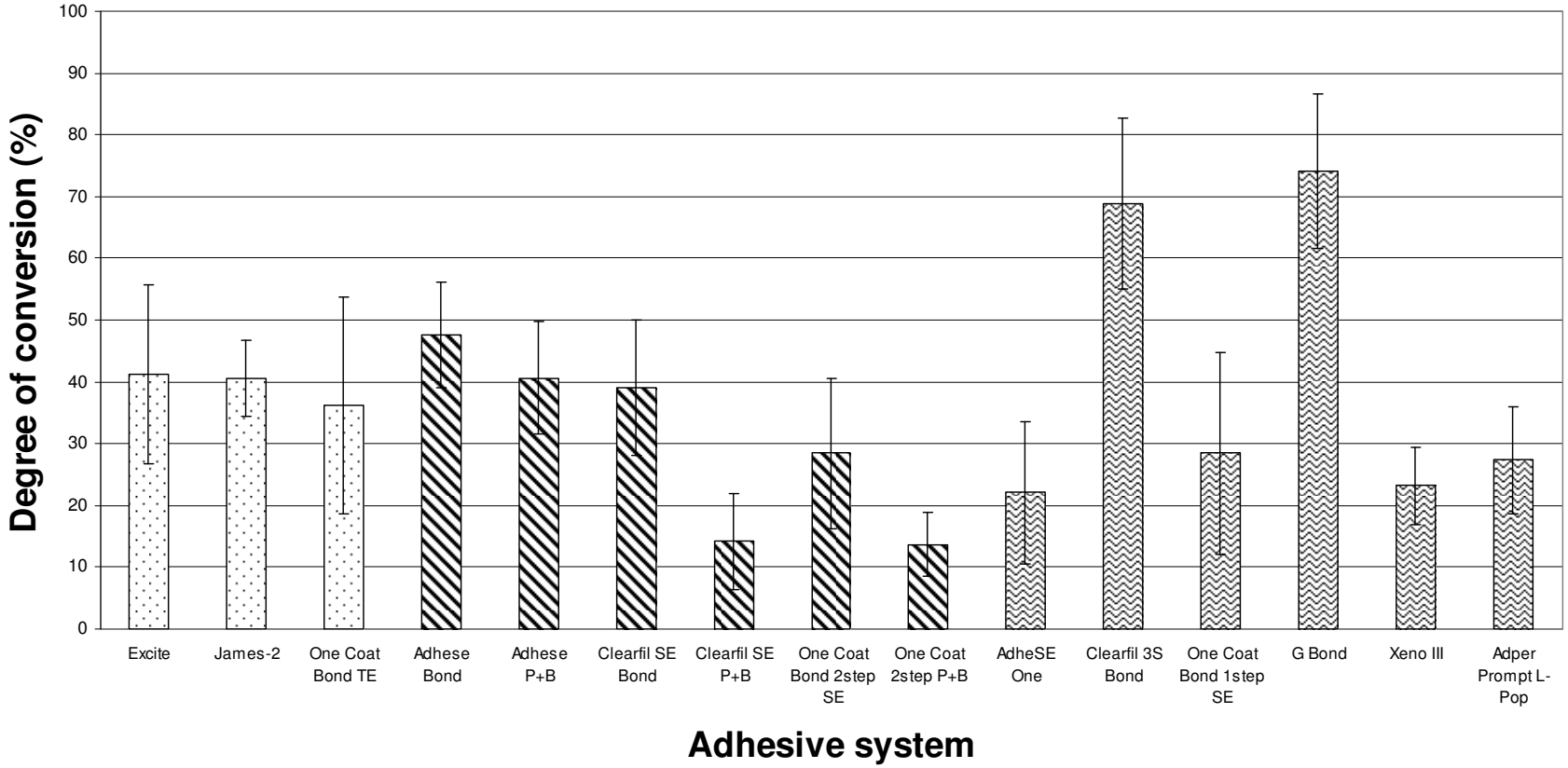

Figure 41. Mean and standard deviation values of the degree of conversion for each adhesive system (5 s curing time).

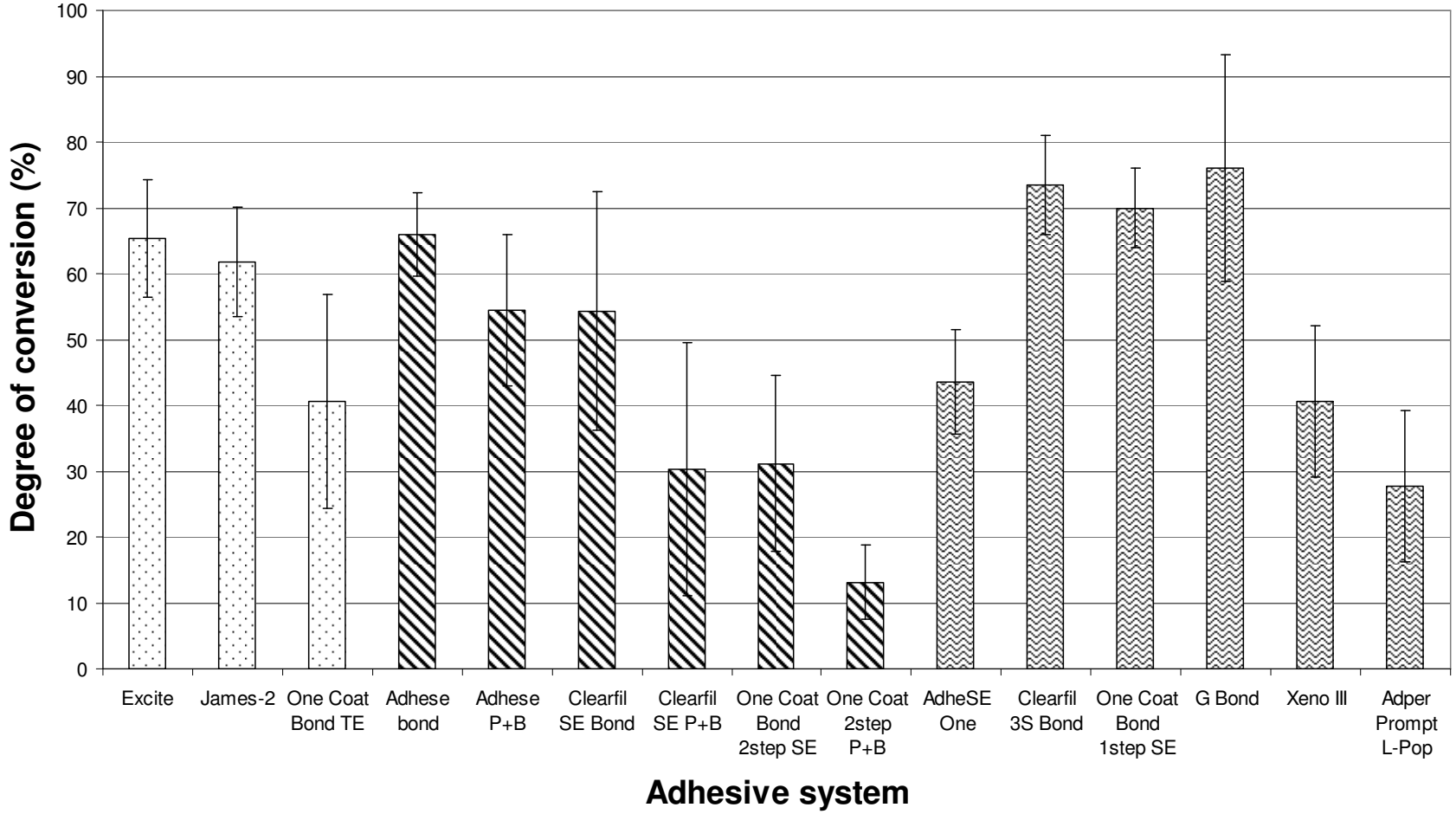

Figure 42. Mean and standard deviation values of the degree of conversion for each adhesive system (10 s curing time).

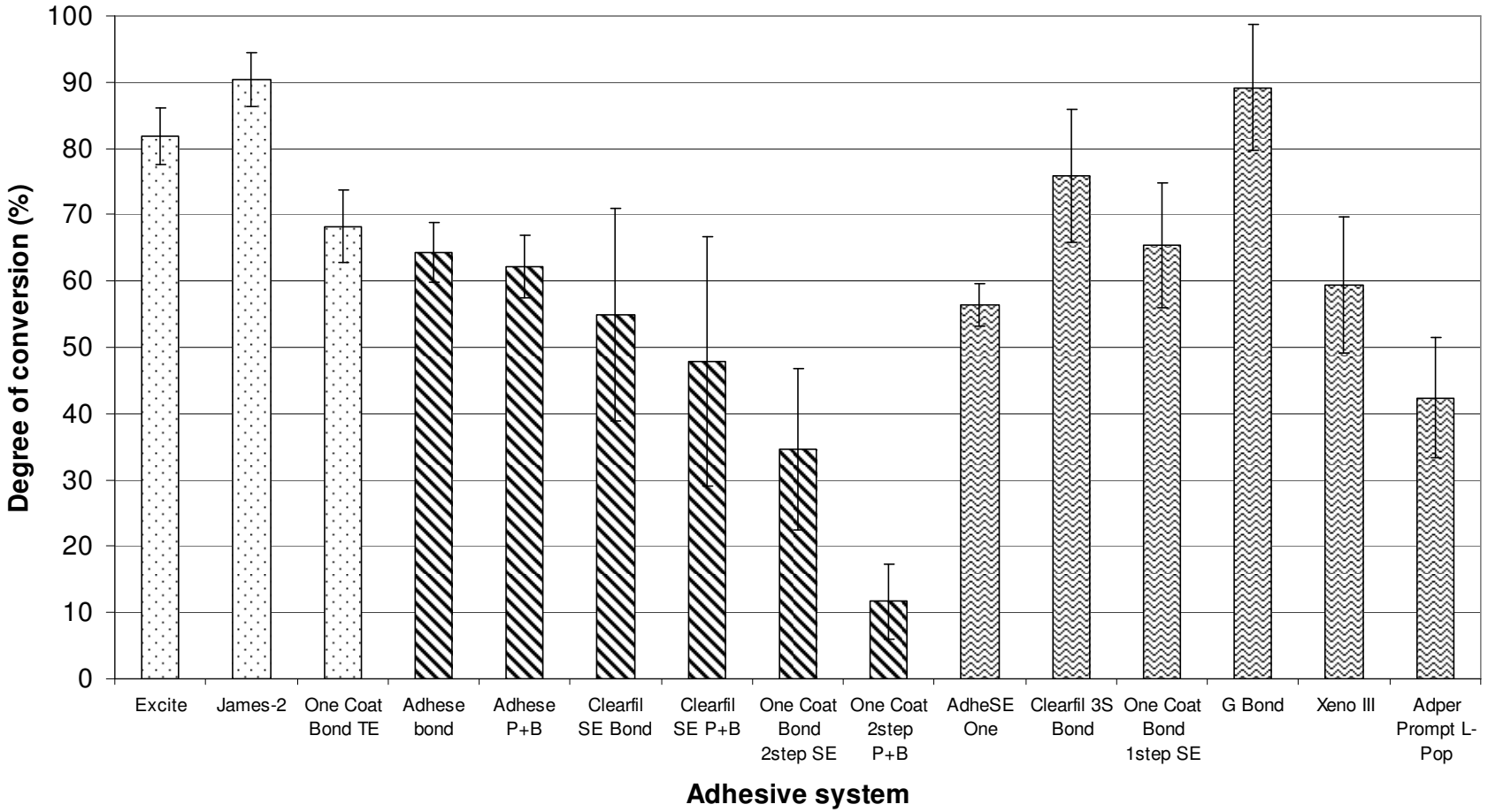

Figure 43. Mean and standard deviation values of the degree of conversion for each adhesive system (20 s curing time).

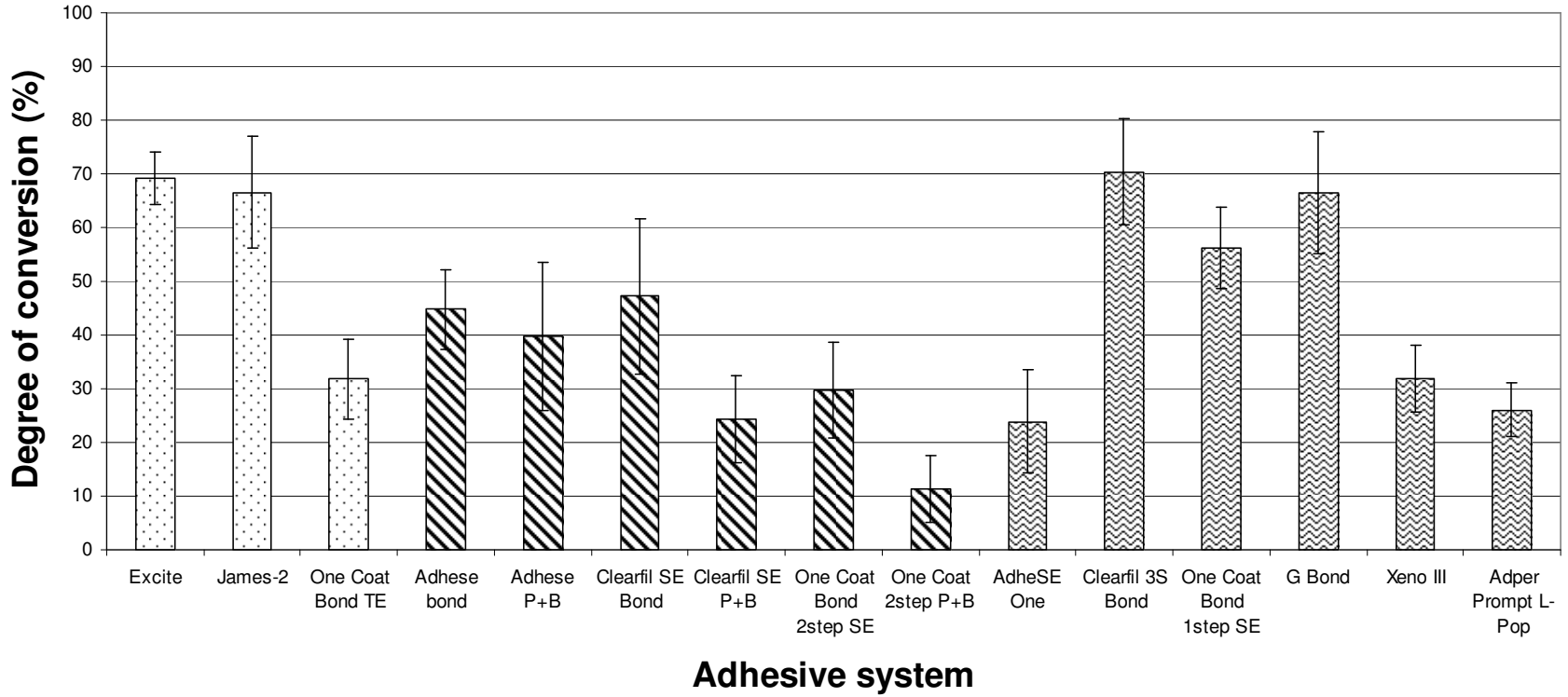

Figure 44. Mean and standard deviation values of the degree of conversion for each adhesive system (10 s soft-start curing time)

Etch-and-rinse adhesive systems

Table 17. The summary of statistical analysis for the etch-and-rinse systems.

Adhesive system	Mean	SD	Minimum	Q1	Median	Q3	Maximum
Excite 5 s	41.21	14.43	14.95	30.70	41.32	54.57	69.57
Excite 10 s [1]	65.28	8.90	44.96	58.59	66.91	71.74	79.36
Excite 20 s	81.31	4.09	76.36	78.21	80.38	84.45	88.68
Excite soft [1]	69.16	4.87	58.87	66.65	69.75	72.64	76.90
James 5 s	40.57	6.12	20.21	37.52	41.26	44.81	51.56
James 10 s [2]	61.72	8.31	46.62	55.49	61.99	66.47	78.46
James 20 s	90.45	4.08	81.38	88.67	91.87	92.99	96.22
James soft [2]	66.51	10.40	55.00	58.68	62.65	70.42	86.54
1Coat TE 5 s [3]	36.11	17.55	11.74	19.58	34.51	55.19	63.06
1Coat TE 10 s [3]	40.61	16.19	11.55	26.36	42.74	55.77	64.66
1Coat TE 20 s	68.25	5.51	59.00	61.60	70.69	71.47	74.48
1Coat TE soft [3]	31.82	7.48	20.36	26.84	31.43	35.40	55.12

Cells with the same superscripts indicate no significant difference within each subgroup ($p>0.05$). Values with no superscipts are significantly different from all other values in their subgroup. Interquartile range is the difference between Q3 and Q1.
SD – standard deviation
Q1 – first quartile
Q3 – third quartile

One Coat Bond TE showed significantly higher DC values when cured for 20 s compared to other curing times including 10 s in the soft-start mode ($p<0.05$). There was no significant difference between the DC values for 5 s and 10 s at 1000 mW/cm^2 and 10 s in the soft-start mode ($p>0.05$). Unlike One Coat Bond TE, 5 s, 10 s and 20 s curing time produced significantly higher DC values for Excite and James 2. However, no significant difference in the DC values was found for 10 s at 1000 mW/cm^2 and 10 s in the soft-start mode for both adhesive systems ($p>0.05$).

Two-step self-etch adhesive systems

Table 18. The summary of statistical analysis for the two-step self-etch systems.

Adhesive system	Mean	SD	Minimum	Q1	Median	Q3	Maximum
Adhese B 5 s [1]	47.49	8.54	29.49	39.01	49.74	54.57	58.56
Adhese B 10 s [2]	65.95	6.27	55.76	62.56	65.98	68.86	78.55
Adhese B 20 s [2]	64.57	4.49	55.57	61.87	64.72	67.02	73.23
Adhese B soft [1]	44.79	7.36	33.43	40.96	42.25	47.85	62.90
Adhese P+B 5 s [3]	40.64	9.09	24.19	34.25	40.01	48.86	55.86
Adhese P+B 10 s [4]	54.38	11.48	34.25	42.24	57.41	65.86	70.98
Adhese P+B 20 s [4]	62.15	4.68	54.26	58.37	61.94	66.69	71.23
Adhese P+B soft [3]	39.79	13.84	22.65	30.83	34.87	43.46	69.63
Clearfil SE B 5 s [5]	38.96	10.98	18.59	30.77	37.63	45.04	63.83
Clearfil SE B 10 s [6]	54.32	18.14	23.16	38.50	54.57	71.39	78.90
Clearfil SE B 20 s [6]	54.85	16.03	25.81	40.59	56.54	70.91	81.00
Clearfil SE B soft [5,6]	47.16	14.44	25.35	33.83	45.96	61.88	70.62
Clearfil SE P+B 5 s	14.16	7.79	0.28	6.95	14.25	21.34	27.81
Clearfil SE P+B 10 s [7]	30.28	19.27	1.82	12.12	31.13	49.41	63.77
Clearfil SE P+B 20 s	47.81	18.84	14.55	28.80	49.27	61.10	77.85
Clearfil SE P+B soft [7]	24.30	8.04	12.21	20.27	22.78	27.50	40.14
1Coat B 5 s [8]	28.48	12.17	3.98	18.98	29.89	37.22	52.83
1Coat B 10 s [8]	31.14	13.34	2.54	19.48	33.94	43.86	52.93
1Coat B 20 s [8]	34.63	12.25	18.37	28.05	31.93	38.83	58.35
1Coat B soft [8]	29.72	9.03	17.99	22.78	29.21	35.36	52.83
1Coat P+B 5 s [9]	13.66	5.20	2.91	10.16	12.65	18.29	24.89
1Coat P+B 10 s [9]	13.16	5.62	3.36	8.10	14.14	18.29	20.71
1Coat P+B 20 s [9]	11.66	5.69	4.53	6.22	11.30	16.03	23.62
1Coat P+B soft [9]	11.25	6.22	1.09	4.74	10.82	15.28	25.49

Legend as for Table 17.

Adhese B and P+B, when cured for 20 s and 10 s at 1000 mW/cm^2, produced similar DC values ($p>0.05$). These values were significantly higher than those obtained for 5 s and 10 s in the soft-start mode ($p<0.05$). No significant differences were found for 5 s and 10 s in the soft-start mode for both systems ($p>0.05$). Clearfil SE B showed similar DC values when cured for 20 s and 10 s at 1000 mW/cm^2 ($p>0.05$). These values were significantly higher than those obtained after 5 s of curing ($p<0.05$). Clearfil SE P+B showed comparable DC values when cured for 20 s and 10 s at 1000 mW/cm^2 ($p>0.05$). These values were significantly higher than those obtained for 5 s and 10 s in the soft-start mode ($p<0.05$). No significant difference was found for 5 s and 10 s in the soft-start mode ($p>0.05$). One Coat B showed similar DC values at 5 s, 10 s, and 20 s and 10 s soft-start mode ($p>0.05$). One Coat P+B showed similar DC values at 5 s, 10 s, and 20 s and 10 s soft-start mode ($p>0.05$).

One-step self-etch adhesive systems

Table 19. The summary of statistical analysis for the one-step self-etch systems.

Adhesive system	Mean	SD	Minimum	Q1	Median	Q3	Maximum
Adhese One 5 s [1]	22.07	11.46	6.98	10.96	19.40	33.63	43.26
Adhese One 10 s	43.52	7.93	24.17	39.20	44.11	49.41	59.16
Adhese One 20 s	56.48	3.20	50.35	54.51	57.51	58.73	60.39
Adhese One soft [1]	23.86	9.64	6.90	15.96	24.27	30.91	42.62
Clearfil 3S 5 s [3,4]	68.85	13.73	40.29	58.17	73.50	79.70	88.99
Clearfil 3S 10 s [3,4]	73.54	7.53	53.32	68.15	73.56	79.32	85.67
Clearfil 3S 20 s [3]	75.90	10.07	50.99	70.79	78.20	82.26	89.83
Clearfil 3S soft [4]	70.35	9.93	55.54	60.28	69.75	78.52	87.68
G Bond 5 s [5,6]	74.12	12.53	44.04	65.59	75.79	85.44	91.48
G Bond 10 s [5]	76.01	17.21	40.14	60.23	79.93	91.85	95.20
G Bond 20 s	89.10	9.51	64.91	88.07	91.25	94.39	96.42
G Bond soft [6]	66.59	11.34	40.80	61.90	70.42	74.40	78.16
Xeno III 5 s	23.18	6.20	5.23	21.16	23.46	26.67	33.90
Xeno III 10 s	40.65	11.45	3.31	36.11	42.99	48.34	55.02
Xeno III 20 s	59.33	10.26	41.19	49.22	62.22	65.66	74.94
Xeno III soft	31.89	6.21	13.25	28.97	33.46	34.36	52.64
Adper PLP 5 s [7]	27.30	8.64	1.89	24.77	29.29	31.61	41.85
Adper PLP 10 s [7]	27.71	11.48	3.80	19.04	30.63	36.08	47.84
Adper PLP 20 s	42.38	9.01	29.72	33.66	43.14	51.01	55.36
Adper PLP soft [7]	26.04	5.02	16.10	22.92	25.25	30.71	36.59
1Coat SE 5 s	28.40	16.31	1.23	13.38	27.50	44.03	55.39
1Coat SE 10 s [8]	69.97	6.05	58.30	64.93	70.08	75.13	78.65
1Coat SE 20 s [8]	65.45	9.37	53.30	56.77	65.02	74.99	83.37
1Coat SE soft	56.29	7.54	42.00	51.15	56.41	61.47	68.20

Legend as for Table 17.

The curing time of 20 s resulted in significantly higher DC values for Adhese One, Xeno III, G Bond and Adper Prompt L-Pop compared to 5 s, 10 s and 10 s soft-start ($p<0.05$). Clearfil 3S gave significantly higher values at 20 s compared to 10 s soft-start ($p<0.05$). One Coat Bond showed similar DC values for 10 s and 20 s ($p>0.05$). Significantly higher DC values were found between 5 s and 10 s as well as between 10 s and 20 s curing times for Xeno III ($p<0.05$).

Adhese One gave significantly higher DC values at 10 s compared to 5 s and 10 s soft-start ($p<0.05$). There was no significant difference between 5 s and 10 s soft-start ($p>0.05$). Adper Prompt L-Pop showed similar results at 5 s and 10 s and also 10 s soft-start ($p>0.05$). G Bond showed similar results at 5 s and 10 s and also 10 s soft-start ($p>0.05$).

Inter-group comparison for the maximum curing time of 20 s

When inter-group comparison of DC values after 20 s was made, Excite, James 2 and G Bond showed the highest median and mean values which were in excess of 80% ($p>0.05$). One Coat Bond TE, Adhese B, Adhese P+B, Clearfil SE B, Clearfil SE P+B, Adhese One, Clearfil 3S, One Coat Bond 1S SE, G Bond and Xeno III showed median and mean DC values between 50% and 70%. One Coat B and Adper Prompt L-Pop gave median and mean DC values between 40% and 50%. Statistically significant differences between adhesive systems are indicated in Table 20. The median and mean DC values for One Coat P+B of about 10% were significantly lower when compared to all the other adhesive systems ($p<0.05$).

Adhese B and P+B as well as Clearfil SE B and P+B showed no statistically significant differences in the DC values after 20 s ($p>0.05$). One Coat B showed significantly higher DC values than One Coat P+B ($p<0.05$).

Table 20. The summary of statistical analysis for inter-group comparison of the degree of conversion of all adhesive systems cured for 20 s.

	James	1Coat TE	Adhese B	Adhese P+B	Clrfil SE B	Clrfil SE P+B	1Coat B	1Coat P+B	Adhese 1	Clrfil 3S	G Bond	Adper	Xeno III	1Coat 1S SE
Excite	NS	NS	P<0.05	P<0.001	P<0.001	P<0.001	P<0.001	P<0.001	P<0.01	NS	NS	P<0.001	P<0.001	NS
James		P<0.001	P<0.001	P<0.001	P<0.001	P<0.001	P<0.001	P<0.001	P<0.001	NS	NS	P<0.001	P<0.001	P<0.001
1Coat TE			NS	NS	NS	P<0.01	P<0.001	P<0.001	P<0.05	NS	P<0.01	P<0.001	NS	NS
Adhese B				NS	NS	NS	P<0.001	P<0.001	NS	NS	P<0.001	P<0.001	NS	NS
Adhese P+B					NS	NS	P<0.001	P<0.001	NS	P<0.05	P<0.001	P<0.05	NS	NS
Clrfil SE B						NS	NS	P<0.001	NS	P<0.001	P<0.001	NS	NS	NS
Clrfil SE P+B							NS	P<0.01	P<0.05	P<0.001	P<0.001	NS	P<0.05	P<0.05
1Coat B								P<0.05	NS	P<0.001	P<0.001	NS	P<0.05	P<0.001
1Coat P+B									P<0.001	P<0.001	P<0.001	P<0.05	P<0.001	P<0.001
Adhese 1										P<0.001	P<0.001	NS	NS	NS
Clrfil 3S											NS	P<0.001	P<0.001	NS
G Bond												P<0.001	P<0.001	P<0.001
Adper													NS	P<0.001
Xeno III														NS

Legend:
Excite – Excite
James – James 2
1Coat TE – etch-and-rinse One Coat Bond
Adhese B – Adhese Bond only
Adhese P+B – Adhese Primer+Bond mixed
Clrfil SE B – Clearfil SE Bond only
Clrfil SE P+B – Clearfil SE Primer+Bond mixed
1Coat B – two-step self-etch One Coat Bond Bond only
1Coat P+B - two-step self-etch One Coat Bond Primer+Bond mixed
Adhese 1 – Adhese One
Clrfil 3S – Clearfil 3S
G Bond – G Bond
Adper – Adper Prompt L-Pop
Xeno III – Xeno III
1Coat 1S SE – one-step self-etch One Coat Bond

8.3. Discussion

The results of the present study indicated that:
(1) With increasing curing times, the DC increased in all studied adhesive systems, however, in 1 out of 12 systems this increase was not significantly different
(2) There are significant differences in the DC values of different adhesive systems after the maximum curing time of 20 s.
Therefore, both null hypotheses were rejected.

In the present study, the DC of 12 adhesive systems was studied as a function of time. The curing time of 10 s was used as the control since it is clinically recommended for curing adhesive systems with LED LCUs at intensities greater than 500 mW/cm^2 by most manufacturers. Additionally, 5 s was chosen as some manufacturers recommend that curing times of less than 10 s may be appropriate for curing adhesives with high-intensity LED LCUs operating at 1000 mW/cm^2 or more. Twenty seconds was chosen to assess whether the DC of adhesive systems increased beyond the manufacturers' recommended time.

As real-time monitoring of the polymerisation process was not available in our laboratory, this study was designed as a substitute. There are Raman spectrometers which allow continuous collection of spectra at intervals of 1 s or less for the duration of adhesive curing. In a previous study by Ye et al. highly sophisticated time-base collection and FTIR were used to monitor polymerisation in real-time (Ye 2007). They showed that polymerisation rate differs in different adhesive systems depending on their chemical composition and light source. The present results confirmed that the DC as a function of time varied in different adhesive systems at 5 s, 10 s and 20 s of curing. The micro-Raman spectroscopy set-up used in the present study did not allow real-time monitoring but the results are in agreement with Ye et al., showing that it may be used as reliably as real-time FTIR.

In the present study, 12 adhesive systems were used. In the etch-and-rinse group, ethanol-BisGMA-HEMA-based, Excite, and two solvent-free UDMA-HEMA-based adhesives, James-2 and One Coat Bond TE, were used. In the two-step self-etch group, two BisGMA-HEMA-based systems, Adhese and Clearfil SE, and one UDMA-HEMA-based system, One Coat Bond, were used. In the one-step self-etch group, two BisGMA-HEMA systems, Clearfil 3S and Adper Prompt L-Pop, two UDMA-based systems, G Bond and Xeno III, one acrylamide-based system, Adhese One, were used as well as One Coat Bond whose monomer composition was not disclosed by the manufacturer. Such a wide selection of adhesive systems allowed the DC as a function of time to be studied in both BisGMA and non-BisGMA-based systems.

The present results showed a general tendency of increased DC values with increased curing times and are in agreement with previous studies (Cadenaro 2005, Kim 2006, Xu 2006, Ye 2007) all of which used fewer adhesive systems. Xu et al. and Kim et al. used conventional halogen LCUs at intensities of 450-600 mW/cm^2 and one or two etch-and-rinse adhesive systems, respectively. Ye et al. used an LED (1200 mW/cm^2) and a halogen LCU (300, 550 and 800 mW/cm^2) and one etch-and-rinse and two one-step self-etch adhesive systems. Cadenaro et al. used one etch-and-rinse, one two-step self-etch and one one-step self-etch system and a conventional halogen LCU.

A linear correlation between the DC and the light energy density (i.e. light intensity multiplied by curing time) was established in a previous study (Xu 2006). However, Xu et al. used only one adhesive system in contrast to the 12 systems used in the present study where no statistical differences were found for different light energy densities in all the adhesive groups. In this respect, the present study is not in a full agreement with the conclusions arrived at by Xu et al. based on only one adhesive system.

In the present study, 1 out of 12 adhesive systems did not follow the general pattern of increased DC with increased curing time, two-step self-etch One Coat Bond. This

suggests that even 5 s or half the recommended curing time was sufficient to produce maximum DC values in this adhesive system in the conditions of the present study.

Adhesive systems from the One Coat Bond "family" showed significant differences in DC values. Furthermore, the required time to reach the highest DC values was different for the three One Coat Bond systems. In contrast to previously mentioned two-step self-etch system, etch-and-rinse One Coat Bond produced DC values between 31% and 68% and required 20 s curing time for the highest conversion. However, it cannot be concluded that these values are maximum conversion values since no longer curing times were used. One-step self-etch One Coat Bond showed DC values between 28% and 70% and required 10 s to reach the highest conversion.

The reason for different behaviour of etch-and-rinse and two-step self-etch One Coat Bond systems is difficult to explain, not only due to multiple variables but also unknown type and wt% of the initiator system. The two-step self etch system contains water as the only solvent in the primer and this may be the likely cause for significantly lower DC values for the P+B mixture compared to B only and the other One Coat Bond systems, since it has been shown that water impairs polymerisation (Wang 2006c).

On the other hand, possible differences in the monomer or initiator system in one-step self-etch One Coat Bond system could account for higher DC values. Furthermore, this system contains ethanol as a solvent unlike previous One Coat Bond systems which may alter the mobility of the system by decreasing its viscosity. The propagation phase of the polymerisation process then occurs in a less restricted environment with a postponed autodeceleration phase (Ye 2007) allowing higher DC values to be reached in a shorter time in one-step self-etch One Coat Bond compared to its predecessors.

Low DC values for Adper Prompt L-Pop (26-42%) found in the present study are in agreement with the findings of Sadek et al. Adper Prompt L-Pop contains water as a solvent and methacrylated phosphoric esters as functional monomers for enamel/dentine

demineralisation. This combination seems unfavourable, since strong hydrogen bonding affinity between the two components may prevent solvent evaporation even after extended drying time (Sadek 2008). The low DC of Adper Prompt L-Pop in the present study could also be associated with the incompatibility of its initiator system and the spectral emission range of the light source. The manufacturer's data do not state the type of the initiator system, but Sadek et al. have stated (without citing their source of information) that Adper Prompt L-Pop contains bisacylphosphine oxide (BAPO). Similarly, Ye et al. claimed that Adper Prompt contains acylphosphine oxide (APO), again without citing their source of information. Both BAPO and APO have shown maximum absorption bands between 365 nm and 416 nm (Ikemura 2008) which is below the spectral emission range of most LED LCUs.

In the present study, lower DC values were found for Clearfil SE P+B than reported in a previous study (Sadek 2008). The reason for this difference could be the fact that Sadek et al. applied the primer to iron moulds and air-dried it for 40 s prior to bond application. This could have resulted in higher water evaporation from the mixture compared to 5 s air-drying in the present study. Furthermore, these authors used a quartz-tungsten halogen LCU at an intensity of 600 mW/cm^2 for 20 s which could also account for the differences in DC values.

Though it was previously reported that primers have a negative effect on polymerisation (Jacobsen & Soderholm 1995, Hotta 1998), this only holds for two-step self-etch One Coat Bond but not for Adhese and Clearfil SE in the present study. In the latter two adhesive systems, the P+B mixture showed lower DC values after 20 s of curing compared to the Bond only but the results were not statistically significant.

The majority of adhesive systems in the present study showed significantly higher DC values after 20 s of curing compared to other curing times. Adper Prompt L-Pop and One Coat Bond TE showed no differences after curing for 5 s and 10 s at 1000 mW/cm^2 or 10 s soft-start. Higher DC values for 10 s at 1000 mW/cm^2 than 10 s in the soft-start

mode were found for Adhese, Adhese One, G Bond, Xeno III, and one-step self-etch One Coat Bond. Though curing time was the same, the amount of delivered energy was different due to differences in light intensity over this time. The energy delivered in the soft-start mode was insufficient to produce DC values in these adhesive systems comparable to 10 s.

The clinical implication, following from the fact that the majority of adhesive systems in the present study showed a significant increase in DC at 20 s compared to 10 s, remains unclear. It has been reported that a decrease in adhesive DC results in a decrease in shear bond strength (Xu 2006). However, no correlation (Sadek 2008) or a negative correlation was found between the DC and microtensile bond strength which was associated with thinner oxygen inhibition zone (Kim 2006). On the other hand, low DC may result in higher permeability (Cadenaro 2005) more water sorption (Yap 2004a) and greater elution of residual uncured monomers from adhesives and RBCs (Yap 2004b). A minimal DC for optimal clinical results is yet to be established not only related to adhesive bond strength but also to the long-term stability of the polymer network.

8.4. Conclusions

Increasing curing times resulted in higher DC values in all adhesive systems except two-step self-etch One Coat Bond. Within the limitations of the study, Adhese, Clearfil SE Bond, Clearfil 3S and one-step self-etch One Coat Bond reached similar DC values after 10 s and 20 s curing time whilst the other adhesive systems showed significantly higher DC values beyond manufacturers' recommended time. It is not possible to specify a clinical curing time that is applicable to all adhesive systems with respect to optimal conversion.

CHAPTER 9

THE DEGREE OF CONVERSION IN ADHESIVE SYSTEMS AS A FUNCTION OF LIGHT SOURCE

The aim of this study was to determine monomer conversion in adhesive systems related to light-curing units (LCUs). The objective was to quantify the DC of adhesive systems related to LCUs. The null hypothesis was that there is neither a significant difference in the DC of a particular adhesive system with respect to different LCUs nor in the DC of different adhesive systems cured with the same LCU.

9.1. Materials and Methods

Adhesive systems used in the present study were an etch-and-rinse system, Excite, a two-step self-etch system, Adhese, and a one-step self-etch system, Adhese One. Adhese was used as Adhese Bond only or Adhese Primer+Bond. The chemical composition of these systems is given in Table 21.

Ten samples of each material were prepared for each LCU. Each sample was prepared by spreading one drop of Excite, Adhese Bond (Adhese B) or Adhese One on a mat black coated, welled microscope slide over an area of approximately 2 mm^2. For Adhese Primer and Bond (Adhese P+B), one drop each of primer and bond was dispensed from the bottles on the welled microscope slide over an area of approximately 2 mm^2. In all cases, the adhesive was gently mixed for 10 s and gently blow-dried for 5 s. These were, then, covered with a Mylar strip and the material was polymerised using one of the four LEDs, or the halogen LCU (Table 22). Curing times were 10 s for the LED and either 10 s or 20 s for Prismetics. Immediately after polymerisation, the Mylar strip was removed and three micro-Raman spectra were obtained for each sample at random sites.

Table 21. Adhesive systems used in the present study.

Material	Manufacturer	Type	Composition
Excite	Ivoclar Vivadent, Schaan, Liechtenstein	Etch-and-rinse	Phosphonic acid acrylate, HEMA, bis-GMA, dimethacrylates, Si-dioxide, ethanol, catalysts, initiators, stabilizers
Adhese		2-step self-etch	**Primer:** Phosphonic acid acrylate, bis-acrylamide, water, initiators, stabilizers **Bond:** HEMA, BisGMA, dimethacrylates, Si-dioxide, initiators, stabilizers
Adhese One		2-step self-etch	**Primer:** Phosphonic acid acrylate, bis-acrylamide, water, initiators, stabilizers **Bond:** HEMA, BisGMA, dimethacrylates, Si-dioxide, initiators, stabilizers

The light intensity of all LCUs was measured using the LED radiometer by Demetron (Kerr Corp., Middleton, WI, USA). The light intensity of the halogen LCU was also measured by the conventional curing radiometer, Model 100 (SDS Kerr, Danbury, CT, USA) to confirm the reading. The light energy density was calculated in both cases by multiplying the curing time by the obtained light intensity values (Table 22).

Micro-Raman analysis was performed within 5 min of curing according to the protocol described in 5.2. Spectra of the two uncured materials were also obtained and used as references for DC calculation. The DC of the adhesive was calculated according to the following formula:

DC = (1 – Rcured / Runcured) X 100

where R is the ratio of aliphatic and aromatic peak intensities at 1639 cm^{-1} and 1609 cm^{-1} in cured and uncured adhesives.

Table 22. Light-curing units used in the present study.

LCUs	Elipar Freelight2	bluephase®	SmartLite™ PS	Coltolux	Prismetics Lite	
Code	Elipar	Bluephase	Smartlite	Coltolux	Prismetics (10 s)	Prismetics (20 s)
Manufacturer	3M ESPE	Ivoclar Vivadent	Dentsply DeTrey	Coltene Whalèdent	Dentsply DeTrey	
Light intensity* (mW/cm^2)	1000	650	710	750	380	380
Curing time	10 s	10 s	10 s	10 s	10 s	20 s
Light energy density (J/cm^2)	10	6.5	7.1	7.5	3.8	7.6

* Actual measurements

The data were analyzed using the two-way ANOVA at the significance level $\alpha=0.05$. The data were fitted in the two-way model for DC in terms of LCU + adhesive and LCU x adhesive interaction. The latter term tested whether the differences in LCU types were consistent across the three adhesive groups. Since the two-way ANOVA showed that the interaction term was significant ($p<0.001$), the differences in LCU types for each material were then tested using one-way ANOVA with the individual significance level for each at 0.0125 instead of 0.05 (Bonferroni correction). Also, two-way and one-way models were fitted for DC squared, rather than DC, since residuals versus fitted values plot showed that groups with larger estimated DC had lower variance than the other groups.

9.2. Results

Table 23 shows mean and SD values of the DC of adhesive systems cured with LCUs. The results of statistical analysis are indicated by superscript numbers. Cells with the

same superscript numbers indicate no statistically significant difference between the LCUs for each adhesive system separately ($p>0.05$).

When curing Excite, Prismetics (20 s) produced statistically higher DC values than the four LEDs and Prismetics (10 s) ($p<0.05$). Prismetics (10 s) gave comparable results as Elipar, Bluephase and Smartlite but higher than Coltolux. There were no significant differences between the LED LCUs ($p>0.05$).

When curing Adhese B, Prismetics (20 s) and Elipar produced statistically higher DC values than Prismetics (10 s) and Bluephase ($p<0.05$) but comparable to Smartlite and Coltolux ($p>0.05$). There were no significant differences between Prismetics (10 s), Bluephase, Smartlite and Coltolux ($p>0.05$).

When curing Adhese P+B, Elipar produced significantly higher DC than Prismetics (10 s) and Coltolux ($p<0.05$) and comparable to Bluephase, Smartlite and Prismetics (20 s) ($p>0.05$). There were no significant differences between Prismetics (10 s) and (20 s), Bluephase, Smartlite and Coltolux ($p>0.05$).

When curing Adhese One, Prismetics (10 s) and (20 s) and Elipar and bluephase produced similar DC values ($p>0.05$). Smartlite produced lower DC values than Prismetics (10 s) and (20 s) ($p<0.05$), but similar to Elipar and Bluephase ($p>0.05$). Coltolux produced lower DC values than all other LCUs ($p<0.05$).

When adhesive systems were compared, Adhese B showed significantly higher DC than Adhese P+B and Adhese One whilst Excite showed higher DC than Adhese B, Adhese P+B and Adhese One ($p<0.05$). There was no statistically significant difference in the DC of Adhese P+B and Adhese One ($p>0.05$).

Table 23. Mean and standard deviation of the degree of conversion of adhesive systems cured with different light-curing units. Within each adhesive group, cells with the same superscript indicate no statistical difference.

Adhesive systems	**Light-curing units**	**Degree of conversion Mean (SD) (%)**
Excite	Elipar[1,2]	68.2 (8.7)
	Bluephase[1,2]	67.3 (5.5)
	Smartlite[1,2]	65.0 (2.9)
	Coltolux[2]	62.0 (4.0)
	Prismetics (10 s)[1]	69.1 (5.5)
	Prismetics (20 s)[3]	76.2 (4.4)
Adhese Primer+Bond	Elipar[2]	50.4 (13.9)
	Bluephase[1,2]	39.6 (12.4)
	Smartlite[1,2]	43.3 (15.2)
	Coltolux[1]	38.1 (11.2)
	Prismetics (10 s)[1]	36.2 (12.6)
	Prismetics (20 s)[1,2]	42.9 (14.8)
Adhese Bond	Elipar[2]	63.4 (1.6)
	Bluephase[1]	58.5 (8.4)
	Smartlite[1,2]	61.3 (4.9)
	Coltolux[1,2]	60.6 (3.9)
	Prismetics (10 s)[1]	58.3 (6.9)
	Prismetics (20 s)[2]	63.0 (1.9)
Adhese One	Elipar[1,2]	39.9 (5.2)
	Bluephase[1,2]	41.3 (7.5)
	Smartlite[2]	39.2 (4.9)
	Coltolux[3]	32.3 (5.9)
	Prismetics (10 s)[1]	45.5 (5.3)
	Prismetics (20 s)[1]	45.4 (7.2)

9.3. Discussion

The results of the present study indicated that:
(1) There was a significant difference in the DC of each adhesive system as a function of light source and
(2) There was a significant difference in the DC of different adhesive systems cured with the same LCU.
Therefore, the null hypothesis was rejected.

The present study investigated the effect of four LED LCUs, a halogen LCU at 10 s and a halogen LCU at 20 s curing times, on the DC of an etch-and-rinse, a self-etch adhesive (Adhese Primer+Bond) and the bond alone. The mean DC values were 62-76% (Excite), 36-50% (Adhese P+B), 58-63% (Adhese B) and 32-45% (Adhese One).

Adhese is a two-step, two-bottle self-etch adhesive with primer and bond in separate bottles. Adhese P+B and Adhese P were compared to investigate the effect of the primer on the DC, similarly to the study in Chapter 8. The same was repeated in the present experiment since a wider range of LCUs was used. The intention was to differentiate whether the negative effect of the primer on the DC of the primer+bond mixtures occurs with other LCUs.

Adhese One was designed to further reduce clinical working time and is applied as a one-step self-etch system. Though it appears to be the successor of Adhese, the chemical composition of Adhese One has been altered by the manufacturer in light of the finding that methacrylate-based adhesives are less hydrolytically stable than acrylamide-based adhesives in acidic aqueous solutions typically found in one-step self-etch systems (Salz 2005b).

Mat black coated microscope slides were chosen to reduce light scattering, and curing on glass eliminated the complicated interaction and biological variability between

adhesives and dentine substrate. Under such circumstances, because there was no diffusion or elution of primer or unreacted monomers into the substrate, lower DC values could be expected. The results should be interpreted in this light.

Manufacturers recommend air-blowing to render the adhesive layer uniform and with solvent containing adhesive resins, this will also promote evaporation (Spreafico 2006). However, complete evaporation is difficult to achieve in clinically relevant air-blowing times (Ikeda 2005, Nunes 2005) and any remaining solvents may compromise polymerisation by dilution of monomers (Nunes 2005). It has, also, been shown that the 'cross linking-facilitated gel phenomenon' is suppressed in adhesives with a high solvent content (Ye 2007). Nevertheless, in order to standardise procedures, manufacturer's recommended time of about 5 s air-blowing was used in the present study. Subsequently, a Mylar strip was applied to prevent oxygen inhibition and curing commenced immediately.

From the manufacturer's instruction, bonding agents should be polymerised for 10 s at a light intensity greater than 400 mW/cm^2 or 20 s at a light intensity below 400 mW/cm^2. In accordance with this, as Prismetics gave an actual reading of 380 mW/cm^2, it was decided to compare light curing times of 10 s and 20 s.

It has been suggested previously that light energy density and not light intensity is the important parameter in determining monomer conversion (Emami & Soderholm 2003) and polymerisation contraction of RBCs (Asmussen & Peutzfeldt 2005). Light energy density for the six tested LCUs was in the range of 3.8-10 J/cm^2. Though Elipar delivered the highest light energy density, it was Prismetics at 20 s that produced higher DC in Excite. There was no significant difference between Elipar and Prismetics when curing Adhese P+B, Adhese B and Adhese One. As expected, Elipar, which had higher light energy density than the other LEDs and Prismetics (10 s), produced comparable or higher DC values for all four adhesive groups. Bluephase, Smartlite and Coltolux produced similar light energy density and there were no differences in DC values for

Adhese but Coltolux produced lower DC values for Adhese One than the other two LCUs.

In the case of Excite, better results obtained by Prismetics (20 s) compared to the LED LCUs may be explained by the differences in the spectral emission range of the two types of light sources. This may also explain why Prismetics (10 s) showed DC values for Excite similar to most LED LCUs and better than Coltolux, even though all LED LCUs had higher light energy density. Halogen LCUs produce a wider spectral range than LED LCUs (Mills 2002, Warnock 2004, Owens & Rodriguez 2007). It is generally accepted that the spectral region greatly affects monomer conversion, and an LCU should match those wavelengths required by the photoinitiator(s) (Hammesfahr 2002). The manufacturer's technical data does not state either the type of photoinitiators or the percentage by weight or volume of these for Excite or Adhese. Differences in either of these may account for the differences in the present results.

In the case of Adhese B and Adhese P+B, Prismetics (20 s) and Elipar at 10 s gave comparable DC values and in the case of Adhese One, Prismetics (20 s), Elipar and bluephase showed similar results, suggesting that factors other than light energy density may be involved in producing similar conversion rates. As Elipar had higher light energy density than Prismetics (10 s) and (20 s), spectral emission range and/or the type and amount of photoinitiators may account for similar results between the two LCUs. Furthermore, Prismetics (10 s) produced comparable DC values for Adhese B and Adhese P+B as LED LCUs except Elipar in spite of lower light energy density. This suggests that higher light energy density may compensate for the effect of a narrower spectral emission range and explain why Elipar produced higher DC than Prismetics (10 s) and comparable to Prismetics (20 s).

The present results indicate that the spectral emission range may have a greater effect on adhesive DC than the light intensity or light energy density. Prismetics (20 s) produced similar or higher DC values in both adhesive systems compared to LED LCUs of higher

light energy density. Even at 10 s, it produced similar results to 3 of the 4 tested LED LCUs at 10 s and in the case of Adhese One, Prismetics (10 s) gave better results than Smartlite and Coltolux. Light energy density seems to be a significant factor when either halogen or LED LCUs are compared since Prismetics (20 s) gave comparable or better results than Prismetics (10 s) as did Elipar compared to the other LED LCUs.

Significantly higher DC values were found in Excite and Adhese B cured with Prismetics (20 s) than (10 s) whilst no statistically significant difference was observed in the Adhese P+B and Adhese One groups. The consensus opinion of the importance of light energy density (Emami & Soderholm 2003, Asmussen & Peutzfeldt 2005) does not hold for Adhese P+B and Adhese One though it does for Excite and Adhese B. The mean DC values in Adhese P+B indicate higher conversion for Prismetics (20 s) than (10 s) but the lack of statistical significance may be due to the large SD values which caused the overlapping of confidence intervals for these curing times. On the other hand, similar results for Prismetics (10 s) and (20 s) for Adhese One, suggest that differences in conversion kinetics in this adhesive system may be due to the differences in chemical composition compared to methacrylate-based systems. The introduction of bisacrylamide and methacrylamide resins in Adhese One requires further investigation of its conversion kinetics.

The present results are in accordance with a previous study which reported higher DC values in an etch-and-rinse (Single Bond) and a self-etch adhesive (Clearfil SE Bond) produced by a conventional halogen compared to an LED LCU (Arrais 2007). Furthermore, a halogen LCU produced higher DC values in commercial orthodontic adhesives than a plasma arc LCU of equivalent light energy density (Bang 2004).

The etch-and-rinse adhesive, Excite, showed higher DC values than Adhese B, Adhese P+B and Adhese One whilst Adhese B showed significantly higher DC values than Adhese P+B and Adhese One. The latter two systems produced similar results.

Adhese P contains the acidic monomers, phosphonic acid acrylate and bis-acrylamide, whereas Adhese B contains no acidic monomers. The lower DC values for Adhese P+B than Adhese B obtained in the present study, suggest that the primer decreases the polymerisation potential of self-etch adhesives. This is in agreement with previous findings (Hotta 1998) and can be attributed to previously mentioned effect of acidic monomers and higher solvent content, especially when the solvent is water, since it has been shown that water impairs polymerisation (Wang 2006c). The higher DC values obtained for Excite than Adhese P+B may be due to the same reasons.

In the case of Adhese P+B, the large variation in DC values was observed. Most probably, this variation is due to the fact that the hydrophilic water-containing primer does not mix well with the hydrophobic solvent-free bond. A 50 nm micro-Raman laser spot is likely to measure in different phases due to phase separation, resulting in the above mentioned variation.

The low viscosity of primers and adhesive resins is partly due to solvent dissolution of monomers (Van Landuyt 2007). Adhese B, containing no solvent, can be expected to have a higher viscosity than Excite, resulting in reduced molecular kinetics and slower polymerisation. This may partly explain why Adhese B alone showed lower DC values than Excite.

9.4. Conclusions

Light source has a significant effect on monomer conversion and DC in adhesive systems. Both the light energy density and the spectral emission range of an LCU are important parameters in monomer conversion in adhesive systems. The halogen LCU at 20 s produced similar or higher DC values compared to the halogen LCU at 10 s and the LED LCUs. Elipar performed similar or better than other LED LCUs. The DC values of the etch-and-rinse adhesive were higher than both self-etch systems. The presence of

primer in the self-etch adhesive compromised polymerisation and resulted in lower DC. One-step self-etch system, Adhese One, showed similar results as Adhese P+B mixture.

CHAPTER 10

QUANTITATIVE AND QUALITATIVE ANALYSIS OF THE ADHESIVE-DENTINE INTERFACE USING MICRO-RAMAN SPECTROSCOPY AND SCANNING ELECTRON MICROSCOPY

The aim of this study was to analyse the quantitative and qualitative aspects of the adhesive-dentine interface using linear and 2D micro-Raman spectroscopy and SEM.

The objectives were:

(1) To quantify the zone of dentine demineralisation, the thickness of the HL and DC of adhesives across the adhesive-dentine interface using linear and 2D micro-Raman spectroscopy;

(2) To quantify the thickness of the HL and qualitatively analyze the appearance of resin tags using SEM;

(3) To compare the values for the HL thickness obtained by micro-Raman spectroscopy and SEM.

The null hypotheses were:

(1) There are no significant differences in dentine demineralisation, the HL thickness, and the DC of different adhesive systems across the adhesive-dentine interface obtained by linear or 2D micro-Raman spectroscopy;

(2) There are no significant differences in the HL thickness among different adhesive systems obtained by SEM;

(3) There are no significant differences in the HL thickness obtained by micro-Raman spectroscopy and SEM.

10.1. Materials and Methods

10.1.1. Sample preparation

Thirty non-carious human third molars were prepared as explained in 5.1 and allocated randomly to six groups of five teeth. Peripheral parts of each tooth were trimmed with a diamond bur in a high-speed handpiece so that the diameter of the tooth did not exceed 8.5 mm which was the diameter of the LCU tip used in the study.

Table 24 lists the adhesive systems used in the present study. For clarity, manufacturers' details for each material are omitted and are given in the List of materials (page XIII).

Table 24. Adhesive systems used in the present study.

Adhesive systems	Type	Composition
Excite	Etch-and-rinse, 1-bottle	Phosphonic acid acrylate, HEMA, BisGMA, dimethacrylates, silica, ethanol, catalysts, stabilizers
Admira		HEMA, HPMA, BisGMA, acetone, catalysts, ormocers, additives
Adhese	2-step self-etch, 2-bottle	Primer: Phosphonic acid acrylate, bis-acrylamide, water, initiators, stabilizers Bond: HEMA, BisGMA, dimethacrylates, Si-dioxide, initiators, stabilizers
Filtek Silorane adhesive system		Primer: Phosphorylated methacrylates, Vitrebond™ copolymer, BisGMA, HEMA, water, ethanol, silane-treated silica filler, initiators, stabilizers Bond: Hydrophobic dimethacrylate, phosphorylated methacrylates, TEGDMA, silane-treated silica filler, initiators, stabilizers
Adhese One	1-step self-etch, 1-bottle	Bis-acrylamide, water, bis-methacrylamide dihydrogen phosphate, amino acid acrylamide, hydroxyl alkyl methacrylamide, highly dispersed silicon dioxide, catalysts, stabilizers
G Bond		4-MET, UDMA, acetone, water, sillanated colloidal silica, initiator

Prior to the application of the etch-and-rinse systems, 37% phosphoric acid was applied to dentine and left for 15 s. Following etching, the acid was removed by water-air spray from the dental unit and the tooth surface was dried with a mild stream of air leaving the dentine moist according to the wet bonding technique.

Each adhesive system was applied according to manufacturers' recommendations and covered with a Mylar strip. The adhesive was cured for 10 s with an LED LCU (Elipar Freelight2) at an intensity of 1000 mW/cm^2 at 1 mm curing distance which was maintained using a custom-made light guide as explained in 5.1. The intensity of the LCU was monitored before and after curing using the Bluephase meter.

After curing, the teeth were stored in distilled water in a light-proof container. The water level was set to 1 mm below the surface of the sample in order to avoid contact with the adhesive system. The temperature and humidity inside the light-proof container were measured using the USB-502 logger. The container was placed in a water bath set at 37°C for 24 h.

After 24 h of storage, the samples were mounted on the Isomet machine and 1 mm thick sections were cut parallel to the long axis of the tooth. Four sections were obtained from each sample. Immediately after sectioning, the sections were analyzed under a light microscope at various magnifications to observe if the adhesive layer remained intact. The dentinal aspect of each section was placed in wet oasis sponge ensuring the adhesive aspect was kept dry. The sections were transported in the light-proof container and micro-Raman analysis started within 30 min.

10.1.2. Micro-Raman spectroscopy

Micro-Raman analysis was done as explained in 5.2. In order to obtain linear spectra, each section was placed on a microscopic slide with the sectioned surface perpendicular

to the adhesive layer facing the Raman laser. The adhesive layer and dentine were identified using x10, x50 and x100 magnification of the Raman microscope. Linear spectra were taken at 1 μm intervals along 30 μm lines across the adhesive-dentine interface at randomly chosen sites within intertubular dentine. The acquisition time was 5 s with 6 accumulations per point. The total time for each micro-Raman linear spectrum was 10 min. Three spectra were taken from each section. Spectra of uncured adhesives were used as reference.

In order to obtain 2D maps, the adhesive-dentine interface was again identified using x10, x50 and x100 magnification. Two-dimensional mapping was performed over 15 x 15 μm or 20 x 20 μm areas across the adhesive-dentine interface at 1 μm intervals in both X and Y axes. These areas included the adhesive layer, the HL, partially demineralised and un-affected dentine. Accumulation time per spectrum was 10 s and 2 spectra were taken per point. Two mappings were performed per section at randomly chosen sites. Samples were kept hydrated throughout the experimental procedure by keeping the dentinal aspect in contact with the moist blotting paper.

Post-processing of data was done as explained in 5.2. The degree of dentine demineralisation was calculated according to the following formula:

Degree of demineralisation=$(1-I_{demineralised} / I_{mineralised}) \times 100$

where I is the intensity of the apatite peak at 960 cm^{-1} in demineralised and mineralised dentine.

The DC of the adhesive system was calculated according to the formula:

DC = $(1 - R_{cured} / R_{uncured}) X 100$

where R is the ratio of aliphatic and aromatic peak intensities at 1639 cm^{-1} and 1609 cm^{-1} in cured and uncured adhesives.

"Modelling analysis" was included in post-processing of 2D maps and allowed spectral components associated with adhesive and dentine to be distinguished. The modelling

algorithms are based on correlation fitting of known reference spectra with raw data. The reference spectra were previously taken from adhesive samples cured on glass slides and un-affected dentine samples. The software uses a direct classical least squares (DCLS) algorithm to identify the distribution of components across a mapped area. The calculation is made on each spectrum associated with the individual pixels of the Raman map. The DCLS analysis calculates a linear combination of the pure component spectra acquired separately before the mapping analysis and provides the closest match to the original raw data spectrum. The resulting combination is in the form "A*spectrum1 + B*spectrum2 +…" where A, B… are constants proportional to the component concentration. This results in a series of chemical images illustrating the distribution of each component across the mapped region and provides a fast and versatile method for component distribution analysis and chemical composition based on the individual Raman spectra.

10.1.3. Scanning electron microscopy

The same samples used for micro-Raman spectroscopy were prepared for and analysed using SEM thereafter. The preparation of samples for SEM is explained in 5.3. The samples were observed under various magnifications, from x200 to x10.000 but the same magnification was used for each adhesive system. On SEM micrographs, the following features of the adhesive-dentine interface were examined: the thickness of the HL and the appearance of resin tags [shape, thickness, length, number per unit area].

10.1.4. Statistical analysis

Data for the depth of dentine demineralisation as well as for adhesive penetration followed a normal distribution. Bartlett's test for equal variances showed significant differences between the groups in both cases ($p<0.05$). Therefore, logarithmic transformation of data [Natural log, ln] was performed and the repeated Bartlett's test

confirmed that differences between group variances were now insignificant (dentine demineralisation p=0.732; adhesive penetration p=0.345). Because both assumptions for parametric testing were met, one-way ANOVA with Tukey's multiple comparisons post-test was used to assess the differences in the depth of dentine demineralisation and adhesive penetration between the adhesive systems.

The mean and SD values for the degree of dentine demineralisation and the DC of adhesive systems as a function of distance were calculated but not subjected to statistical analysis. A power calculation showed that the required number of teeth would exceed 100 for dentine demineralisation and 50 for DC for the test to detect the difference of 10% with the power of 0.80. Therefore, no further statistical testing was done regarding the degree of dentine demineralisation and the DC of adhesive systems as a function of distance.

Data for the DC of adhesive systems within the adhesive layer as well as the HL showed normal distribution. Bartlett's test for equal variances showed significant differences between the groups in spite of several attempts to transform data ($p<0.001$). Therefore, a non-parametric test, the Kruskal-Wallis test with Dunn's multiple comparisons post-test was used to evaluate the differences in the DC between adhesive systems.

Though data for HL thickness obtained by 2D micro-Raman spectroscopy and SEM followed a normal distribution, Bartlett's test showed significant differences in variances ($p<0.001$). After the transformation of data using the square root function, Bartlett's test showed equal variances (micro-Raman spectroscopy p=0.601; SEM p=0.329). Therefore, the differences between adhesive systems were compared using one-way ANOVA with Tukey's post-test whilst the data for HL thickness of each adhesive system, obtained by the two methods, were compared using the paired t-tests with the p values for each adjusted for multiple comparisons and set at 0.008 instead of 0.05 (Bonferroni correction).

10.2. Results

10.2.1. Depth and degree of dentine demineralisation

Figure 45 shows the depth of dentine demineralisation for each adhesive system. Significant differences between the means were found for all adhesive systems ($p<0.05$) except for Excite vs. Admira, Adhese vs. G Bond and Filtek Silorane vs. Adhese One ($p>0.05$).

Phosphoric acid treatment prior to the application of Excite and Admira resulted in significantly deeper dentine demineralisation than that produced by both two-step and one-step self-etch adhesive systems ($p<0.05$). Adhese produced significantly deeper dentine demineralisation than Filtek Silorane adhesive system ($p<0.05$) but comparable to G Bond ($p>0.05$). Adhese One produced significantly thinner dentine demineralisation than Adhese and G Bond ($p<0.05$) but comparable to Filtek Silorane ($p>0.05$).

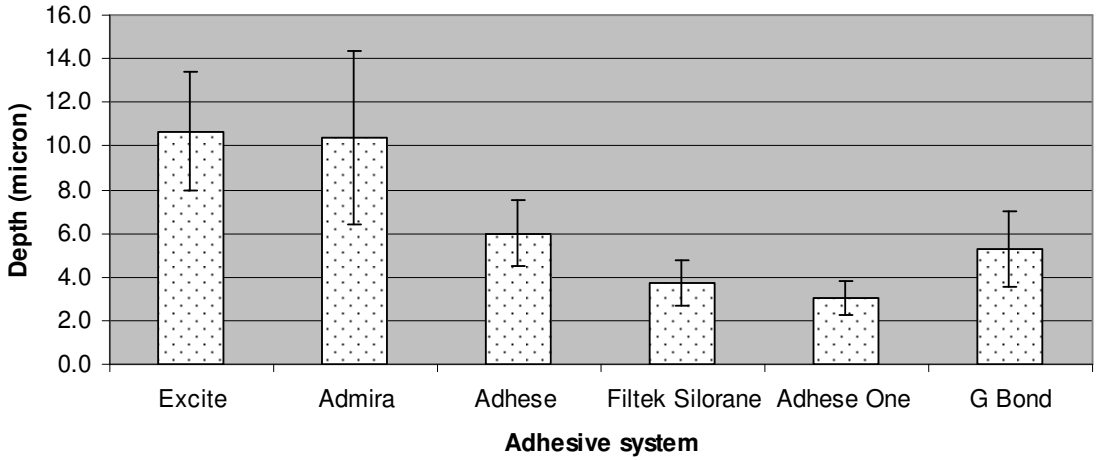

Figure 45. Mean and standard deviation of the depth of dentine demineralisation for each adhesive system.

The mean and SD values for the degree of dentine demineralisation are given in Table 25 for each micron across the adhesive-dentine interface. Figure 46 shows the mean values for the degree of dentine demineralisation across the adhesive-dentine interface. The SD values were omitted for clarity of presentation. Excite and Admira, etch-and-rinse systems used with phosphoric acid, showed higher mean values for the degree of dentine demineralisation compared to self-etch adhesive systems. Self-etch systems showed a more abrupt decrease in the degree of dentine demineralisation as a function of distance. The two-step self-etch system, Filtek Silorane showed similar decrease in dentine demineralisation as one-step self-etch systems, Adhese One and G Bond.

Table 25. Mean and standard deviation of the degree of dentine demineralisation at 1 μm intervals across the adhesive-dentine interface. The values are given in %.

Depth (μm)	Excite		Admira		Adhese		Filtek Silorane		Adhese One		G Bond	
	Mean	SD	Mean	SD	Mean	SD	Mean	SD	Mean	SD	Mean	SD
1	91.00	2.53	86.43	6.60	83.24	6.87	80.52	7.80	80.67	10.61	73.82	12.09
2	87.31	5.86	85.30	6.03	71.62	11.30	54.27	21.22	47.30	26.10	61.61	18.08
3	74.93	12.88	81.02	10.57	58.07	18.83	38.77	25.05	20.48	16.04	51.94	20.84
4	66.63	15.64	69.61	16.71	46.54	20.99	22.41	16.22	15.67	11.25	31.62	20.69
5	60.73	15.46	58.32	27.96	40.25	21.85	23.24	16.58			19.58	18.10
6	53.95	15.27	49.05	26.45	29.29	25.66					14.94	17.35
7	48.10	20.72	43.98	25.91	25.12	18.59					16.19	12.05
8	43.65	20.26	41.32	26.49							11.62	10.54
9	31.71	14.02	48.58	27.89								
10	19.02	11.44	38.81	20.29								
11	26.18	16.96	30.14	21.95								
12	13.85	8.97	21.35	3.41								
13	5.34	4.99	25.27	12.65								

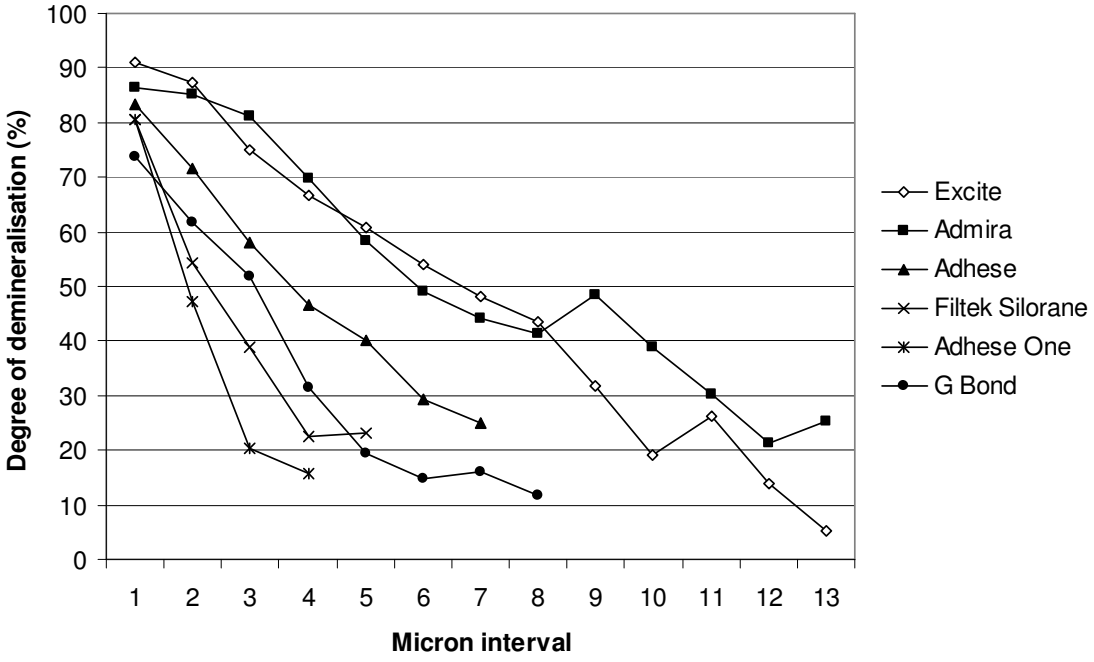

Figure 46. Degree of dentine demineralisation micron by micron across the adhesive-dentine interface for each adhesive system. [Mean values]

10.2.2. Depth of adhesive penetration

Figure 47 shows the mean and SD values for the depth of adhesive penetration. The same numbers next to adhesive name indicate no statistically significant differences in adhesive penetration between different systems ($p>0.05$).

Excite showed comparable depth of adhesive penetration to Admira, and significantly greater than the self-etch systems. The difference between Admira and Adhese was not statistically significant ($p>0.05$) but Admira showed significantly deeper adhesive penetration compared to Filtek Silorane, Adhese One and G Bond ($p<0.05$). There were no statistically significant differences between Adhese, Adhese One, Filtek Silorane and G Bond ($p>0.05$).

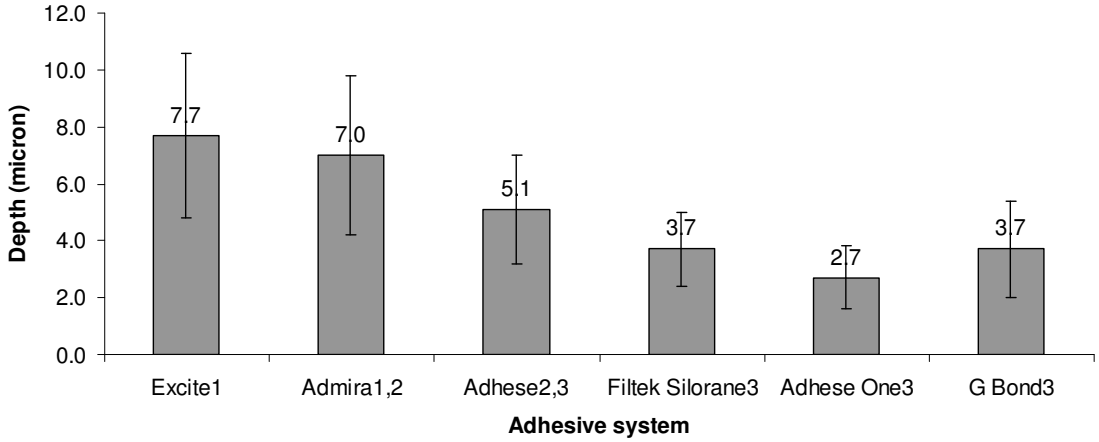

Figure 47. Mean and standard deviation of the depth of adhesive penetration for each system. Same numbers next to each adhesive name on the x-axis indicate no statistically significant differences in adhesive penetration ($p>0.05$).

10.2.3. The degree of conversion in adhesive systems

Adhesive layer

Table 26 and Figure 48 show the results of the DC within the adhesive layer for each system. Cells with the same superscripts are not statistically significant ($p>0.05$). Excite and FS Primer showed similar DC values ($p>0.05$) as did Excite and Adhese ($p>0.05$). Admira produced lower DC values than Excite and FS Primer ($p<0.05$) but similar to Adhese ($p>0.05$). There was no significant difference between FS Bond and Adhese One ($p<0.05$) but both FS Bond and Adhese One showed significantly lower DC values compared to other systems ($p<0.05$).

The aliphatic 1639 cm^{-1} peak could not be identified in spectra of any G Bond samples. This suggested that there were no C=C double bonds left within the adhesive layer or that their concentration was undetectable by micro-Raman spectroscopy. Therefore, the

data for G Bond are not included in the statistical analysis. Figure 49 shows a representative micro-Raman spectrum from within the adhesive layer of G Bond.

Table 26. Descriptive statistics and statistical differences in the degree of conversion within the adhesive layer for each adhesive system. DC values are given in %.

Adhesive system	Mean	SD	Minimum	Q1	Median	Q3	Maximum
Excite [1,2]	84.48	6.45	72.06	79.37	85.40	89.39	95.00
Admira [3]	76.17	5.35	62.21	72.50	77.00	80.22	85.01
Adhese [1,3]	80.93	4.54	71.95	77.08	81.73	84.44	88.78
FS Primer [2]	87.41	5.19	71.43	83.24	89.73	91.49	95.96
FS Bond [4]	64.67	4.75	54.57	60.30	64.02	69.44	78.00
Adhese One [4]	55.99	8.80	40.52	48.15	56.46	62.39	75.05

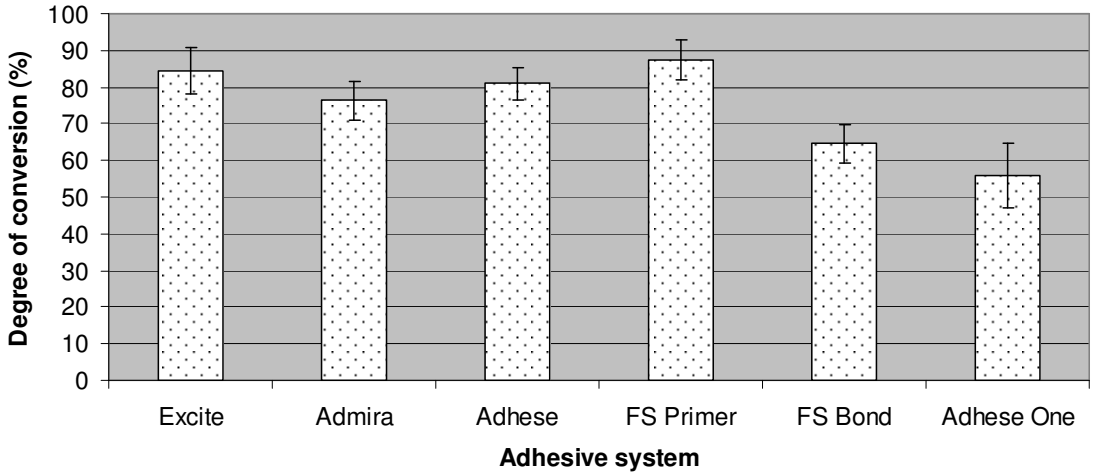

Figure 48. Mean and standard deviation of the degree of conversion within the adhesive layer for each adhesive system.

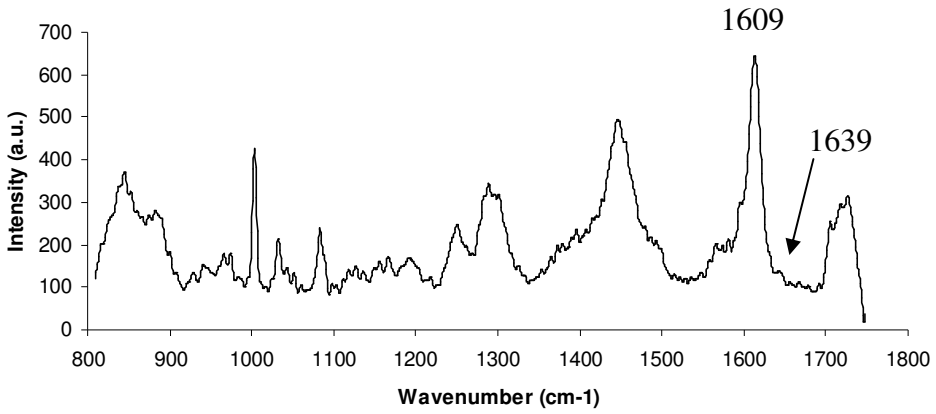

Figure 49. A representative micro-Raman spectrum from within the adhesive layer of G Bond. No 1639 cm^{-1} peak detectable.

Hybrid layer

Table 27 and Figure 50 show the results of the DC within the hybrid layer for each system. The aliphatic 1639 cm^{-1} peak for G Bond was detectable in 15 sections. Sections in which this peak was not detectable were not included in statistical analysis. Cells with the same superscripts are not significantly different ($p>0.05$).

Table 27. Descriptive statistics and statistical differences in the degree of conversion within the hybrid layer for each adhesive system. DC values are given in %.

Adhesive system	Mean	SD	Minimum	Q1	Median	Q3	Maximum
Excite [1]	57.20	12.43	35.29	47.25	56.00	65.08	84.09
Admira [2]	71.77	8.88	38.10	68.05	74.53	77.61	81.35
Adhese [2]	65.40	15.04	23.19	60.25	67.71	75.28	85.61
FS Primer [3]	78.48	9.66	57.20	72.86	80.31	86.66	90.49
Adhese One[4]	41.06	15.31	6.30	29.69	44.65	52.97	67.10
G Bond [2]	71.42	10.32	43.31	64.29	71.73	79.09	90.13

FS Primer showed significantly higher DC values than other adhesive systems ($p<0.05$). Admira, Adhese and G Bond gave similar results ($p>0.05$). Significantly lower DC values were found for Excite compared to FS Primer, Admira, Adhese and G Bond but higher than Adhese One ($p<0.05$). Adhese One produced significantly lower DC values than all other systems ($p<0.05$).

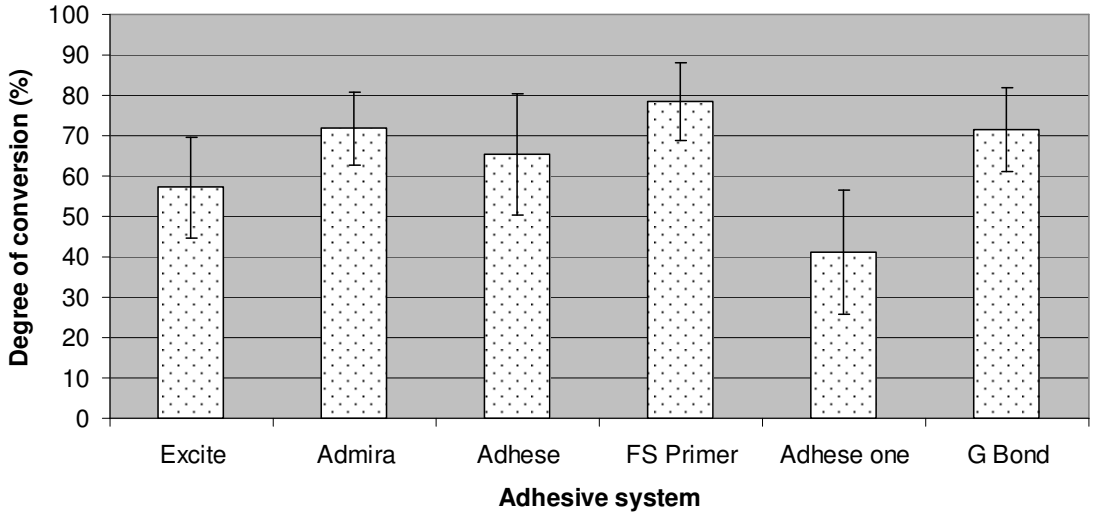

Figure 50. Mean and standard deviation of the degree of conversion within the hybrid layer for each adhesive system.

DC micron by micron

Table 28 shows the mean and SD values for the DC of adhesive systems as a function of distance across the adhesive – dentine interface. Figure 51 shows the trend of the DC across the adhesive-dentine interface. The SD values are omitted for clarity of presentation.

Table 28. Mean and standard deviation of the degree of conversion of adhesive systems at 1 μm intervals across the adhesive-dentine interface. DC values are given in %.

	Depth (μm)	Excite		Admira		Adhese		Filtek Silorane Primer		Adhese One		G Bond	
		Mean	SD	Mean	SD	Mean	SD	Mean	SD	Mean	SD	Mean	SD
Adhesive layer	1	85.16	5.63	77.39	6.01	80.15	4.41	87.64	6.16	56.00	9.66		
	2	83.55	6.89	76.50	5.83	80.05	5.40	90.89	3.86	57.68	10.64		
	3	84.34	6.46	75.04	3.25	81.71	3.79	85.98	5.25	57.87	8.31		
	4	84.86	6.82	75.77	6.33	81.84	4.57	85.12	5.48	52.47	6.57		
Hybrid layer	5	60.30	14.26	74.75	7.63	73.94	8.28	82.73	5.94	50.89	9.19	78.25	6.88
	6	61.33	15.69	75.93	8.50	67.03	14.85	76.37	11.17	42.82	16.60	70.26	11.59
	7	59.39	7.18	71.81	8.41	63.15	19.10	76.65	10.81	40.92	16.39	61.15	12.93
	8	58.95	8.16	71.77	4.75	62.75	21.88						
	9	54.73	7.89	71.39	6.10	72.39	8.71						
	10	50.00	20.59	69.55	9.39								
	11	53.11	14.69	67.17	15.70								

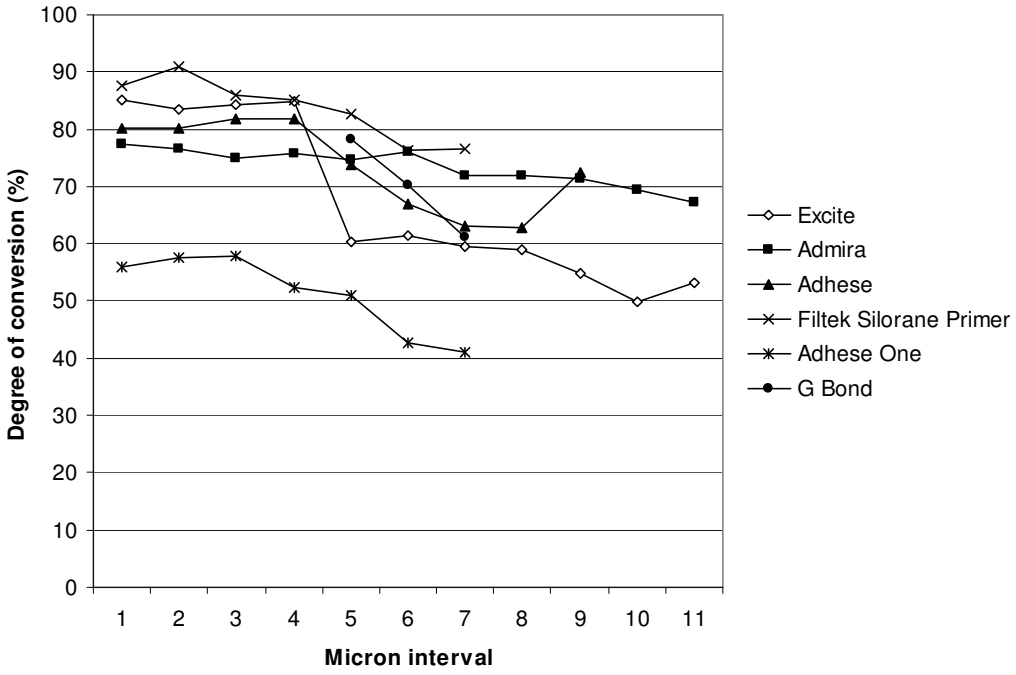

Figure 51. The degree of conversion of adhesive systems micron by micron across the adhesive-dentine interface. [Mean values]

Microns 1-4 correspond to the adhesive layer. Microns 5-11 correspond to the HL. Values for G Bond presented only for the HL.

10.2.4. Two-dimensional micro-Raman spectroscopy and SEM

Figures 52-57 show representative 2D micro-Raman maps and SEM micrographs of the adhesive-dentine interface. The HL from 2D micro-Raman maps was defined as the overlapping of spectral intensities of bands associated with aromatic and aliphatic groups representing adhesive resins and the phosphate group representing dentine hydroxyapatite. The thickness of the HL on SEM micrographs was measured starting from the 'electron dense edge effect' at the base of the adhesive layer to the next 'electron dense edge effect', which is usually considered the limit of the HL.

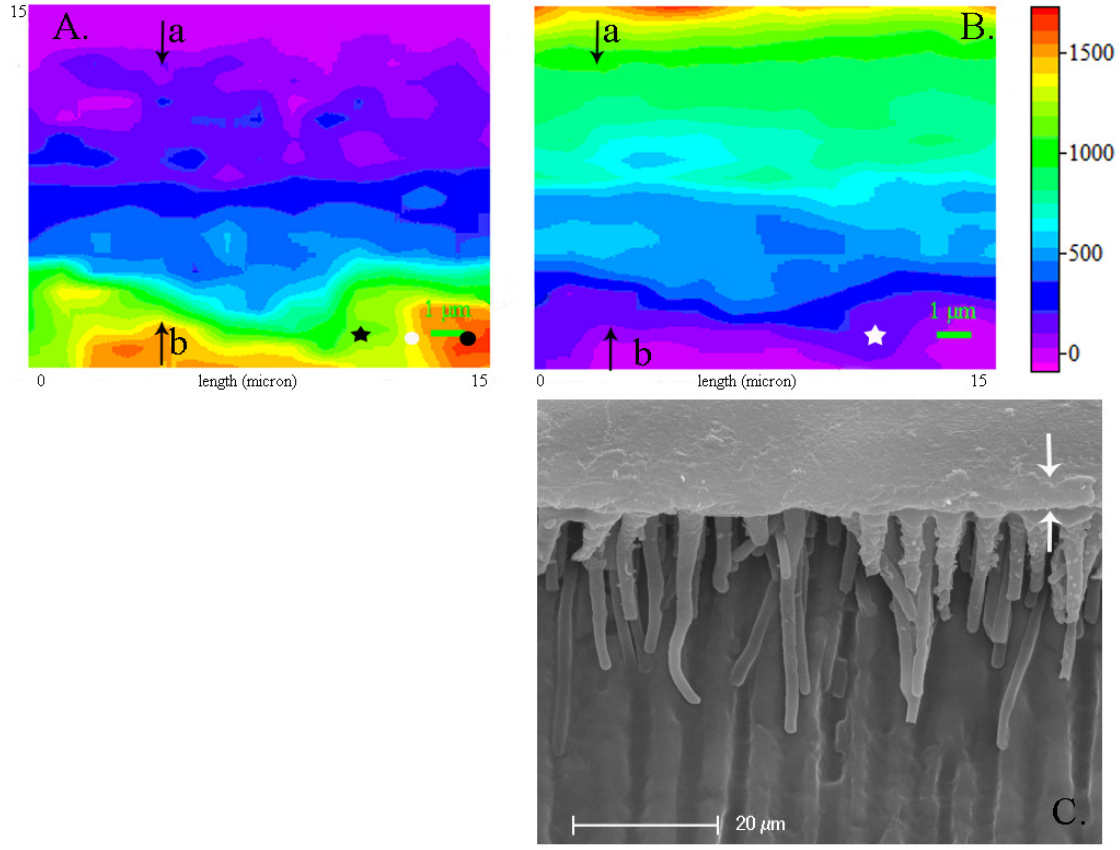

Figure 52. A representative 2D micro-Raman map and the corresponding SEM micrograph of the Excite-dentine interface.

A. The range of intensity of spectral features associated with dentine, ranging from the least intensity corresponding to maximum demineralised dentine (point

a, black arrow) to maximum intensity corresponding to unaffected dentine (point b, black arrow). The black star indicates a dentinal tubule, the black circle peritubular dentine and the white circle intertubular dentine.

B. The identical specimen area and the range of intensity of spectral features associated with adhesive resin starts from maximum intensity indicating pure adhesive (point a, black arrow), to the minimum intensity indicating no adhesive resin (point b, black arrow). The white star indicates a resin tag.

The colour scale shows intensity in arbitrary units for both A. and B.

There is an inverse relationship between the spectral intensities of the dentine hydroxyapatite moieties (left) and aliphatic and aromatic moieties in adhesive resin (right).

Point a indicates the beginning of dentine demineralisation and is taken as the top of the HL. Point b indicates un-affected dentine and is considered the bottom of the HL.

C. SEM micrograph obtained from the same sections used to collect micro-Raman data. The white arrows depict the HL. Excite formed numerous funnel-shaped resin tags. Lateral branching of resin tags was predominantly found in the proximity of the HL, down to about 20 µm. Further down the resin tags, lateral extensions were less frequent until no lateral branching was observed. The thickness of the resin tags varied from about 3.5 µm in the funnel-shaped regions close to the HL to about 1.4 µm further down.

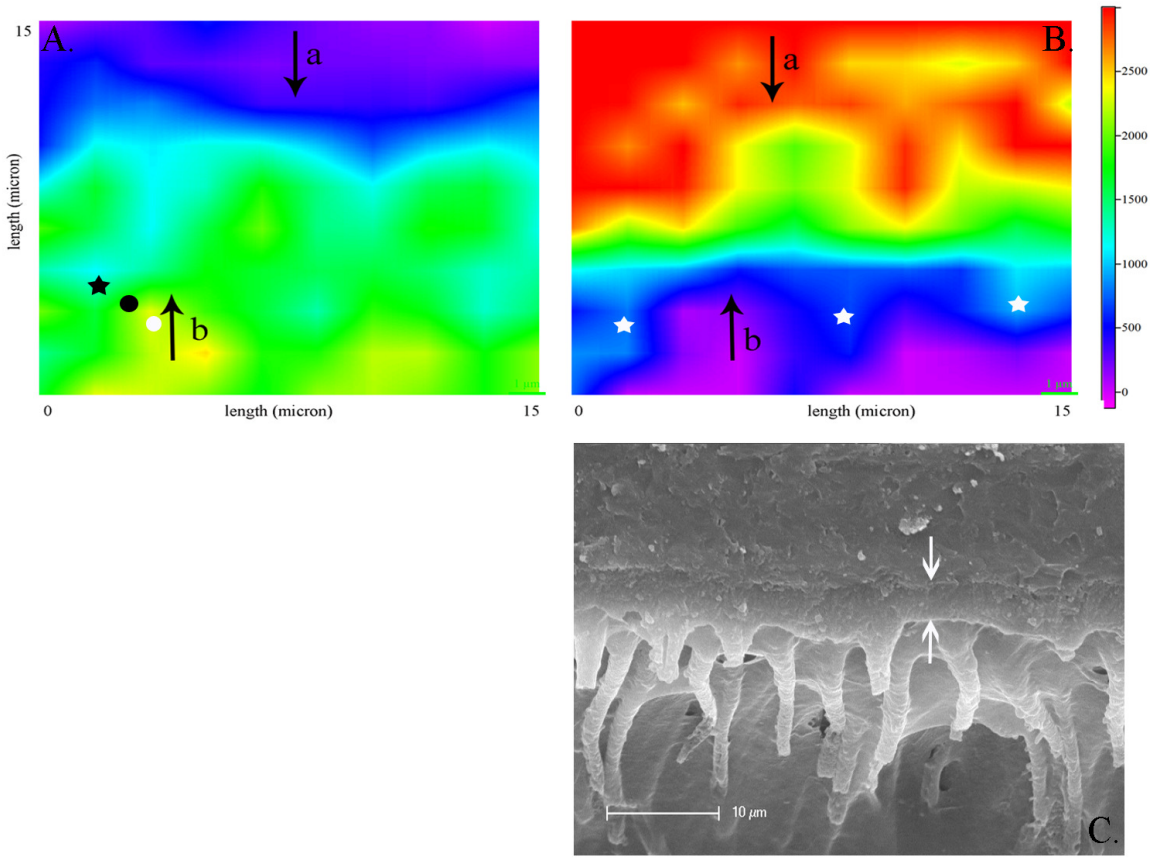

Figure 53. A representative 2D micro-Raman map and the corresponding SEM micrograph of the Admira-dentine interface. Explanations for A. and B. are as for Figure 52.

C. SEM micrograph obtained from the same sections used to collect micro-Raman data. The white arrows depict the HL. The number and shape of resin tags formed by Admira bond is similar to Excite. Lateral branching observed for Admira but to a less extent than that found for Excite. The thickness of the resin tags varied from about 3.6 μm in the funnel-shaped regions close to the HL to about 1.4 μm further down.

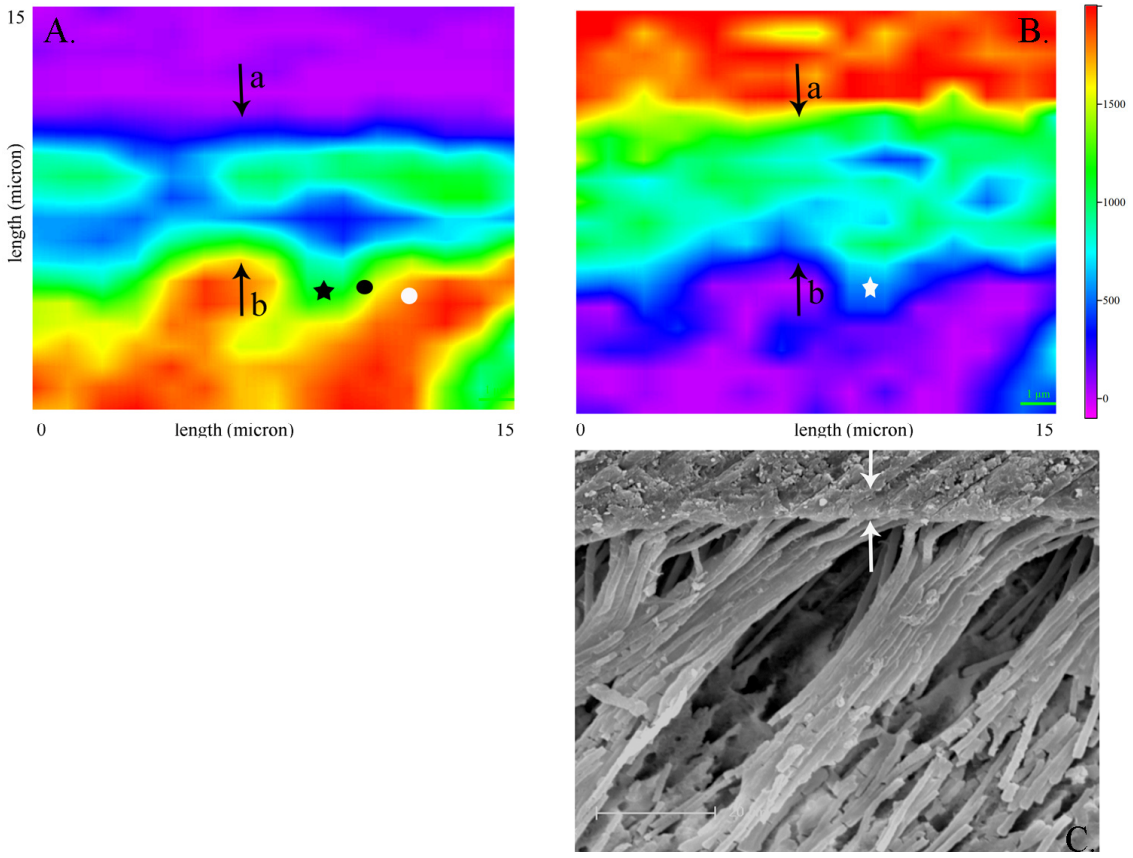

Figure 54. A representative 2D micro-Raman map and the corresponding SEM micrograph of the Adhese-dentine interface. Explanations for A. and B. are as for Figure 52.

C. SEM micrograph of Adhese. The white arrows depict the HL. Adhese formed numerous straight, long and thin resin tags with no funnel-shape as seen in Excite. Lateral branching was less frequent than previously found in Excite. The resin tags formed bundles most likely during preparation of SEM and may not be a genuine finding in dentine. The thickness of the resin tags of Adhese from about 2.0 µm in the proximity of the HL to about 1.2 µm further down.

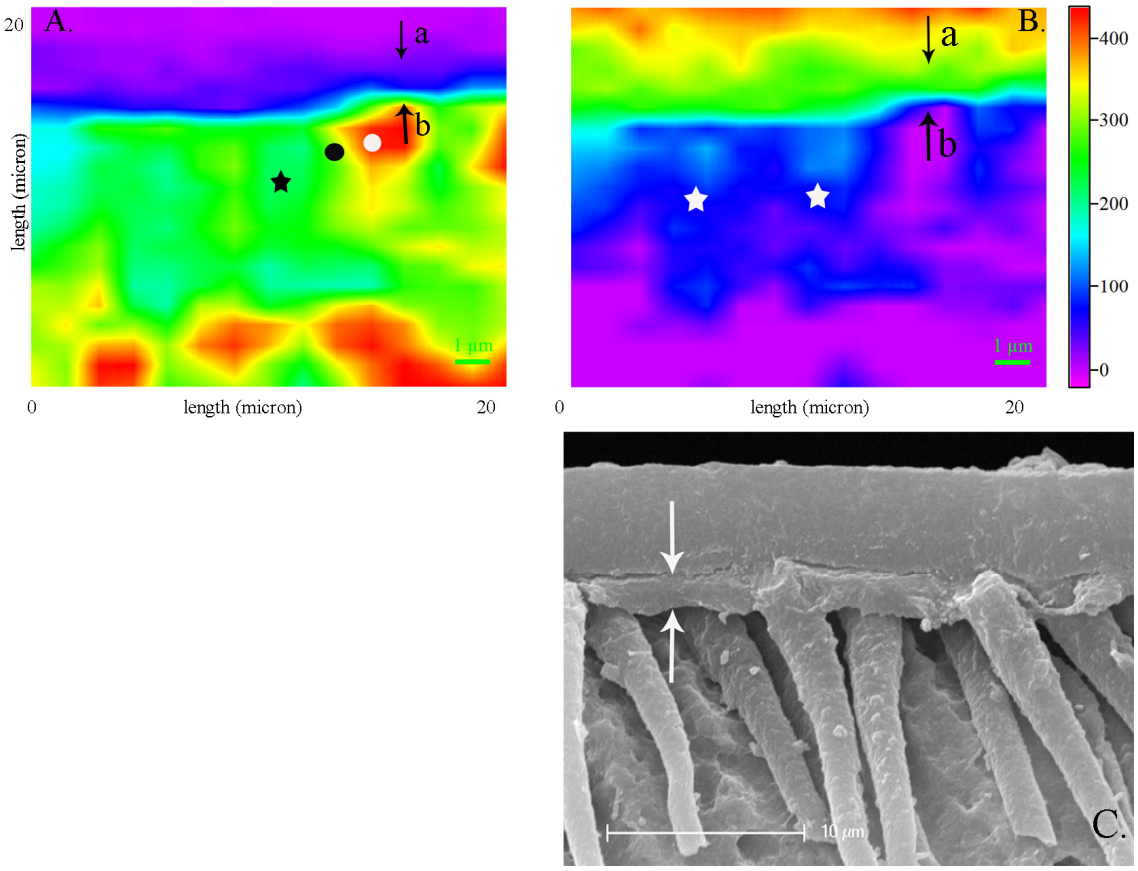

Figure 55. A representative 2D micro-Raman map and the corresponding SEM micrograph of the Filtek Silorane adhesive-dentine interface. Explanations for A. and B. are as for Figure 52.

C. SEM micrograph of Filtek Silorane adhesive system. The white arrows depict the HL. Though this adhesive system consisted of two separately cured components, Primer and Bond, no interface between the two was identified on SEM micrographs at various magnifications, up to x10.000. The resin tags were funnel-shaped similarly to Excite but with less lateral branching which was seen in the proximity of the HL. The thickness of the resin tags varied from about 3.3 µm in the funnel-shaped regions to about 1.4 µm in straight regions further away from the HL.

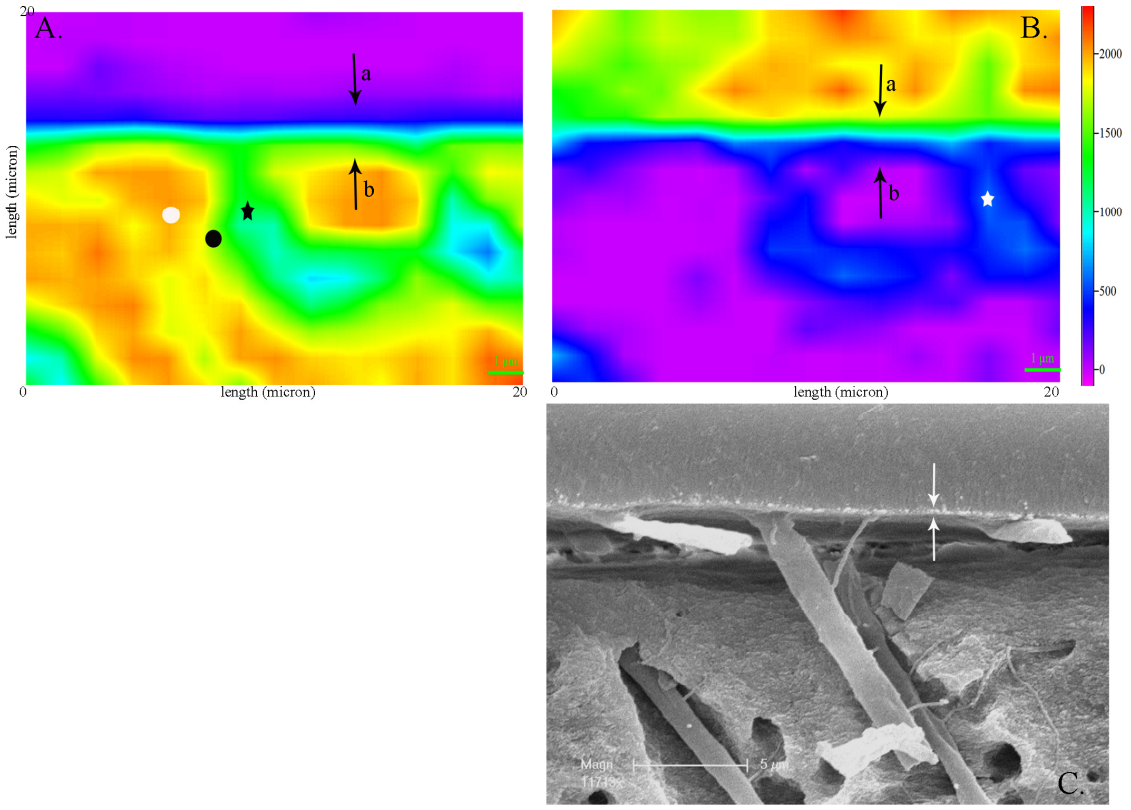

Figure 56. A representative 2D micro-Raman map and the corresponding SEM micrograph of the Adhese One-dentine interface. Explanations for A. and B. are as for Figure 52.

C. SEM micrograph of Adhese One. The white arrows depict the HL. Adhese One showed fewer resin tags per unit area than previous adhesive systems. The resin tags were straight, thin and shorter than those found in Adhese. Scarce very thin lateral extensions were seen in the proximity of the HL. The thickness of Adhese One resin tags was uniform along their length, from about 1.5 µm close to the HL to about 1.1 µm further down.

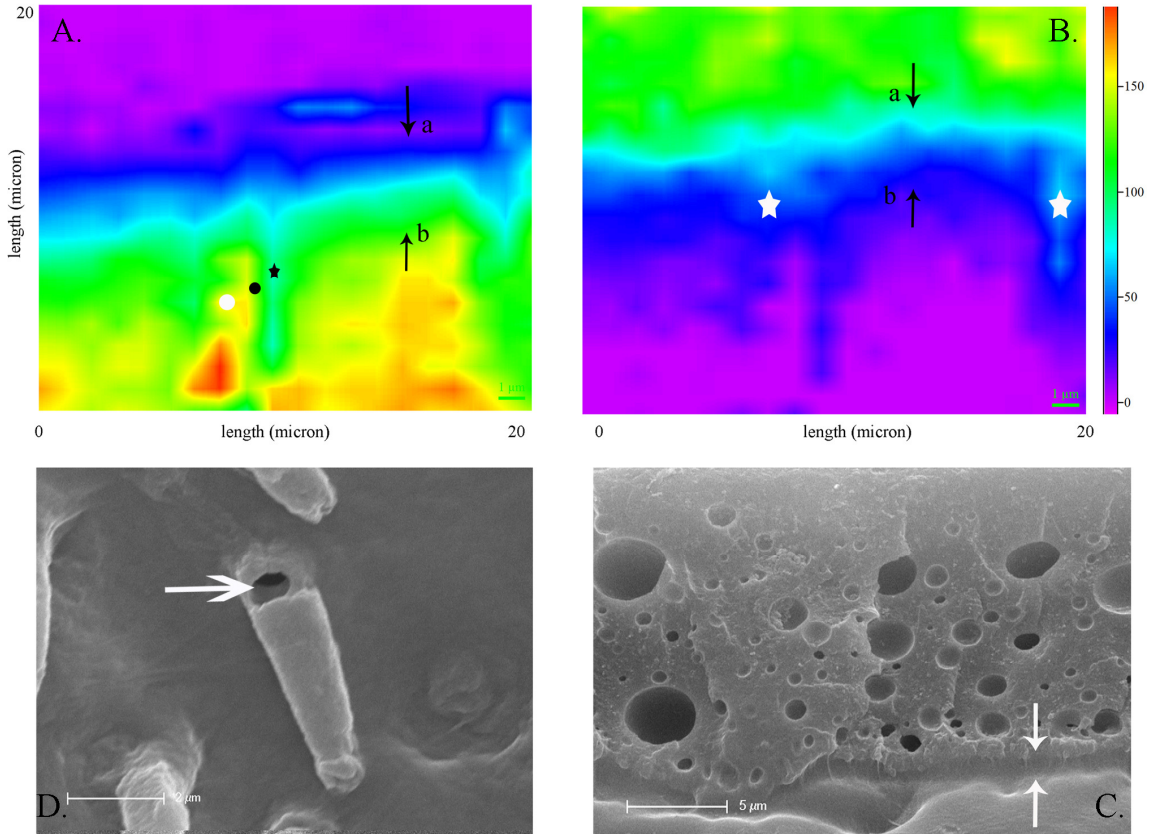

Figure 57. A representative 2D micro-Raman map and the corresponding SEM micrographs of the G Bond-dentine interface. Explanations for A. and B. are as for Figure 52.

C. SEM micrograph of G Bond. The white arrows depict the HL. The adhesive layer of G Bond was found to be extremely porous with voids of various diameters, from less than 1 µm to more than 5 µm.

D. Resin tags were shorter than in other adhesive systems and in many cases appeared as resin plugs occluding the orifices of dentinal tubules. Furthermore, some resin tags were porous which corresponded to the voids found in the adhesive layer. The white arrow indicates a void in a resin tag. The thickness of the resin tags was about 1.2 µm. No lateral branching of resin tags was observed for G Bond.

In addition, Figure 58 shows the distribution of Filtek Silorane Primer and Bond across the adhesive-dentine interface as a function of distance. An intermediate transition zone of about 1 µm can be identified between the primer and bond, between 4 µm and 6 µm. This zone was not identified on SEM micrographs even at the highest magnification.

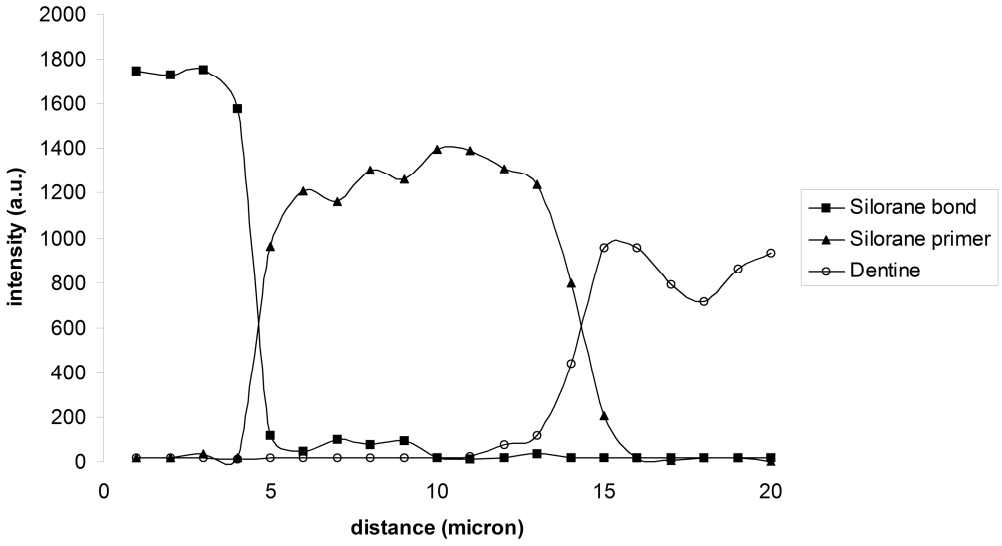

Figure 58. An intermediate zone of circa 1 µm between Filtek Silorane Primer and Bond with spectral features corresponding to both components of the Filtek Silorane adhesive system.

Table 29 shows the descriptive statistics and statistical differences for the HL thickness of each adhesive system obtained from 2D micro-Raman data. Cells with the same superscript numbers are not significantly different ($p>0.05$). Etch-and-rinse systems, Excite and Admira, produced comparable HL thickness ($p>0.05$) but significantly greater than self-etch systems ($p<0.05$). Adhese produced significantly greater HL thickness than Filtek Silorane adhesive system and the two one-step self-etch systems, Adhese One and G Bond ($p<0.05$). No statistically significant difference was observed for the HL thickness of Filtek Silorane adhesive system and G Bond ($p>0.05$). Adhese One showed the least HL thickness of all tested adhesive systems ($p<0.05$).

Table 29. Descriptive statistics for the hybrid layer thickness of each adhesive system [Micro-Raman spectroscopy]. HL thickness values are given in µm.

Adhesive system	Mean	SD	Minimum	Q1	Median	Q3	Maximum
Excite [1]	7.5	1.5	6.0	7.0	7.0	8.0	10.0
Admira [1]	7.5	1.6	5.0	6.0	7.0	9.0	10.0
Adhese[4]	5.3	1.6	3.0	4.0	5.0	7.0	8.0
Filtek Silorane [2, 3]	3.1	0.8	2.0	2.0	3.0	4.0	4.0
Adhese One [3]	2.3	1.0	1.0	2.0	2.5	3.0	4.0
G Bond [2]	3.8	1.3	2.0	3.0	3.0	4.7	6.0

Table 30 shows the descriptive statistics and statistical differences for the HL thickness of each adhesive system obtained from SEM data. Cells with the same superscript numbers are not statistically significant ($p>0.05$). Excite, Admira and Adhese showed comparable values for HL thickness ($p>0.05$) but significantly higher than Filtek Silorane adhesive system, Adhese One and G Bond ($p<0.05$). Filtek Silorane showed comparable results with G Bond ($p>0.05$) and Adhese One produced the thinnest HL compared to all other systems ($p<0.05$).

Table 30. Descriptive statistics for the hybrid layer thickness of each adhesive system [SEM]. HL thickness values are given in µm.

Adhesive system	Mean	SD	Minimum	Q1	Median	Q3	Maximum
Excite [1]	5.0	1.1	3.3	4.1	4.5	6.4	7.3
Admira [1]	4.4	1.5	2.8	3.4	3.9	4.7	8.1
Adhese [1]	3.7	1.1	2.1	2.9	3.7	4.5	5.4
Filtek Silorane [2]	1.9	0.9	1.0	1.3	1.9	2.6	2.6
Adhese One[3]	0.8	0.3	0.5	0.8	0.8	1.2	1.2
G Bond [2]	1.5	0.8	1.1	1.4	1.4	1.6	2.7

Table 31 shows statistical differences between the data for HL thickness of each adhesive system obtained using the two methods, 2D micro-Raman spectroscopy and SEM. In each adhesive group, the HL thickness as calculated from micro-Raman data was significantly greater than that measured on SEM micrographs ($p<0.05$).

Table 31. Statistical differences in hybrid layer thickness values for each adhesive system obtained by micro-Raman spectroscopy and SEM.

Adhesive system	**p value**	**Significance**
Excite – Raman vs. SEM	0.002	S
Admira – Raman vs. SEM	<0.001	S
Adhese – Raman vs. SEM	0.001	S
Filtek Silorane – Raman vs. SEM	0.004	S
Adhese One – Raman vs. SEM	<0.001	S
G Bond – Raman vs. SEM	<0.001	S

10.3. Discussion

The results of the present study indicated that:

(1) There were significant differences in dentine demineralisation, the HL thickness and the DC of different adhesive systems across the adhesive – dentine interface obtained by micro-Raman spectroscopy;

(2) There were significant differences in the HL thickness among adhesive systems obtained by SEM;

(3) There were significant differences in the HL thickness obtained by micro-Raman spectroscopy and SEM.

Therefore, all three null hypotheses were rejected.

In the present study, six adhesive systems were chosen, two from each of the following groups: (1) etch-and-rinse system, Excite and Admira, (2) two-step self-etch systems, Adhese and Filtek Silorane and (3) one-step self-etch systems, Adhese One and G Bond. The reason for selecting these particular adhesives was that, within each group, the two adhesive systems showed considerable variations in chemical composition with respect to the organic resin component, functional monomers and solvents. In this way, the objectives of the present study could be evaluated against a wide range of possible chemical compositions. On the other hand, three systems from each group, Excite, Adhese and Adhese One come from the same manufacturer and it can be expected that manufacturers tend to have an underlying philosophy regarding adhesive chemistry. By using systems from the same manufacturer, certain chemical variations are eliminated, allowing a more controlled evaluation of the progression from etch-and-rinse through two-step to one-step self-etch systems. Filtek Silorane adhesive system was selected because it matches the novel silorane-based RBC whose organic resin component is different compared to the "traditional" dimethacrylate-based RBCs. Though the adhesive system itself is a two-step self-etch system, it differs from all currently available two-step self-etch systems in that the primer is cured prior to the application of the bonding agent.

Each sample was its own control because linear spectra contained data from both demineralised and mineralised dentine. The intensity of the apatite peak varied in each spectrum since it is given in arbitrary units, but within each spectrum it showed a distinctive plateau at different depths within dentine. This plateau was taken as the unaffected mineralised zone and the mean intensity of the apatite peak was calculated from three different points and used as the control value for mineralised dentine in each linear spectrum.

DC values in the HL are given for the distance which corresponds to the mean depth of adhesive penetration. Values for further distances do not reflect the whole sample since adhesive penetration beyond the mean value was found in fewer number of samples.

Inclusion of these DC values would artificially increase the DC beyond the mean value of adhesive penetration. This is also the reason why the mean and SD values for the HL as a whole slightly differ from the ones given in Table 28 which includes all DC values irrespective of the distance in the HL. More homogeneous dispersion of DC values was observed for the adhesive layer compared to the HL for all adhesive systems.

10.3.1. Dentine demineralisation

The results of the present study have shown significantly deeper dentine demineralisation with etch-and-rinse than self-etch systems. This is in agreement with previous SEM (Abu-Hanna 2004) and micro-Raman studies (Carvalho 2005, Wang 2007). No significant difference was observed between the two etch-and-rinse systems, Excite and Admira, which are both applied after dentine is etched with phosphoric acid. The depth of dentine demineralisation with phosphoric acid varied from 6 to 14 µm and larger SD values in this group compared to self-etch systems indicated a more variable pattern of dentine demineralisation. Deeper demineralisation produced by phosphoric acid and self-etch systems, Adhese and G Bond, was associated with greater variability than in the other self-etch systems, Filtek Silorane and Adhese One.

The depth of dentine demineralisation for self-etch adhesive systems could not be associated with the number of application steps, often used to classify these systems. Adhese, a two-step, and G Bond, a one-step system, showed deeper demineralisation than Filtek Silorane, a two-step, and Adhese One, a one-step system. The depth of dentine demineralisation may be associated with specific types of functional acidic monomers in these systems. Van Landuyt et al. stated that the etching potential depends on the acidity of monomers which decreases in the following order: sulfonic acid>phosphonic>phosphoric>carboxylic acid>>alcohol (Van Landuyt 2007). Phosphonic acid acrylate, in Adhese, had a stronger acidic potential than phosphorylated methacrylates found in Filtek Silorane. Though carboxylic acid is weaker than

phosphates, G Bond contains 4-MET, with two carboxylic groups, resulting in pH<2 (Monticelli 2007). This is considered sufficient for a satisfactory etching potential for both enamel and dentine (Moszner 2005). Given the fact that dihydrogen acids are always more acidic than their monohydrogen counterparts, as they dissociate to more protons (Tay & Pashley 2001), it was rather unexpected that Adhese One, containing a dihydrogen phosphate-based acidic monomer, produced the least dentine demineralisation.

A higher degree of dentine demineralisation was associated with phosphoric acid in the etch-and-rinse system, Excite and Admira, compared to that produced by acidic monomers in self-etch adhesive systems. The degree of demineralisation produced by self-etch adhesives in the present study was comparable to phosphoric acid only in the first 1-2 μm. Deeper than 2 μm, there was a rapid decrease in their demineralisation potential. The trend of dentine demineralisation as a function of distance, suggests a linear decrease for etch-and-rinse adhesives and two-step self-etch Adhese, whilst for the other systems, Filtek Silorane, Adhese One and G Bond it had an exponential decrease [Figure 46]. This means that with more aggressive etchants, there is a more abrupt change between partially demineralised and un-affected dentine than with less aggressive acidic monomers in one-step self-etch systems.

10.3.2. Adhesive penetration

Deeper dentine demineralisation was accompanied by deeper adhesive penetration with Excite and Admira compared to self-etch adhesives. The results of the present study have confirmed that adhesive penetration for etch-and-rinse systems is always less than the extent of dentine demineralisation as reported in previous studies (Sano 1994, Hashimoto 2002, Wang 2007). On the other hand, the extent of adhesive penetration with self-etch systems was virtually equal to the extent of dentine demineralisation and, in most cases there was less than 1 μm of demineralised dentine unfilled with adhesive.

Filtek Silorane adhesive system showed equal dentine demineralisation and adhesive penetration whilst the greatest discrepancy between dentine demineralisation and adhesive penetration in self-etch systems was seen for G Bond. The results of the present study indicate that, for most self-etch systems, the problem of differential demineralisation and adhesive infiltration is not completely eliminated.

10.3.3. The degree of conversion in adhesive systems

In addition to addressing the problem of adhesive penetration, consideration must also be given to the question of the adhesive DC in the HL. In previous studies, it has been suggested that a 'pool' of unreacted monomers remains after incomplete polymerisation of the adhesive system within the HL (Sano 1999, Hashimoto 2002). However, in these studies, this conclusion was based on indirect evidence, i.e. increased micro porosity within the HL after 1 year storage or the relative comparison of peak heights in micro-Raman spectra. No details, either on the DC values or the depth of adhesive penetration were given in these studies. In the present study, it was possible to quantify the remaining C=C double bonds after determining the intensities of the aliphatic and aromatic peaks and calculating the DC using the previously quoted formula. Furthermore, by taking linear scans across the adhesive-dentine interface, it was possible to calculate a series of DC values at 1 µm intervals.

When compared to previous experiments detailed in Chapter 8 where the adhesive systems were applied to glass slides, the current experiment, when adhesives were applied to dentine, showed substantially higher DC values for all systems. This highlights the importance of substrate as another factor influencing the DC of adhesive systems in addition to previously mentioned factors related to LCU (Arrais 2007, D'Alpino 2007, Ye 2007), curing parameters (Kim 2006, Xu 2006, Feng 2009) or the chemical composition of adhesive systems (Imazato 1997, Imazato 2003b, Bae 2005, Dickens & Cho 2005, Kim 2005, Ogliari 2006, Wang 2006c, Ogliari 2007, Guo 2008a).

In previous studies using FTIR, adhesive systems were applied to potassium bromide pellet/crystal, glass slides, acetate strips but not to dentine. Adhesive systems, especially self-etch ones, are designed to be self-limiting, which means that the original chemical composition changes during interaction with dentine. Acidic monomers are neutralised through an interaction with hydroxyapatite. Any remaining solvents, ethanol or acetone, are known to be "water chasers" as they both exhibit the azeotropic effect through hydrogen bonding with water and this may result in phase separation (Van Landuyt 2007). Separation has been shown to occur between adhesive components due to different hydrophilicity of monomers (Spencer 2002) and affinity to form hydrogen bonds with the substrate (Van Landuyt 2005).

Substantial differences in the DC of adhesive systems on dentine and other substrates indicate that no direct extrapolation of DC values should be made from such in vitro studies to clinical conditions, as dentine seems to play an important role in polymerisation kinetics of adhesive systems. However, inert substrates may be used for studying and comparing the effect of various curing parameters, as was done in Chapters 8 and 9. Inert substrates eliminate the variations which may occur when adhesive systems interact with dentine. This interaction with dentine is unique for each adhesive formulation but also depends on biological variations in dentine, as was previously shown (Wang 2007).

There is limited information on the DC of adhesive systems across the adhesive-dentine interface. One of a few studies has shown a decrease in the DC of an "all-in-one" adhesive system, Prompt L-Pop, from about 90% in the adhesive layer to about 79% in resin tags, 50 μm deep. This was attributed to an increased water content within the dentinal tubules (Wang & Spencer 2005). A recent study by Navarra et al. has shown significantly higher DC values for Filtek Silorane Primer than Bond. Furthermore, higher DC values in the HL, but lower in the adhesive layer, have been reported for Filtek Silorane adhesive system compared to Clearfil SE Bond (Navarra 2009).

When discussing the DC of adhesive systems, irrespective of their chemical composition, two distinctive layers can be identified, the adhesive layer and the HL. The adhesive layer lies on top of the HL and is formed by adhesive only whilst the HL consists of both the adhesive and dentine and, therefore, should be considered separately. The DC of Excite, Adhese and Filtek Silorane Primer were in excess of 80% in the adhesive layer with Admira slightly lower than 80%, indicating a relatively high conversion of C=C double bonds. The DC of G Bond could not be calculated for the adhesive layer since the 1639 cm^{-1} peak associated with unreacted C=C double bonds could not be identified [Figure 49]. In the hypothetical situation of complete polymerisation, there would be a near elimination of C=C double bonds. However, in the current situation, it is more likely that the non-detection of the 1639 cm^{-1} peak is indicative of the number of unreacted C=C double bonds being below the threshold for detection by the micro-Raman spectrometer. A similar finding was reported by Suzuki et al. who studied the interface between dentine and 4META/MMA-TBB resin (Suzuki 1991). 4-META was hydrolyzed to 4-MET, which is the constituent of G Bond, and MMA is a predecessor monomer for all dimethacrylate-based systems, including G Bond. These authors also reported the absence of the 1639 cm^{-1} peak, not only in the adhesive layer but also in the HL.

Filtek Silorane Bond and Adhese One, on the other hand, produced significantly lower DC than the other adhesive systems. Adhese One showed the lowest DC, which was comparable to the results obtained in Chapter 8 when Adhese One was cured on glass slides for twice the manufacturer's recommended curing time. This may indicate that Adhese One has a maximum DC in the range of 55-60%, probably due to its chemical composition rather than the substrate. Adhese One is a one-step self-etch system with substantially different chemical composition compared to other systems. It contains bis-acrylamide and bis-methacrylamide cross-linking monomers which are hydrolytically more stable in acidic aqueous solutions than methacrylate monomers (Salz 2005b). However, it seems that these monomers cause inferior polymerisation kinetics than traditionally used methacrylates resulting in lower DCs. Though Adhese also contains

bis-acrylamide in the primer, it exhibits high DC values which may be attributed to BisGMA and HEMA in the bonding agent. The results of the present study as well as those presented in Chapter 8 indicate the complexity of the effect of chemical composition on polymerisation kinetics within different adhesive systems.

In addition to the effect of bis-acrylamide, Adhese One may have lower DC due to possible acid-base reaction between the amine and peroxide-based initiators and acidic monomers which has been shown to impair polymerisation (Salz 2005a). Furthermore, it is widely known that co-initiators, such as PPD or Lucirin fall out with the emission range of most LED LCUs (Moszner 2005). The manufacturer's technical data does not state the initiator system in Adhese One so, there may be several factors affecting lower DC in this adhesive system compared to the others.

Filtek Silorane Primer showed significantly higher DC values compared to Filtek Silorane Bond. The same finding has been recently reported by another study using NIR micro-Raman spectroscopy (Navarra 2009). This discrepancy in conversion needs to be further investigated with regard to the longevity of the Filtek Silorane Primer-Bond interface. Since their chemical composition is substantially different, it is difficult to estimate the actual amount of remaining unreacted monomers. It has been previously shown that the DC is only indicative of the number of unreacted C=C double bonds and not the amount of unreacted monomers. Emami & Soderholm have shown that the number of C=C double bonds per gram resin varies significantly among similar resin formulations, even from the same manufacturer, depending on the percentage weight of monomers and their molecular weights (Emami & Soderholm 2003). Filtek Silorane Primer and Bond contain different cross-linking monomers in addition to the unknown formulation of the unique hydrophobic dimethacrylate with an unknown number of C=C double bonds per gram resin. It is therefore, impossible to conclude whether the difference in DC between Primer and Bond will affect the clinical performance of Filtek Silorane adhesive system.

All adhesive systems except Admira showed greater or less decrease in the DC in the HL compared to the adhesive layer [Figure 51]. In most systems, the values of DC decreased as soon as the HL was reached. With Admira, however, the DC values in the adhesive layer and the HL were less variable.

The greatest decrease in the DC between the adhesive layer and the HL was seen in Excite. Whilst the mean DC was found to be in excess of 80% in the adhesive layer, it dropped to mean values between 50% and 60% in the HL. Thus, not only was demineralised dentine left un-infiltrated by this etch-and-rinse adhesive, but also a substantial amount of monomers remained unpolymerised. The DC of Adhese, Filtek Silorane Primer and G Bond remained above 60% and 70% within the HL, even though this is a significant decrease compared to the values found in their adhesive layers.

The HL is created by the diffusion of adhesive monomers into the water-filled spaces created by the demineralisation process and collagen exposure (Nakabayashi 1982). Water, however, interferes with the polymerisation process (Wang & Spencer 2005) and this could be the reason for a significant drop in DC values in the HL compared to the adhesive layer, observed in the aforementioned adhesive systems. The difference in extent to which the DC decreased in different systems could be related to the extent of dentine demineralisation and the interference of the polymerisation process by water. Compared to Excite, self-etch systems show a milder demineralisation potential, exposing less collagen fibres and fewer water voids probably resulting in less water interference with the polymerisation process (Pashley & Carvalho 1997).

Though Admira is also an etch-and-rinse adhesive system, it showed relative consistency in the DC throughout the adhesive and HL and seemed less affected by dentine substrate than Excite. This may be explained by the differences in the solvent content of the two systems. Acetone has a much better evaporation potential than ethanol which may result in less solvent content after the application to dentine. Solvent evaporation can facilitate polymerisation by reducing the distance between monomers

which may result in increased polymerisation rates and DC values (Jacobsen & Soderholm 1995, Giannini 2008). Furthermore, it has been shown that adding 10% of acetone to water increases vapour pressure by 300% resulting in increased evaporation of surface water (Chaudhry 1980).

Not only was the DC of most of the adhesive systems lower in the HL than the adhesive layer, larger variations of DC were observed for all the adhesive systems across the HL. This further elucidates the complex mechanism of interaction between the adhesive systems and dentine substrate and indicates that less predictable polymerisation kinetics occurs in the HL.

Previous studies have suggested that inferior polymer formation in the HL may be prone to degradation by water uptake, swelling of polymer chains and plasticization (Finer & Santerre 2004, De Munck 2005, Sideridou & Achilias 2005). Inferior polymer formation may be associated with lower DC of adhesive systems and the differences between the depth of demineralisation and adhesive penetration found in the present study. Furthermore, it has been shown that exposed collagen fibres are susceptible to degradation by host-derived matrix metalloproteinases even in the absence of bacteria (Pashley 2004). Therefore, the HL may be the weakest link which affects the longevity of the adhesive-dentine interface. It has been shown that the fracture of the adhesive-dentine interface typically occurs within the HL and not the adhesive layer (Hashimoto 2000, Hashimoto 2002, Bedran-de-Castro 2004, Monticelli 2007).

10.3.4. Two-dimensional micro-Raman spectroscopy versus SEM

The morphology of the HL has been studied using scanning electron microscopy (SEM), transmission electron microscopy (TEM) and staining techniques or a combination of these. The disadvantages of microscopic methods have been reviewed (Van Meerbeek 2000). Strong acids used in preparation dissolve both the mineral within the HL that is

not protected by the resin, as well as the un-affected dentine. The organic component of the HL is also affected by the organicolytic potential of NaOCl. Any information about the tooth tissue structure to which the adhesive was bonded, is lost. The low resistance of the HL to argon ion preparation treatment makes it easily distinguished from the adjacent adhesive and dentine (Van Meerbeek 1993a) though listed drawbacks include the formation of surface granules and porosities, which mimic poorly infiltrated demineralised dentine by polishing (Yoshiyama 1995). Specimen embedding into freshly mixed epoxy resin, for TEM, may cause two-directional movement of unreacted monomer molecules. Epoxy resin contains bisphenol A, which may infiltrate any porosity in the specimen, either originally present or created during EDTA decalcification (Nakabayashi 1998a). Acid dyes have been recently used to stain and identify type I collagen in the HL and it remains uncertain whether these acidic dyes and acetic acid, used in the staining preparation, cause further dentine demineralisation and possible exposure of collagen fibres (Wang & Spencer 2004a). Alcohol, used as a drying medium in staining preparations, may facilitate uncured monomer leaching or dissolution of poorly formed polymer networks, resulting in artefactual dye spread. The disadvantages of all three preparation methods limit the ability to observe the true extent of altered dentine substrate hybridization.

On the other hand, micro-Raman spectroscopic specimens can be observed under normal atmospheric conditions without chemical preparation procedures that may alter the interface. Moreover, data can be acquired from moist specimens, as water is a weak Raman scatterer. 2D micro-Raman maps, obtained in the present study, are a compilation of 15 x 15 µm or 20 x 20 µm scans from which data is acquired for statistical analysis. Confocal micro-Raman spectroscopy allows subsurface information to be obtained and data so gathered are analysed in the dedicated LabSpec software using a DCLS algorithm to identify the distribution of components across a mapped area. In addition to this, linear data can be extracted from a 2D map to calculate the degree of dentine demineralisation or adhesive DC across the adhesive-dentine interface.

The present study has indicated comparable results regarding the degree of dentine demineralisation and adhesive DC obtained from linear spectra and 2D maps. Since the acquisition of linear spectra is less time consuming, linear micro-Raman spectroscopy may be used to gather this type of information as long as the spectra are taken from random locations at the adhesive-dentine interface.

On the other hand, slight discrepancies were noted between the data obtained by linear and 2D micro-Raman spectroscopy with regard to adhesive penetration within the HL [Figure 47 and Table 29]. Since 2D maps cover a wider area compared to 1 µm linear scan across the adhesive-dentine interface, 2D mapping may be more reliable in determining the true HL thickness. Though linear scans of the HL are taken from the areas between the dentinal tubules, signals from lateral branches in close proximity to the HL may result in false conclusions about the adhesive penetration within the HL. Two-dimensional imaging provides visual information about the adhesive-dentine interface and allows resin tags, intertubular and peritubular areas to be identified. Therefore, the possibility of an erroneous interpretation of the HL thickness is reduced in 2D maps compared to linear scans.

The present results of 2D micro-Raman spectroscopic analysis have shown significantly thicker HL for Excite and Admira than self-etch adhesives. Filtek Silorane adhesive system produced thinner HL than Adhese and comparable to one-step self-etch G Bond. Adhese One showed the least HL thickness of all tested systems, comparable to the findings of adhesive penetration in linear micro-Raman analysis. The distribution of spectral features associated with adhesive and dentine indicates that the HL is a gradual transition zone between the adhesive layer and un-affected dentine for both etch-and-rinse and self-etch systems. This has been previously suggested for etch-and-rinse systems with different conditioning procedures (Van Meerbeek 1993b) or one-step self-etch adhesive systems (Sato & Miyazaki 2005) using linear micro-Raman spectroscopy. The present linear micro-Raman spectroscopic analysis indicates gradual changes in the degree of dentine demineralisation and adhesive DC across the adhesive-dentine

interface. 2D maps further indicate the gradual changes in the amount of adhesive and dentine based on the changes in the intensity of spectral features associated with adhesive and dentine.

The micro-Raman data from the present study confirm a complex interaction between adhesive and demineralised dentine, not always obvious from SEM and TEM findings (Van Meerbeek 1993a, Shimada 1995, Ferrari 1996, Sunico 2002, Sato & Miyazaki 2005, Sidhu 2007). These latter techniques suggest that a sudden and distinct change occurs between the adhesive and dentine. Moreover, 2D micro-Raman maps showed a very heterogeneous distribution of demineralisation on the horizontal axis as well as heterogeneous penetration of monomer into this affected dentine which was not suggested by linear data collection (Van Meerbeek 1993b, Wang & Spencer 2004b, Sato & Miyazaki 2005).

It has been shown previously that collagen fibres at the bottom of the HL often remain exposed due to the discrepancy between dentine demineralisation and adhesive penetration. The zone of exposed and un-infiltrated collagen fibres has been identified as one of the reasons for inferior mechanical properties of the adhesive-dentine bond (Hashimoto 2000) and areas of potential degradation (Pashley & Carvalho 1997, Pashley 2004, Carvalho 2005). In addition to this discrepancy, a potential problem may be that the reduced amount and decreased DC of adhesive resin, towards the bottom of the HL, may not be sufficient to 'compete' with water within interfibrillar spaces. This suggests that the actual zone of fully infiltrated collagen fibres is smaller than previously considered. In areas where adhesive resin is detected by micro-Raman spectroscopy, and therefore, by definition, part of the HL, the amount and DC of this adhesive may not be sufficient to provide adequate micro-mechanical interlocking to withstand mechanical, chemical and biological challenges.

The thickness of the HL obtained from micro-Raman data was significantly greater than that measured on SEM micrographs for all adhesives and this may be attributed to the previously discussed limitations of SEM.

With micro-Raman spectroscopy it was possible to distinguish a 1 μm transitional zone between Filtek Silorane Primer and Bond, which was not identified on SEM micrographs [Figure 58]. Micro-Raman showed distinctive spectra for both Primer and Bond, indicating separately cured layers. SEM micrographs showed a homogeneous zone, without any discernable interface. To ensure bonding with hydrated dentine, Silorane primer contains hydrophilic monomers whereas the bond has hydrophobic bi-functional monomers to match the hydrophobic Silorane resin. The bond is placed on the cured primer surface prior to be cured itself. Raman spectra indicated an intervening zone of circa 1 μm of mixed spectral features associated with both primer and bond. This zone of mixed primer and bond spectral features may result from an oxygen inhibition layer remaining at the cured primer surface. This zone may prove to be a weak link in the bonding system and further research is required. These features are not shown on SEM micrographs at x10000.

In micro-Raman spectra of the cured primer, the decrease of 1609 cm^{-1} band associated with unreacted aliphatic groups suggested further saturation of these groups during the curing of Silorane bond. It was not possible to differentiate how much of this saturation was contributed by the interaction with Silorane bond aliphatic groups or remaining unreacted aliphatic groups within Silorane primer itself.

Though SEM lacks data which were obtained by micro-Raman spectroscopy, it is a very useful adjunct tool in studying the adhesive-dentine interface, especially regarding the appearance of resin tags. These are exposed during sample preparation by an acid-base treatment using HCl and NaOCl (Van Meerbeek 2000). Further critical point drying prevents the formation of cracks and allows the original appearance of resin tags and their connection to the adhesive layer to be preserved.

In agreement with previous studies, the present results have shown differences in the frequency, shape, length and thickness as well as lateral branching of resin tags for different adhesive systems (Ferrari 1996, Santini 2001, Yoshiyama 2002, Radovic 2006). Etch-and-rinse adhesives, Excite and Admira, showed numerous, funnel-shaped resin tags some of which were thick and short whilst some were thin and long. Lateral branching was predominantly located on the short and thick resin tags. The shape of resin tags and lateral branching pattern are indicative of the aggressiveness of phosphoric acid, which removed not only the smear layer but also affected peritubular dentine allowing the spread of adhesive resin. Further dentine demineralisation along the dentinal tubules enabled enlargement and opening of the orifices to lateral canals especially those close to the HL. Thicker resin tags with extensive lateral branching were also seen after prolonged etching times (Ferrari 1997) so the ability of adhesive systems to form lateral branches depends mainly on the etching potential of either phosphoric acid or acidic monomers in self-etch systems.

Conversely, self-etch systems, especially Adhese and Adhese One formed thin and long resin tags with a few slender lateral branches. Less numerous tags were observed for one-step self-etch system, Adhese One. Filtek Silorane adhesive system formed thicker and shorter resin tags compared to Adhese and Adhese One.

SEM micrographs of G Bond showed numerous voids within the adhesive layer and also in the resin tags. Voids in G Bond have been previously reported using TEM (Sidhu 2007) and SEM (Monticelli 2007) and may be due to the lack of HEMA and phase separation. Furthermore, acetone, a co-solvent in G Bond, may induce phase separation and precipitation of adhesive components due to the changing water:acetone ratio during evaporation (Moszner 2005). G Bond does not contain HEMA, a low viscous monomer that increases dentine wetting and solubility of other adhesive monomers that may account for short and thick resin tags. These can also be considered resin plugs since they only occupied the orifice and several microns of the dentinal tubules. Though the acidic monomer 4-MET was able to produce deeper dentine demineralisation than the

other one-step self-etch adhesive, Adhese One, this was not followed by adequate adhesive penetration of G Bond resin. Voids in the adhesive layer and resin tags together with the discrepancy between dentine demineralisation and adhesive penetration may be factors associated with reduced bond durability of G Bond (Monticelli 2007). The same authors reported the G Bond failure at the top of the HL which further substantiates the present results as well as other papers (Hashimoto 2000, Hashimoto 2002, Bedran-de-Castro 2004).

10.4. Conclusions

The mean depth of dentine demineralisation for etch-and-rinse systems was about 10 μm which was significantly greater than 3-6 μm found for self-etch systems. Furthermore, higher degree of dentine demineralisation, as a function of distance, across the adhesive-dentine interface was associated with etch-and-rinse systems. All systems showed a discrepancy between dentine demineralisation and the HL thickness.

All adhesive systems showed a decrease in DC in the HL compared to the adhesive layer, with Admira bond showing the most uniform DC values. Significant differences in DC were observed for Filtek Silorane Primer and Bond. Adhese One showed the lowest DC across the adhesive-dentine interface. All systems showed less predictable polymerisation kinetics with larger variances of DC values in the HL compared to the adhesive layer. The DC values were in the range of 56-87% for the adhesive layer and 41-78% for the HL.

More unreacted C=C double bonds within the HL, and reduced amount of adhesive resin in the deepest zones of the HL, indicated that the zone of exposed collagen fibres was greater than defined in previous studies by the difference in dentine demineralisation and adhesive penetration. In a clinical context, this may be associated with inferior

mechanical properties of the polymer network and the whole adhesive-dentine bond as well as susceptibility to biodegradation and pulpal irritation.

2D confocal micro-Raman spectroscopy showed high discriminatory powers at a molecular level and not only gave a more precise indication of dentine demineralisation and monomer infiltration, but also highlighted the intermediate zone of circa 1 μm between Filtek Silorane Primer and Bond, not visible with SEM at x10.000 magnification. Furthermore, 2D micro-Raman spectroscopy indicated that the HL is a gradual transition zone between the adhesive layer and the un-affected dentine.

Micro-Raman spectroscopy and SEM showed that the etch-and-rinse adhesive systems, Excite and Admira, produced thicker HL compared to Silorane, G Bond and Adhese One. Micro-Raman spectroscopy showed that the Filtek Silorane adhesive system produced HL of comparable thickness to one-step self-etch adhesives. SEM analysis suggested that Filtek Silorane HL was of comparable thickness to methacrylate-based G Bond but significantly thicker than acrylamide-based Adhese One.

SEM analysis showed that etch-and-rinse systems produced numerous resin tags, with two distinctive types: short and thick with considerable lateral branching and longer but thinner with virtually no lateral branching. Self-etch adhesives, Adhese and Adhese One, showed a considerably different pattern of resin tags, long and thin with a few lateral branches. Filtek Silorane produced resin tags which resembled those of etch-and-rinse adhesives whilst G Bond showed numerous voids throughout the adhesive layer and very short and thick resin tags and resin plugs.

CHAPTER 11

QUANTITATIVE AND QUALITATIVE ANALYSIS OF THE RESIN-BASED COMPOSITE-ADHESIVE-DENTINE INTERFACE USING MICRO-RAMAN SPECTROSCOPY AND SCANNING ELECTRON MICROSCOPY

The aim of this study was to analyse the quantitative and qualitative aspects of the RBC-adhesive-dentine interface using linear and 2D micro-Raman spectroscopy and SEM.

The objectives were:
(1) To quantify the DC of RBCs and adhesive systems using micro-Raman spectroscopy;
(2) To evaluate the RBC-adhesive interface using 2D micro-Raman spectroscopy and SEM.

The null hypotheses are:
(1) There is no significant difference in the DC of the different adhesive systems after placement of their corresponding RBCs;
(2) There is no significant difference in the DC of RBCs.

11.1. Materials and Methods

11.1.1. Sample preparation

Thirty non-carious human third molars were prepared as explained in 5.1 and allocated randomly to six groups of five teeth. Peripheral parts of each tooth were trimmed with a diamond bur in a high-speed handpiece so that the diameter did not exceed 8.5 mm which was the diameter of the LCU tip used in the study.

Table 32 lists the adhesive systems and RBCs used in the present study. For simplicity, manufacturers' details for each material are omitted from Table 32 and are to be found in the comprehensive list of materials and devices on page XIII.

Prior to the application of the etch-and-rinse systems, Excite and Admira, 37% phosphoric acid was applied to dentine and left for 15 s. Following etching, the acid was rinsed with water and the tooth surface was dried with a mild stream of air leaving dentine moist according to the wet bonding technique.

Each adhesive system was applied according to the manufacturers' recommendations and covered with a Mylar strip. The adhesive was cured for 10 s with an LED LCU, Elipar Freelight2, at an intensity of 1000 mW/cm^2 at 1 mm tip-to-surface curing distance.

A matrix band was placed around each tooth so that the height of the band above the dentine surface was 3 mm. The RBC corresponding to the adhesive system was placed as a single increment up to a previously made mark 1 mm from the top of the matrix band. This created a 2 mm single increment RBC on top of the adhesive system with 1 mm remaining unfilled which acted as a standard light guide. Each sample was cured for 20 s using the Elipar Freelight2 at an intensity of 1000 mW/cm^2. The intensity of the LCU was monitored before and after curing of the adhesive and the RBC using a Bluephase meter. Immediately after curing, the matrix bands were discarded and the teeth were stored for 24 h in distilled water in light-proof containers, in a water bath set at 37ºC.

Table 32. Adhesive systems and resin-based composites used in the present study.

Materials	Type	Composition
Adhesive systems		
Excite	Etch-and-rinse, 1-bottle	Phosphonic acid acrylate, HEMA, BisGMA, dimethacrylates, silica, ethanol, catalysts, stabilizers
Admira		HEMA, HPMA, BisGMA, acetone, catalysts, ormocers, additives
Adhese	2-step self-etch, 2-bottle	Primer: Phosphonic acid acrylate, bis-acrylamide, water, initiators, stabilizers Bond: HEMA, BisGMA, dimethacrylates, Si-dioxide, initiators, stabilizers
Filtek Silorane adhesive system		Primer: Phosphorylated methacrylates, Vitrebond™ copolymer, BisGMA, HEMA, water, ethanol, silane-treated silica filler, initiators, stabilizers Bond: Hydrophobic dimethacrylate, phosphorylated methacrylates, TEGDMA, silane-treated silica filler, initiators, stabilizers
Adhese One	1-step self-etch, 1-bottle	Bis-acrylamide, water, bis-methacrylamide dihydrogen phosphate, amino acid acrylamide, hydroxyl alkyl methacrylamide, highly dispersed silicon dioxide, catalysts, stabilizers
G Bond		4-MET, UDMA, acetone, water, sillanated colloidal silica, initiator
Resin-based composites		
Tetric EvoCeram	dimethacrylate-based, nanohybrid	Dimethacrylates, prepolymers, barium glass, ytterbium trifluoride, mixed oxide fillers, additives, catalysts, stabilizers, pigments
Admira	ormocer-based, microhybrid	BisGMA, UDMA, ormocer, silicate filler, catalysts, additives
Filtek Silorane RBC	silorane-based, microhybrid	Silorane resin, CQ, iodonium salt, quartz filler, yttrium fluoride, stabilizers, pigments
Gradia Direct	dimethacrylate-based, microhybrid	UDMA, silica powder, alumino-silicate glass, organic filler

After 24 h of storage, the samples were mounted on the Isomet and 1 mm thick sections were cut parallel to the long axis of the tooth. From each sample, four sections were

obtained. The sections were analyzed under a light microscope at various magnifications to observe if the adhesive layer remained intact. The dentinal aspect of each section was placed in wet oasis sponge ensuring the adhesive aspect was kept dry. The sections were transported in the light-proof container and micro-Raman analysis started within 30 min.

11.1.2. Micro-Raman spectroscopy

Micro-Raman analysis was done as explained in 5.2. and 10.1.2. In addition to linear and 2D spectra taken across the adhesive-dentine interface, 30 μm linear and 20 x 20 μm 2D maps were taken at random sites of the RBC-adhesive interface. Post-processing of data was done as explained in 5.2. and 10.1.2.

11.1.3. Scanning electron microscopy

The same samples used for micro-Raman spectroscopy were prepared for and analysed using SEM. The preparation of samples for SEM was done as explained in 5.3. and the analysis is detailed in 10.1.3.

11.1.4. Statistical analysis

Though the data for DC of adhesive systems within the adhesive layer and the HL showed a normal (Gaussian) distribution, Bartlett's test showed significant differences in variances between the groups ($p<0.001$) despite several attempts to transform data. Therefore, the non-parametric Kruskal-Wallis test with Dunn's multiple comparisons post-test was used to evaluate the differences in DC values.

The data for DC of RBCs showed a normal distribution, but Bartlett's test showed significant difference between variances ($p<0.001$). However, after the transformation of data, no significant differences were observed ($p=0.091$) and the one-way ANOVA with Tukey's post-test was used to evaluate differences between groups.

11.2. Results

11.2.1. Adhesive systems

There were no statistically significant differences in the depth or degree of dentine demineralisation and adhesive penetration for any of the adhesive systems compared to data presented in 10.2. Therefore, these data are not presented here to avoid duplication.

Table 33 shows the descriptive statistics and statistical differences for the DC of adhesive systems within the adhesive layer. Cells with the same superscripts are not significantly different ($p>0.05$). The highest DC values were observed for Filtek Silorane Primer and the lowest for Adhese One ($p<0.05$). Excite, Admira and Adhese produced comparable results ($p>0.05$). Filtek Silorane Primer showed significantly higher DC than Filtek Silorane Bond ($p<0.05$). The DC of G Bond could not be calculated because the aliphatic peak at 1639 cm^{-1} was undetectable, so this adhesive system was not included in the statistical analysis for the adhesive layer.

Table 33. Descriptive statistics and statistical differences in the degree of conversion within the adhesive layer for each adhesive system. DC values are given in %.

Adhesive system	**Mean**	**SD**	**Minimum**	**Q1**	**Median**	**Q3**	**Maximum**
Excite [1]	82.07	7.37	71.10	75.05	82.11	87.45	96.08
Admira [1]	82.56	7.31	67.29	76.67	83.99	88.79	95.13
Adhese [1]	83.01	6.86	70.72	76.00	84.52	89.07	95.24
FS Primer[2]	90.91	3.90	81.11	89.45	91.66	93.31	97.13
FS Bond[3]	73.15	6.32	62.09	66.08	73.96	79.12	90.77
Adhese One[4]	53.16	7.32	41.09	48.21	51.79	57.33	69.42

Table 34 shows the descriptive statistics and statistical differences for the DC of adhesive systems within the HL. Cells with the same superscripts are not significantly different ($p>0.05$). Filtek Silorane Primer produced higher DC values than the other adhesive systems ($p<0.05$), but comparable to Adhese ($p>0.05$). Adhese produced significantly higher DC values than Excite ($p<0.05$) but comparable to Admira and G Bond ($p>0.05$). Excite, Admira and G Bond produced comparable DC values within the HL ($p>0.05$). Adhese One showed significantly lower DC than all other systems ($p<0.05$).

Table 34. Descriptive statistics and statistical differences in the degree of conversion within the hybrid layer for each adhesive system. DC values are given in %.

Adhesive system	**Mean**	**SD**	**Minimum**	**Q1**	**Median**	**Q3**	**Maximum**
Excite [1]	69.44	12.65	36.85	59.66	68.91	79.25	86.39
Admira [1,2]	73.25	7.18	56.88	68.31	73.33	77.86	86.02
Adhese [2,4]	77.86	9.58	54.44	71.25	79.89	85.94	93.96
FS Primer [4]	83.90	8.58	67.86	76.25	83.11	91.28	96.11
Adhese One[3]	32.55	11.96	15.05	21.85	30.30	42.70	58.83
G Bond [1,2]	73.76	10.43	57.31	64.25	72.08	83.09	91.00

11.2.2. Resin-based composites

Table 35 shows the descriptive statistics and statistical differences for the DC of RBCs. Cells with the same superscripts are not significantly different ($p>0.05$). No significant differences were observed for Tetric EvoCeram used with Excite, Adhese or Adhese One ($p>0.05$). Admira showed significantly higher DC values compared to other RBCs ($p<0.05$). Filtek Silorane RBC showed significantly lower DC values compared to other

RBCs ($p<0.05$), whilst Gradia Direct showed significantly lower DC than Tetric EvoCeram and Admira ($p<0.05$).

Table 35. Descriptive statistics and statistical differences in the degree of conversion of resin-based composites. DC values are given in %.

Resin-based composite	Mean	SD	Minimum	Q1	Median	Q3	Maximum
TEC–Excite [1]	66.64	5.26	55.21	63.48	66.47	71.11	78.07
TEC–Adhese [1]	66.30	6.40	54.67	59.38	67.48	72.26	75.62
TEC–Adhese One [1]	65.58	6.71	55.05	59.17	65.40	71.16	80.60
Filtek Silorane[2]	55.07	7.94	42.34	47.94	54.75	62.97	69.10
Gradia Direct[3]	59.94	9.98	24.29	56.52	60.76	67.50	77.54
Admira RBC[4]	71.27	8.64	52.68	63.96	72.32	79.23	83.70

11.2.3. Two-dimensional micro-Raman spectroscopy and SEM

Figures 59-64 show 2D micron-Raman maps for the adhesive-dentine and RBC-adhesive interface and SEM micrographs for each adhesive system and its corresponding RBC. The adhesive-dentine interface for each adhesive system is similar to previously presented in 10.2.4. when only adhesive was applied to dentine without a subsequent RBC. The RBC-adhesive interface showed differences between various systems. In contrast to an indistinctive transitional zone for Tetric EvoCeram-Excite, Tetric EvoCeram-Adhese and Gradia Direct-G Bond, these zones were clearly demarcated for Tetric EvoCeram-Adhese One and Filtek Silorane RBC-adhesive. The transitional zone for Admira RBC-Admira bond was distinctive but to a less extent compared to the latter two RBC-adhesive interfaces. Spectral features characteristic for Admira RBC did not completely disappear in the adhesive but were of lower intensity compared to the RBC.

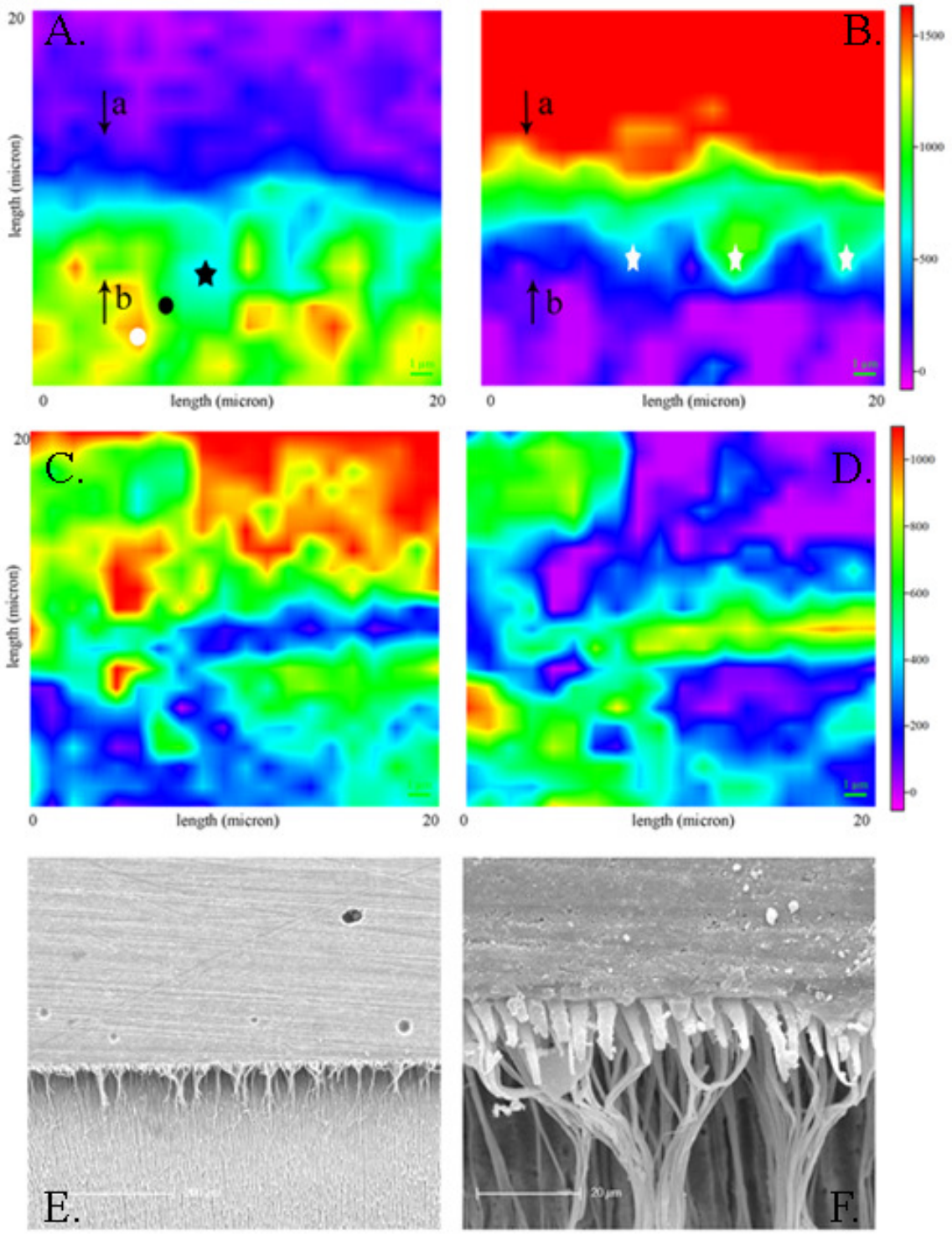

Figure 59. Representative 2D micro-Raman maps and the corresponding SEM micrographs of Excite-dentine and Tetric EvoCeram-Excite interfaces.

A. The range of intensity of spectral features associated with dentine, ranging from the least intensity corresponding to maximum demineralised dentine (point a, black arrow) to maximum intensity corresponding to unaffected dentine (point b, black arrow). The black star indicates a dentinal tubule, the black circle peritubular dentine and the white circle intertubular dentine.

B. The identical specimen area and the range of intensity of spectral features associated with adhesive resin starts from maximum intensity indicating pure adhesive (point a, black arrow), to the minimum intensity indicating no adhesive resin (point b, black arrow). The white star indicates a resin tag.

The colour scale shows intensity in arbitrary units for both A. and B.

There is an inverse relationship between the spectral intensities of the dentine hydroxyapatite moieties (left) and aliphatic and aromatic moieties in adhesive resin (right).

Point a indicates the beginning of dentine demineralisation and is taken as the top of the HL. Point b indicates un-affected dentine and is considered the bottom of the HL.

2D micro-Raman map of the Tetric EvoCeram-Excite interface shows no distinctive junction between the two materials. C. The distribution of the RBC; D. The distribution of the adhesive system.

E&F. SEM micrographs show no distinctive junction between the RBC and adhesive. Two types of resin tags produced by Excite, and previously observed in Figure 52, were more distinctive: short and thick with numerous very short lateral branches and long and much thinner, smooth sided tags. The short tags were about 9 µm long whilst the long tags were more than 50 µm long, converging about 20 µm deep to form a thick rope-like bundle, the whole appearance being like the delta of a river. Both types of resin tags occurred in the same zone.

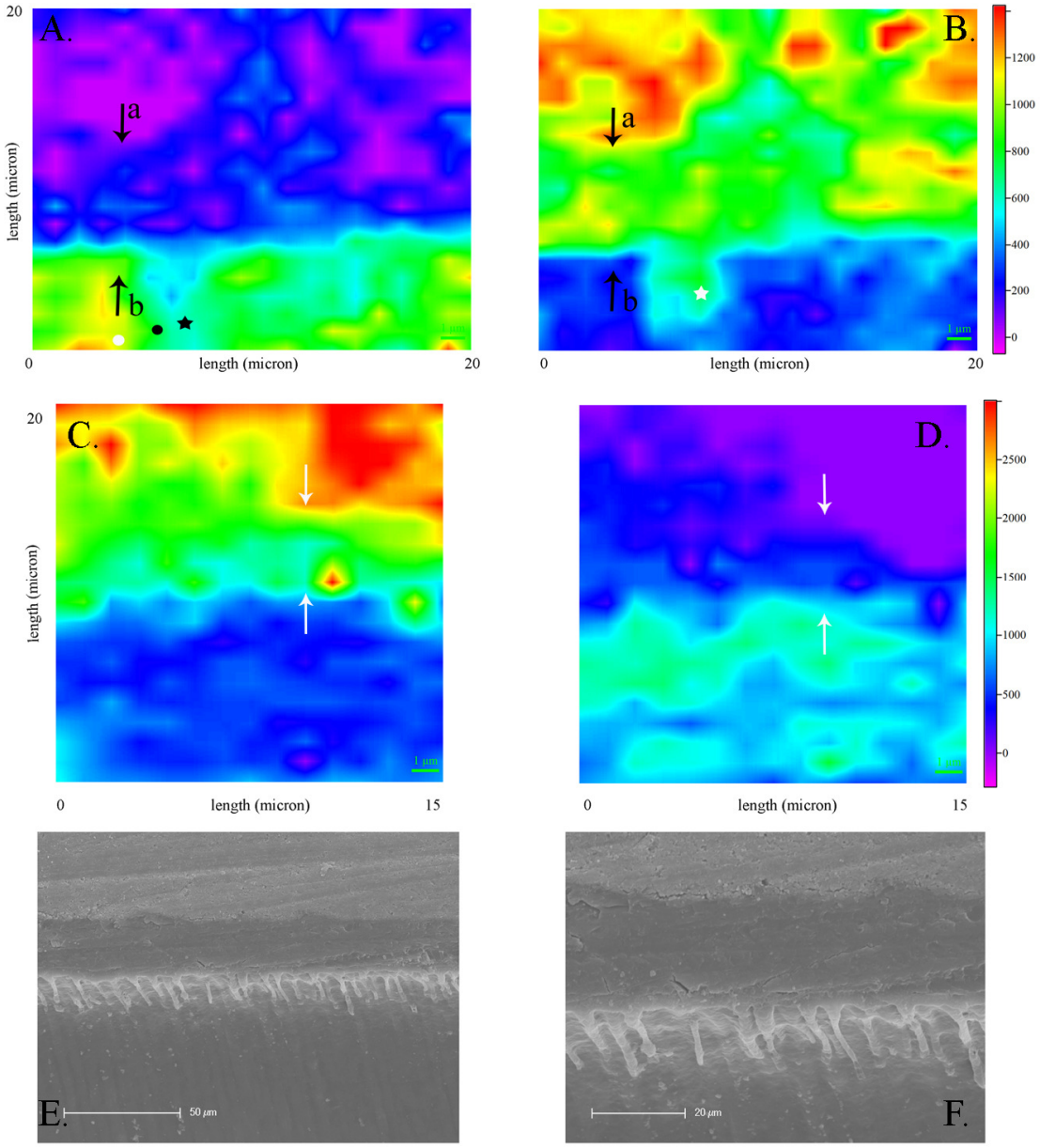

Figure 60. Representative 2D micro-Raman maps and the corresponding SEM micrographs of Admira bond-dentine and Admira RBC-Admira bond interfaces. The description for the adhesive-dentine and RBC-adhesive interface is as given for Figure 59. The 2D micro-Raman map of Admira RBC-Admira bond interface shows an intervening zone of about 3 µm with both spectral features associated with the Admira RBC and Admira bond.

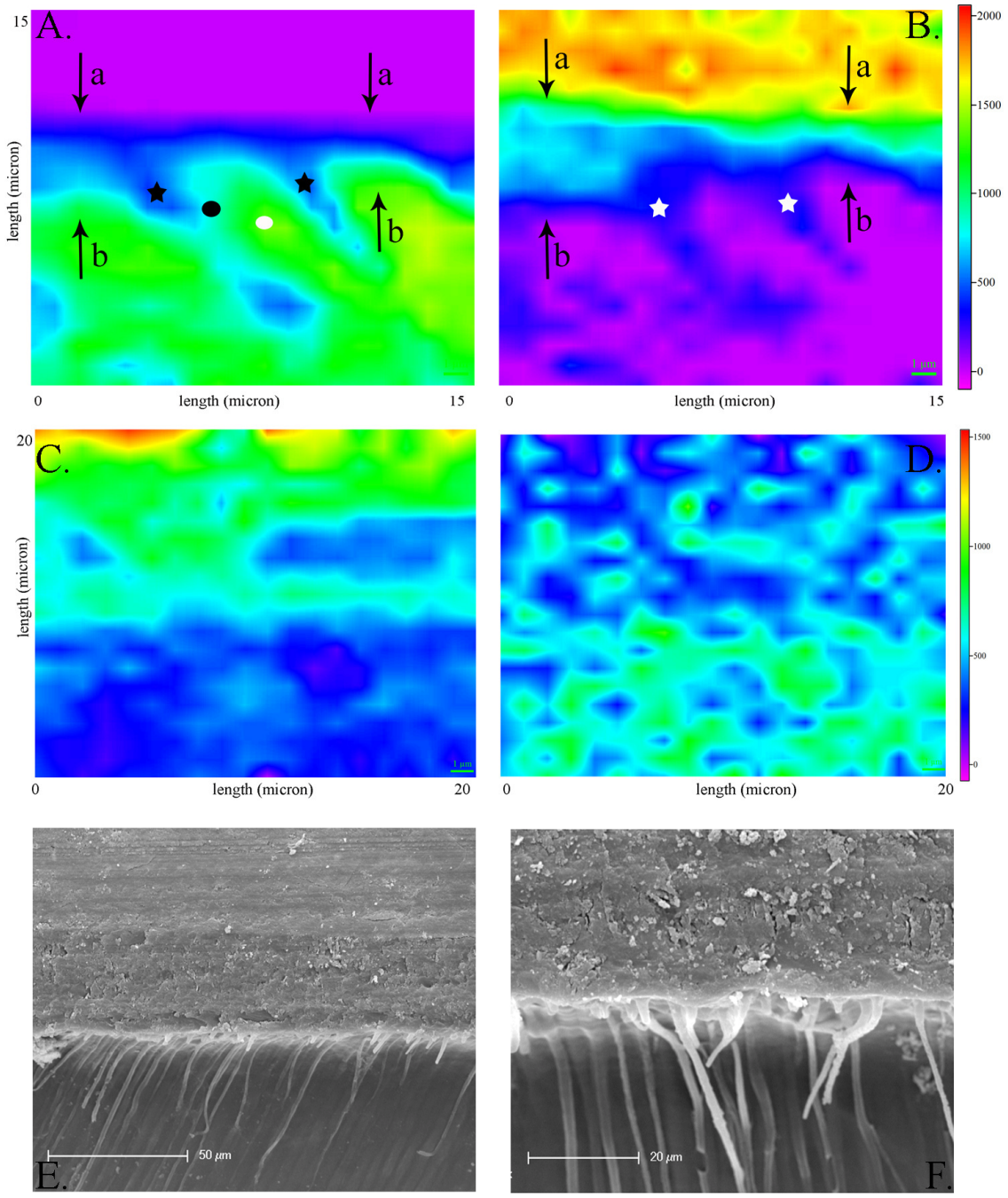

Figure 61. Representative 2D micro-Raman maps and the corresponding SEM micrographs of Adhese-dentine and Tetric EvoCeram-Adhese interfaces. The description for Adhese-dentine interface and RBC-adhesive is as given for Figure 59. The 2D micro-Raman map of Tetric EvoCeram-Adhese interface shows an unclear junction between the two materials with the spectral features

associated with both Tetric EvoCeram and Adhese overlapping over a relatively large area of about 9 μm. On the other hand, SEM micrographs show a distinctive electron dense line at the RBC-adhesive interface.

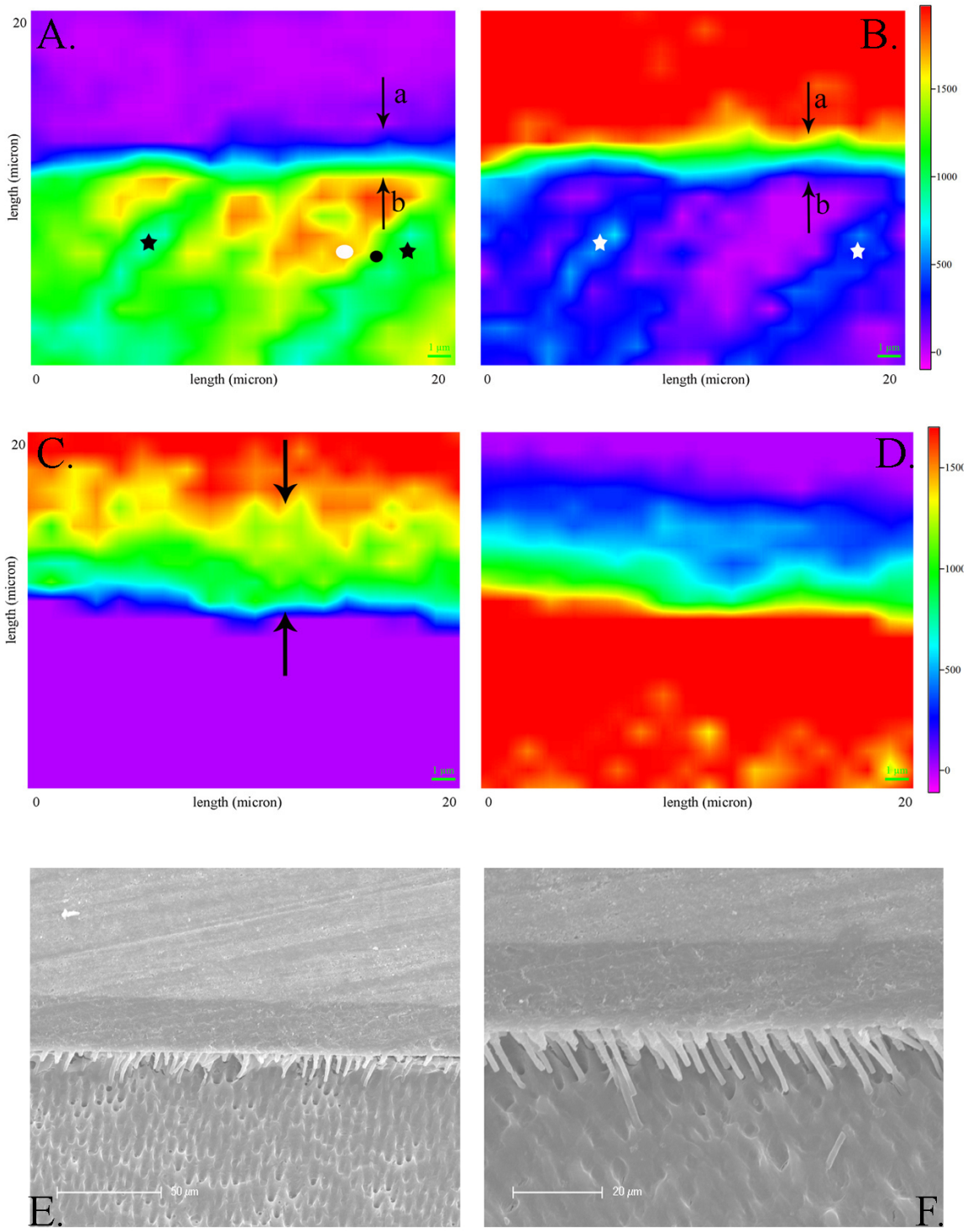

Figure 62. Representative 2D micro-Raman maps and the corresponding SEM micrographs of Filtek Silorane adhesive-dentine and Filtek Silorane RBC-adhesive interfaces. The description for the adhesive-dentine and RBC-

adhesive interface is as given for Figure 59. The 2D micro-Raman map of Filtek Silorane RBC-adhesive interface shows a distinct zone of separation with about 5 μm of gradual transition between spectral features associated with the RBC and the adhesive system.

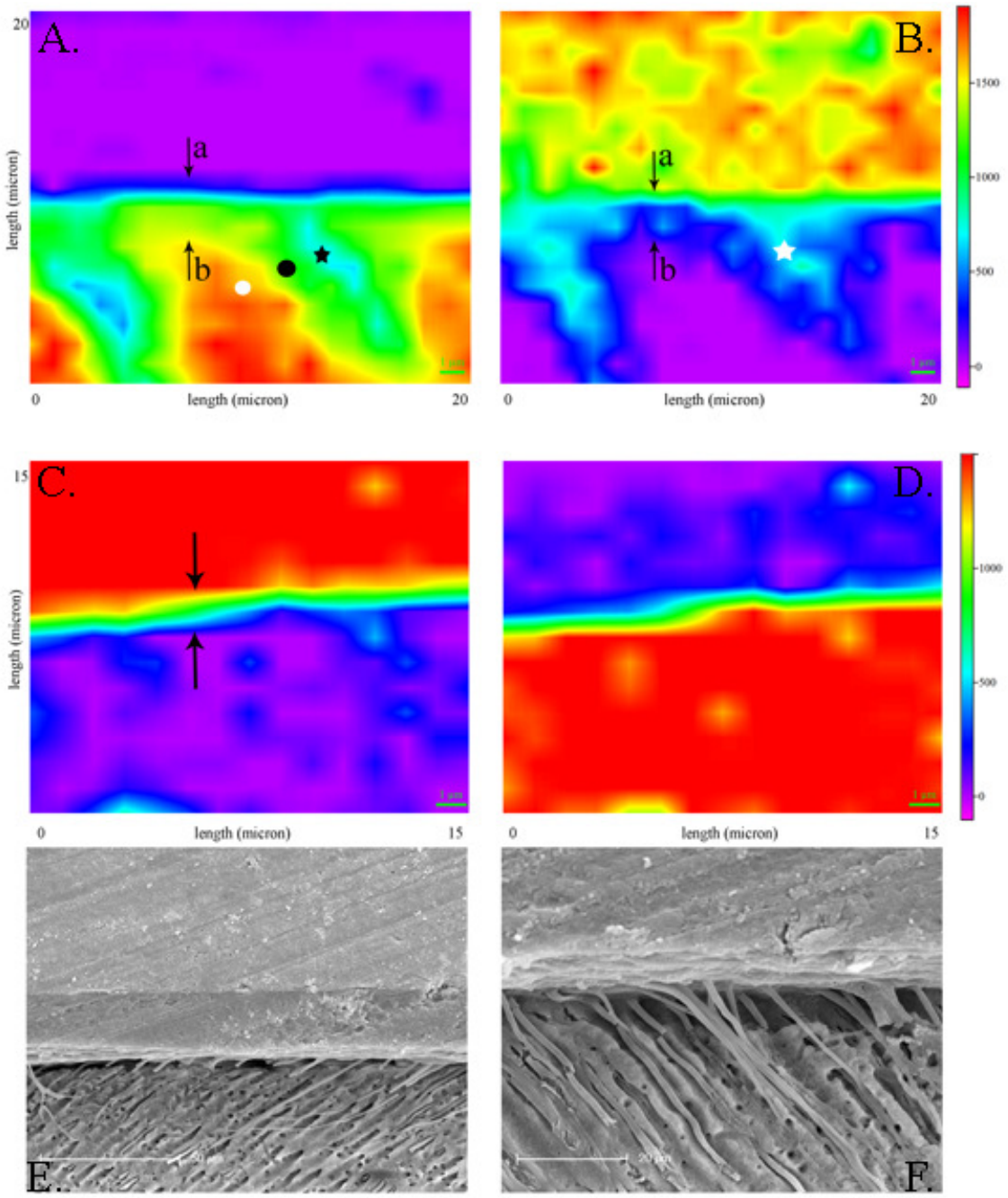

Figure 63. Representative 2D micro-Raman maps and the corresponding SEM micrographs of Adhese One-dentine and Tetric EvoCeram-Adhese One interfaces. The description for the adhesive-dentine interface and RBC-adhesive is as given for Figure 59. The 2D micro-Raman map of Tetric EvoCeram-Adhese One interface shows an abrupt change between the RBC and the adhesive

system. This zone between the two materials is clearly visible on SEM micrographs. A very thin HL and the appearance of resin tags are similar to those in Figure 53.

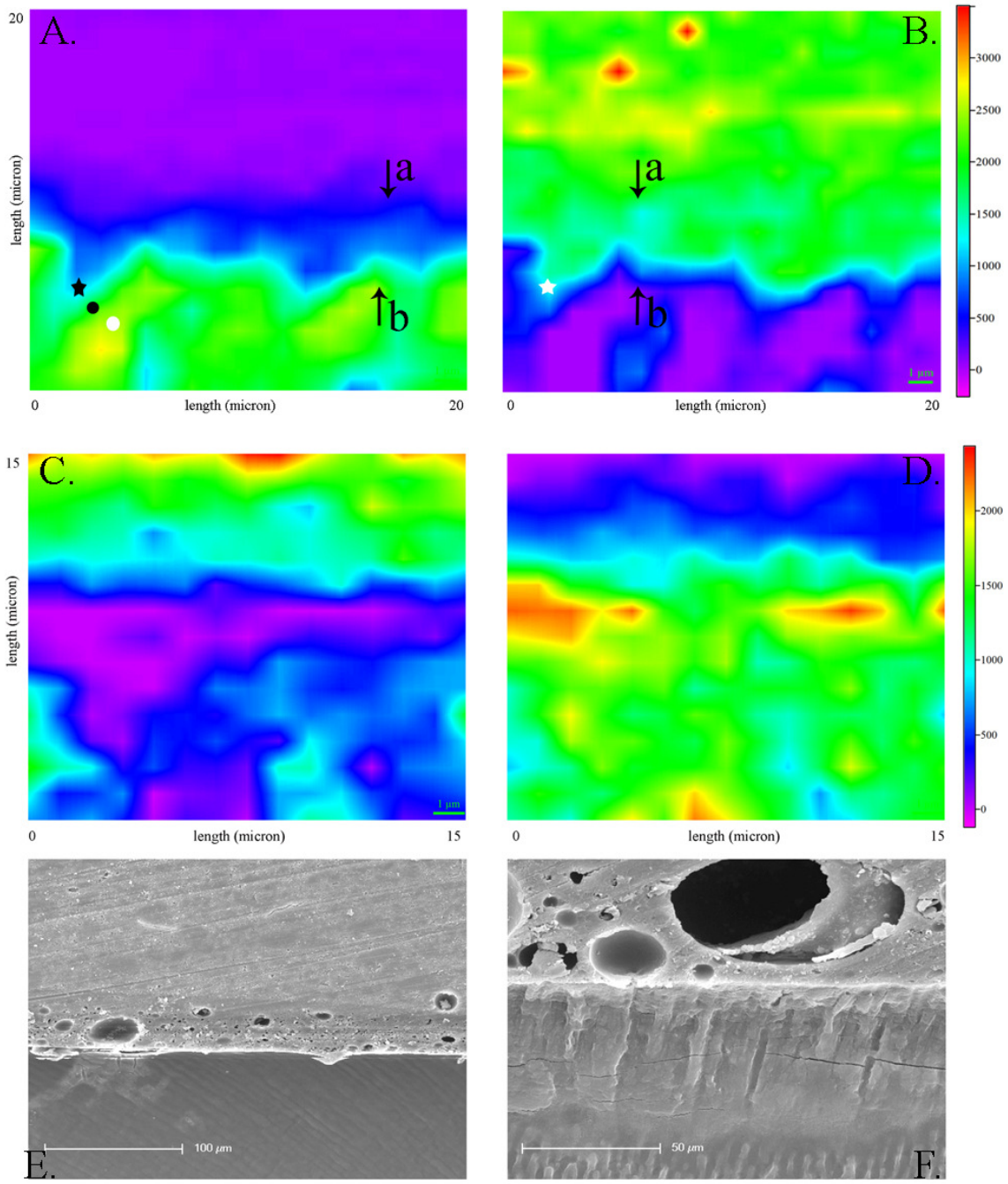

Figure 64. Representative 2D micro-Raman maps and the corresponding SEM micrographs of G Bond-dentine and Gradia Direct-G Bond interfaces. The description for G Bond-dentine and RBC-adhesive interface is as given for Figure 59. The 2D micro-Raman map of Gradia Direct-G Bond interface shows a distinct but less sharp transition between the RBC and the adhesive system

compared to RBC-adhesive systems in Figures 62 (Filtek Silorane) and 63 (Tetric EvoCeram-Adhese One). SEM micrographs show a zone of transition between the RBC and adhesive. The adhesive layer and the HL for G Bond are similar to those in Figure 57. Voids are clearly seen throughout the adhesive layer.

11.3. Discussion

The results indicated that:
(1) There were significant differences in the DC of different adhesive systems after the placement of their corresponding RBCs;
(2) There were significant differences in the DC of RBCs;
Therefore, all null hypotheses were rejected.

In the present study, the same adhesive systems were used as in Chapter 10 where the adhesive-dentine interface was studied after the placement of adhesive alone, without an RBC. In addition to reasons given in 10.3. for the use of Excite, Adhese and Adhese One, these adhesives were selected because they are manufactured by the same company and are compatible with Tetric EvoCeram. Other RBCs used in this study, Admira, Gradia Direct and Filtek Silorane RBC were chosen because they have significantly different chemical composition. This allowed the assessment of the polymerisation kinetics of a variety of RBC formulations. However, the present study did not include all available RBC formulations and the discussion must be interpreted in this light.

No differences were observed for the depth or degree of dentine demineralisation or the HL thickness in the present study compared to 10.2. This indicates that dentine demineralisation and adhesive penetration are virtually complete after adhesive placement and curing and are unaffected by the subsequent RBC curing. It has been reported that self-etch adhesive systems retain their etching potential after curing due to

the presence of unreacted acidic monomers and poorly polymerised oligomers (Wang & Spencer 2005). These may dissolve in dentinal water and continue to etch the surrounding dentine. The hydrolysis of ester bonds within the acidic monomers, over time, could also produce phosphoric acid which would demineralise the adjacent dentine. However, there are no data about the extent of these processes or subsequent changes in the original depth and degree of dentine demineralisation and the HL thickness.

Certain differences were observed from Tables 26 and 33 as well as Tables 27 and 34 for the DC of several adhesive systems before and after the placement and curing of their corresponding RBCs. The increased DC was found for Admira bond, Filtek Silorane Primer and Bond within the adhesive layer and Excite, Adhese and Filtek Silorane Primer within the HL. However, data from Chapter 10 were not statistically compared to the current study because these two studies were designed and carried out as separate experiments. More importantly, statistical subgroup analyses would require Bonferrroni correction for multiple comparisons which would significantly reduce the power of each test. The power and sample size calculations were initially done based on the alpha value of 0.05 and in this case, the correction would result in $p<0.008$ for each test.

In spite of this, the observation of increased DC values in adhesive systems after the placement of RBCs indicates that certain adhesive systems do not completely polymerise during adhesive curing and retain substantial polymerisation potential. At least two factors may induce further adhesive polymerisation during the curing of the applied RBCs: (1) light transmission through the RBC may deliver additional energy to the adhesive and further excite CQ and co-initiators (Stewardson 2004, Arikawa 2007, Masotti 2007, dos Santos 2008) and (2) heat generated during the polymerisation of RBCs may induce further polymerisation in adhesive systems with an increase in DC (Bagis & Rueggeberg 1997a). No data were found in the literature on the effect of heat on adhesive DC after their initial polymerisation. It has been previously shown that

heating RBCs in an oven to 50ºC for as short a time as 30 s significantly increased their DC (Bagis & Rueggeberg 1997a). On the other hand, it has been shown that a substantial amount of heat is generated within silorane-based, ormocer-based and dimethacrylate-based RBCs during curing. Temperature in excess of 70ºC was recorded during curing of Filtek Silorane RBC which was significantly higher than temperatures for ormocer-based and dimethacylate-based materials which were around 55ºC (Miletic 2009a). The effect of this heat on the DC of adhesive systems needs to be further investigated.

In the present study, the DC within the adhesive layer was found to be higher for Filtek Silorane Primer than Bond and this was in agreement with the results in 10.2. In the present study, where further energy was applied during the curing of Filtek Silorane RBC, the DC of Filtek Silorane Bond increased significantly compared to the Primer which remained virtually the same.

The DC of G Bond within the adhesive layer could not be calculated because the 1639 cm^{-1} peak was undetectable, as previously reported in 10.2. The one-step self-etch system, Adhese One, repeatedly showed the lowest DC values compared to all other adhesive systems.

In the present study, the DC of all adhesive systems decreased in the HL compared to the adhesive layer, as has been previously reported. Admira, showed differences between the adhesive layer and the HL but this was due to the increase in the DC in the adhesive layer, whilst the DC within the HL remained comparable to values reported in the previous study (10.2.). Adhesive DC for all systems was less predictable and less uniform in the HL than in the adhesive layer, as larger variances were observed, similarly to the previous study (10.2.).

According to the manufacturer's technical data, Tetric EvoCeram is an isofilled and nanofilled RBC containing a dimetharylate-based organic matrix with a certain amount

of prepolymerised particles. Admira RBC is an ormocer-based RBC containing an inorganic SiO_2 backbone with attached dimethacrylate monomers which constitute this unique polymerizable unit – ormocer. Admira also contains a small amount of free dimethacrylates. Gradia Direct is a UDMA-based RBC with up to 5% dimethacrylates and Filtek Silorane is a silorane-based RBC whose organic matrix consists of a combination of oxiranes and siloxanes brought together to form the unique silorane unit.

The DC of Tetric EvoCeram was found to be similar in combination with all three corresponding adhesive systems, Excite, Adhese and Adhese One. This indicates that the DC of adhesive systems has no effect on the DC of the overlying RBCs. The DC of Gradia Direct and Filtek Silorane RBC were significantly lower than Tetric EvoCeram, but still in excess of 50%. Admira RBC showed significantly higher DC compared to other RBCs. The DC of about 71% found in Admira RBC was higher than previously reported using FTIR spectroscopy (Bala 2005, Fleming 2007). The differences could be due to the fact that in the studies by Bala et al. and Fleming et al. the DC was calculated after curing of RBC samples in moulds where the effect of oxygen inhibition could be more profound compared to the placement and curing of RBCs on top of cured adhesives on dentine discs.

The unique micro-Raman spectrum of Filtek Silorane RBC reflected its profoundly different chemical composition compared to methacrylate-based RBCs. The 1639 cm^{-1} and 1609 cm^{-1} peaks were not identified since this material does not contain aliphatic and aromatic C=C double bonds. The C-O-C group from the oxirane component takes part in the polymerisation of Filtek Silorane. There are no literature data on micro-Raman characterisation and DC calculation of Filtek Silorane RBC. FTIR spectroscopy has been previously used to study the DC of this novel RBC (Palin 2003, Palin 2005, Ilie & Hickel 2006). However, both research groups used silorane-based experimental materials and not the commercially available Filtek Silorane RBC. Both research groups identified and associated the 883 cm^{-1} band in silorane absorbance spectra with C-O-C groups. Because the experimental silorane-based materials in these studies varied in

chemical composition, different bands were used as internal standards. Whilst Ilie & Hickel (2006) used the C-H associated 1257 cm^{-1} peak, Palin et al. (2003, 2005) used the aromatic C=C 1609 cm^{-1} peak.

In the present study, a peak at 790 cm^{-1} was identified in the micro-Raman spectrum of Filtek Silorane RBC, which was similar to epoxide ring stretching vibrations found in a previous study (Wu & Soucek 2000). This peak was used for DC calculations and the 1410-1460 cm^{-1} peak associated with CH_2 was used as the internal standard.

Since the main cross-linking monomer in Gradia Direct is UDMA, which does not contain aromatic rings, the 1720 cm^{-1} peak associated with C=O vibrations was used as the internal standard in preference to the 1609 cm^{-1} peak. The 1609 cm^{-1} peak was of low intensity in the uncured material and may be associated with the small amounts of other dimethacrylate monomers, unspecified by the manufacturer. Both 1639 cm^{-1} and 1720 cm^{-1} peaks are associated with UDMA indicating the constant and linear ratio with different molar concentrations of UDMA in RBC formulations.

The 2D micro-Raman spectra have shown substantially different transitional zones between different RBC-adhesive systems. Whilst Tetric EvoCeram-Excite, TetricEvoCeram-Adhese and to a certain extent Admira RBC-Admira bond and Gradia Direct-G Bond showed a blurry and indistinct junction, Tetric EvoCeram-Adhese One and Filtek Silorane RBC-adhesive showed a distinct change between the two components. This was very abrupt for Tetric EvoCeram-Adhese One whilst Filtek Silorane RBC-adhesive formed a 5 μm zone of gradual transition.

The characteristics of an RBC-adhesive interface may be associated with the chemical composition of the two materials. It is to be expected that the more similar the composition of adhesive and RBC, the more indistinctive the junction will be. This difference was clearly demonstrated in the case of Excite and Adhese One and Tetric EvoCeram. Tetric EvoCeram and Excite are dimethacrylate-based RBC and adhesive

system, respectively. Conversely, Adhese One contains bis-acrylamide and bis-methacrylamide cross-linking monomers. Excite and Tetric EvoCeram were able to form a homogeneous transitional polymer network in the oxygen inhibition layer of Excite which would blend into the polymer networks of both the RBC and the adhesive system. This was not the case for dimethacylate cross-linking monomers from Tetric EvoCeram and their acrylamide counterparts in Adhese One when a distinct zone was observed. It is not known to what extent the differences in the RBC-adhesive interface, distinct transition versus homogeneous zone, contribute to the longevity in terms of the bond strength or susceptibility of degradation. Spectral features characteristic for Admira RBC were found in the adhesive layer but were of lower intensity compared to the RBC. This could be due to the fact that ormocer molecules are present in both Admira bond and Admira RBC but in greater amount in the RBC.

Though the HL has been previously identified as the weakest link in the RBC-adhesive-dentine bonding (Hashimoto 2000, Hashimoto 2002, Bedran-de-Castro 2004, De Munck 2005, Wang & Spencer 2005), the RBC-adhesive interface may be of great importance in the assessment of composite repairs which are being increasingly utilised in clinical practice (Mjor & Gordan 2002). No uncertainty in clinical decision-making exists with one-bottle systems, either etch-and-rinse or self-etch ones. However, clinicians may be indecisive with two-bottle systems, whether to apply both primer and bond or bond only to the surface of an old RBC restoration which needs repair. From the point of view of material composition and the DC, there is no exclusive answer since adhesive systems from different manufacturers vary to a great extent. For example, the amount of photoinitiators may be designed in such a way that only the combined use of primer and bond is required for maximum conversion. On the other hand, higher solvent content and acidity of the primer may impair polymerisation of the entire adhesive system if applied together with the bonding agent to the surface of an old RBC. In this respect, manufacturers' instructions for use for most adhesive systems lack the detailed information for composite repairs.

11.4. Conclusions

The placement of RBCs on adhesive systems cured in situ did not affect dentine demineralisation and the HL thickness but had a significant effect on the DC values of adhesive systems in the adhesive layer and the HL. However, even with the additional curing, the DC of adhesive systems remained lower in the HL than in the adhesive layer. The DC in the HL also showed greater variance compared to the adhesive layer which indicated lower predictability of monomer conversion in the HL. Filtek Silorane Primer showed the highest and Adhese One the lowest DC values in both the adhesive layer and the HL. Filtek Silorane Primer showed significantly higher DC values than Filtek Silorane Bond. The DC values were in the range of 53-91% for the adhesive layer and 32-84% for the HL.

Admira showed the highest and Filtek Silorane the lowest DC values of all tested RBCs. Tetric EvoCeram produced similar DC values with different adhesive systems under the same curing conditions. The DC of the tested RBCs was in the range of 55-71%.

Filtek Silorane RBC was characterised using micro-Raman spectroscopy for the first time. The 790 cm^{-1} peak was associated with the epoxide C-O-C vibrations and used for DC calculations.

The quality of the transitional zone between RBCs and the adhesive systems depended on the chemical composition of the associated materials. Systems with dissimilar chemistry formed distinctive junctions with abrupt changes between the RBC and the adhesive system. Conversely, systems with more similar chemical composition formed gradual transitional zones and indistinctive junctions between the two components. Clinically, the compatibility of RBCs and adhesives and the quality of the transitional zone may be important for the durability and bond strength of the RBC-adhesive interface.

CHAPTER 12

CORRELATION OF MONOMER ELUTION WITH THE DEGREE OF CONVERSION IN ADHESIVE SYSTEMS

The aim of this study was to correlate monomer elution with monomer conversion in adhesive systems.

The objectives were to:
(1) To quantify the elution of HEMA, TEGDMA and BisGMA from etch-and-rinse and self-etch adhesive systems using reverse-phase high-performance liquid chromatography (HPLC);
(2) To quantify the DC of adhesive systems before and after elution using micro-Raman spectroscopy;
(3) To correlate monomer elution and the DC of adhesive systems.

The null hypotheses are:
(1) There is no significant difference in the amount of monomer elution as a function of time;
(2) There is no significant difference in the DC of adhesive systems;
(3) There is no correlation between monomer elution and the DC adhesive systems.

12.1. Materials and Methods

12.1.1. Sample preparation

Thirty intact human third molars of similar size, extracted for orthodontic reasons, were prepared to expose flat dentine surfaces as explained in 5.1. One dentine disc, 1 mm

thick, was cut from the mid-coronal portion of each tooth. The discs were randomly allocated to five groups of six and stored in distilled water in a refrigerator at 4ºC for no more than 24 h. Prior to the experiment, the containers were allowed to attain room temperature (20±1ºC).

Table 36 lists the following adhesive systems used in the present study. For simplicity, the manufacturer's details are omitted from the table and are to be found in the comprehensive list of materials and devices on page XIII.

Table 36. Adhesive systems used in the present study.

Adhesive systems	Type	Composition
Excite	Etch-and-rinse, 1-bottle	Phosphonic acid acrylate, HEMA, BisGMA, dimethacrylates, silica, ethanol, catalysts, stabilizers
Admira		HEMA, HPMA, BisGMA, acetone, catalysts, ormocers, additives
Clearfil SE	2-step self-etch, 2-bottle	Primer: MDP, HEMA, dimethacrylate hydrophilic, camphorquinone, N,N-diethanol p-toluidine, water. Adhesive: MDP, BisGMA, HEMA, dimethacrylate hydrophobic, camphorquinone, N,N-diethanol p-toluidine, silica
Filtek Silorane adhesive system		Primer: Phosphorylated methacrylates, Vitrebond™ copolymer, BisGMA, HEMA, water, ethanol, silane-treated silica filler, initiators, stabilizers Bond: Hydrophobic dimethacrylate, phosphorylated methacrylates, TEGDMA, silane-treated silica filler, initiators, stabilizers
Clearfil 3S	1-step self-etch, 1-bottle	MDP, BisGMA, HEMA, initiator, stabilizer, ethanol, water, filler

Prior to the application of Excite and Admira, dentine was first etched with 37% phosphoric acid for 15 s, rinsed with water for 10 s and blot-dried in accordance with the conventional wet bonding technique. No dentine pre-treatment was done for self-etch adhesive systems except for blot-drying. Prior to applying adhesives, each disc was

weighed (m_0) using a Mettler-Toledo balance (AB104, Mettler-Toledo Inc., Columbus, Ohio, USA)

In Excite group, Excite was applied to the dentine surface, gently agitated for 10 s and immediately dried by a stream of air for 3 s. In Admira group, Admira was applied to the dentine surface, left for 30 s and gently air-dried. In Clearfil SE group, Clearfil SE Primer was applied to the dentine surface and left in place for 20 s. It was then dried with a mild stream of air. Clearfil SE Bond was then applied to the dentine surface and air-dried. In Filtek Silorane group, Filtek Silorane Primer was applied for 15 s followed by gentle air-dispersion and 10 s of curing. Filtek Silorane Bond was applied on top of the primer and gently air-dried. In Clearfil 3S group, Clearfil 3S was applied to the dentine surface and left in place for 20 s. The entire surface was then air-dried for 10 s.

In all groups, immediately after the adhesive application to dentine discs, a Mylar strip was placed on top and the adhesive was cured for 10 s using an LED LCU, Elipar Freelight2, at an intensity of 1000 mW/cm^2, at 1 mm tip-to-surface distance. The intensity of the LCU was monitored by a Bluephase meter throughout the experiment. The Mylar strip was discarded immediately after curing and the discs were weighed (m_1). The amount of applied adhesive was calculated as $m=m_1-m_0$.

For all adhesive systems, the application and curing was done in accordance with manufacturers' instructions. The whole procedure was conducted in a small fume cupboard in which the temperature and humidity were constantly monitored by a USB-502 logger and remained at 20±1ºC and 50±2%. The procedure for each individual disc took less than 2 min and moisture evaporation under such conditions was considered to be negligible.

12.1.2. Micro-Raman spectroscopy

Following curing, micro-Raman spectroscopy was performed as explained in 5.2. Three point spectra were taken on the top surface of the adhesive at randomly chosen locations with 10 s accumulation time and six acquisitions for each point. Spectra of uncured adhesive systems were taken during the same session and were used as reference.
Post-processing of data was done as explained in 5.2. The DC for each adhesive system was calculated in accordance with the following formula:

$$\mathbf{DC = (1 - R_{cured} / R_{uncured}) X 100}$$

where R is the ratio of aliphatic and aromatic peak intensities at 1639 cm^{-1} and 1609 cm^{-1} in cured and uncured adhesives.

12.1.3. High-performance liquid chromatography

Immediately after micro-Raman spectroscopy, each sample was immersed in 1 ml of 75% ethanol/water solution (HPLC Gradient Grade solvents) in a separate glass vial and stored in a water bath at 37ºC. HPLC measurements were done 1 h, 6 h, 24 h, 96 h and 7 days after immersion. After each time interval, the whole solution was taken up for analysis, dentine discs were air-dried with the very mild stream of air and immersed in the fresh 1 ml of ethanol/water solution.

Quantitative analysis was performed on an Agilent 1100 Series HPLC system (Agilent Technologies, Santa Clara, CA, USA) equipped with a G1311A QuatPump, a G1313A Standard Autosampler and a G1315A DAD UV-Vis Detector. The column used was a reverse-phase Phenomenex Prodigy 5 ODS 310CA (Phenomenex, Torrance, CA, USA) (Figure 65). The mobile phase was a mixture of HPLC Grade water, containing 0.1% trifluoroacetic acid, and HPLC Grade acetonitrile, containing 0.04% trifluoroacetic acid. The gradient was applied according to the method shown in Table 37.

The flow rate was 1 mL min^{-1} and the injector volume was always 20 µL. UV detection was performed at 210 nm to monitor the elution of HEMA and TEGDMA and 275 nm for BisGMA. The compounds were identified by comparison of their elution times with those of the reference compounds under the same HPLC conditions. All measurements were done in triplicate.

Figure 65. Agilent 1100 Series HPLC system used in the present study.

Table 37. Time programme of the mobile phase gradient.

Time (min)	**Eluents (%)**	
	H_2O	**CH_3CN**
0	90	10
7.0	40	60
10.0	0	100
17.0	0	100
17.1	90	10
20.0	90	10

For calibration purposes, stock solutions of reference standards were prepared in 75% ethanol/water solution and the solutions were stored in a refrigerator at 4°C. The calibration solutions were prepared from these stock solutions by dilution with 75% ethanol to give final concentrations of 1.0, 5.0, 10.0, 15.0, 25.0 and 50.0 ppm. Triple 20 µL injections were made for each standard solution; the peak area for appropriate monomers was determined and plotted versus concentration using linear regression analysis.

12.1.4. Statistical analysis

The data for eluted monomers and DC were tested for normality using Kolmogorov-Smirnov test and for the equal variances using Bartlett's test. The data followed Gaussian (normal) distribution for both datasets ($p>0.15$). However, Bartlett's test showed significant differences between variances and therefore, the data were transformed so that both assumptions for the analysis of variance (ANOVA) were met. One–way ANOVA was used to test differences for either monomer elution or the DC between the adhesives. The paired t-test was used to test the differences in BisGMA and HEMA elution from the same adhesive system with the p value for each at 0.01 instead of 0.05 (Bonferroni correction). Pearson's correlation coefficient was used to measure the degree of linear relationship between the amount of eluted monomer and the DC for each adhesive.

12.2. Results

12.2.1. Monomer elution – High-performance liquid chromatography

Figure 66 shows the superimposed representative chromatograms for the three monomers.

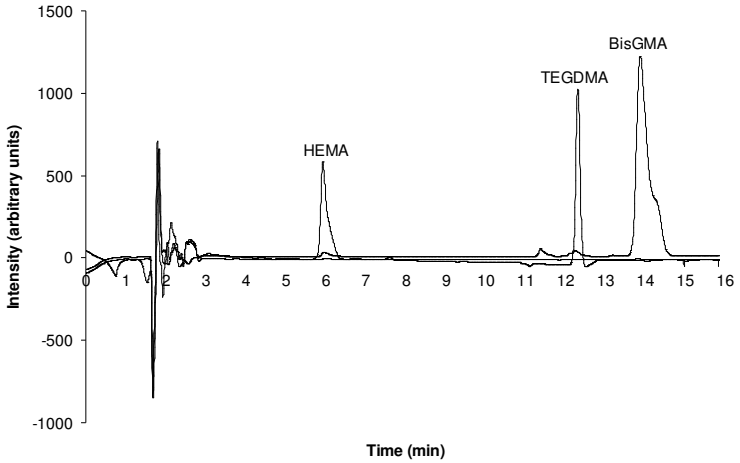

Figure 66. Representative chromatograms of HEMA, TEGDMA and BisGMA standard solutions.

The regression equations and R^2 values were as follows:

HEMA: conc(X)= (area Y – 94.2)/145.2, R^2=0.9980

TEGDMA: conc(X)= (area Y – 225.2)/179.7, R^2=0.9844

BisGMA: conc(X)= (area Y – 4.9)/23.2, R^2=0.9995

Tables 38 and 39 show the amount of eluted BisGMA and HEMA from five tested adhesive systems. The same superscript numbers / letters indicate no significant differences (one-way ANOVA).

More than 90% of the whole elution occurred during the first 1 h after immersion and was nearly complete after 24 h. In Clearfil SE and Admira less than 0.5 ppm of BisGMA was detected after 96 h whereas the concentration of BisGMA increased in Filtek Silorane from 6 h to 96 h. No elution of BisGMA from any adhesive system was detected after 7 days. The amount of eluted BisGMA was significantly different for all adhesives ($p<0.05$), except for Excite and Clearfil 3S ($p>0.05$).

HEMA showed similar elution kinetics to BisGMA. It eluted completely after 6 h from Clearfil 3S and after 24 h from Excite, Clearfil SE and Filtek Silorane. No HEMA was detected from Admira between 6 h and 96 h. At 96 h and 7 days, 1.1 ppm and 1.6 ppm

were detected, respectively. The differences in HEMA elution between adhesive systems were statistically significant ($p<0.05$), except for Excite and Admira ($p>0.05$).

There was a statistically significant difference between the elution of BisGMA and HEMA for each adhesive (paired t-test; $p<0.001$).

The total amount of eluted TEGDMA from Filtek Silorane adhesive system was detected during the first 1 h, the mean (SD) values being 8.6(3.7) ppm.

Table 38. Elution of BisGMA per mg adhesive.

Adhesive system		**Time**				
		1 h	**6 h**	**24 h**	**96 h**	**7 days**
Excite[1]	Mean (ppm)	14.2	2.5	0.2	0.0	0.0
	SD (ppm)	2.1	1.4	0.3	0.0	0.0
Clearfil SE	Mean	29.2	3.2	0.5	0.2	0.0
	SD	7.9	1.9	0.4	0.3	0.0
Clearfil 3S[1]	Mean	18.9	0.5	0.1	0.0	0.0
	SD	4.0	0.1	0.2	0.0	0.0
Admira	Mean	8.8	0.6	0.5	0.3	0.0
	SD	2.2	0.2	0.3	0.4	0.0
Filtek Silorane	Mean	2.0	1.9	2.6	4.9	0.0
	SD	0.7	0.5	1.0	1.5	0.0

Table 39. Elution of HEMA per mg adhesive.

Adhesive		Time				
		1 h	**6 h**	**24 h**	**96 h**	**7 days**
Excite[A]	Mean (ppm)	25.7	0.9	0.4	0.0	0.0
	SD (ppm)	7.6	0.4	0.3	0.0	0.0
Clearfil SE	Mean	49.9	1.6	0.3	0.0	0.0
	SD	7.1	0.6	0.0	0.0	0.0
Clearfil 3S	Mean	13.1	0.7	0.0	0.0	0.0
	SD	2.7	0.6	0.0	0.0	0.0
Admira[A]	Mean	26.7	0.8	0.0	1.1	1.6
	SD	6.1	0.7	0.0	0.4	0.5
Filtek Silorane	Mean	2.6	0.9	0.5	0.0	0.0
	SD	1.9	0.7	0.1	0.0	0.0

The weight% of eluted BisGMA and HEMA was calculated using the total amount of these two monomers in the uncured adhesive as a baseline. BisGMA varied from 3.8 wt% for Excite to 23.1 wt% for Admira. HEMA varied from 3.9 wt% for Clearfil 3S to 32.5wt% for Admira (Table 40). The same letters indicate no significant differences (one-way ANOVA). There were statistically significant differences between all adhesives with respect to wt% of HEMA ($p<0.05$). For BisGMA, the differences were statistically significant between all adhesives ($p<0.05$), except Clearfil SE and Clearfil 3S ($p>0.05$).

Table 40. Elution of BisGMA and HEMA relative to the amount of either monomer in uncured adhesive (wt%) per mg adhesive.

Monomer		**Adhesive system**			
		Excite	Clearfil SE	Clearfil 3S	Admira
BisGMA	Mean (ppm)	3.8	11.9	12.0	23.1
	SD (ppm)	0.6	2.9	2.5	5.7
	Significance	A	B	B	C
HEMA	Mean (ppm)	8.6	12.7	3.9	32.5
	SD (ppm)	2.5	1.8	0.9	7.9
	Significance	A	B	C	D

12.2.2. The degree of conversion – Micro-Raman spectroscopy

Figure 67 shows the DC values for all adhesive systems immediately after curing, after 24 h and after 7 days. One–way ANOVA confirmed that the differences were statistically significant for all adhesive systems ($p<0.05$), except for Excite and Clearfil SE, at the same time intervals ($p>0.05$). In all groups, the DC was significantly higher after 24 h and 7 days than the DC calculated immediately after curing ($p<0.05$). A significant difference between 24 h and 7-day intervals was observed only in the Filtek Silorane group ($p<0.05$).

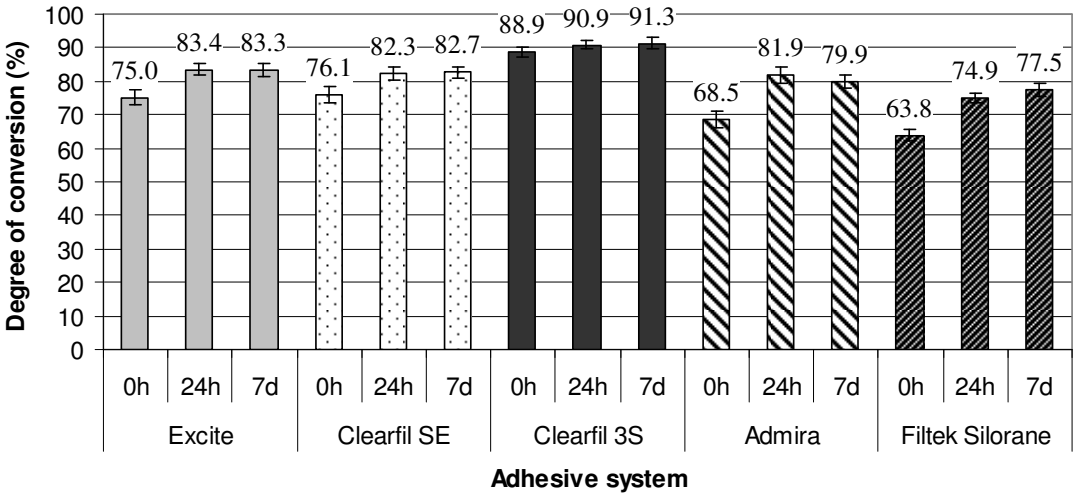

Figure 67. The degree of conversion of adhesive systems obtained immediately after curing, 24 h and 7 days post-curing.

12.2.3. Correlation analysis

The linear relationship was determined between the elution of BisGMA and HEMA in Excite (Pearson's correlation coefficient r=0.540), Admira (r=0.698) and Filtek Silorane (r=0.809) ($p<0.05$). Since the Pearson coefficient values were in the range $0<r<1$, the correlation was positive i.e. the more BisGMA eluted, the more HEMA eluted from the adhesive system as well. There was no linear relationship between the elution of BisGMA and HEMA in Clearfil SE and Clearfil 3S ($p>0.05$).

A negative correlation was found between the amount of eluted HEMA and the DC for Clearfil 3S (r= -0.758, $p<0.001$). It was found that Clearfil 3S samples with lower initial DC values eluted more HEMA than samples with higher DC. There was no linear relationship between the amount of eluted monomers and the DC for any other adhesive system ($p>0.05$).

12.3. Discussion

The results indicated that:
(1) There were significant differences in the amount of monomer elution per time;
(2) There were significant differences in the DC of adhesive systems;
(3) At least one of the materials showed correlation between elution and the DC.
Therefore, all three null hypotheses were rejected.

In the present study, monomer elution from different adhesive systems was quantified using HPLC and correlated with the DC determined by micro-Raman spectroscopy. The adhesive systems were chosen based on the classification of etch-and-rinse, two-step self-etch and one-step self-etch systems with the addition of two adhesives based on ormocer and silorane chemistry. Another criterion for adhesive selection was that the organic component was based on BisGMA/HEMA. Although Filtek Silorane Bond contains TEGDMA, the Primer is based on BisGMA/HEMA.

In all five adhesives, virtually all HEMA was eluted by 24 h, with more than 90% eluted in the first 1 h. BisGMA followed a similar pattern except in the case of Filtek Silorane where it increased up to 96 h and dropped thereafter to undetectable levels at 7 days.

It was reported that the elution of monomers from RBCs was 85-100% were eluted within 24 h (Ferracane & Condon 1990). It should be noted that only one material was investigated by these authors and, though four of the five adhesive systems in the current study had a similar pattern, the elution of BisGMA from Filtek Silorane was very different. More recent studies, using the more sensitive methodology of HPLC, have shown that monomer elution extends beyond 24 h for RBCs, experimental resin mixtures (Munksgaard 2000, Sideridou & Achilias 2005) as well as fissure sealants (Moon 2000). The current study substantiates this for dental adhesives though only trace amounts are identifiable after 24 h in most cases.

A previous study has reported that monomer elution from cured adhesives is about 1.5-2.5% of adhesive total weight (Kaga 2001). In the present study, the amount of eluents relative to the total weight of adhesives was not considered appropriate for material comparison due to significant qualitative and quantitative differences in monomer content in various adhesive systems. Therefore, the amount of eluted monomers relative to the total amount of monomers in uncured adhesives was calculated. Weight % for HEMA and BisGMA was calculated for Excite, Clearfil SE, Clearfil 3S and Admira but could not be calculated for Filtek Silorane because spontaneous polymerisation occurred during HPLC preparation in spite of efforts to overcome this problem.

Large variations were observed for eluted BisGMA and HEMA between the adhesives. The highest wt% of eluted BisGMA and HEMA was associated with Admira, 23.1wt% and 32.5wt%, respectively. The manufacturer's data states that Admira contains monomers attached to a SiO_2 backbone as well as a pool of free monomers. The manufacturer was requested to supply ormocers contained in the adhesive system to be used as reference. As this was denied, it was impossible to determine the amount of monomers attached to the ormocer molecules and, therefore, only the free monomers were quantified. It is unclear whether the high amount of eluted monomers from Admira, found in the present study, originated solely from the pool of free monomers or from degraded unpolymerised ormocers as well.

The wt% of eluted HEMA from Excite was more than twice the value of eluted HEMA from Clearfil 3S. It has been shown that the smear layer and smear plugs retain in self-etch adhesives (Tay & Pashley 2001) which may represent a diffusion barrier (Wang & Hume 1988). It has been shown that the outward fluid movement through both the smear layer and the cured adhesives is lower in self-etch than etch-and-rinse adhesives (Hashimoto 2004). This phenomenon could account for lower HEMA elution in the one-step self-etch system, Clearfil 3S, than the etch-and-rinse system, Excite, in the present study.

The increased wt% of eluted HEMA from the two-step self-etch adhesive system, Clearfil SE may be partly explained by the fact that HEMA is also contained in the bond liquid and contributes to a pool of free HEMA in the cured adhesive layer.

According to the manufacturer's data on Filtek Silorane adhesive system, the main monomers in the primer are BisGMA and HEMA and the main named constituent of the bond is TEGDMA. A previous study, using 2D micro-Raman spectroscopic mapping of the adhesive-dentine interface, has shown the presence of two separate layers (primer and bond) in the Filtek Silorane adhesive system. Elution of both HEMA and BisGMA from the primer through the overlying bond indicated the permeable nature of the bond which was not sufficient to prevent elution of HEMA and BisGMA. In a previous study, an inverse correlation was found between the DC and the permeability of dental adhesives (Cadenaro 2005). Differences in the elution kinetics for BisGMA and HEMA occurred probably due to the larger size and greater rigidity due to the bulky aromatic moieties which contribute to the lower mobility of BisGMA compared to HEMA.

TEGDMA was completely eluted from Filtek Silorane after 1 h and was not detected in the remainder of the 7 day period. TEGDMA showed faster elution than BisGMA in the other adhesives. This may be due to the differences in stereochemistry of the two dimethacrylates, the flexibility and the lack of bulky aromatic moieties of TEGDMA which may favour its faster release even through the highly cross-linked 3D networks.

Absolute values of monomer elution are important for evaluating adverse biological effects of monomers on vital cells. Depending on the study design, these values indicate the range of monomer concentrations that the cells may be exposed to in clinical conditions. The present study design was chosen to favour maximum polymerisation of adhesives when applied to dentine as well as maximum elution of unreacted monomers into an organic solvent. When saliva and distilled water are used as solvents rather than ethanol/water, there is significantly lower elution of monomers from RBCs (Ferracane & Condon 1990, Kim & Chung 2005, Zhang & Xu 2008). Moreover, the use of pure

methanol as solvent enabled detection of a broad range of monomers in dental adhesives and the reliable retention prediction even of hydrophilic monomers, such as HEMA (Silikas & Watts 2000). The most commonly used organic solvent for studying monomer elution from resin-based dental materials is ethanol/water solution (Ferracane & Condon 1990, Ferracane 1994, Eliades 1995, Moon 2000, Sideridou & Achilias 2005). Ethanol/water has been recommended by the US Food and Drug Administration for the use as a saliva substitute. Ethanol/water solution favours solvent penetration into the polymer matrix and enlargement of spaces between polymer chains (Sideridou & Achilias 2005), resulting in greater elution of unreacted monomers which would otherwise remain trapped within the polymer network. Even with organic solvents, certain amounts of unreacted monomers remain because the elution process is affected not only by the solvent but also by polymer morphology and monomer distribution. It has been shown that the unreacted monomers are more likely to remain within microgels than micropores of the polymer network (Simon 1989).

Although distilled water or artificial saliva may simulate more clinically relevant conditions, it is well-known that neither fully resembles the composition of human saliva. Furthermore, variations in natural salivary composition and flow rate may result in variations of monomer elution. It may, therefore, be more appropriate to create a framework of possible elution concentrations than to try and simulate every possible clinical situation.

It has been stated that residual BisGMA may be metabolised to bisphenol A which is believed to have estrogenic activity (Olea 1996). Although reported TC50 concentrations for BisGMA (Hanks 1991, Ratanasathien 1995, Kostoryz 2001), HEMA (Ratanasathien 1995) and TEGDMA (Hanks 1991, Ratanasathien 1995) vary in different studies, other studies have shown that even sub-toxic doses of monomers and extracts of dental resins may alter cellular functions such as secretion, homeostasis, dentinogenesis, or tissue repair (Kostoryz 2001, Schweikl 2006).

In the present study, the greatest elution was observed per mg Clearfil SE – about 30 ppm BisGMA and 50 ppm HEMA. Nearly 20 ppm BisGMA eluted from Excite and Clearfil 3S whereas about 10 ppm was detected from Admira and Filtek Silorane. As for HEMA, following Clearfil SE, Excite and Admira showed the highest absolute values of 25-27 ppm. Less than 10 ppm of TEGDMA was detected per mg Filtek Silorane adhesive system. Future studies are necessary to determine the effect of such concentrations on cellular functions and metabolism.

Positive correlation occurred between BisGMA and HEMA elution for Excite, Admira and Filtek Silorane indicating that an increase in the amount of eluted BisGMA is associated with an increased amount of eluted HEMA. This relationship was not observed in Clearfil SE and Clearfil 3S.

HEMA seems to be a good predictor of the DC for Clearfil 3S since a direct negative correlation was found. However, the overall result of the study indicates that no direct correlation exists between the DC of adhesives and the elution of unreacted monomers. Although it is often hypothesized that greater elution indicates lower DC, this is not substantiated by the present study.

Filtek Silorane showed lower DC than other adhesive systems. Since the micro-Raman spectra were taken from the surface of the adhesive, the calculated DC values corresponded to Filtek Silorane Bond. It has been shown that the reactivity of dimethacrylates in the formation of homopolymers increases with increasing distance between the methacrylate groups (Peutzfeldt 1997). It could be expected that a system containing TEGDMA shows higher DC than found in the present study. However, the reactivity of TEGDMA could be impaired by phosphorylated methacrylates contained in the bond whose primary role is priming the dentine (Hotta 1998). Their role may be hindered by the presence of the cured primer between the bond and dentine and could result in a higher content of these phosphorylated methacrylates and lower pH of the bond. Furthermore, the nature and chemical characteristics of the hydrophobic

dimethacrylate, developed to match the silorane resin, remains unknown and undisclosed by the manufacturer.

Significantly higher DC of Clearfil 3S than Clearfil SE is in accordance with the previous view that primers are associated with a reduced DC of adhesive systems. The lower DC of Admira compared to Excite, Clearfil SE and Clearfil 3S may indicate lower reactivity of the complex ormocer molecules compared to free cross-linking monomers.

12.4. Conclusions

The etch-and-rinse, self-etch, ormocer-based and silorane-based adhesive systems investigated in the present study showed different monomer elution kinetics. More than 90% of the named monomers in all adhesives systems, except for BisGMA from Filtek Silorane adhesive system, eluted during the first 1 h. Both the absolute amount and wt% of eluted monomers varied in all systems. The highest absolute amount of eluted monomers was observed for Clearfil SE whereas the highest wt% of eluted monomers was detected from Admira.

Filtek Silorane adhesive system showed the lowest and Clearfil 3S the highest DC values both initially and after elution. In all adhesive systems, there was an increase in the DC after monomer elution.

The overall result of the study indicated that no direct correlation exists between the DC of adhesives and the elution of unreacted monomers, although a negative correlation was found for the elution of HEMA and the DC of Clearfil 3S.

CHAPTER 13

GENERAL CONCLUSIONS

The current investigations showed that the degree of conversion in dental adhesive systems is always less than 100% irrespective of the curing conditions.

The mean degree of conversion in most tested adhesive systems, cured on glass slides for the manufacturers' recommended time, was in the range of 40-76%. Eight out of 12 systems showed significantly higher conversion when cured for twice the recommended time. It was impossible to specify one curing time applicable to all adhesive systems, due to differences in conversion kinetics.

The light source had a significant effect on the degree of conversion in the tested adhesive systems. Both light energy density and spectral emission range of the light source are important parameters in the conversion process. Irrespective of the light source, the tested etch-and-rinse system showed higher conversion than the tested two-step and one-step self-etch systems.

The tested etch-and-rinse systems were associated with greater depth and degree of dentine demineralisation and thicker hybrid layers compared to the tested self-etch systems. All tested systems showed deeper dentine demineralisation than adhesive penetration. The degree of conversion was significantly lower in the hybrid layer compared to the adhesive layer. The mean degree of conversion was 56-87% in the adhesive layer and 41-78% in the hybrid layer for all tested adhesive systems. Filtek Silorane Primer showed the highest and Adhese One the lowest DC values in both the adhesive layer and the HL. The curing of resin-based composites over cured adhesives significantly increased the degree of conversion in several adhesive systems. Micro-

Raman analysis gave a more precise indication of dentine demineralisation and adhesive penetration than scanning electron microscopy. It was shown that the hybrid layer is a gradual zone of transition between the adhesive layer and un-affected dentine. Furthermore, micro-Raman spectroscopy identified an intermediate zone of circa 1 μm with combined spectral features associated with Filtek Silorane Primer and Bond which was not detectable using scanning electron microscopy.

The transitional zone between resin-based composites and adhesive systems showed variations depending on their relative chemical composition. Systems with dissimilar chemical composition formed distinctive junctions with abrupt changes between the spectral features associated with the resin-based composite and adhesive system. Conversely, systems with more similar chemical composition formed gradual transitional zones and indistinctive junctions between the two materials. The DC of the tested RBCs was in the range of 55-71%.

More than 90% of BisGMA, TEGDMA and HEMA eluted from adhesive systems within the first 1 h after immersion in 75% ethanol/water solution, with the exception of BisGMA from Filtek Silorane adhesive which continuously eluted up to 96 h post-immersion. The absolute amounts of eluted monomers varied from about 10-33 ppm for BisGMA and 4-52 ppm for HEMA in different adhesive systems. The mean absolute amount of TEGDMA eluted from Filtek Silorane was 8.6 ppm. The highest weight percent of eluted monomers was found for Admira bond. Overall, no direct correlation was found between the degree of conversion and monomer elution from adhesive systems.

CHAPTER 14

FUTURE WORK

When currently available adhesive systems are compared, it is difficult to arrive at any definite conclusion as to what causes differences in the degree of conversion, due to the many inherent variables, such as the type and amount of functional and cross-linking monomers, initiators, solvents, fillers and/or additives. Therefore, future work will be carried out using experimental adhesive mixtures in which the effect of individual components will be assessed systematically.

The current investigations studied the elution of BisGMA, HEMA and TEGDMA from adhesive systems. Future studies will investigate elution of other leachable components from commercially available and experimental adhesive systems and resin-based composites. Future work will also be aimed at the identification and quantification of local and systemic biological effects of eluted components.

Novel adhesive systems and resin-based composites have been continuously marketed in an attempt to overcome current problems such as polymerisation shrinkage of resin-based composites or clinical application procedures for adhesive systems. Novel systems will, therefore, be incorporated into the future work regarding monomer conversion and elution.

REFERENCES

1. ISO 4049:2000 - Dentistry -- Polymer-based filling, restorative and luting materials.
2. ISO TR 11405: Dental materials - guidance on testing of adhesion to tooth structure 1994.
3. Abdalla AI, Davidson CL. Comparison of the marginal and axial wall integrity of in vivo and in vitro made adhesive class V restorations. J Oral Rehabil 1993; 20: 257-269.
4. Abdalla AI, Garcia-Godoy F. Morphological characterization of single bottle adhesives and vital dentin interface. Am J Dent 2002; 15: 31-34.
5. Abu-Hanna A, Gordan VV, Mjor I. The effect of variation in etching times on dentin bonding. Gen Dent 2004; 52: 28-33.
6. Agee KL, Pashley EL, Itthagarun A, Sano H, Tay FR, Pashley DH. Submicron hiati in acid-etched dentin are artifacts of desiccation. Dent Mater 2003; 19: 60-68.
7. Altintas SH, Usumez A. HPLC analysis of HEMA released from two different adhesive systems. J Biomed Mater Res B Appl Biomater 2009.
8. Arikawa H, Kanie T, Fujii K, Takahashi H, Ban S. Effect of filler properties in composite resins on light transmittance characteristics and color. Dent Mater J 2007; 26: 38-44.
9. Armstrong SR, Vargas MA, Fang Q, Laffoon JE. Microtensile bond strength of a total-etch 3-step, total-etch 2-step, self-etch 2-step, and a self-etch 1-step dentin bonding system through 15-month water storage. J Adhes Dent 2003; 5: 47-56.
10. Arrais CA, Pontes FM, Santos LP, Leite ER, Giannini M. Degree of conversion of adhesive systems light-cured by LED and halogen light. Braz Dent J 2007; 18: 54-59.
11. Arvidsson A, Liedberg B, Moller K, Lyven B, Sellen A, Wennerberg A. Chemical and topographical analyses of dentine surfaces after Carisolv treatment. J Dent 2002; 30: 67-75.
12. Asmussen E. Factors affecting the quantity of remaining double bonds in restorative resin polymers. Scand J Dent Res 1982; 90: 490-496.
13. Asmussen E, Peutzfeldt A. Mechanical properties of heat treated restorative resins for use in the inlay/onlay technique. Scand J Dent Res 1990; 98: 564-567.
14. Asmussen E, Peutzfeldt A. Influence of UEDMA BisGMA and TEGDMA on selected mechanical properties of experimental resin composites. Dent Mater 1998; 14: 51-56.
15. Asmussen E, Peutzfeldt A. Polymerization contraction of resin composite vs. energy and power density of light-cure. Eur J Oral Sci 2005; 113: 417-421.
16. Atai M, Motevasselian F. Temperature rise and degree of photopolymerization conversion of nanocomposites and conventional dental composites. Clin Oral Investig 2008.
17. Atai M, Watts DC. A new kinetic model for the photopolymerization shrinkage-strain of dental composites and resin-monomers. Dent Mater 2006; 22: 785-791.
18. Aw TC, Lepe X, Johnson GH, Mancl L. One-year clinical evaluation of an ethanol-based and a solvent-free dentin adhesive. Am J Dent 2004; 17: 451-456.

19. Aw TC, Lepe X, Johnson GH, Mancl LA. A three-year clinical evaluation of two-bottle versus one-bottle dentin adhesives. J Am Dent Assoc 2005; 136: 311-322.
20. Bae JH, Cho BH, Kim JS, Kim MS, Lee IB, Son HH et al. Adhesive layer properties as a determinant of dentin bond strength. J Biomed Mater Res B Appl Biomater 2005; 74: 822-828.
21. Bagis YH, Rueggeberg FA. Effect of post-cure temperature and heat duration on monomer conversion of photo-activated dental resin composite. Dent Mater 1997a; 13: 228-232.
22. Bagis YH, Rueggeberg FA. Mass loss in urethane/TEGDMA- and Bis-GMA/TEGDMA-based resin composites during post-cure heating. Dent Mater 1997b; 13: 377-380.
23. Baharav H, Abraham D, Cardash HS, Helft M. Effect of exposure time on the depth of polymerization of a visible light-cured composite resin. J Oral Rehabil 1988; 15: 167-172.
24. Bala O, Olmez A, Kalayci S. Effect of LED and halogen light curing on polymerization of resin-based composites. J Oral Rehabil 2005; 32: 134-140.
25. Bang HC, Lim BS, Yoon TH, Lee YK, Kim CW. Effect of plasma arc curing on polymerization shrinkage of orthodontic adhesive resins. J Oral Rehabil 2004; 31: 803-810.
26. Baran G, Boberick K, McCool J. Fatigue of restorative materials. Crit Rev Oral Biol Med 2001; 12: 350-360.
27. Baratieri LN, Canabarro S, Lopes GC, Ritter AV. Effect of resin viscosity and enamel beveling on the clinical performance of Class V composite restorations: three-year results. Oper Dent 2003; 28: 482-487.
28. Barnes DM, Thompson VP, Blank LW, McDonald NJ. Microleakage of Class 5 composite resin restorations: a comparison between in vivo and in vitro. Oper Dent 1993; 18: 237-245.
29. Bassiouny MA, Grant AA. A visible light-cured composite restorative. Clinical open assessment. Br Dent J 1978; 145: 327-330.
30. Bayne SC, Heymann HO, Swift EJ, Jr. Update on dental composite restorations. J Am Dent Assoc 1994; 125: 687-701.
31. Bedran-de-Castro AK, Pereira PN, Pimenta LA, Thompson JY. Effect of thermal and mechanical load cycling on microtensile bond strength of a total-etch adhesive system. Oper Dent 2004; 29: 150-156.
32. Beun S, Glorieux T, Devaux J, Vreven J, Leloup G. Characterization of nanofilled compared to universal and microfilled composites. Dent Mater 2007; 23: 51-59.
33. Bonilla ED, Stevenson RG, 3rd, Yashar M, Caputo AA. Effect of application technique and dentin bonding agent interaction on shear bond strength. Oper Dent 2003; 28: 568-573.
34. Bouschlicher MR, Rueggeberg FA, Wilson BM. Correlation of bottom-to-top surface microhardness and conversion ratios for a variety of resin composite compositions. Oper Dent 2004; 29: 698-704.
35. Bowen R. Dental filling material comprising vinyl silane treated fused silica and a binder consisting of the reaction product of Bis-phenol and glycidyl acrylate. In: Office USP, editor.; 1962.

36. Bowen RL. Adhesive bonding of various materials to hard tooth tissues II. Bonding to dentin promoted by a surface-active comonomer. J Dent Res 1965; 44: 895-902.
37. Bowen RL, Marjenhoff WA. Dental composites/glass ionomers: the materials. Adv Dent Res 1992; 6: 44-49.
38. Braga RR, Ferracane JL. Contraction stress related to degre of conversion and reaction kinetics. J Dent Res 2002; 81: 114-118.
39. Brannstrom M, Garberoglio R. Occlusion of dentinal tubules under superficial attrited dentine. Swed Dent J 1980; 4: 87-91.
40. Breschi L, Cadenaro M, Antoniolli F, Sauro S, Biasotto M, Prati C et al. Polymerization kinetics of dental adhesives cured with LED: correlation between extent of conversion and permeability. Dent Mater 2007; 23: 1066-1072.
41. Breschi L, Mazzoni A, Ruggeri A, Cadenaro M, Di Lenarda R, De Stefano Dorigo E. Dental adhesion review: aging and stability of the bonded interface. Dent Mater 2008; 24: 90-101.
42. Breschi L, Perdigao J, Lopes MM, Gobbi P, Mazzotti G. Morphological study of resin-dentin bonding with TEM and in-lens FESEM. Am J Dent 2003; 16: 267-274.
43. Brodsky B, Sha N. The triples helix motif in proteins. FASEB J 1995; 9: 1537-1546.
44. Bulucu B, Ozsezer E. Influence of light-curing units on dentin bond strength after bleaching. J Adhes Dent 2007; 9: 183-187.
45. Buonocore M. Adhesive sealing of pits and fissures for caries prevention, with use of ultraviolet light. J Am Dent Assoc 1970; 80: 324-330.
46. Buonocore MG. A simple method of increasing the adhesion of acrylic filling materials to enamel surfaces. J Dent Res 1955; 34: 849-853.
47. Buonocore MG, Wileman, W, Brudevold F. A report on a resin composition capable of bonding to human dentin surfaces. J Dent Res 1956; 35: 846-851.
48. Burger KM, Cooley RL, Garcia-Godoy F. Effect of thermocycling times on dentin bond strength. J Esthet Dent 1992; 4: 197-198.
49. Burrow MF, Inokoshi S, Tagami J. Water sorption of several bonding resins. Am J Dent 1999; 12: 295-298.
50. Burrow MF, Satoh M, Tagami J. Dentin bond durability after three years using a dentin bonding agent with and without priming. Dent Mater 1996; 12: 302-307.
51. Burrow MF, Tyas MJ. 1-year clinical evaluation of one-step in non-carious cervical lesions. Am J Dent 1999; 12: 283-285.
52. Cadenaro M, Antoniolli F, Sauro S, Tay FR, Di Lenarda R, Prati C et al. Degree of conversion and permeability of dental adhesives. Eur J Oral Sci 2005; 113: 525-530.
53. Cadenaro M, Breschi L, Antoniolli F, Mazzoni A, Di Lenarda R. Influence of whitening on the degree of conversion of dental adhesives on dentin. Eur J Oral Sci 2006; 114: 257-262.
54. Cadenaro M, Breschi L, Antoniolli F, Navarra CO, Mazzoni A, Tay FR et al. Degree of conversion of resin blends in relation to ethanol content and hydrophilicity. Dent Mater 2008; 24: 1194-1200.
55. Cagidiaco MC, Ferrari M, Vichi A, Davidson CL. Mapping of tubule and intertubule surface areas available for bonding in Class V and Class II preparations. J Dent 1997; 25: 379-389.

56. Calheiros FC, Braga RR, Kawano Y, Ballester RY. Relationship between contraction stress and degree of conversion in restorative composites. Dent Mater 2004; 20: 939-946.
57. Camerlingo C, Lepore M, Gaeta GM, Riccio R, Riccio C, De Rosa A, De Rosa M. Er:YAG laser treatments on dentine surface: micro-Raman spectroscopy and SEM analysis J Dent 2004; 32: 399-405.
58. Camilotti V, Grullon PG, Mendonca MJ, D'Alpino PH, Gomes JC. Influence of different light curing units on the bond strength of indirect resin composite restorations. Braz Oral Res 2008; 22: 164-169.
59. Carvalho RM, Chersoni S, Frankenberger R, Pashley DH, Prati C, Tay FR. A challenge to the conventional wisdom that simultaneous etching and resin infiltration always occurs in self-etch adhesives. Biomaterials 2005; 26: 1035-1042.
60. Carvalho RM, Yoshiyama M, Brewer PD, Pashley DH. Dimensional changes of demineralized human dentine during preparation for scanning electron microscopy. Arch Oral Biol 1996a; 41: 379-386.
61. Carvalho RM, Yoshiyama M, Pashley EL, Pashley DH. In vitro study on the dimensional changes of human dentine after demineralization. Arch Oral Biol 1996b; 41: 369-377.
62. Casciani FS EE, Newbury DE, Doty SB. Raman microprobe studies of two mineralizing tissues: enamel of the rat incisor and and the embryonic chick tibia. Scanning Electron Microsc 1979; 2: 383-391.
63. Cassoni A, Ferla Jde O, Shibli JA, Kawano Y. Knoop microhardness and FT-Raman spectroscopic evaluation of a resin-based dental material light-cured by an argon ion laser and halogen lamp: an in vitro study. Photomed Laser Surg 2008; 26: 531-539.
64. Caughman WF, Caughman GB, Shiflett RA, Rueggeberg F, Schuster GS. Correlation of cytotoxicity, filler loading and curing time of dental composites. Biomaterials 1991; 12: 737-740.
65. Caughman WF, Rueggeberg FA, Curtis JW, Jr. Clinical guidelines for photocuring restorative resins. J Am Dent Assoc 1995; 126: 1280-1282, 1284, 1286.
66. Chan DC, Reinhardt, JW, Schulein, TM. Bond strengths of restorative materials to dentin. Gen Dent 1985; 33: 236-238.
67. Chaudhry M, Van Ness HC, Abbott MM. Excess thermodynamic functions for ternary systems. Total-pressure data and GE for acetone-ethanol-water at 500C. Journal of Chemical & Engineering Data 1980; 25: 254-257.
68. Chohayeb AA. Bonding to tooth structure: clinical and biological considerations. Int Dent J 1988; 38: 105-111.
69. Chung K, Greener EH. Degree of conversion of seven visible light-cured posterior composites. J Oral Rehabil 1988; 15: 555-560.
70. Cook WD. Factors affecting the depth of cure of UV-polymerized composites. J Dent Res 1980; 59: 800-808.
71. Craig RG. Chemistry, composition, and properties of composite resins. Dent Clin North Am 1981; 25: 219-239.
72. Cribb AM, Scott JE. Tendon response to tensile stress: An ultrastructural investigation of collagen: Proteoglycan interactions in stressed tendon. J Anat 1995; 187: 423-428.

73. Crivello JV. Cationic polymerisation of iodonium and sulfonium salt photoinitiators. Advanced Polymer Science 1984; 62: 1-48.
74. D'Alpino PH, Svizero NR, Pereira JC, Rueggeberg FA, Carvalho RM, Pashley DH. Influence of light-curing sources on polymerization reaction kinetics of a restorative system. Am J Dent 2007; 20: 46-52.
75. da Silva EM, Almeida GS, Poskus LT, Guimaraes JG. Relationship between the degree of conversion, solubility and salivary sorption of a hybrid and a nanofilled resin composite. J Appl Oral Sci 2008; 16: 161-166.
76. Darvell BW. Materials Science for Dentistry. Honk Kong: Darvell BW; 2002: p. 119-128.
77. Datar R, Rueggeberg FA, Caughman GB, Wataha JC, Lewis J, Schuster GS. Effects of subtoxic concentrations of benzoyl peroxide on cell lipid metabolism. J Biomed Mater Res A 2004; 71: 685-692.
78. Davidson-Kaban SS, Davidson CL, Feilzer AJ, de Gee AJ, Erdilek N. The effect of curing light variations on bulk curing and wall-to-wall quality of two types and various shades of resin composites. Dent Mater 1997; 13: 344-352.
79. Davidson CL, de Gee AJ. Light-curing units, polymerization, and clinical implications. J Adhes Dent 2000; 2: 167-173.
80. Davidson CL, de Gee AJ, Feilzer A. The competition between the composite-dentin bond strength and the polymerization contraction stress. J Dent Res 1984; 63: 1396-1399.
81. Davidson CL, Feilzer AJ. Polymerization shrinkage and polymerization shrinkage stress in polymer-based restoratives. J Dent 1997; 25: 435-440.
82. de Gee AF, Feilzer AJ, Davidson CL. True linear polymerization shrinkage of unfilled resins and composites determined with a linometer. Dent Mater 1993; 9: 11-14.
83. De Munck J, Van Landuyt K, Peumans M, Poitevin A, Lambrechts P, Braem M et al. A critical review of the durability of adhesion to tooth tissue: methods and results. J Dent Res 2005; 84: 118-132.
84. De Munck J, Van Meerbeek B, Satoshi I, Vargas M, Yoshida Y, Armstrong S et al. Microtensile bond strengths of one- and two-step self-etch adhesives to bur-cut enamel and dentin. Am J Dent 2003a; 16: 414-420.
85. De Munck J, Van Meerbeek B, Yoshida Y, Inoue S, Suzuki K, Lambrechts P. Four-year water degradation of a resin-modified glass-ionomer adhesive bonded to dentin. Eur J Oral Sci 2004; 112: 73-83.
86. De Munck J, Van Meerbeek B, Yoshida Y, Inoue S, Vargas M, Suzuki K et al. Four-year water degradation of total-etch adhesives bonded to dentin. J Dent Res 2003b; 82: 136-140.
87. Dennison JB, Craig RG. Characterization of enamel surfaces prepared with commercial and experimental etchants. J Am Dent Assoc 1978; 97: 799-805.
88. DeWald JP, Ferracane JL. A comparison of four modes of evaluating depth of cure of light-activated composites. J Dent Res 1987; 66: 727-730.
89. Dickens SH, Cho BH. Interpretation of bond failure through conversion and residual solvent measurements and Weibull analyses of flexural and microtensile bond strengths of bonding agents. Dent Mater 2005; 21: 354-364.

90. Dickens SH, Stansbury JW, Choi KM, Floyd CJE. Photopolymerization kinetics of methacrylate dental resins. Macromolecules 2003; 36: 6043-6053.
91. Donmez N, Belli S, Pashley DH, Tay FR. Ultrastructural correlates of in vivo/in vitro bond degradation in self-etch adhesives. J Dent Res 2005; 84: 355-359.
92. dos Santos GB, Alto RV, Filho HR, da Silva EM, Fellows CE. Light transmission on dental resin composites. Dent Mater 2008; 24: 571-576.
93. Douglas WH. Clinical status of dentine bonding agents. J Dent 1989; 17: 209-215.
94. Duke ES, Lindemuth J. Polymeric adhesion to dentin: contrasting substrates. Am J Dent 1990; 3: 264-270.
95. Dunne SM, Davies BR, Millar BJ. A survey of the effectiveness of dental light-curing units and a comparison of light testing devices. Br Dent J 1996; 180: 411-416.
96. Durey K, Santini A, Miletic V. Pulp chamber temperature rise during curing of resin-based composites with different light-curing units. Prim Dent Care 2008; 15: 33-38.
97. Eckert GJ, Platt JA. A statistical evaluation of microtensile bond strength methodology for dental adhesives. Dent Mater 2007; 23: 385-391.
98. Eick JD, Byerley TJ, Chappell RP, Chen GR, Bowles CQ, Chappelow CC. Properties of expanding SOC/epoxy copolymers for dental use in dental composites. Dent Mater 1993; 9: 123-127.
99. Eick JD, Gwinnett AJ, Pashley DH, Robinson SJ. Current concepts on adhesion to dentin. Crit Rev Oral Biol Med 1997; 8: 306-335.
100. Eick JD, Kotha SP, Chappelow CC, Kilway KV, Giese GJ, Glaros AG et al. Properties of silorane-based dental resins and composites containing a stress-reducing monomer. Dent Mater 2007; 23: 1011-1017.
101. Eick JD, Smith RE, Pinzino CS, Kostoryz EL. Stability of silorane dental monomers in aqueous systems. J Dent 2006; 34: 405-410.
102. Eliades G, Vougiouklakis G, Palaghias G. Effect of dentin primers on the morphology, molecular composition and collagen conformation of acid-demineralized dentin in situ. Dent Mater 1999; 15: 310-317.
103. Eliades GC, Vougiouklakis GJ, Caputo AA. Degree of double bond conversion in light-cured composites. Dent Mater 1987; 3: 19-25.
104. Eliades T, Eliades G, Bradley TG, Watts DC. Degree of cure of orthodontic adhesives with various polymerization initiation modes. Eur J Orthod 2000; 22: 395-399.
105. Eliades T, Eliades G, Brantley WA, Johnston WM. Residual monomer leaching from chemically cured and visible light-cured orthodontic adhesives. Am J Orthod Dentofacial Orthop 1995; 108: 316-321.
106. Eliades T, Hiskia A, Eliades G, Athanasiou AE. Assessment of bisphenol-A release from orthodontic adhesives. Am J Orthod Dentofacial Orthop 2007; 131: 72-75.
107. Emami N, Soderholm KJ. How light irradiance and curing time affect monomer conversion in light-cured resin composites. Eur J Oral Sci 2003; 111: 536-542.
108. Emami N, Soderholm KJ. Influence of light-curing procedures and photo-initiator/co-initiator composition on the degree of conversion of light-curing resins. J Mater Sci Mater Med 2005; 16: 47-52.

109. Emami N, Soderholm KJ, Berglund LA. Effect of light power density variations on bulk curing properties of dental composites. J Dent 2003; 31: 189-196.
110. Endo T, Osada T, Finger WJ, Hoffmann M, Kanehira M, Komatsu M. Effect of oxygen inhibition of self-etching adhesives on enamel-dentin polymer bond. J Adhes Dent 2007; 9: 33-38.
111. Faria-e-Silva AL, Casselli DS, Lima GS, Ogliari FA, Piva E, Martins LR. Kinetics of conversion of two dual-cured adhesive systems. J Endod 2008; 34: 1115-1118.
112. Faria e Silva AL, Arias VG, Soares LE, Martin AA, Martins LR. Influence of fiber-post translucency on the degree of conversion of a dual-cured resin cement. J Endod 2007; 33: 303-305.
113. Faust R, Shaffer, TD. Cationic polymerization. American Chemical Society; 1997.
114. Feilzer AJ, Dauvillier BS. Effect of TEGDMA/BisGMA ratio on stress development and viscoelastic properties of experimental two-paste composites. J Dent Res 2003; 82: 824-828.
115. Feilzer AJ, De Gee AJ, Davidson CL. Setting stress in composite resin in relation to configuration of the restoration. J Dent Res 1987; 66: 1636-1639.
116. Feng L, Carvalho R, Suh BI. Insufficient cure under the condition of high irradiance and short irradiation time. Dent Mater 2009; 25: 283-289.
117. Ferracane JL. Elution of leachable components from composites. J Oral Rehabil 1994; 21: 441-452.
118. Ferracane JL, Condon JR. Rate of elution of leachable components from composite. Dent Mater 1990; 6: 282-287.
119. Ferracane JL, Greener EH. Fourier transform infrared analysis of degree of polymerization in unfilled resins--methods comparison. J Dent Res 1984; 63: 1093-1095.
120. Ferrari M, Cagidiaco MC, Kugel G, Davidson CL. Dentin infiltration by three adhesive systems in clinical and laboratory conditions. Am J Dent 1996; 9: 240-244.
121. Ferrari M, Mannocci F, Vichi A, Davidson CL. Effect of two etching times on the sealing ability of Clearfil Liner Bond 2 in Class V restorations. Am J Dent 1997; 10: 66-70.
122. Ferrari M, Yamamoto K, Vichi A, Finger WJ. Clinical and laboratory evaluation of adhesive restorative systems. Am J Dent 1994; 7: 217-219.
123. Finer Y, Santerre JP. The influence of resin chemistry on a dental composite's biodegradation. J Biomed Mater Res A 2004; 69: 233-246.
124. Finer Y, Santerre JP. Influence of silanated filler content on the biodegradation of bisGMA/TEGDMA dental composite resins. J Biomed Mater Res A 2007; 81: 75-84.
125. Fleming GJ, Khan S, Afzal O, Palin WM, Burke FJ. Investigation of polymerisation shrinkage strain, associated cuspal movement and microleakage of MOD cavities restored incrementally with resin-based composite using an LED light curing unit. J Dent 2007; 35: 97-103.
126. Fowler CS, Swartz ML, Moore BK. Efficacy testing of visible-light-curing units. Oper Dent 1994; 19: 47-52.
127. Frankenberger R, Perdigao J, Rosa BT, Lopes M. "No-bottle" vs "multi-bottle" dentin adhesives--a microtensile bond strength and morphological study. Dent Mater 2001; 17: 373-380.

128. Frankenberger R, Strobel WO, Kramer N, Lohbauer U, Winterscheidt J, Winterscheidt B et al. Evaluation of the fatigue behavior of the resin-dentin bond with the use of different methods. J Biomed Mater Res B Appl Biomater 2003; 67: 712-721.
129. Fukushima T, Inoue Y, Miyazaki K, Itoh T. Effect of primers containing N-methylolacrylamide or N-methylolmethacrylamide on dentin bond durability of a resin composite after 5 years. J Dent 2001; 29: 227-234.
130. Gale MS, Darvell BW. Thermal cycling procedures for laboratory testing of dental restorations. J Dent 1999; 27: 89-99.
131. Gale MS, Darvell BW, Cheung GS. Three-dimensional reconstruction of microleakage pattern using a sequential grinding technique. J Dent 1994; 22: 370-375.
132. Garberoglio R, Brannstrom M. Scanning electron microscopic investigation of human dentinal tubules. Arch Oral Biol 1976; 21: 355-362.
133. Garcia-Godoy F, Tay FR, Pashley DH, Feilzer A, Tjaderhane L, Pashley EL. Degradation of resin-bonded human dentin after 3 years of storage. Am J Dent 2007; 20: 109-113.
134. Gauthier M, Stangel I, Ellis TH, Zhu XX. A new method for quantifying the intensity of the C=C band of dimethacrylate dental monomers in their FTIR and Raman spectra. Biomaterials 2005a; 26: 6440-6448.
135. Gauthier M, Stangel I, Ellis TH, Zhu XX. Oxygen inhibition in dental resins. J Dent Res 2005b; 84: 725-729.
136. Gerzina TM, Hume WR. Effect of hydrostatic pressure on the diffusion of monomers through dentin in vitro. J Dent Res 1995; 74: 369-373.
137. Geurtsen W, Spahl W, Muller K, Leyhausen G. Aqueous extracts from dentin adhesives contain cytotoxic chemicals. J Biomed Mater Res 1999; 48: 772-777.
138. Ghosh TK, Jasti B.R. Theory and practice of contemporary pharmaceutics. Boca Raton: CRC Press; 2005: p. 37-41.
139. Giannini M, Arrais CA, Vermelho PM, Reis RS, dos Santos LP, Leite ER. Effects of the solvent evaporation technique on the degree of conversion of one-bottle adhesive systems. Oper Dent 2008; 33: 149-154.
140. Giannini M, Seixas CA, Reis AF, Pimenta LA. Six-month storage-time evaluation of one-bottle adhesive systems to dentin. J Esthet Restor Dent 2003; 15: 43-48; discussion 49.
141. Gilchrist F, Santini A, Harley K, Deery C. The use of micro-Raman spectroscopy to differentiate between sound and eroded primary enamel. Int J Paediatr Dent 2007; 17: 274-280.
142. Guo X, Peng Z, Spencer P, Wang Y. Effect of initiator on photopolymerization of acidic, aqueous dental model adhesives. J Biomed Mater Res A 2008a.
143. Guo X, Wang Y, Spencer P, Ye Q, Yao X. Effects of water content and initiator composition on photopolymerization of a model BisGMA/HEMA resin. Dent Mater 2008b; 24: 824-831.
144. Gwinnett AJ, Buonocore MG. Adhesives and Caries Prevention; a Preliminary Report. Br Dent J 1965; 119: 77-80.
145. Gwinnett AJ, Kanca JA, 3rd. Micromorphology of the bonded dentin interface and its relationship to bond strength. Am J Dent 1992; 5: 73-77.

146. Hammesfahr P, O'Connor MT, Wang X. Light-curing technology: Past, present, future. Compend Contin Educ Dent 2002; 23: 18-24.
147. Han L, Abu-Bakr N, Okamoto A, Iwaku M. WDX study of resin-dentin interface on wet vs. dry dentin. Dent Mater J 2000; 19: 317-325.
148. Hanks CT, Strawn SE, Wataha JC, Craig RG. Cytotoxic effects of resin components on cultured mammalian fibroblasts. J Dent Res 1991; 70: 1450-1455.
149. Hannig M, Bott B. In-vitro pulp chamber temperature rise during composite resin polymerization with various light-curing sources. Dent Mater 1999; 15: 275-281.
150. Hansen EK, Asmussen E. Reliability of three dental radiometers. Scand J Dent Res 1993; 101: 115-119.
151. Hashimoto M, Ito S, Tay FR, Svizero NR, Sano H, Kaga M et al. Fluid movement across the resin-dentin interface during and after bonding. J Dent Res 2004; 83: 843-848.
152. Hashimoto M, Ohno H, Kaga M, Endo K, Sano H, Oguchi H. In vivo degradation of resin-dentin bonds in humans over 1 to 3 years. J Dent Res 2000; 79: 1385-1391.
153. Hashimoto M, Ohno H, Kaga M, Sano H, Endo K, Oguchi H. The extent to which resin can infiltrate dentin by acetone-based adhesives. J Dent Res 2002; 81: 74-78.
154. Heintze SD. Systematic reviews: I. The correlation between laboratory tests on marginal quality and bond strength. II. The correlation between marginal quality and clinical outcome. J Adhes Dent 2007; 9 Suppl 1: 77-106.
155. Heymann HO, Bayne SC. Current concepts in dentin bonding: focusing on dentinal adhesion factors. J Am Dent Assoc 1993; 124: 26-36.
156. Hitmi L, Bouter D, Degrange M. Influence of drying and HEMA treatment on dentin wettability. Dent Mater 2002; 18: 503-511.
157. Ho SP, Sulyanto RM, Marshall SJ, Marshall GW. The cementum-dentin junction also contains glycosaminoglycans and collagen fibrils. J Struct Biol 2005; 151: 69-78.
158. Hotta K, Mogi M, Mura F, Nakabayashi N. Effect of 4-MET on bond strength and penetration of monomers into enamel. Dent Mater 1992; 8: 173-175.
159. Hotta M, Kondoh K, Kamemizu H. Effect of primers on bonding agent polymerization. J Oral Rehabil 1998; 25: 792-799.
160. Hsu S. Infrared spectroscopy. In: Settle FA, editor. Handbook of Instrumental Techniques for Analytical Chemistry: Prentice Hall; Har/Cdr edition; 1997.
161. Ikeda T, De Munck J, Shirai K, Hikita K, Inoue S, Sano H et al. Effect of evaporation of primer components on ultimate tensile strengths of primer-adhesive mixture. Dent Mater 2005; 21: 1051-1058.
162. Ikemura K, Ichizawa K, Yoshida M, Ito S, Endo T. UV-VIS spectra and photoinitiation behaviors of acylphosphine oxide and bisacylphosphine oxide derivatives in unfilled, light-cured dental resins. Dent Mater J 2008; 27: 765-774.
163. Ilie N, Hickel R. Silorane-based dental composite: behavior and abilities. Dent Mater J 2006; 25: 445-454.
164. Imazato S. Antibacterial properties of resin composites and dentin bonding systems. Dent Mater 2003a; 19: 449-457.
165. Imazato S, Imai T, Russell RR, Torii M, Ebisu S. Antibacterial activity of cured dental resin incorporating the antibacterial monomer MDPB and an adhesion-promoting monomer. J Biomed Mater Res 1998; 39: 511-515.

166. Imazato S, Kinomoto Y, Tarumi H, Ebisu S, Tay FR. Antibacterial activity and bonding characteristics of an adhesive resin containing antibacterial monomer MDPB. Dent Mater 2003b; 19: 313-319.
167. Imazato S, Kinomoto Y, Tarumi H, Torii M, Russell RR, McCabe JF. Incorporation of antibacterial monomer MDPB into dentin primer. J Dent Res 1997; 76: 768-772.
168. Imazato S, McCabe JF, Tarumi H, Ehara A, Ebisu S. Degree of conversion of composites measured by DTA and FTIR. Dent Mater 2001; 17: 178-183.
169. Imazato S, Tarumi H, Kobayashi K, Hiraguri H, Oda K, Tsuchitani Y. Relationship between the degree of conversion and internal discoloration of light-activated composite. Dent Mater J 1995; 14: 23-30.
170. Indrani DJ, Cook WD, Televantos F, Tyas MJ, Harcourt JK. Fracture toughness of water-aged resin composite restorative materials. Dent Mater 1995; 11: 201-207.
171. Inoue S, Van Meerbeek B, Abe Y, Yoshida Y, Lambrechts P, Vanherle G et al. Effect of remaining dentin thickness and the use of conditioner on micro-tensile bond strength of a glass-ionomer adhesive. Dent Mater 2001a; 17: 445-455.
172. Inoue S, Vargas MA, Abe Y, Yoshida Y, Lambrechts P, Vanherle G et al. Microtensile bond strength of eleven contemporary adhesives to dentin. J Adhes Dent 2001b; 3: 237-245.
173. Jacobsen T, Soderholm KJ. Some effects of water on dentin bonding. Dent Mater 1995; 11: 132-136.
174. Kaga M, Noda M, Ferracane JL, Nakamura W, Oguchi H, Sano H. The in vitro cytotoxicity of eluates from dentin bonding resins and their effect on tyrosine phosphorylation of L929 cells. Dent Mater 2001; 17: 333-339.
175. Kalliyana K, Yamuna V. Effect of initiator concentration, exposure time and particle size of the filler upon the mechanical properties of a light-curing radiopaque dental composite. J Oral Rehabil 1998; 25: 747-751.
176. Kanca J, 3rd. Improving bond strength through acid etching of dentin and bonding to wet dentin surfaces. J Am Dent Assoc 1992a; 123: 35-43.
177. Kanca J, 3rd. Resin bonding to wet substrate. 1. Bonding to dentin. Quintessence Int 1992b; 23: 39-41.
178. Kanca J, 3rd. Wet bonding: effect of drying time and distance. Am J Dent 1996; 9: 273-276.
179. Kanehira M, Finger WJ, Hoffmann M, Endo T, Komatsu M. Relationship between degree of polymerization and enamel bonding strength with self-etching adhesives. J Adhes Dent 2006; 8: 211-216.
180. Karjalainen S, Soderling E, Pelliniemi L, Foidart JM. Immunohistochemical localization of types I and III collagen and fibronectin in the dentine of carious human teeth. Arch Oral Biol 1986; 31: 801-806.
181. Kato G, Nakabayashi N. The durability of adhesion to phosphoric acid etched, wet dentin substrates. Dent Mater 1998; 14: 347-352.
182. Kidd EA. Microleakage: a review. J Dent 1976; 4: 199-206.
183. Kim JG, Chung CM. Elution from light-cured dental composites: comparison of trimethacrylate and dimethacrylate as base monomers. J Biomed Mater Res B Appl Biomater 2005; 72: 328-333.

184. Kim JS, Cho BH, Lee IB, Um CM, Lim BS, Oh MH et al. Effect of the hydrophilic nanofiller loading on the mechanical properties and the microtensile bond strength of an ethanol-based one-bottle dentin adhesive. J Biomed Mater Res B Appl Biomater 2005; 72: 284-291.
185. Kim JS, Choi YH, Cho BH, Son HH, Lee IB, Um CM et al. Effect of light-cure time of adhesive resin on the thickness of the oxygen-inhibited layer and the microtensile bond strength to dentin. J Biomed Mater Res B Appl Biomater 2006; 78: 115-123.
186. Knezevic A, Tarle Z, Meniga A, Sutalo J, Pichler G, Ristic M. Degree of conversion and temperature rise during polymerization of composite resin samples with blue diodes. J Oral Rehabil 2001; 28: 586-591.
187. Knezevic A, Tarle Z, Meniga A, Sutalo J, Pichler G, Ristic M. Photopolymerization of composite resins with plasma light. J Oral Rehabil 2002; 29: 782-786.
188. Korkmaz Y, Attar N. Dentin bond strength of composites with self-etching adhesives using LED curing lights. J Contemp Dent Pract 2007; 8: 34-42.
189. Koshiro K, Inoue S, Sano H, De Munck J, Van Meerbeek B. In vivo degradation of resin-dentin bonds produced by a self-etch and an etch-and-rinse adhesive. Eur J Oral Sci 2005; 113: 341-348.
190. Kostoryz EL, Tong PY, Strautman AF, Glaros AG, Eick JD, Yourtee DM. Effects of dental resins on TNF-alpha-induced ICAM-1 expression in endothelial cells. J Dent Res 2001; 80: 1789-1792.
191. Kuboki Y, Ohgushi K, Fusayama T. Collagen biochemistry of the two layers of carious dentin. J Dent Res 1977; 56: 1233-1237.
192. Kugel G, Ferrari M. The science of bonding: from first to sixth generation. J Am Dent Assoc 2000; 131 Suppl: 20S-25S.
193. Kwong SM, Cheung GS, Kei LH, Itthagarun A, Smales RJ, Tay FR et al. Micro-tensile bond strengths to sclerotic dentin using a self-etching and a total-etching technique. Dent Mater 2002; 18: 359-369.
194. Kwong SM, Tay FR, Yip HK, Kei LH, Pashley DH. An ultrastructural study of the application of dentine adhesives to acid-conditioned sclerotic dentine. J Dent 2000; 28: 515-528.
195. Lee HL, Orlowski JA, Rogers BJ. A comparison of ultraviolet-curing and self-curing polymers in preventive, restorative and orthodontic dentistry. Int Dent J 1976; 26: 134-151.
196. Lee SY, Greener EH, Mueller HJ, Chiu CH. Effect of food and oral simulating fluids on dentine bond and composite strength. J Dent 1994; 22: 352-359.
197. Lee SY, Lin CT. Storage effect on dentine structure and on resultant composite bond strengths. J Oral Rehabil 1997; 24: 823-834.
198. Leloup G, D'Hoore W, Bouter D, Degrange M, Vreven J. Meta-analytical review of factors involved in dentin adherence. J Dent Res 2001; 80: 1605-1614.
199. Leloup G, Holvoet PE, Bebelman S, Devaux J. Raman scattering determination of the depth of cure of light-activated composites: influence of different clinically relevant parameters. J Oral Rehabil 2002; 29: 510-515.

200. Lim YK, Lee YK. Influence of light transmittance and background reflectance on the light curing of adhesives used to bond esthetic brackets. Am J Orthod Dentofacial Orthop 2007; 132: 5 e17-24.
201. Lohbauer U, Rahiotis C, Kramer N, Petschelt A, Eliades G. The effect of different light-curing units on fatigue behavior and degree of conversion of a resin composite. Dent Mater 2005; 21: 608-615.
202. Lohbauer U, Zinelis S, Rahiotis C, Petschelt A, Eliades G. The effect of resin composite pre-heating on monomer conversion and polymerization shrinkage. Dent Mater 2009; 25: 514-519.
203. Lopez-Suevos F, Dickens SH. Degree of cure and fracture properties of experimental acid-resin modified composites under wet and dry conditions. Dental Materials 2008; 24: 778-785.
204. Loshaek S, Fox TG. Cross-Linked Polymers .1. Factors Influencing the Efficiency of Cross-Linking in Copolymers of Methyl Methacrylate and Glycol Dimethacrylates. Journal of the American Chemical Society 1953; 75: 3544-3550.
205. Lundin SA, Koch G. Cure profiles of visible-light-cured Class II composite restorations in vivo and in vitro. Dent Mater 1992; 8: 7-9.
206. Lutz F, Krejci I, Barbakow F. Quality and durability of marginal adaptation in bonded composite restorations. Dent Mater 1991; 7: 107-113.
207. Lutz F, Phillips RW. A classification and evaluation of composite resin systems. J Prosthet Dent 1983; 50: 480-488.
208. Mair LH. An investigation into the permeability of composite materials using silver nitrate. Dent Mater 1989; 5: 109-114.
209. Marshall GW, Jr. Dentin: microstructure and characterization. Quintessence Int 1993; 24: 606-617.
210. Marshall GW, Jr., Marshall SJ, Kinney JH, Balooch M. The dentin substrate: structure and properties related to bonding. J Dent 1997; 25: 441-458.
211. Masotti AS, Onofrio AB, Conceicao EN, Spohr AM. UV-vis spectrophotometric direct transmittance analysis of composite resins. Dent Mater 2007; 23: 724-730.
212. McClelland JF, Bajic SJ, Jones RW, Seaverson LM Photoacoustic spectroscopy in modern techniques in applied molecular spectroscopy. NY: FM Mirabella; 1998.
213. McLean JW. Glass-ionomer cements. Br Dent J 1988; 164: 293-300.
214. Meiers JC, Young D. Two-year composite/dentin bond stability. Am J Dent 2001; 14: 141-144.
215. Michelsen VB, Lygre H, Skalevik R, Tveit AB, Solheim E. Identification of organic eluates from four polymer-based dental filling materials. Eur J Oral Sci 2003; 111: 263-271.
216. Michelsen VB, Moe G, Strom MB, Jensen E, Lygre H. Quantitative analysis of TEGDMA and HEMA eluted into saliva from two dental composites by use of GC/MS and tailor-made internal standards. Dent Mater 2008; 24: 724-731.
217. Miletic V, Ivanovic V, Dzeletovic B, Lezaja M. Temperature changes in silorane-, ormocer-, and dimethacrylate-based composites and pulp chamber roof during light-curing. J Esthet Restor Dent 2009a; 21: 122-131; discussion 132.

218. Miletic V, Santini A, Trkulja I. Quantification of monomer elution and carbon-carbon double bonds in dental adhesive systems using HPLC and micro-Raman spectroscopy. J Dent 2009b; 37: 177-184.
219. Milia E, Santini A. Ultrastructural transmission electron microscopy (TEM) study of hybrid layers formed beneath a one-bottle adhesive system using the total-etch technique and a self-etching system. Quintessence Int 2003; 34: 447-452.
220. Millen C, Ormond M, Richardson G, Santini A, Miletic V, Kew P. A study of temperature rise in the pulp chamber during composite polymerization with different light-curing units. J Contemp Dent Pract 2007; 8: 29-37.
221. Millich F, Jeang L, Eick JD, Chappelow CC, Pinzino CS. Elements of light-cured epoxy-based dental polymer systems. J Dent Res 1998; 77: 603-608.
222. Mills RW, Uhl A, Jandt KD. Optical power outputs, spectra and dental composite depths of cure, obtained with blue light emitting diode (LED) and halogen light curing units (LCUs). Br Dent J 2002; 193: 459-463; discussion 455.
223. Mjor IA, Gordan VV. Failure, repair, refurbishing and longevity of restorations. Oper Dent 2002; 27: 528-534.
224. Monticelli F, Osorio R, Pisani-Proenca J, Toledano M. Resistance to degradation of resin-dentin bonds using a one-step HEMA-free adhesive. J Dent 2007; 35: 181-186.
225. Moon H-J, Lim B-S, Lee Y-K, Kim C-W. Determination of Residual Monomers in Dental Pit and Fissure Sealants Using Food/Oral Simulating Fluids. Bull Korean Chem Soc 2000; 21: 1115-1118.
226. Moon HJ, Lee YK, Lim BS, Kim CW. Effects of various light curing methods on the leachability of uncured substances and hardness of a composite resin. J Oral Rehabil 2004; 31: 258-264.
227. Moszner N, Salz U, Zimmermann J. Chemical aspects of self-etching enamel-dentin adhesives: A systematic review. Dent Mater 2005; 21: 895-910.
228. Munksgaard EC, Peutzfeldt A, Asmussen E. Elution of TEGDMA and BisGMA from a resin and a resin composite cured with halogen or plasma light. Eur J Oral Sci 2000; 108: 341-345.
229. Musanje L, Ferracane JL. Effects of resin formulation and nanofiller surface treatment on the properties of experimental hybrid resin composite. Biomaterials 2004; 25: 4065-4071.
230. Nakabayashi N. Bonding of restorative materials to dentine: the present status in Japan. Int Dent J 1985; 35: 145-154.
231. Nakabayashi N, Kojima K, Masuhara E. The promotion of adhesion by the infiltration of monomers into tooth substrates. J Biomed Mater Res 1982; 16: 265-273.
232. Nakabayashi N, Pashley DH. Hybridization of dental hard tissues. Tokyo: Quintessence Publishing Co, Ltd; 1998a: p. 62-63.
233. Nakabayashi N, Pashley DH. Hybridization of dental hard tissues. Tokyo: Quintessence Publishing Co, Ltd; 1998b: p. 8-9.
234. Nakajima M, Okuda M, Ogata M, Pereira PN, Tagami J, Pashley DH. The durability of a fluoride-releasing resin adhesive system to dentin. Oper Dent 2003; 28: 186-192.
235. Nakaoki Y, Nikaido T, Pereira PN, Inokoshi S, Tagami J. Dimensional changes of demineralized dentin treated with HEMA primers. Dent Mater 2000; 16: 441-446.

236. Navarra CO, Cadenaro M, Armstrong SR, Jessop J, Antoniolli F, Sergo V et al. Degree of conversion of Filtek Silorane Adhesive System and Clearfil SE Bond within the hybrid and adhesive layer: an in situ Raman analysis. Dent Mater 2009; 25: 1178-1185.
237. Newman SM, Murray GA, Yates JL. Visible lights and visible light-activated composite resins. J Prosthet Dent 1983; 50: 31-35.
238. Nikaido T, Kunzelmann KH, Chen H, Ogata M, Harada N, Yamaguchi S et al. Evaluation of thermal cycling and mechanical loading on bond strength of a self-etching primer system to dentin. Dent Mater 2002a; 18: 269-275.
239. Nikaido T, Kunzelmann KH, Ogata M, Harada N, Yamaguchi S, Cox CF et al. The in vitro dentin bond strengths of two adhesive systems in class I cavities of human molars. J Adhes Dent 2002b; 4: 31-39.
240. Nishino M, Yamashita S, Aoba T, Okazaki M, Moriwaki Y. The laser-Raman spectroscopic studies on human enamel and precipitated carbonate containing apatite. J Dent Res 1981; 60: 751-755.
241. Nishiyama N, Asakura T, Suzuki K, Sato T, Nemoto K. Adhesion mechanisms of resin to etched dentin primed with N-methacryloyl glycine studied by 13C-NMR. J Biomed Mater Res 1998; 40: 458-463.
242. Nishiyama N, Suzuki K, Asakura T, Komatsu K, Nemoto K. Adhesion of N-methacryloyl-omega-amino acid primers to collagen analyzed by 13C NMR. J Dent Res 2001; 80: 855-859.
243. Nomoto R. Effect of light wavelength on polymerization of light-cured resins. Dent Mater J 1997; 16: 60-73.
244. Nunes MF, Swift EJ, Perdigao J. Effects of adhesive composition on microtensile bond strength to human dentin. Am J Dent 2001; 14: 340-343.
245. Nunes TG, Ceballos L, Osorio R, Toledano M. Spatially resolved photopolymerization kinetics and oxygen inhibition in dental adhesives. Biomaterials 2005; 26: 1809-1817.
246. O'Shea DC BM, Young RA. Compositional analysis of apatites with laser-raman spectroscopy: (OH, F, Cl) apatites Arch Oral Biol 1974; 19: 995-1006.
247. Odian G. Principles of polymerization. New York: Willey Interscience; 2004.
248. Ogliari FA, de Sordi ML, Ceschi MA, Petzhold CL, Demarco FF, Piva E. 2,3-Epithiopropyl methacrylate as functionalized monomer in a dental adhesive. J Dent 2006; 34: 472-477.
249. Ogliari FA, Ely C, Petzhold CL, Demarco FF, Piva E. Onium salt improves the polymerization kinetics in an experimental dental adhesive resin. J Dent 2007; 35: 583-587.
250. Okazaki M, Douglas WH. Comparison of surface layer properties of composite resins by ESCA, SEM and X-ray diffractometry. Biomaterials 1984; 5: 284-288.
251. Olea N, Pulgar R, Perez P, Olea-Serrano F, Rivas A, Novillo-Fertrell A. Estrogenicity of resin-based composites and sealants used in dentistry. Environmental Health Perspectives 1996; 104: 298-305.
252. Oooka S, Miyazaki M, Takamizawa T, Tsubota K, Kurokawa H, Rikuta A. Influence of adhesive polymerization mode on dentin bond strength of direct core foundation systems. J Oral Sci 2004; 46: 185-189.

253. Ortengren U, Wellendorf H, Karlsson S, Ruyter IE. Water sorption and solubility of dental composites and identification of monomers released in an aqueous environment. J Oral Rehabil 2001; 28: 1106-1115.
254. Owens BM, Rodriguez KH. Radiometric and spectrophotometric analysis of third generation light-emitting diode (LED) light-curing units. J Contemp Dent Pract 2007; 8: 43-51.
255. Oysaed H, Ruyter IE, Sjovik Kleven IJ. Release of formaldehyde from dental composites. J Dent Res 1988; 67: 1289-1294.
256. Ozturk B, Ozturk AN, Usumez A, Usumez S, Ozer F. Temperature rise during adhesive and resin composite polymerization with various light curing sources. Oper Dent 2004; 29: 325-332.
257. Palin WM, Fleming GJ, Burke FJ, Marquis PM, Randall RC. Monomer conversion versus flexure strength of a novel dental composite. J Dent 2003; 31: 341-351.
258. Palin WM, Fleming GJ, Nathwani H, Burke FJ, Randall RC. In vitro cuspal deflection and microleakage of maxillary premolars restored with novel low-shrink dental composites. Dent Mater 2005; 21: 324-335.
259. Pashley DH. Dentin: a dynamic substrate--a review. Scanning Microsc 1989; 3: 161-174; discussion 174-166.
260. Pashley DH. Clinical considerations of microleakage. J Endod 1990; 16: 70-77.
261. Pashley DH. Clinical correlations of dentin structure and function. J Prosthet Dent 1991; 66: 777-781.
262. Pashley DH. Dynamics of the pulpo-dentin complex. Crit Rev Oral Biol Med 1996; 7: 104-133.
263. Pashley DH, Carvalho RM. Dentine permeability and dentine adhesion. J Dent 1997; 25: 355-372.
264. Pashley DH, Ciucchi B, Sano H, Horner JA. Permeability of dentin to adhesive agents. Quintessence Int 1993; 24: 618-631.
265. Pashley DH, Tay FR, Yiu C, Hashimoto M, Breschi L, Carvalho RM et al. Collagen degradation by host-derived enzymes during aging. J Dent Res 2004; 83: 216-221.
266. Paul SJ, Welter DA, Ghazi M, Pashley D. Nanoleakage at the dentin adhesive interface vs microtensile bond strength. Oper Dent 1999; 24: 181-188.
267. Perdigao J, Baratieri LN, Lopes M. Laboratory evaluation and clinical application of a new one-bottle adhesive. J Esthet Dent 1999; 11: 23-35.
268. Perdigao J, Frankenberger R. Effect of solvent and rewetting time on dentin adhesion. Quintessence Int 2001; 32: 385-390.
269. Perdigao J, Geraldeli S, Carmo AR, Dutra HR. In vivo influence of residual moisture on microtensile bond strengths of one-bottle adhesives. J Esthet Restor Dent 2002; 14: 31-38.
270. Perdigao J, Lambrechts P, Van Meerbeek B, Braem M, Yildiz E, Yucel T et al. The interaction of adhesive systems with human dentin. Am J Dent 1996; 9: 167-173.
271. Peutzfeldt A. Resin composites in dentistry: the monomer systems. Eur J Oral Sci 1997; 105: 97-116.
272. Peutzfeldt A, Asmussen E. Influence of aldehydes on selected mechanical properties of resin composites. J Dent Res 1992; 71: 1522-1524.

273. Puckett AD, Fitchie JG, Kirk PC, Gamblin J. Direct composite restorative materials. Dent Clin North Am 2007; 51: 659-675, vii.
274. Radovic I, Vulicevic ZR, Garcia-Godoy F. Morphological evaluation of 2- and 1-step self-etching system interfaces with dentin. Oper Dent 2006; 31: 710-718.
275. Raspanti M, Alessandrini A, Gobbi P, Ruggeri A. Collagen fibril surface: TMAFM, FEG-SEM and freeze-etching observations. Microsc Res Tech 1996; 35: 87-93.
276. Ratanasathien S, Wataha JC, Hanks CT, Dennison JB. Cytotoxic interactive effects of dentin bonding components on mouse fibroblasts. J Dent Res 1995; 74: 1602-1606.
277. Rock WP. The effect of etching of human enamel upon bond strengths with fissure sealant resins. Arch Oral Biol 1974; 19: 873-877.
278. Rode KM, Kawano Y, Turbino ML. Evaluation of curing light distance on resin composite microhardness and polymerization. Oper Dent 2007; 32: 571-578.
279. Rosales-Leal JI. Microleakage of Class V composite restorations placed with etch-and-rinse and self-etching adhesives before and after thermocycling. J Adhes Dent 2007; 9 Suppl 2: 255-259.
280. Rosales-Leal JI, Osorio R, Holgado-Terriza JA, Cabrerizo-Vilchez MA, Toledano M. Dentin wetting by four adhesive systems. Dent Mater 2001; 17: 526-532.
281. Rueggeberg F, Craig RG. Correlation of parameters used to estimate monomer conversion in a light-cured composite. J Dent Res 1988; 67: 932-937.
282. Rueggeberg F, Hashinger DT, Fairhurst CW. Calibration of FTIR conversion analysis of contemporary dental resin composites. Dent Mater 1990; 6: 241-249.
283. Rueggeberg F, Tamareselvy K. Resin cure determination by polymerization shrinkage. Dent Mater 1995; 11: 265-268.
284. Rueggeberg FA, Margeson DH. The effect of oxygen inhibition on an unfilled/filled composite system. J Dent Res 1990; 69: 1652-1658.
285. Ruyter IE, Svendsen SA. Remaining methacrylate groups in composite restorative materials. Acta Odontol Scand 1978; 36: 75-82.
286. Sadek FT, Calheiros FC, Cardoso PE, Kawano Y, Tay F, Ferrari M. Early and 24-hour bond strength and degree of conversion of etch-and-rinse and self-etch adhesives. Am J Dent 2008; 21: 30-34.
287. Sakoolnamarka R, Burrow MF, Prawer S, Tyas MJ. Raman spectroscopic study of noncarious cervical lesions. Odontology 2005; 93: 35-40.
288. Salz U, Zimmermann J, Salzer T. Self-curing, self-etching adhesive cement systems. J Adhes Dent 2005a; 7: 7-17.
289. Salz U, Zimmermann J, Zeuner F, Moszner N. Hydrolytic stability of self-etching adhesive systems. J Adhes Dent 2005b; 7: 107-116.
290. Sano H, Shono T, Takatsu T, Hosoda H. Microporous dentin zone beneath resin-impregnated layer. Oper Dent 1994; 19: 59-64.
291. Sano H, Takatsu T, Ciucchi B, Horner JA, Matthews WG, Pashley DH. Nanoleakage: leakage within the hybrid layer. Oper Dent 1995; 20: 18-25.
292. Sano H, Yoshikawa T, Pereira PN, Kanemura N, Morigami M, Tagami J, Pashley DH. Long-term durability of dentin bonds made with a self-etching primer, in vivo. J Dent Res 1999; 78: 906-911.

293. Santerre J, Shajii L, Leung BW. Relation of dental composite formulations to their degradation and the release of hydrolyzed polymeric-resin-derived products. Crit Rev Oral Biol Med 2001; 12: 136-151.
294. Santini A, Ivanovic V, Ibbetson R, Milia E. Influence of cavity configuration on microleakage around Class V restorations bonded with seven self-etching adhesives. J Esthet Restor Dent 2004; 16: 128-135; discussion 136.
295. Santini A, Miletic V. Comparison of the hybrid layer formed by Silorane adhesive, one-step self-etch and etch and rinse systems using confocal micro-Raman spectroscopy and SEM. J Dent 2008; 36: 683-691.
296. Santini A, Plasschaert AJ, Mitchell S. Effect of composite resin placement techniques on the microleakage of two self-etching dentin-bonding agents. Am J Dent 2001; 14: 132-136.
297. Santos GB, Medeiros IS, Fellows CE, Muench A, Braga RR. Composite depth of cure obtained with QTH and LED units assessed by microhardness and micro-Raman spectroscopy. Oper Dent 2007; 32: 79-83.
298. Sato M, Miyazaki M. Comparison of depth of dentin etching and resin infiltration with single-step adhesive systems. J Dent 2005; 33: 475-484.
299. Schneider LF, Pfeifer CS, Consani S, Prahl SA, Ferracane JL. Influence of photoinitiator type on the rate of polymerization, degree of conversion, hardness and yellowing of dental resin composites. Dent Mater 2008; 24: 1169-1177.
300. Schrader B. Infrared and Raman Spectroscopy: Methods and Applications. New York: Wiley-VCH Verlag GmbH 1995.
301. Schroeder WF, Cook WD, Vallo CI. Photopolymerization of N,N-dimethylaminobenzyl alcohol as amine co-initiator for light-cured dental resins. Dent Mater 2008; 24: 686-693.
302. Schroeder WF, Vallo CI. Effect of different photoinitiator systems on conversion profiles of a model unfilled light-cured resin. Dent Mater 2007; 23: 1313-1321.
303. Schulze K, Balooch M, Balooch G, Marshall GW, Marshall SJ. Micro-Raman spectroscopic investigation of dental calcified tissues. J Biomed Mater Res 2004; 69: 286-293.
304. Schweikl H, Spagnuolo G, Schmalz G. Genetic and cellular toxicology of dental resin monomers. J Dent Res 2006; 85: 870-877.
305. Shimada Y, Harnirattisai C, Inokoshi S, Burrow MF, Takatsu T. In vivo adhesive interface between resin and dentin. Oper Dent 1995; 20: 204-210.
306. Shin WS, Li XF, Schwartz B, Wunder SL, Baran GR. Determination of the degree of cure of dental resins using Raman and FT-Raman spectroscopy. Dent Mater 1993; 9: 317-324.
307. Shono Y, Terashita M, Shimada J, Kozono Y, Carvalho RM, Russell CM et al. Durability of resin-dentin bonds. J Adhes Dent 1999; 1: 211-218.
308. Sideridou I, Tserki V, Papanastasiou G. Effect of chemical structure on degree of conversion in light-cured dimethacrylate-based dental resins. Biomaterials 2002; 23: 1819-1829.
309. Sideridou ID, Achilias DS. Elution study of unreacted Bis-GMA, TEGDMA, UDMA, and Bis-EMA from light-cured dental resins and resin composites using HPLC. J Biomed Mater Res B Appl Biomater 2005; 74: 617-626.

310. Sidhu SK, Omata Y, Tanaka T, Koshiro K, Spreafico D, Semeraro S et al. Bonding characteristics of newly developed all-in-one adhesives. J Biomed Mater Res B Appl Biomater 2007; 80: 297-303.
311. Silikas N, Kavvadia K, Eliades G, Watts D. Surface characterization of modern resin composites: A multitechnique approach. Am J Dent 2005; 18: 95-100.
312. Silikas N, Watts DC. High pressure liquid chromatography of dentin primers and bonding agents. Dent Mater 2000; 16: 81-88.
313. Silva Soares L, Rocha R, Martin AA, Pinheiro AL, Zampieri M. Monomer conversion of composite dental resins photoactivated by a halogen lamp and a LED: a FT-Raman spectroscopy study. Quim Nova 2005; 28: 229-232.
314. Simon G, Allen PEM, Bennett DJ, Williams DRG, Williams EH. . Nature of residual unsaturation during cure of dimethacrylates examined by CPPEMAS 13C NMR and simulation using a kinetic gelation model. Macromolecules 1989; 22: 3555-3561.
315. Skrtic D, Antonucci JM. Effect of bifunctional comonomers on mechanical strength and water sorption of amorphous calcium phosphate- and silanized glass-filled Bis-GMA-based composites. Biomaterials 2003; 24: 2881-2888.
316. Skrtic D, Stansbury JW, Antonucci JM. Volumetric contraction and methacrylate conversion in photo-polymerized amorphous calcium phosphate/methacrylate composites. Biomaterials 2003; 24: 2443-2449.
317. Soares LE, Martin AA, Pinheiro AL, Pacheco MT. Vicker's hardness and Raman spectroscopy evaluation of a dental composite cured by an argon laser and a halogen lamp. J Biomed Opt 2004; 9: 601-608.
318. Soh MS, Yap AU, Yu T, Shen ZX. Analysis of the degree of conversion of LED and halogen lights using micro-Raman spectroscopy. Oper Dent 2004; 29: 571-577.
319. Spencer P, Wang Y. Adhesive phase separation at the dentin interface under wet bonding conditions. J Biomed Mater Res 2002; 62: 447-456.
320. Spencer P, Wang Y, Walker MP, Wieliczka DM, Swafford JR. Interfacial chemistry of the dentin/adhesive bond. J Dent Res 2000; 79: 1458-1463.
321. Spencer P, Wang Y, Bohaty B. Interfacial chemistry of moisture-aged class II composite restorations. J Biomed Matr Res part B: Applied Biomater 2006; 77: 234-240.
322. Spreafico D, Semeraro S, Mezzanzanica D, Re D, Gagliani M, Tanaka T et al. The effect of the air-blowing step on the technique sensitivity of four different adhesive systems. J Dent 2006; 34: 237-244.
323. St-Georges AJ, Swift EJ, Thompson JY, Heymann HO. Irradiance effects on the mechanical properties of universal hybrid and flowable hybrid resin composites. Dent Mater 2003; 19: 406-413.
324. Stansbury JW. Synthesis and evaluation of new oxaspiro monomers for double ring-opening polymerization. J Dent Res 1992; 71: 1408-1412.
325. Steele D. Theory of vibrational spectroscopy. W.B. Saunders; 1971.
326. Stewardson DA, Shortall AC, Harrington E, Lumley PJ. Thermal changes and cure depths associated with a high intensity light activation unit. J Dent 2004; 32: 643-651.
327. Sun GJ, Chae KH. Properties of 2,3-butanedione and 1-phenyl-1,2-propanedione as new photosensitizers for visible light cured dental resin composites Polymer 2000; 41: 6205-6212.

328. Sunico MC, Shinkai K, Medina VO, 3rd, Shirono M, Tanaka N, Katoh Y. Effect of surface conditioning and restorative material on the shear bond strength and resin-dentin interface of a new one-bottle nanofilled adhesive. Dent Mater 2002; 18: 535-542.
329. Suzuki M, Kato H, Wakumoto S. Vibrational analysis by Raman spectroscopy of the interface between dental adhesive resin and dentin. J Dent Res 1991; 70: 1092-1097.
330. Suzuki S, Leinfelder KF, Kawai K, Tsuchitani Y. Effect of particle variation on wear rates of posterior composites. Am J Dent 1995; 8: 173-178.
331. Takahashi A, Inoue S, Kawamoto C, Ominato R, Tanaka T, Sato Y et al. In vivo long-term durability of the bond to dentin using two adhesive systems. J Adhes Dent 2002; 4: 151-159.
332. Tanimoto Y, Hayakawa T, Nemoto K. Analysis of photopolymerization behavior of UDMA/TEGDMA resin mixture and its composite by differential scanning calorimetry. J Biomed Mater Res B Appl Biomater 2005; 72: 310-315.
333. Tarle Z, Knezevic A, Demoli N, Meniga A, Sutalo J, Unterbrink G et al. Comparison of composite curing parameters: effects of light source and curing mode on conversion, temperature rise and polymerization shrinkage. Oper Dent 2006; 31: 219-226.
334. Tarle Z, Meniga A, Knezevic A, Sutalo J, Ristic M, Pichler G. Composite conversion and temperature rise using a conventional, plasma arc, and an experimental blue LED curing unit. J Oral Rehabil 2002; 29: 662-667.
335. Tay FR, Moulding KM, Pashley DH. Distribution of nanofillers from a simplified-step adhesive in acid-conditioned dentin. J Adhes Dent 1999; 1: 103-117.
336. Tay FR, Pang KM, Gwinnett AJ, Wei SH. A method for microleakage evaluation along the dentin/restorative interface. Am J Dent 1995; 8: 105-108.
337. Tay FR, Pashley DH. Aggressiveness of contemporary self-etching systems. I: Depth of penetration beyond dentin smear layers. Dent Mater 2001; 17: 296-308.
338. Tay FR, Pashley DH, Yoshiyama M. Two modes of nanoleakage expression in single-step adhesives. J Dent Res 2002; 81: 472-476.
339. Toledano M, Osorio R, Osorio E, Aguilera FS, Yamauti M, Pashley DH et al. Effect of bacterial collagenase on resin-dentin bonds degradation. J Mater Sci Mater Med 2007; 18: 2355-2361.
340. Tomlins P, Palin WM, Shortall AC, Wang RK. Time-resolved simultaneous measurement of group index and physical thickness during photopolymerization of resin-based dental composite. J Biomed Opt 2007; 12: DOI:10.117/111.2709877.
341. Tramini P, Bonnet B, Sabatier R, Maury L. A method of age estimation using Raman microspectrometry imaging of the human dentin. Forensic Science International 2001; 118: 1-9.
342. Tramini P, Pelissier B, Valacarcel J, Bonnet B, Maury L. A Raman spectroscopic investigation of dentin and enamel structure modified by lactic acid. Caries Res 2000; 34: 233-240.
343. Tsuda H, Arends J. Raman spectra of human dental calculus. J Dent Res 1993; 72: 1609-1613.
344. Tsuda H, Arends J. Orientational micro-Raman spectroscopy on hydroxyapatite single crystals and human enamel crystallites. J Dent Res 1994; 73: 1703-1710.

345. Tsuda H, Jongebloed WL, Stokroos I, Arends J. Combined Raman and SEM study on CaF2 formed on/in enamel by APF treatments. Caries Res 1993; 27: 445-454.
346. Tsuda H, Jongebloed WL, Stokroos I, Arends J. A micro-Raman spectroscopic study of hydrazine-treated human dental calculus. Scanning Microsc 1996a; 10: 1015-1023; discussion 1023-1014.
347. Tsuda H, Ruben J, Arends J. Raman spectra of human dentin mineral. Eur J Oral Sci 1996b; 104: 123-131.
348. Turssi CP, Ferracane JL, Vogel K. Filler features and their effects on wear and degree of conversion of particulate dental resin composites. Biomaterials 2005; 26: 4932-4937.
349. Unemori M, Matsuya Y, Matsuya S, Akashi A, Akamine A. Water absorption of poly(methyl methacrylate) containing 4-methacryloxyethyl trimellitic anhydride. Biomaterials 2003; 24: 1381-1387.
350. Uno S, Inoue H, Finger WJ, Inoue S, Sano H. Microtensile bond strength evaluation of three adhesive systems in cervical dentin cavities. J Adhes Dent 2001; 3: 333-341.
351. Usumez S, Buyukyilmaz T, Karaman AI, Gunduz B. Degree of conversion of two lingual retainer adhesives cured with different light sources. Eur J Orthod 2005; 27: 173-179.
352. Uzunova Y, Lukanov L, Filipov I, Vladimirov S. High-performance liquid chromatographic determination of unreacted monomers and other residues contained in dental composites. J Biochem Biophys Methods 2008; 70: 883-888.
353. Vaidyanathan J, Vaidyanathan TK, Kerrigan JE. Evaluation of intermolecular interactions of self-etch dentin adhesive primer molecules with type 1 collagen: computer modeling and in vitro binding analysis. Acta Biomater 2007; 3: 705-714.
354. Vaidyanathan TK, Vaidyanathan J. Recent advances in the theory and mechanism of adhesive resin bonding to dentin: a critical review. J Biomed Mater Res B Appl Biomater 2009; 88: 558-578.
355. Van Landuyt KL, De Munck J, Snauwaert J, Coutinho E, Poitevin A, Yoshida Y et al. Monomer-solvent phase separation in one-step self-etch adhesives. J Dent Res 2005; 84: 183-188.
356. Van Landuyt KL, Snauwaert J, De Munck J, Peumans M, Yoshida Y, Poitevin A et al. Systematic review of the chemical composition of contemporary dental adhesives. Biomaterials 2007; 28: 3757-3785.
357. Van Meerbeek B, Braem M, Lambrechts P, Vanherle G. Morphological characterization of the interface between resin and sclerotic dentine. J Dent 1994; 22: 141-146.
358. Van Meerbeek B, Conn LJ, Jr., Duke ES, Eick JD, Robinson SJ, Guerrero D. Correlative transmission electron microscopy examination of nondemineralized and demineralized resin-dentin interfaces formed by two dentin adhesive systems. J Dent Res 1996; 75: 879-888.
359. Van Meerbeek B, Dhem A, Goret-Nicaise M, Braem M, Lambrechts P, VanHerle G. Comparative SEM and TEM examination of the ultrastructure of the resin-dentin interdiffusion zone. J Dent Res 1993a; 72: 495-501.

360. Van Meerbeek B, Mohrbacher H, Celis JP, Roos JR, Braem M, Lambrechts P et al. Chemical characterization of the resin-dentin interface by micro-Raman spectroscopy. J Dent Res 1993b; 72: 1423-1428.
361. Van Meerbeek B, Perdigao J, Lambrechts P, Vanherle G. The clinical performance of adhesives. J Dent 1998; 26: 1-20.
362. Van Meerbeek B, Vargas M, Inoue S, Yoshida Y, Perdigao J, Lambrechts P, Vanherle G. Microscopy investigations. Techniques, results, limitations. American Journal of Dentistry 2000; 13: 3D-18D.
363. Van Noort R, Noroozi S, Howard IC, Cardew G. A critique of bond strength measurements. J Dent 1989; 17: 61-67.
364. Vandewalle KS, Roberts HW, Tiba A, Charlton DG. Thermal emission and curing efficiency of LED and halogen curing lights. Oper Dent 2005; 30: 257-264.
365. Veis A, Lambrianides T, Nicolaou A. Area-metric analysis of dye leakage for evaluation of sealing ability of root canal obturation techniques. Endod Dent Traumatol 1996; 12: 222-226.
366. Venhoven BA, de Gee AJ, Davidson CL. Polymerization contraction and conversion of light-curing BisGMA-based methacrylate resins. Biomaterials 1993; 14: 871-875.
367. Venhoven BA, de Gee AJ, Davidson CL. Light initiation of dental resins: dynamics of the polymerization. Biomaterials 1996; 17: 2313-2318.
368. Versluis A, Douglas WH, Sakaguchi RL. Thermal expansion coefficient of dental composites measured with strain gauges. Dent Mater 1996; 12: 290-294.
369. Vodak D, Braun M, Iordanidis L, Plvert J, Stevens M, Beck L, Spence JCH, O'Keeffe M, Yaghi OM. One-Step Synthesis and Structure of an Oligo(spiro-orthocarbonate). J Am Chem Soc 2002; 124: 4942-4943.
370. Walters PA. Dentinal hypersensitivity: a review. J Contemp Dent Pract 2005; 6: 107-117.
371. Wang JD, Hume WR. Diffusion of hydrogen ion and hydroxyl ion from various sources through dentine. Int Endod J 1988; 21: 17-26.
372. Wang Y, Spencer P. Effect of acid etching time and technique on interfacial characteristics of the adhesive-dentin bond using differential staining. Eur J Oral Sci 2004a; 112: 293-299.
373. Wang Y, Spencer P. Physiochemical interactions at the interfaces between self-etch adhesive systems and dentine. J Dent 2004b; 32: 567-579.
374. Wang Y, Spencer P. Continuing etching of an all-in-one adhesive in wet dentin tubules. J Dent Res 2005; 84: 350-354.
375. Wang Y, Spencer P. Interfacial chemistry of class II composite restorations: Structure analysis. J Biomed Mater Res 2005; 75: 580-587.
376. Wang Y, Spencer P, Hager C, Bohaty B. Comparison of interfacial characteristics of adhesive bonding to superficial versus deep dentine using SEM and staining techniques. J Dent 2006a; 34: 26-34.
377. Wang Y, Spencer P, Walker MP. Chemical profile of adhesive/caries-affected dentin interfaces using Raman microspectroscopy. J Biomed Mater Res A 2007; 81: 279-286.

378. Wang Y, Spencer P, Yao X. Micro-Raman imaging analysis of monomer/mineral distribution in intertubular region of adhesive/dentin interfaces. J Biomed Opt 2006b; 11: 024005.
379. Wang Y, Spencer P, Yao X, Ye Q. Effect of coinitiator and water on the photoreactivity and photopolymerization of HEMA/camphoquinone-based reactant mixtures. J Biomed Mater Res A 2006c; 78: 721-728.
380. Warnock R, Rueggeberg FA. Curing kinetics of a photo-polymerized dental sealant. Am J Dent 2004; 17: 457-461.
381. Watanabe I, Nakabayashi, N. Bonding durability of of photocured Phenyl-P in TEGDMA to smear layer-retained bovine dentin Quintessence Int 1993; 24: 335-342.
382. Weinmann W, Thalacker C, Guggenberger R. Siloranes in dental composites. Dent Mater 2005; 21: 68-74.
383. Wentrup-Byrne E, Armstrong CA, Armstrong RS, Collins BM. Fourier transform Raman microscopic mapping of the molecular components in a human tooth. J Raman Spectrosc 1997; 27: 151-158.
384. Wertz JE, Bolton JR. Electron Spin Resonance: Elementary Theory and Practical Applications. NY: McGraw-Hill; 1972.
385. Wieliczka D, Spencer P, Kruger MB. Raman mapping of the dentin/adhesive interface. Appl Spectrosc 1996; 50: 1500-1504.
386. Williams D, Fleming I. Spectroscopic methods in organic chemistry. Berkshire: McGraw-Hill Publishing; 1995.
387. Witzel MF, Calheiros FC, Goncalves F, Kawano Y, Braga RR. Influence of photoactivation method on conversion, mechanical properties, degradation in ethanol and contraction stress of resin-based materials. J Dent 2005; 33: 773-779.
388. Wu S, Soucek MD. Crosslinking of acrylic latex coatings with cycloaliphatic diepoxide. Polymer 2000; 41: 2017-2028.
389. Wunderlich B. Thermal analysis of polymeric materials. NY: Springer; 2005.
390. Xie B, Dickens SH, Giuseppetti AA. Microtensile bond strength of thermally stressed composite-dentin bonds mediated by one-bottle adhesives. Am J Dent 2002; 15: 177-184.
391. Xu X, Sandras DA, Burgess JO. Shear bond strength with increasing light-guide distance from dentin. J Esthet Restor Dent 2006; 18: 19-27; discussion 28.
392. Yamada M, Miyazaki M, Moore BK. Influence of interchanging adhesive resins and self-etching primers on the mechanical properties of adhesive resins. Oper Dent 2004; 29: 532-537.
393. Yamauchi J, Nakabayashi, N, Masuhara E. Adhesive agents for hard tissue containing phosphoric acid monomers. ACS, Div Polym Chem, Polym Prepr 1979; 20: 594-595.
394. Yap A, Soh MS, Han VTS, Siow KS. Influence of curing lights and modes on cross-link density of dental composites. Oper Dent 2004a; 29: 410-415.
395. Yap AU, Han VT, Soh MS, Siow KS. Elution of leachable components from composites after LED and halogen light irradiation. Oper Dent 2004b; 29: 448-453.
396. Ye Q, Wang Y, Spencer P. Nanophase separation of polymers exposed to simulated bonding conditions. J Biomed Mater Res B Appl Biomater 2008.

397. Ye Q, Wang Y, Williams K, Spencer P. Characterization of photopolymerization of dentin adhesives as a function of light source and irradiance. J Biomed Mater Res B Appl Biomater 2007; 80: 440-446.
398. Yoshida Y, Van Meerbeek B, Nakayama Y, Snauwaert J, Hellemans L, Lambrechts P et al. Evidence of chemical bonding at biomaterial-hard tissue interfaces. J Dent Res 2000; 79: 709-714.
399. Yoshida Y, Van Meerbeek B, Nakayama Y, Yoshioka M, Snauwaert J, Abe Y et al. Adhesion to and decalcification of hydroxyapatite by carboxylic acids. J Dent Res 2001; 80: 1565-1569.
400. Yoshioka M, Yoshida Y, Inoue S, Lambrechts P, Vanherle G, Nomura Y et al. Adhesion/decalcification mechanisms of acid interactions with human hard tissues. J Biomed Mater Res 2002; 59: 56-62.
401. Yoshiyama M, Carvalho R, Sano H, Horner J, Brewer PD, Pashley DH. Interfacial morphology and strength of bonds made to superficial versus deep dentin. Am J Dent 1995; 8: 297-302.
402. Yoshiyama M, Tay FR, Doi J, Nishitani Y, Yamada T, Itou K et al. Bonding of self-etch and total-etch adhesives to carious dentin. J Dent Res 2002; 81: 556-560.
403. Yoshiyama M, Urayama A, Kimochi T, Matsuo T, Pashley DH. Comparison of conventional vs self-etching adhesive bonds to caries-affected dentin. Oper Dent 2000; 25: 163-169.
404. Zhang Y, Xu J. Effect of immersion in various media on the sorption, solubility, elution of unreacted monomers, and flexural properties of two model dental composite compositions. J Mater Sci Mater Med 2008; 19: 2477-2483.

ACKNOWLEDGEMENTS

My most sincere gratitude is extended to Dr Ario Santini, Director of Biomaterials Research at the Edinburgh Postgraduate Dental Institute, The University of Edinburgh, for giving me the opportunity to continue my postgraduate education in Edinburgh, his supervision of my PhD work and the invaluable advice regarding all aspects of research methodology and writing of my thesis. Working with Dr Santini has been the most outstanding time of my career and a true inspiration for my future professional journey.

I am indebted to Professor Richard Ibbetson, Director of Edinburgh Postgraduate Dental Institute, The University of Edinburgh, for his generosity and support which enabled me to undertake my PhD studies in Edinburgh.

My sincere thanks go to Professor Vladimir Ivanovic, Department of Restorative Dentistry and Endodontics, the School of Dentistry, the University of Belgrade, without whose recommendation, support and encouragement, I would not have been able to study in Edinburgh.

I am also grateful to Professor Lesley Yellowlees, Head of the School of Chemistry, The University of Edinburgh, and Professors Colin Pulham and Mark Bradley of the School of Chemistry, The University of Edinburgh, for allowing me unrestricted access to, and use of micro-Raman spectroscopy and high-performance liquid chromatography facilities.

I would like to thank Dr Ivan Trkulja, postdoctoral fellow of the School of Chemistry, The University of Edinburgh, for his selfless help with high-performance liquid chromatography.

I would like to express my gratitude to all of my colleagues at the Department of Restorative Dentistry and Endodontics, the School of Dentistry, the University of Belgrade, for their continuous support during my PhD work.

APPENDIX

MICRO-RAMAN SPECTRA OF TISSUES AND MATERIALS

This appendix contains representative micro-Raman spectra of all tissues and materials used in this thesis.

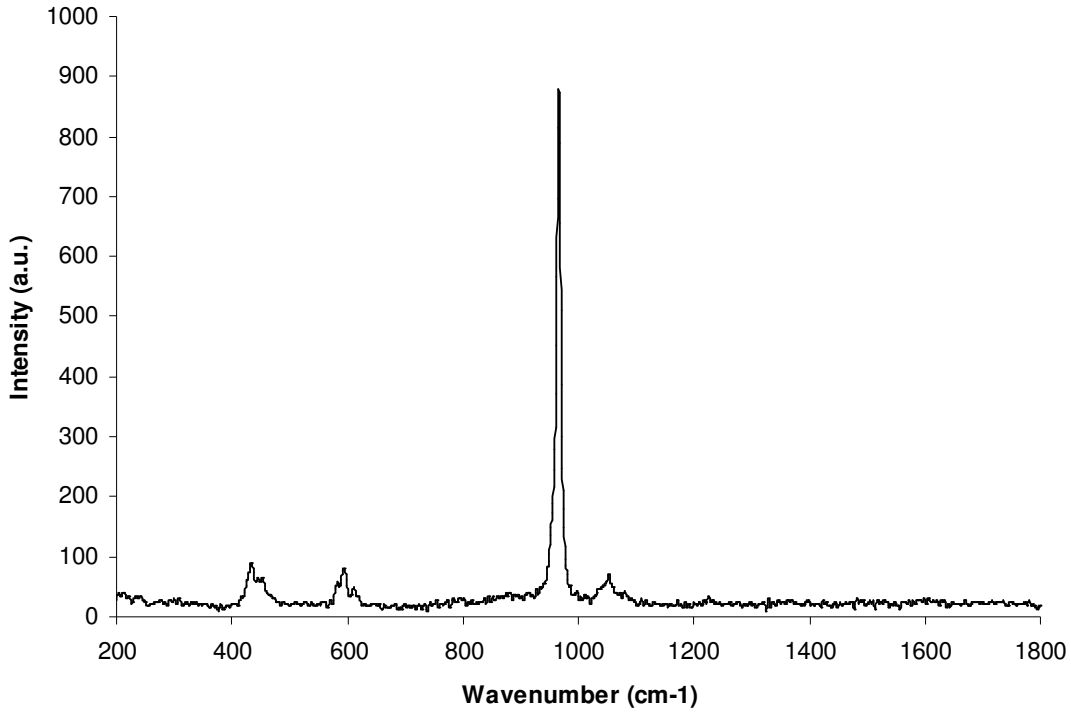

Spectrum 1. Hydroxyapatite.

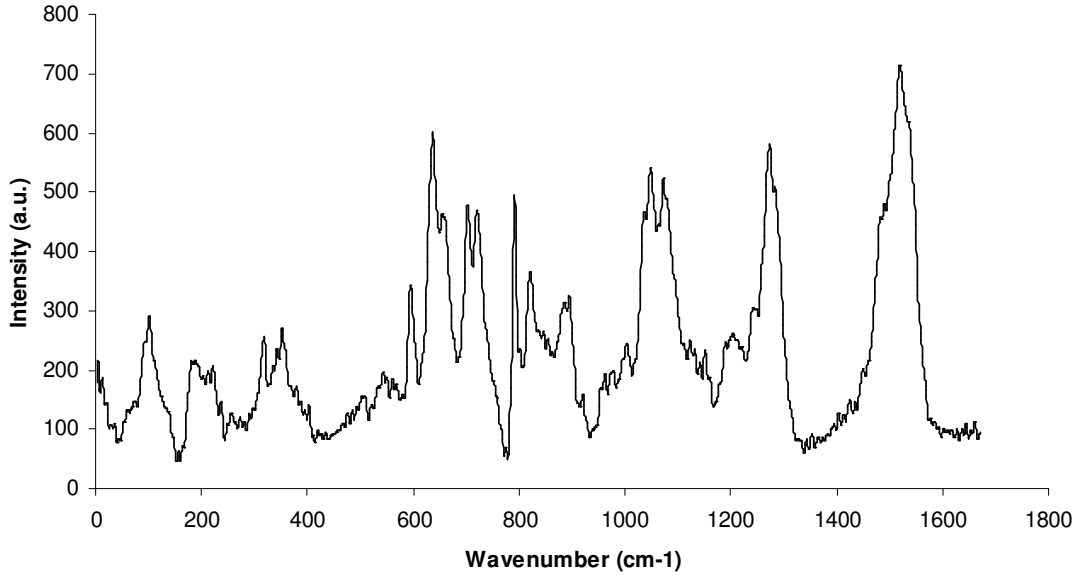

Spectrum 2. Collagen type I (wavenumber range 0-1800 cm^{-1}).

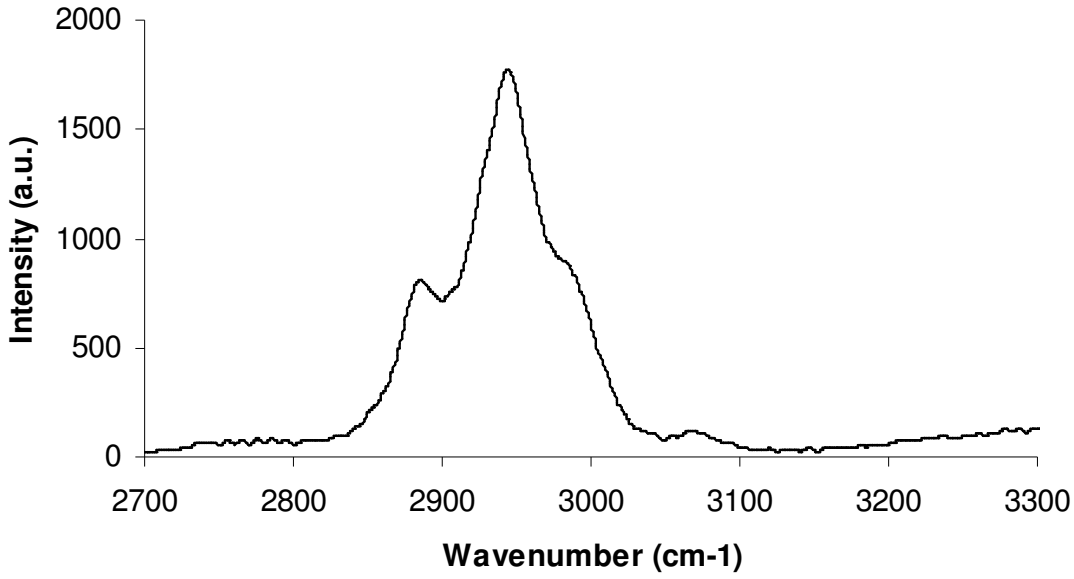

Spectrum 3. Collagen type I (wavenumber range 2700-3300 cm^{-1}).

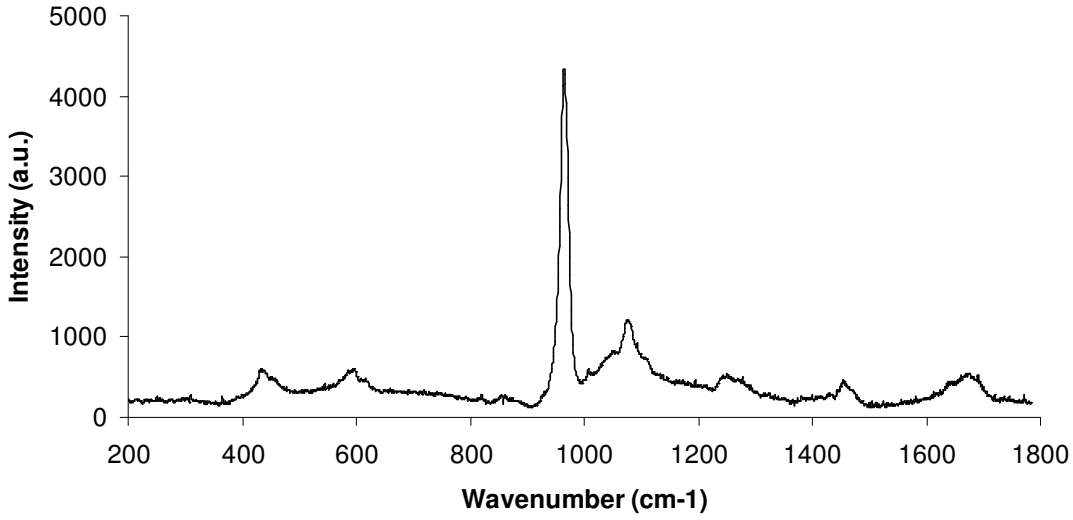

Spectrum 4. Dentine.

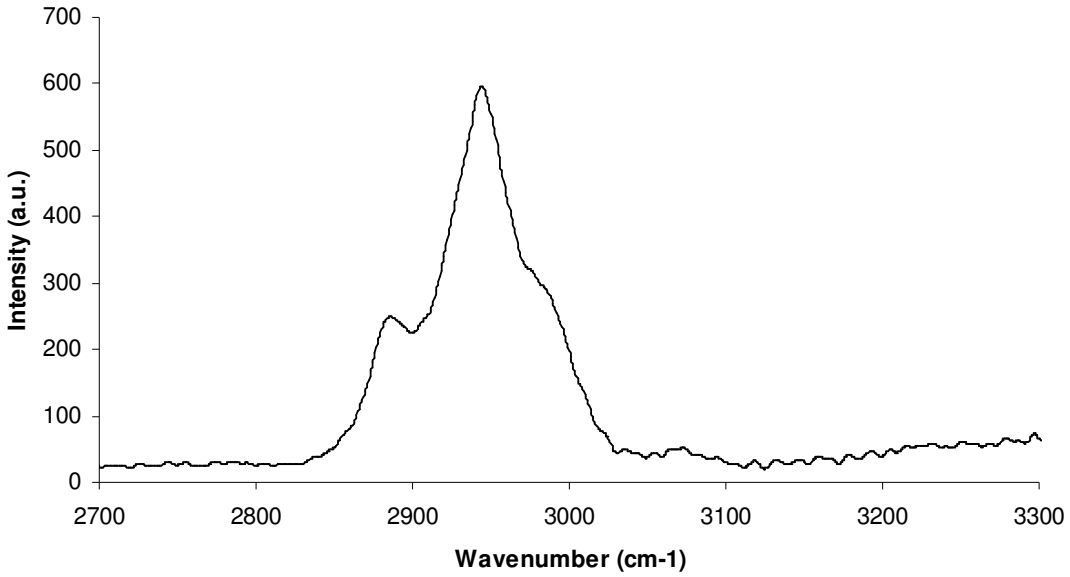

Spectrum 5. Dentine (wavenumber range 2700-3300 cm^{-1}).

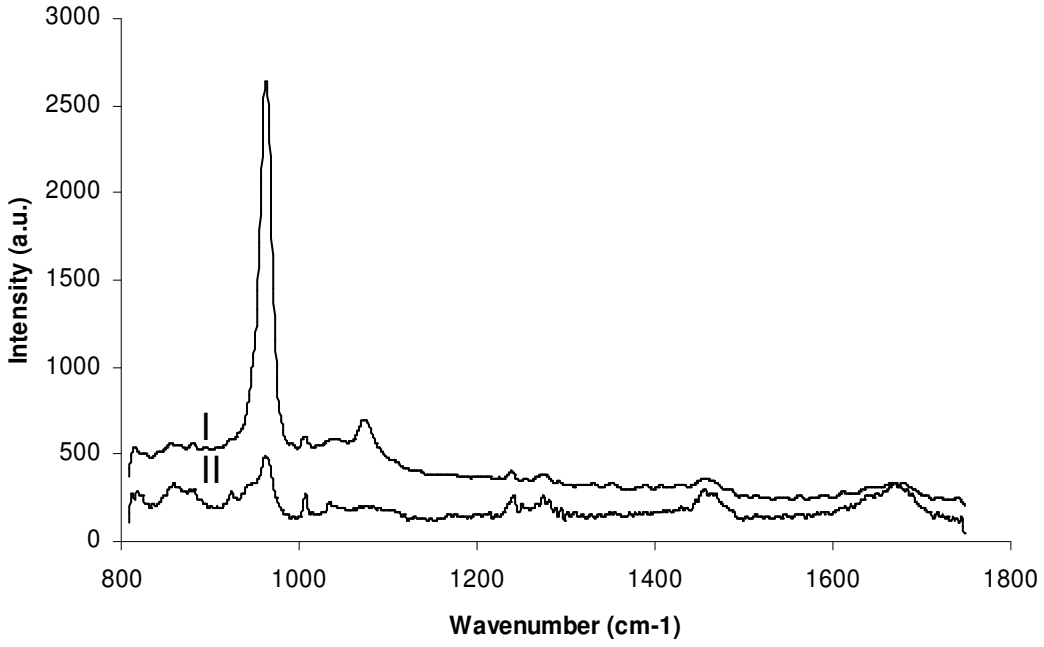

Spectra 6. Change in dentine mineral content after acid etching; I – Dentine before etching; II – Dentine after etching.

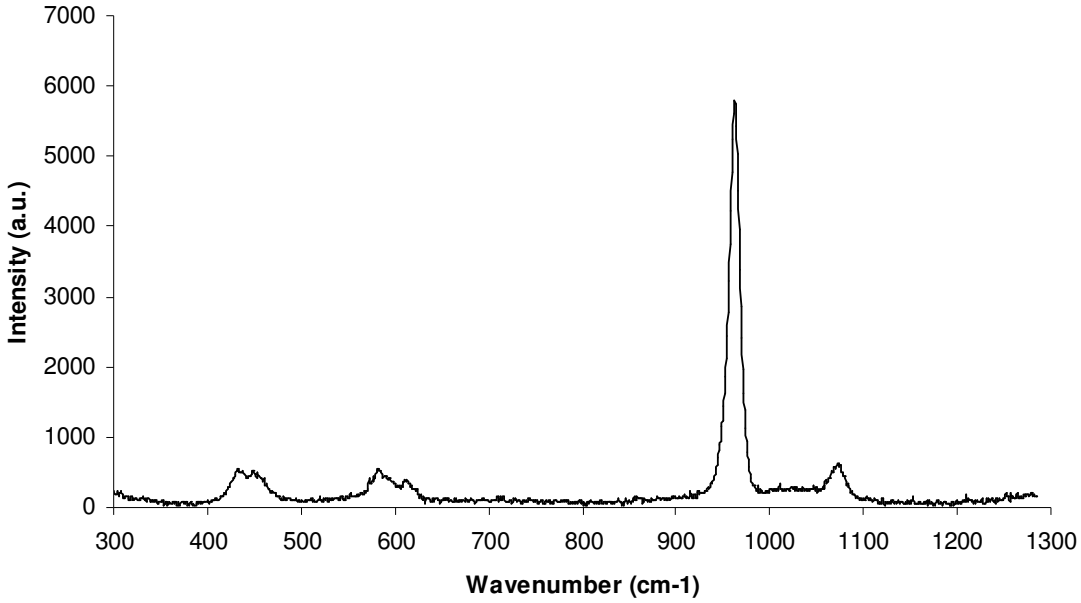

Spectrum 7. Enamel.

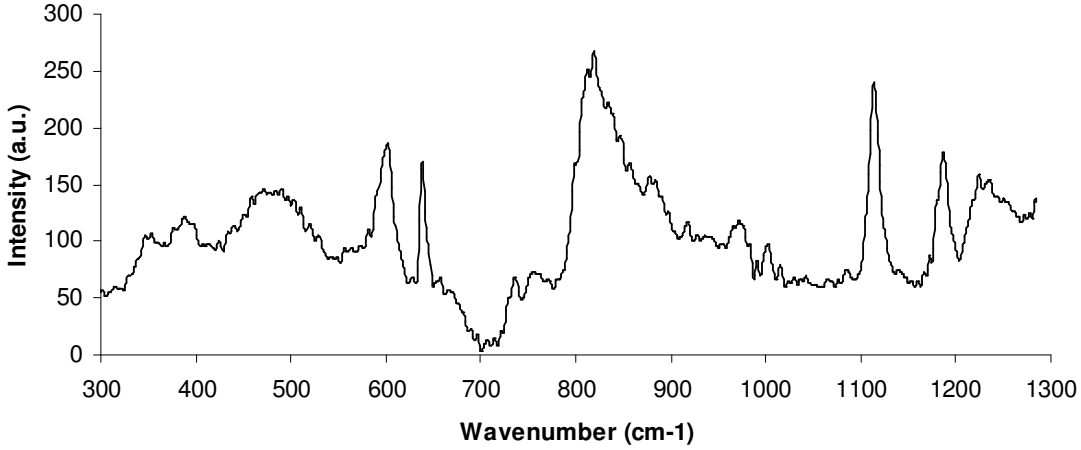

Spectrum 8. Fillers.

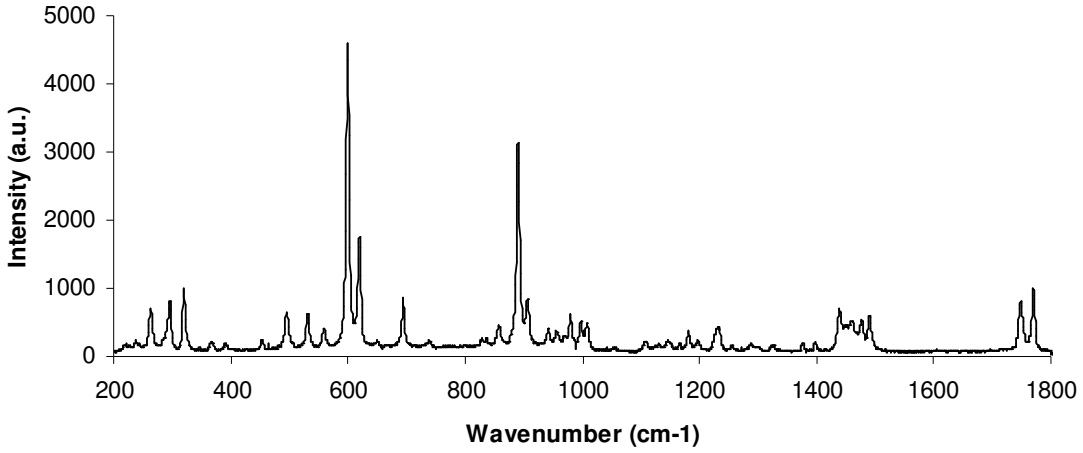

Spectrum 9. Camphorquinone.

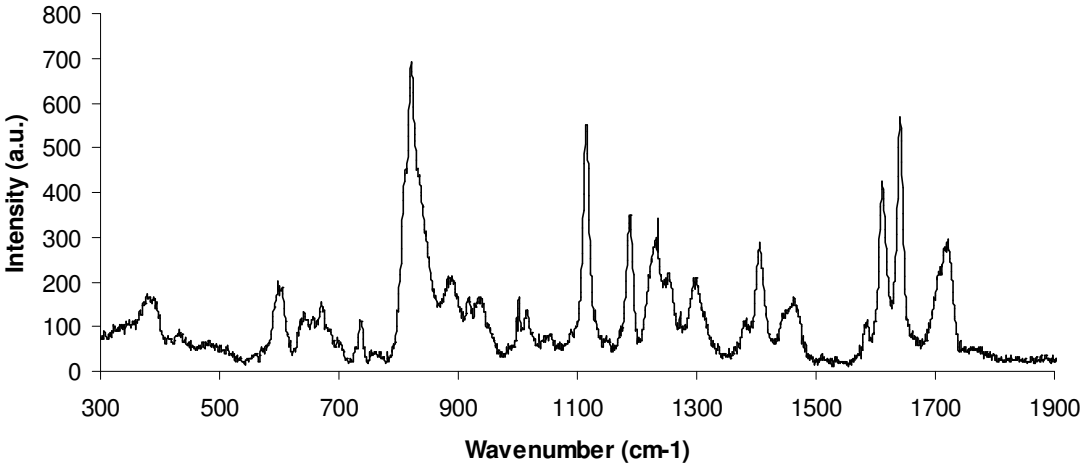

Spectrum 10. BisGMA.

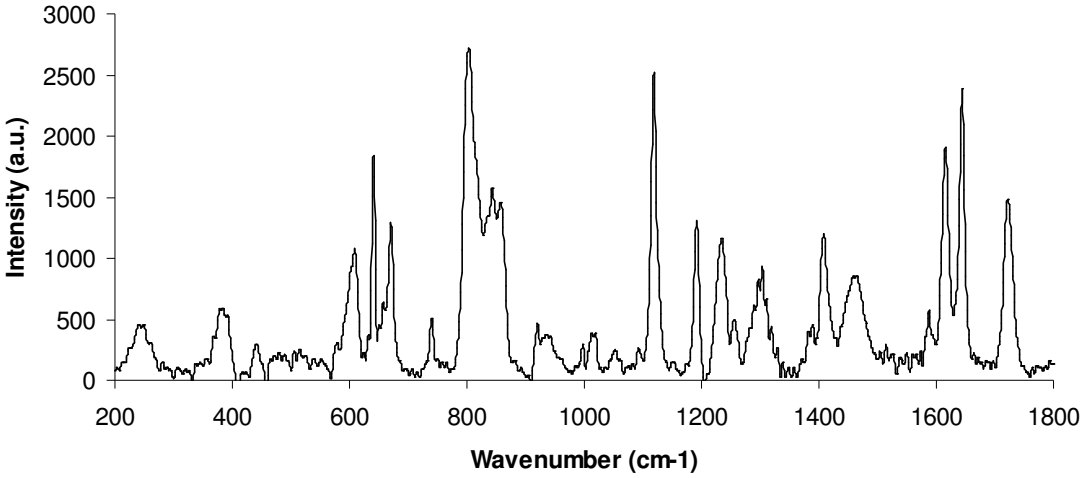

Spectrum 11. BisEMA.

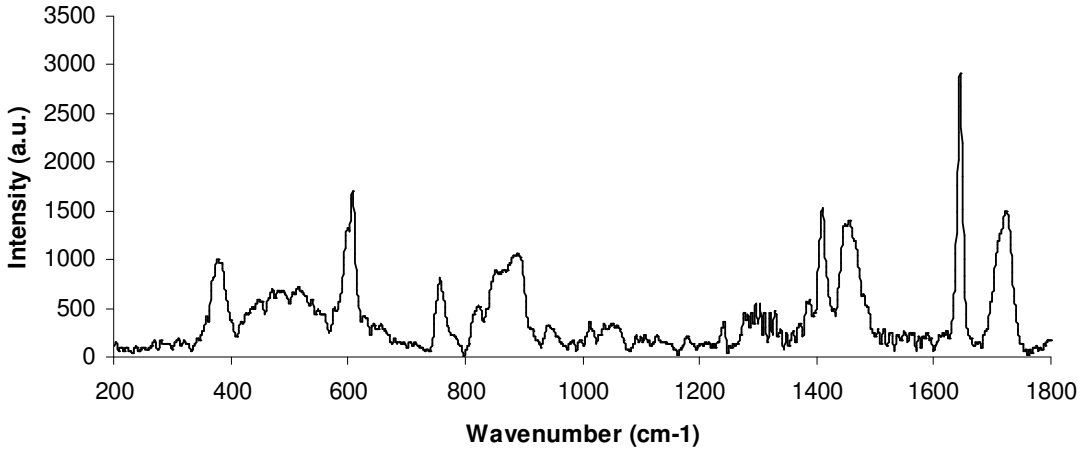

Spectrum 12. UDMA.

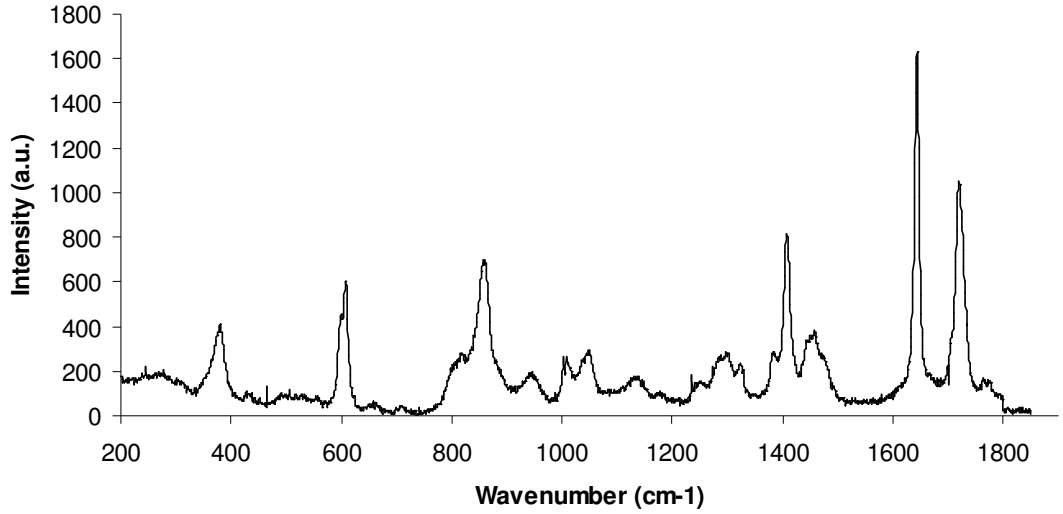

Spectrum 13. TEGDMA.

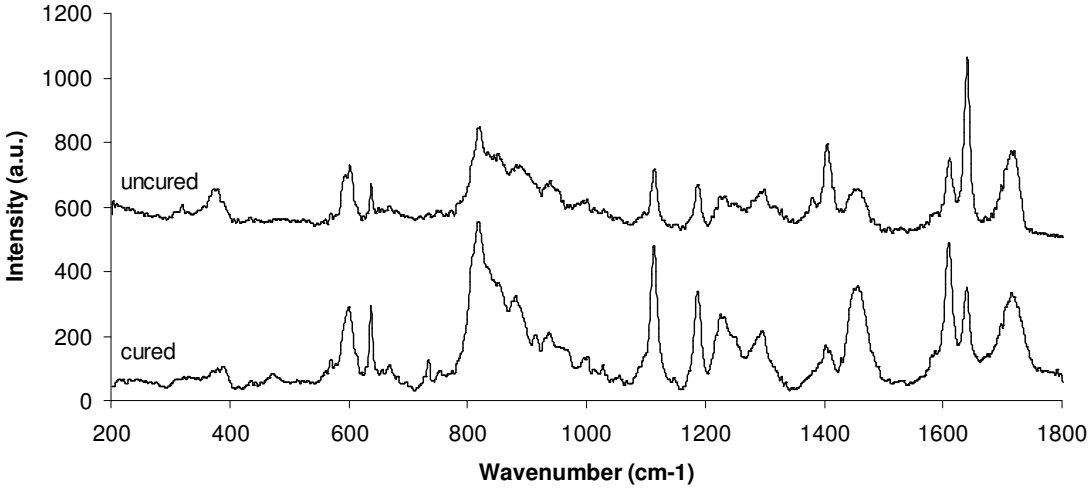

Spectra 14. Excite.

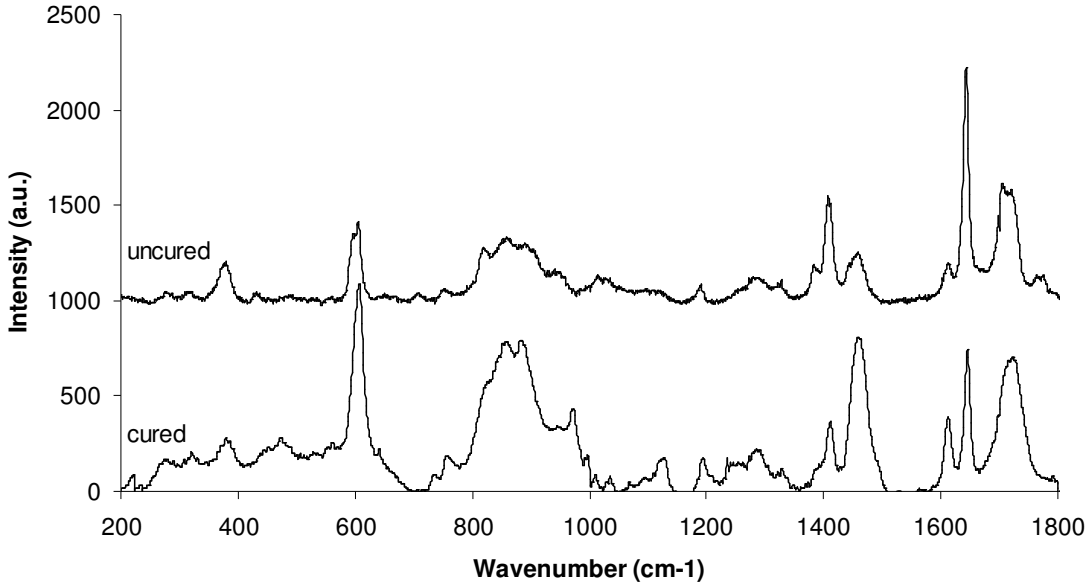

Spectra 15. James -2.

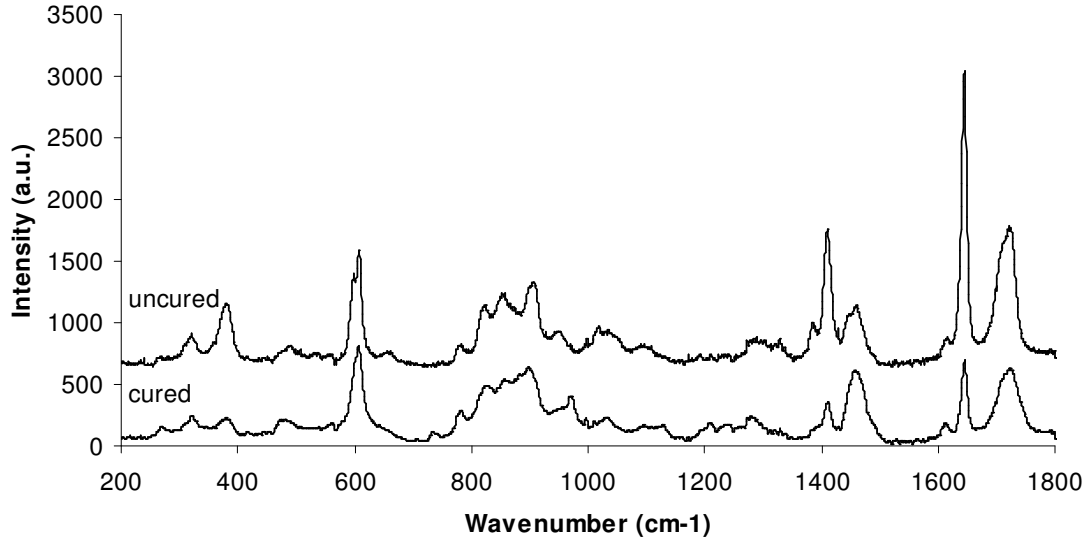

Spectra 16. One Coat Bond [etch-and-rinse].

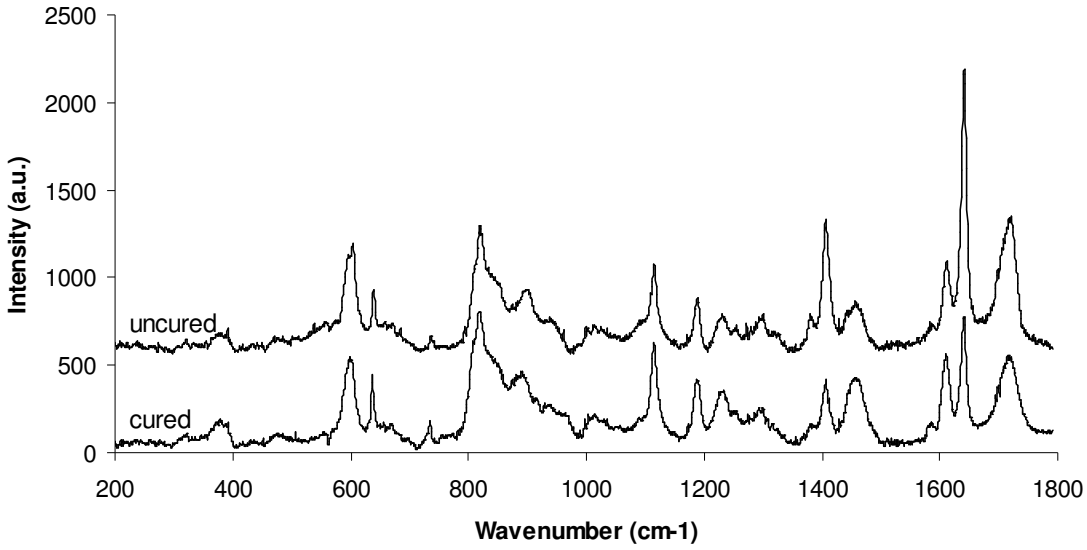

Spectra 17. AdheSE Bond.

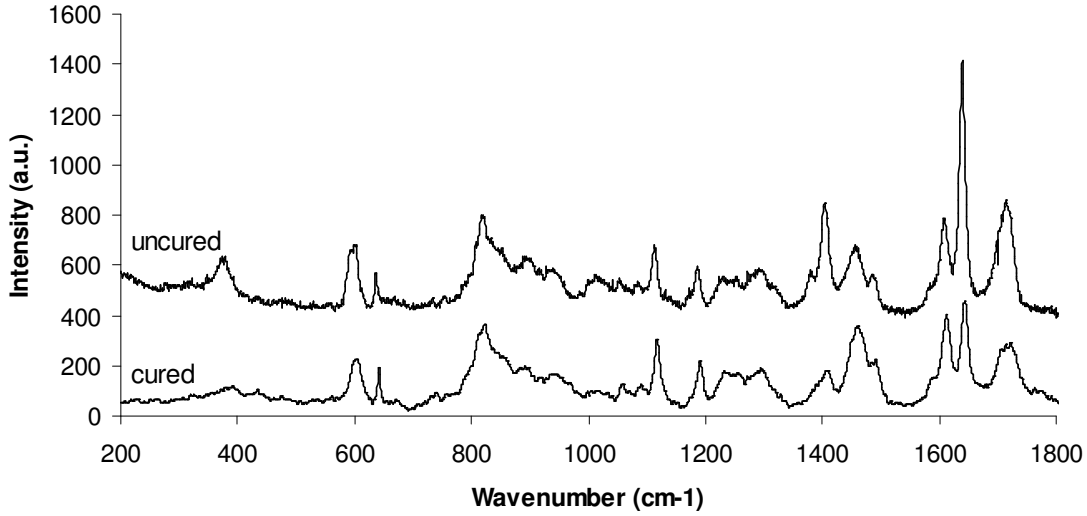

Spectra 18. AdheSE Primer + Bond.

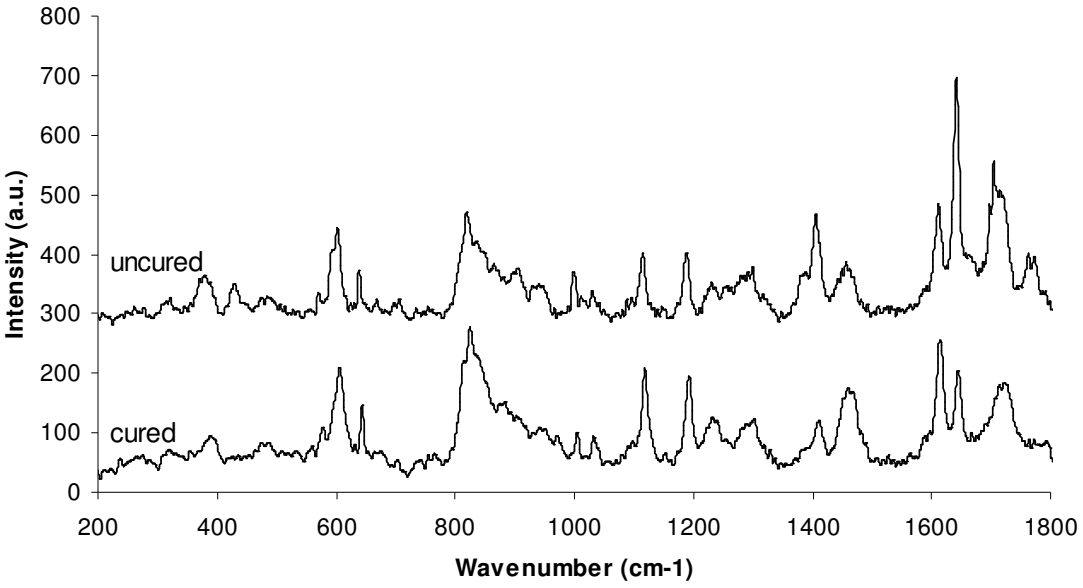

Spectra 19. Cleafil SE Bond.

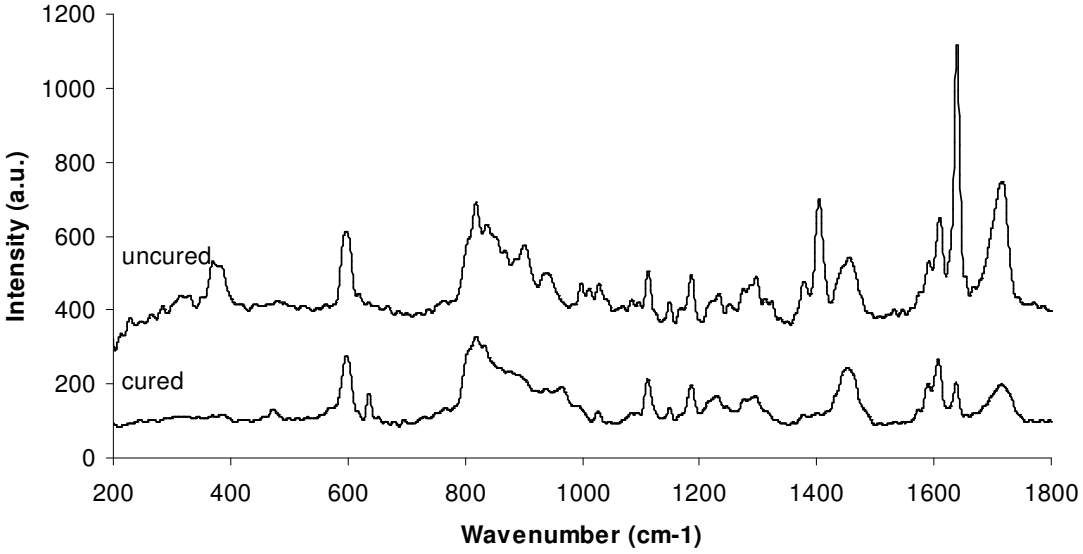

Spectra 20. Clearfil SE Primer + Bond.

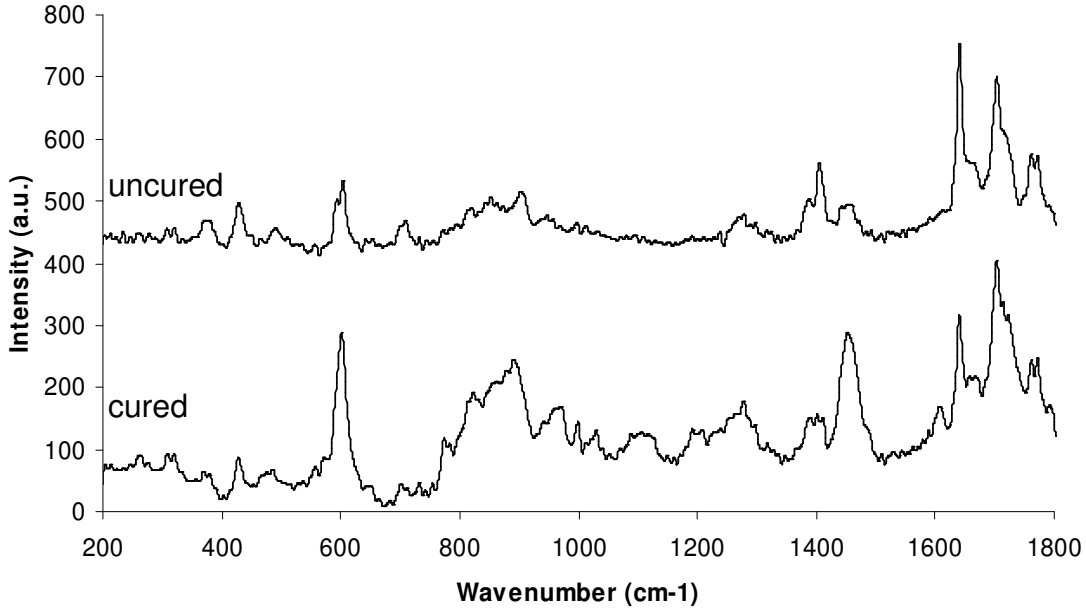

Spectra 21. One Coat Bond 2-step self-etch (Bond only).

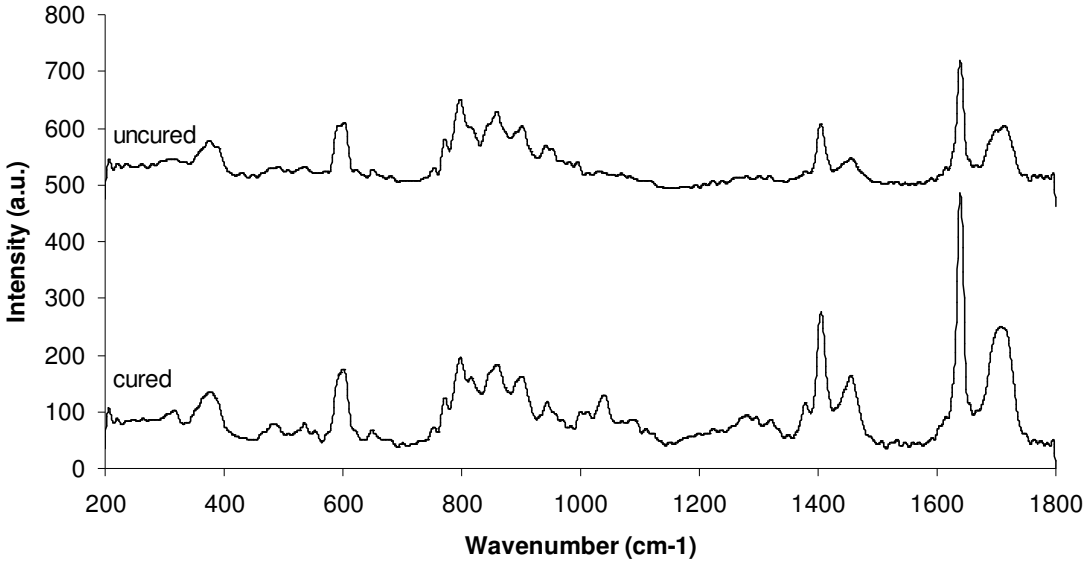

Spectra 22. One Coat Bond 2-step self-etch (Primer + Bond).

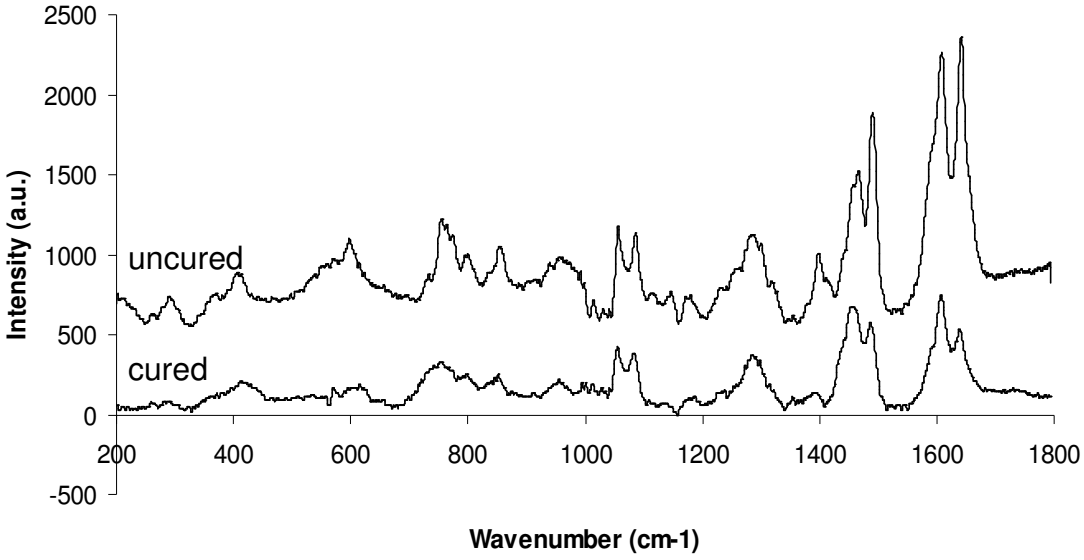

Spectra 23. AdheSE One.

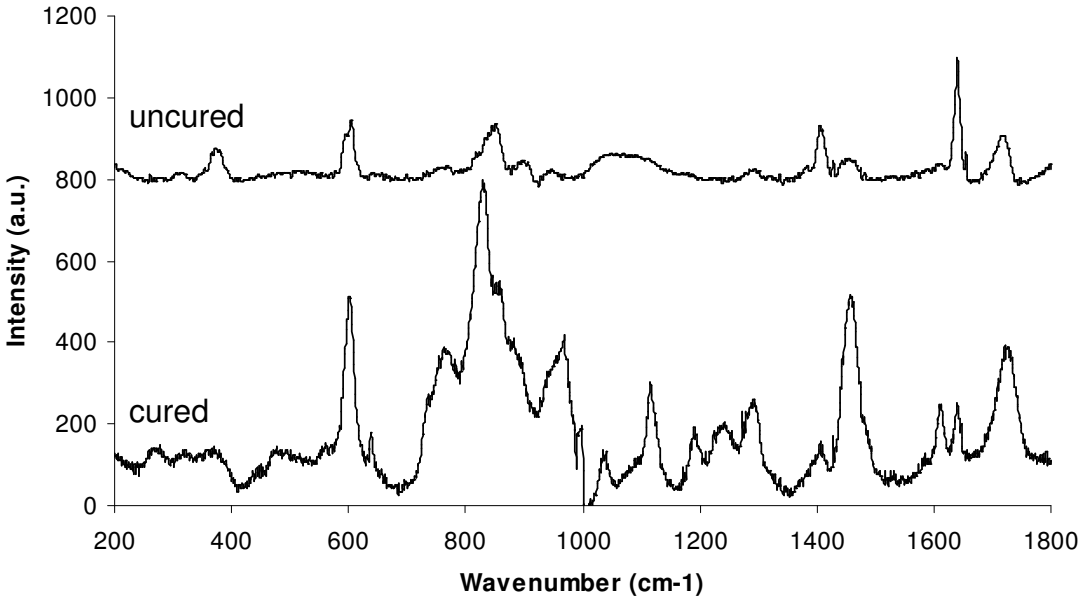

Spectra 24. Adper prompt L-Pop.

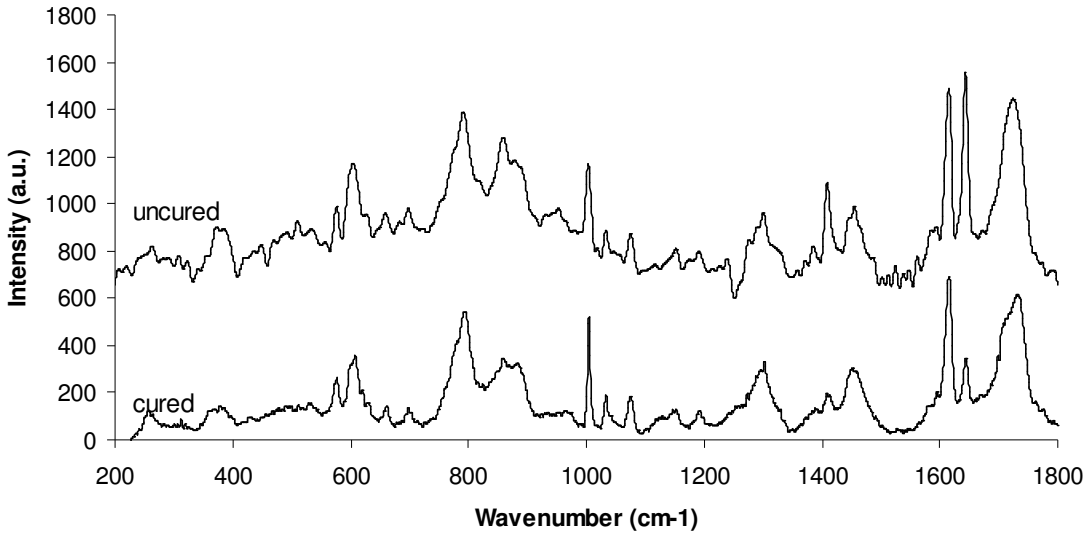

Spectra 25. G Bond.

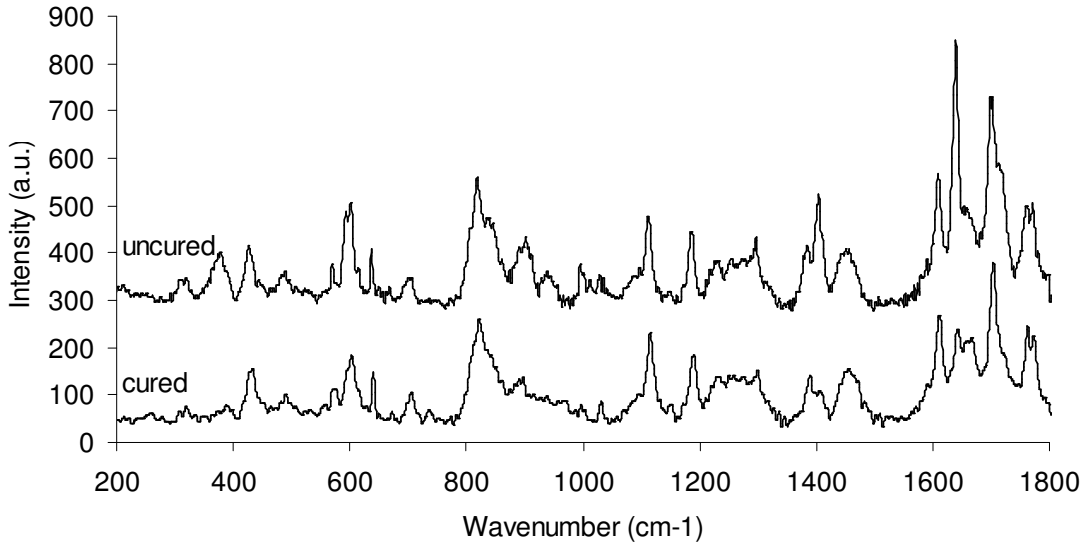

Spectra 26. Clearfil 3S Bond.

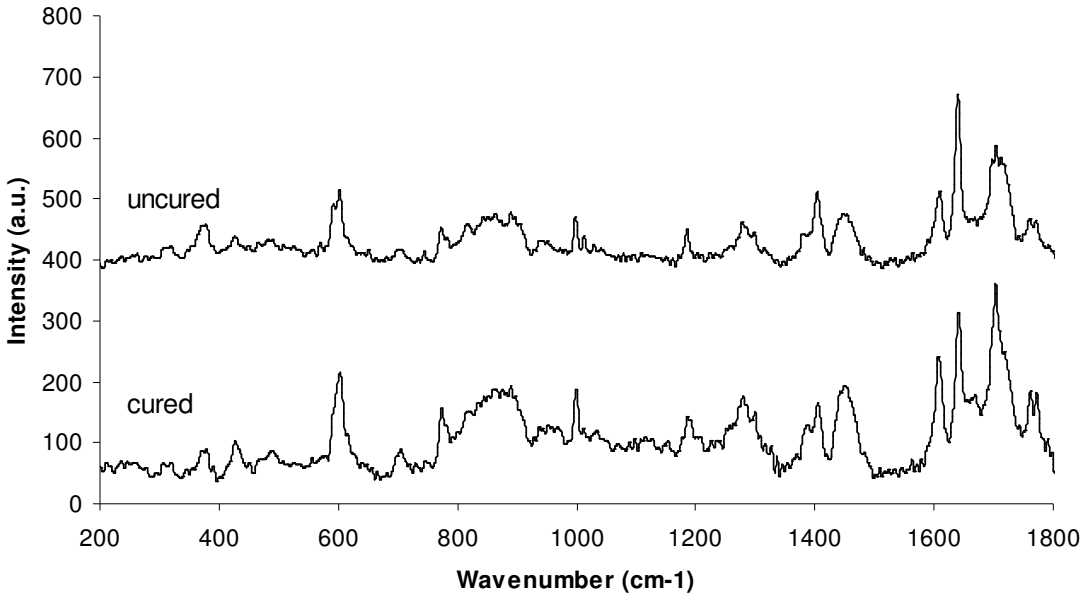

Spectra 27. One Coat Bond 1-step self-etch.

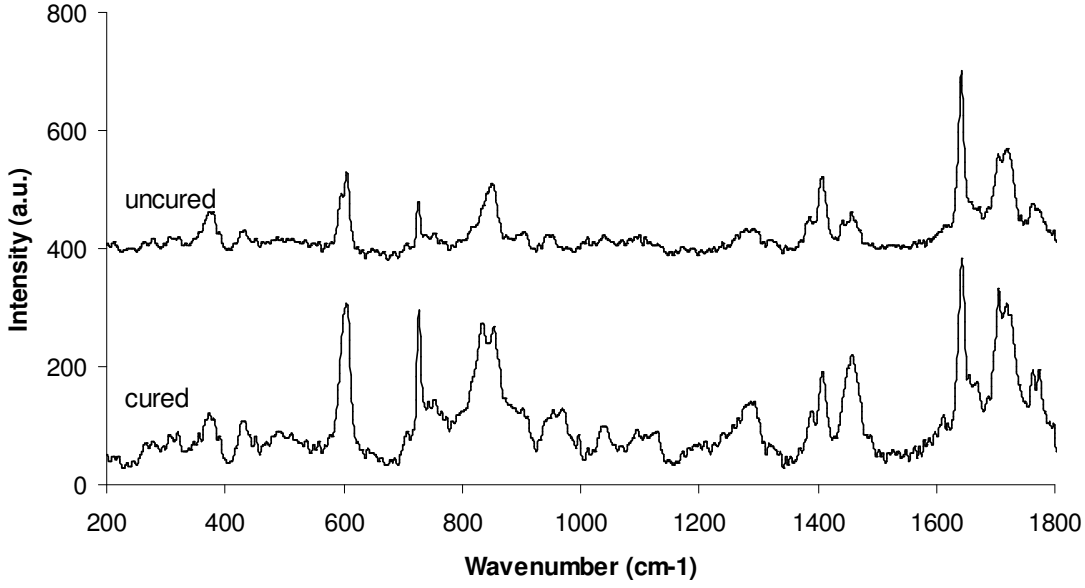

Spectra 28. Xeno III (liquid A + liquid B).

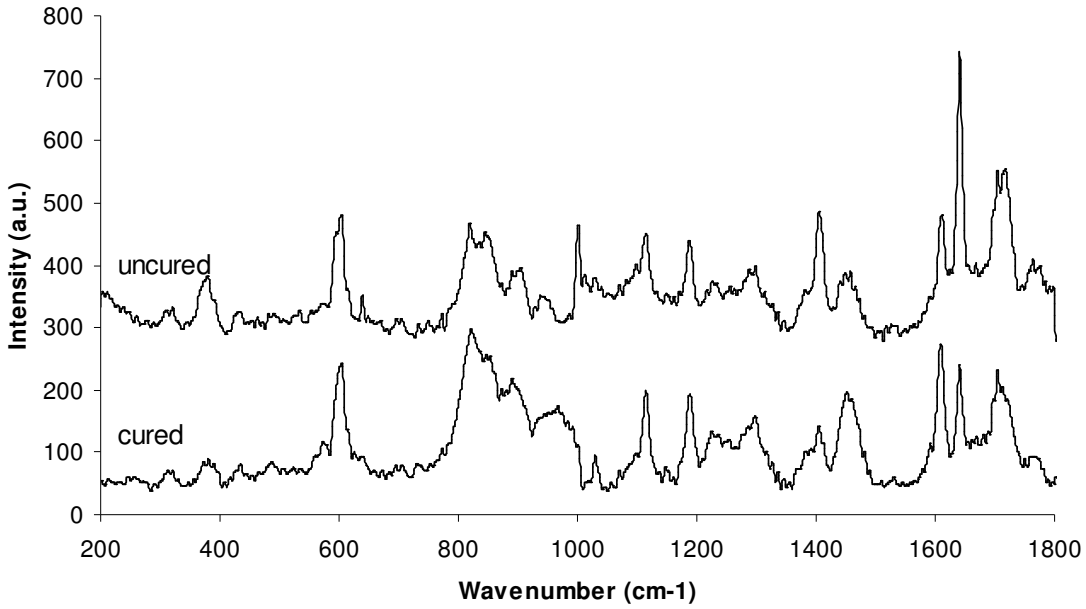

Spectra 29. Filtek Silorane Primer.

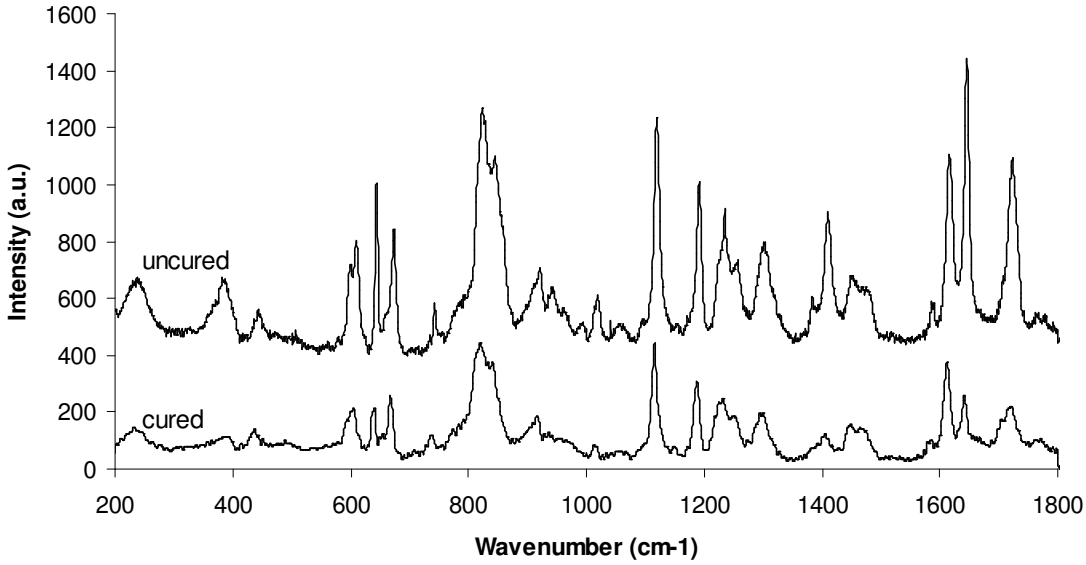

Spectra 30. Filtek Silorane Bond.

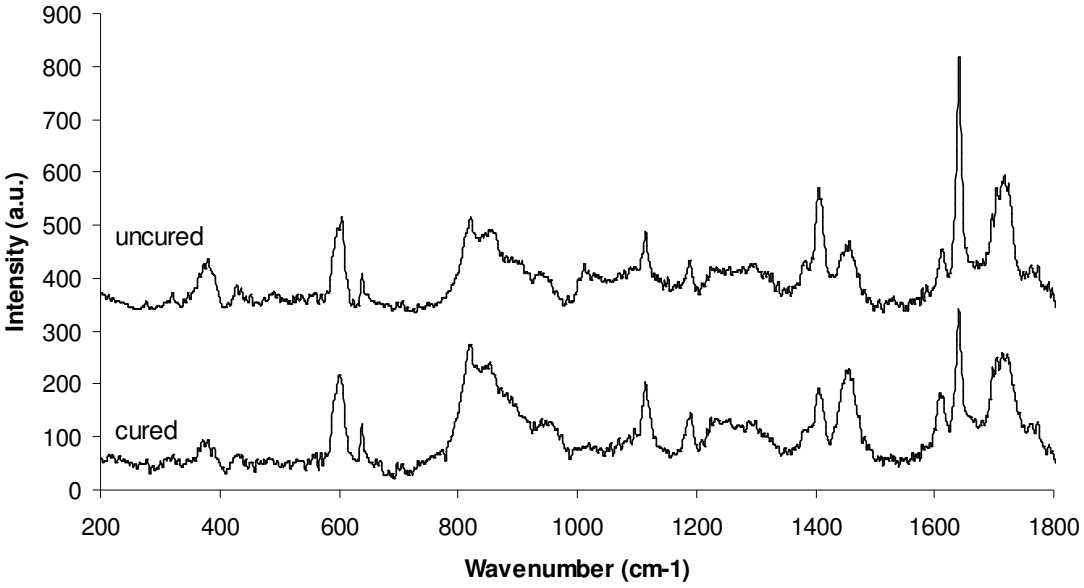

Spectra 31. Admira bond.

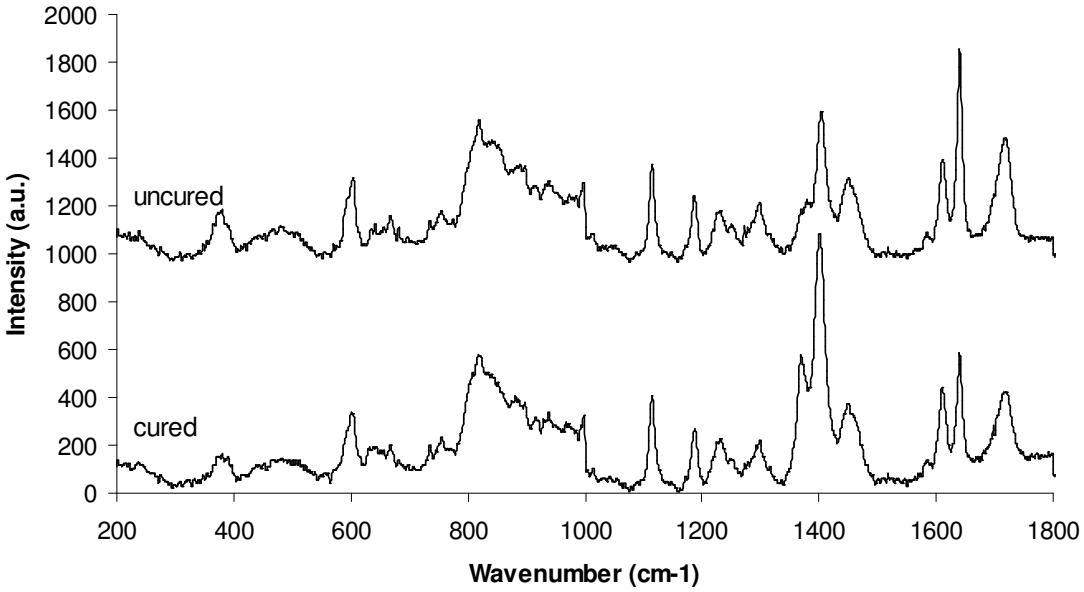

Spectra 32. Tetric EvoCeram.

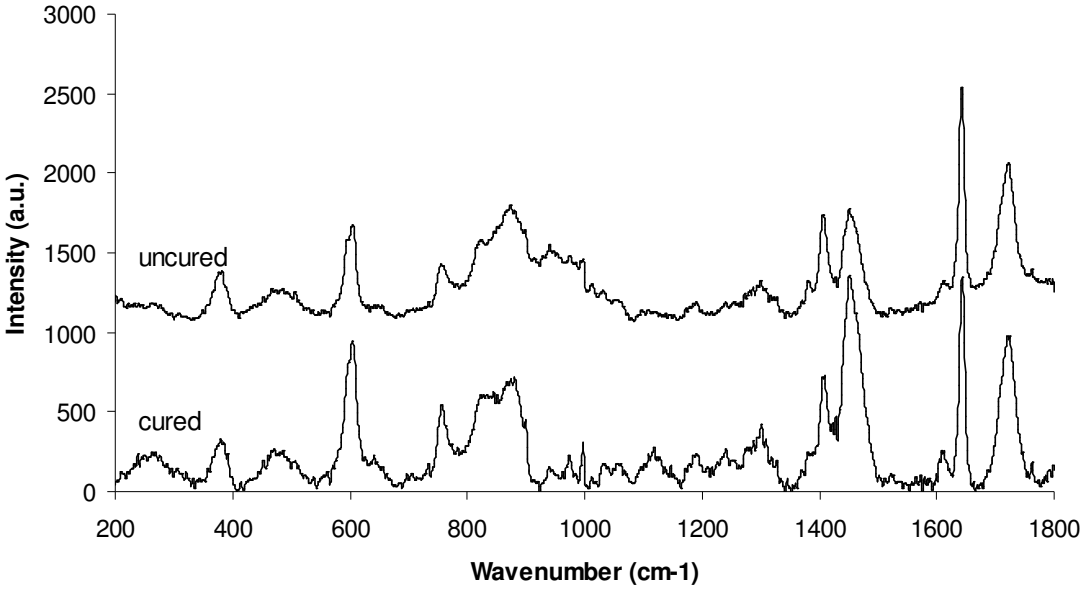

Spectra 33. Gradia Direct.

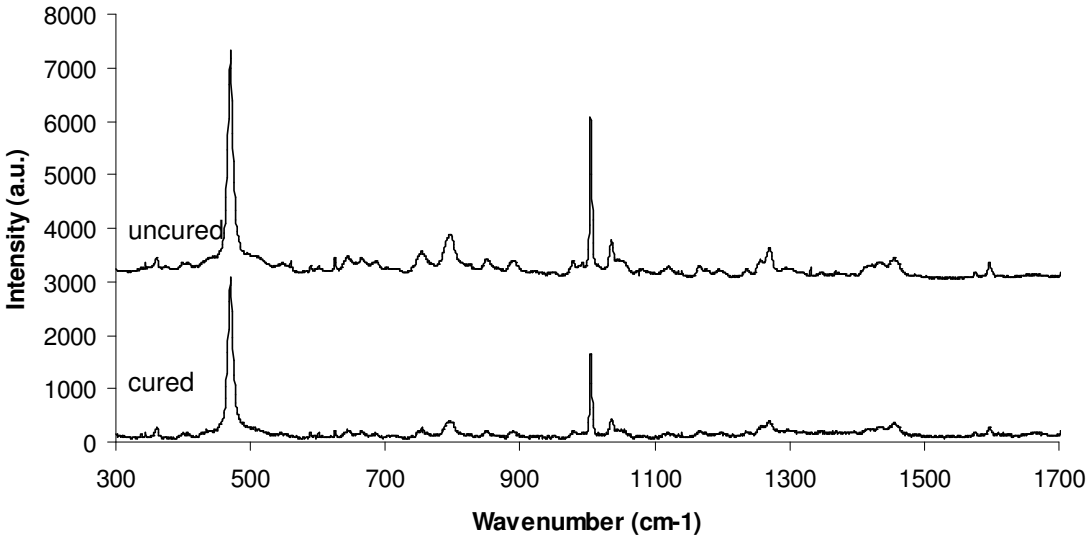

Spectra 34. Filtek Silorane.

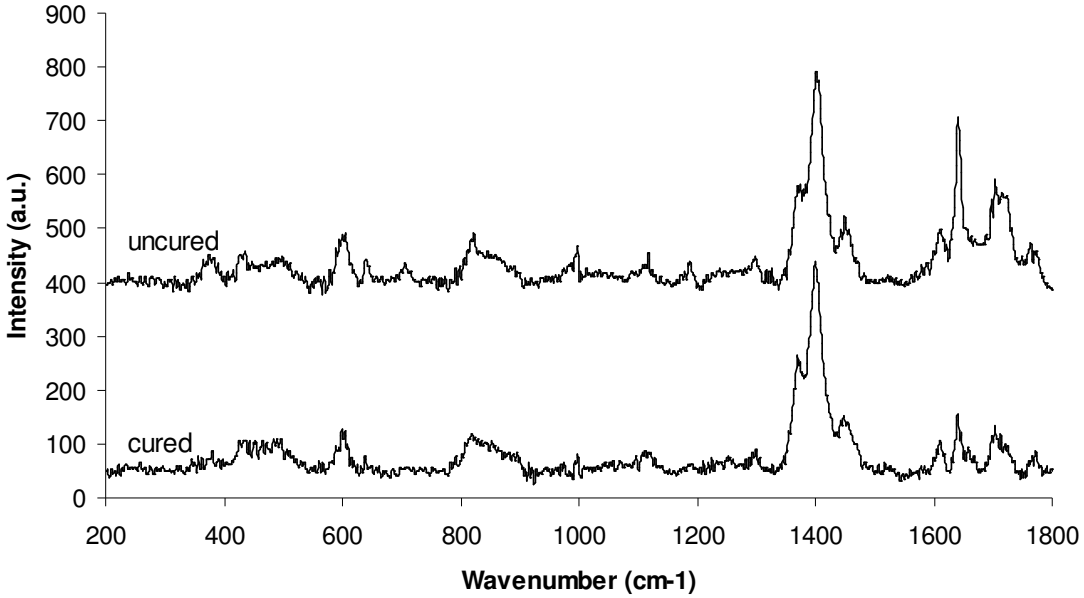

Spectra 35. Admira.

PUBLISHED PAPERS

Reprinted from:

Miletic V, Santini A. Remaining Unreacted Methacrylate Groups in Resin-Based Composite With Respect to Sample Preparation and Storing Conditions Using Micro-Raman Spectroscopy. J Biomed Mater Res Part B: Appl Biomater 2008:87B;468-474. ©2008 Journal of Biomedical Materials Research, with permission from John Wiley & Sons Inc.

Santini A, Miletic V. Quantitative micro-Raman assessment of dentine demineralization, adhesive penetration, and degree of conversion of three dentine bonding systems. Eur J Oral Sci 2008:116;177-183. ©2008 European Journal of Oral Sciences, with permission from John Wiley & Sons Inc.

Santini A, Miletic V. Comparison of the hybrid layer formed by Silorane adhesive, one-step self-etch and etch and rinse systems using confocal micro-Raman spectroscopy and SEM. J Dent 2008:36;683-691. ©2008 Journal of Dentistry, with permission from Elsevier.

Miletic V, Santini A, Trkulja I. Quantification of monomer elution and carbon–carbon double bonds in dental adhesive systems using HPLC and micro-Raman spectroscopy. J Dent 2009:37;177-184. ©2009 Journal of Dentistry, with permission from Elsevier.

Permissions include parts of Chapters 7, 9, 10 and 12.

Remaining Unreacted Methacrylate Groups in Resin-Based Composite With Respect to Sample Preparation and Storing Conditions Using Micro-Raman Spectroscopy

Vesna J. Miletic, Ario Santini

Postgraduate Dental Institute, University of Edinburgh, Edinburgh EH3 9HA, United Kingdom

Received 19 November 2007; revised 8 February 2008; accepted 27 March 2008
Published online 27 May 2008 in Wiley InterScience (www.interscience.wiley.com). DOI: 10.1002/jbm.b.31128

Abstract: The aim of this study was to measure degree of conversion (DC) of resin-based composites (RBCs) using micro-Raman spectroscopy followed by different sample preparation procedures and storing conditions. Ninety samples of Tetric EvoCeram (Ivoclar Vivadent, Schaan, Liechtenstein) were prepared in standardized molds and cured with a high powered LED light-curing unit, bluephase® (Ivoclar Vivadent, Schaan, Liechtenstein) for 20 s. Samples were allocated to eight groups. DC of groups 1 and 2 was recorded without or after polishing. DC in groups 3 and 4 was recorded from vertically sectioned samples *versus* "split" samples. DC in groups 5–8 was recorded after storing samples at room temperature and humidity, in 90 ± 2% humidity at 37 ± 1°C, distilled water at 37 ± 1°C or buffered incubation medium (BIM) at 37 ± 1°C for 24 h. Mean values of DC in polished and unpolished samples were 63.6% (±3.2%) and 54.7% (±5.2%), respectively ($p < 0.0001$). There was no significant difference in DC after sample-sectioning ($p > 0.05$). Significantly higher DC values were obtained after storing samples in BIM (76.8% ± 2.1%) than in distilled water (59.7% ± 5.7%), extreme humidity (60.3% ± 3.9%) or in room conditions (63.6% ± 3.2%) ($p < 0.001$). DC of an RBC measured by micro-Raman spectroscopy may be affected by differences in sample preparation and storing conditions, making it difficult to extrapolate data from *in vitro* studies into clinically relevant information. © 2008 Wiley Periodicals, Inc. J Biomed Mater Res Part B: Appl Biomater 87B: 468–474, 2008

Keywords: micro-Raman spectroscopy; degree of conversion; resin-based composites; adhesive restorations; dental materials

INTRODUCTION

The composition of resin-based composites (RBCs), their degree of conversion (DC) and reaction kinetics are important parameters determining the loss of mechanical function[1] and leaching of components from the RBCs in the clinical situation.[2–4]

In particular, the DC of RBCs affects their structure in terms of mechanical properties as well as chemical stability. As shown in previous studies, DC is never 100%,[1,5–7] and when less than optimal, the mechanical properties, such as wear,[1] fracture toughness, flexural modulus, hardness,[8] and flexural fatigue,[9] are compromised. The leaching of monomers from restorations, and their diffusion through intervening dentine, may have a detrimental effect on the dental pulp.[10] Unreacted monomers have been detected in saliva during the first 24 h after polymerization.[11] Moreover, the chemical instability of underpolymerized RBCs leads to accelerated biodegradation due to hydrolysis and plasticization resulting in the increase of available monomers and oligomers.[12]

Micro-Raman spectroscopy has been used in dentistry to identify the mineral component of intact teeth,[13–16] teeth after various treatment modalities,[17,18] to determine the polymerization rate of various materials,[6,7,19-22] and to investigate tooth tissue/material interfaces.[23–26] DC has been measured by various methods.[6,7,22,27–32] Micro-Raman spectroscopy is a nondestructive technique without the need for physical alteration of samples prior to analysis, and therefore, it is a useful tool for studying the DC. However, the literature search reveals that different preparation procedures have been used in studies determining DC of RBCs, thus, making the results difficult to compare (Table I).

The aim of this study was to measure and compare the DC values of an RBC as affected by different sample preparation procedures and storing conditions. The null hypothesis was that there would be no significant difference regarding sample preparation and storage conditions on DC.

Correspondence to: V. Miletic (e-mail: vesna.miletic@gmail.com)

TABLE I. Differences in Preparation Procedures Used in Previous Studies

Procedure	Variable	Reference
Polishing	Polished	32
	Not polished	6,7,19
Storage time	1 h	7,19
	24 h	19,21
	48 h	23
	Immediate use	6
	Unknown time	32
Humidity	90%	23
	Unknown humidity	6,7,19,23,32
Temperature	Room temperature	7
	37°C	21–23
	Unknown temperature	6
Medium	Distilled water	21
	Delbecco's solution	23
	Air	19
	unknown	32

MATERIALS AND METHODS

Table II shows the details on the RBC used in this study.

Preparation of Acrylic Molds and RBC Samples

A precision metal rod 5 mm in diameter was placed vertically in a rubber mold $3 \times 3 \times 6$ cm^3 and freshly mixed acrylic was poured round this and cured for 24 h at 55°C and 3 bar pressure. After curing, the metal rod was removed, leaving an acrylic block with a 5 mm diameter internal cylinder. Eight such acrylic blocks were made. From these acrylic blocks, using an Isomet saw (Buehler, Lake Bluff, IL), 20 standardized acrylic molds 1 mm thick and 70 molds 2 mm thick were sectioned and polished until they were exactly 1 mm or 2 mm thick. The dimensions of acrylic molds were verified using electronic digital calipers with an accuracy of ±0.02 mm per 100 mm reading at 0–40°C and at 20–80% relative humidity (Jade Products, Rugby, UK).

From these molds, samples of RBC were prepared in the following manner. The acrylic mold was placed on a glass-mixing slab, and filled with the RBC. To standardize the amount of material in the mold, a constant load was applied when filling by first placing a Mylar strip (DuPont, Stevenage, Herts, UK) on top of the material followed by a metal sheet. A 5 kg weight was used to compress the material into the mold. The RBC was subsequently photopolymerized by a bluephase® light-curing unit (LCU) (Ivoclar Vivadent, Schaan, Liechtenstein) for 20 s at 1100 mW/cm^2. To achieve a constant distance between the tip of the LCU and the surface of the RBC during curing, a custom-made jig was fabricated. Two discs, 10 mm in diameter, were cut from 1 mm thick plastic sheets. Into the first, a hole was cut, just smaller than the tip of the LCU and into the second, a hole just larger than the tip of the LCU. The two discs were glued together creating a well with an internal rim. The tip of the LCU rested on this internal rim and was maintained at 1 mm from the RBC surface during curing. The light intensity was verified using the integrated radiometer immediately prior to and after curing. The loading of the molds and curing of the RBC was done at room temperature and humidity, which were constantly monitored throughout this procedure using a temperature and humidity data logger (USB-500 Series Data Logger, Measurement Computing Corp, Norton, USA) and were always within the range of 22 ± 2°C and humidity 45 ± 3%. Immediately after curing, the Mylar strip was discarded and samples were randomly allocated to various groups for appropriate treatment.

After the preparation appropriate to each subgroup, samples were stored in light-proof containers at 22 ± 2°C for 24 h before micro-Raman spectra were obtained using a LABRAM 300 (HORIBA Jobin Yvon, Stanmore, Middlesex, UK) with red argon-ion laser at 632.817 nm. Spatial resolution was 1.5 μm and spectral resolution was ~2.5 cm^{-1}.

Prior to each session, the micro-Raman spectrometer was calibrated internally for zero and then, using a silicon sample, calibrated for coefficient values. Acquisition time for each spectrum was 20 s with ten accumulations. The laser beam was focused through a ×100 objective lens (Olympus UK, London, UK). Labspec 4.18 (HORIBA Jobin Yvon, Stanmore, Middlesex, UK) is dedicated software for data acquisition and analysis, and has been specially designed by Horiba Jobin Yvon, the manufacturer of LabRam system. Using this software, "band fitting" can be accomplished, which allows accurate calculation of peaks and band positions, the elimination of extraneous peaks, and the subsequent calculation of peak amplitude, band width, and integrated areas.

Effect of Polishing. Twenty samples of RBC, 5 mm by 2 mm, were randomly allocated to two subgroups.

Group I was polished according to the following protocol: 240-grit, 600-grit, and 1000-grit silicone carbide discs in wet conditions, for 30 s each and finished with a soft cloth with SiO_2 solution (Buehler, Lake Bluff, IL) for 30 s.

Group II was not polished.

TABLE II. Constituents of TetricEvoCeram (Ivoclar Vivadent AG, Schaan, Liechtenstein)

Composition	% (v/v)
Dimethacrylates (including BisGMA)	16.8
Barium glass, ytterbium trifluoride, mixed oxide	48.5
Prepolymers (copolymer)	34
Additives	0.4
Stabilizers, catalysts	0.3
Pigments	<0.1

Type of RBC: Isofilled, nanofilled.
Filler size: 0.4–0.7 μm, nanofillers < 100 nm.

TABLE III. The Composition of the Buffered Incubation Medium (per mL)

Calcium chloride	0.15 mg
Magnesium chloride	15 mg
Sodium chloride	0.05 mg
Potassium chloride	1.2 mg
Dibasic sodium phosphate	0.28 mg
Sorbitol	30 mg

Three spectral measurements were obtained for both top and bottom surfaces of each sample. The repeated acquisition of spectra was conducted to analyze the consistency of spectral features, that is, spectral overlap, particularly in the "finger print" region and to calculate a mean DC value, using Labspec 4.18. At the same time, spectra from uncured material were taken under the same instrumentation parameters.

Effect of Sectioning. Group 1 (Vertical sectioning): Ten samples of RBC, 5 mm by 2 mm, were used. Each sample was sectioned vertically on the Isomet saw through its greatest diameter.

Group 2 ("Split" sample technique): The "split" sample was constructed from two 1 mm molds. One mold was placed on top of a Mylar strip on a glass mixing slab and filled with RBC. A second Mylar strip was placed on top of this and a second mold added, sandwiching the Mylar strip between the two molds. The second mold was filled with RBC and the RBC in both molds was simultaneously cured as previously described.

In Group 1 ("sectioned" samples), spectra were taken at three points within each sample, on top and bottom surfaces and in the middle of the section. In Group 2 ("split" samples), spectra were taken on top and bottom surfaces of both parts of the "split" sample. At the same time, spectra from uncured material were taken under the same instrumentation parameters.

Values from corresponding regions in both "sectioned" and "split" samples were statistically analyzed, top with top, bottom with bottom, and middle sectioned with bottom of the upper "split" sample.

Effect of Different Storing Conditions. Forty samples of RBC, 5 mm by 2 mm, were used. All samples were polished immediately after curing according to the following protocol: 240-grit, 600-grit, and 1000-grit silicone carbide discs in wet conditions, for 30 s each, and finished with soft cloth with SiO_2 solution for 30 s.

Group A was stored at room temperature (22 ± 2°C) and (45 ± 3%) humidity (±3%) for 24 h.

Group B was stored at body temperature (37 ± 1°C) and (90 ± 2%) humidity for 24 h.

Group C was stored in distilled water at body temperature (37 ± 1°C) for 24 h.

Group D was stored in a buffered incubation medium (BIM) (Saliveze®, LOT:20266-02, EXP: 2009.08, Wyvern Medical, Ledbury, UK) at body temperature (37 ± 1°C) for 24 h. The pH of BIM was monitored before storage of RBC samples. The composition of BIM is given in Table III.

With all parameters set as previously described, spectra were obtained from top and bottom surfaces of each sample, after they had been air-dried with a mild stream of air from a dental syringe, and from uncured material.

Calculation of Degree of Conversion

The DC was calculated according to the formula:

$$DC = [1 - R_{cured}/R_{uncured}] \times 100$$

R is the ratio of peak heights at 1640 and 1610 cm^{-1} in cured and uncured material.

Aliphatic C=C bonds in cured and uncured samples corresponded to the 1640 cm^{-1} peak in the micro-Raman spectrum whilst aromatic C=C bonds corresponded to the 1610 cm^{-1} peak. Since aromatic bonds do not undergo any changes during the polymerization process, unlike aliphatic bonds, the 1610 cm^{-1} peak was used as an internal standard for DC calculations. The complete loss of aliphatic C=C bonds was not expected, as it has been shown that the DC of resin-based materials is never 100%.[1,5–7]

Data were analyzed using nonparametric Mann–Whitney test and Kruskal–Wallis test (GraphPad InStat, version 3.00, GraphPad Software, San Diego, CA).

RESULTS

Repeated spectra showed consistency and overlapping of spectral features in the "finger print" region in all groups of cured and uncured samples.

The mean DC of polished RBC samples was 63.6% (±3.2% SD), whereas mean DC of unpolished material was found to be 54.7% (±5.2%). There was a statistically significant difference between DC of polished and unpolished samples ($p < 0.0001$).

Figure 1 shows mean and SD values for the DC of sectioned *versus* "split" samples of RBC. Mean DC of sectioned samples were on top 64.5% (±4.2%), in the middle

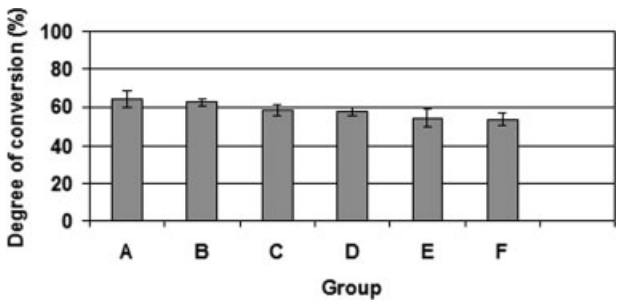

Figure 1. Mean and SD of the degree of conversion of sectioned vs. 'split' samples of Tetric EvoCeram. Legend: A-section top; B-split top; C-section middle; D-split middle; E-section bottom; F-split bottom.

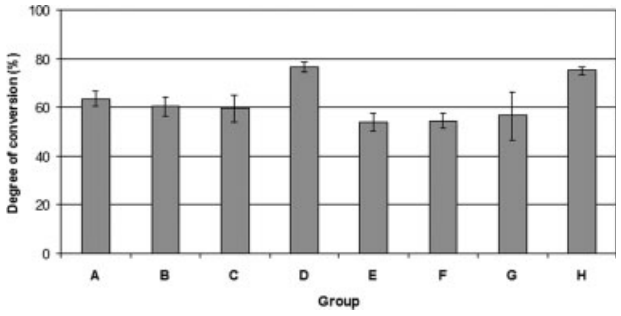

Figure 2. Mean and SD of DC of RBC samples stored in different storing conditions. Top: (A) 22°C, 45% RH; (B) 37°C, 90% RH; (C) 37°C, distilled H_2O; (D) 37°C, BIM. Bottom: (E) 22°C, 45% RH; (F) 37°C, 90% RH; (G) 37°C, distilled H_2O; (H) 37°C, BIM.

58.5% (±2.8%), and at the bottom 54.2 (±4.4%). Mean DC of "split" samples were on top 62.7% (±1.7%), in the middle 57.8% (±2.3%), and at the bottom 53.8% (±3.3%). There was no statistically significant difference between top ($p = 0.3095$), middle ($p = 0.6991$), and bottom ($p = 0.8182$) surfaces of sectioned and "split" samples.

Figure 2 presents mean and SD values of the DC of samples kept in different storing conditions:

Group A: Room temperature (22 ± 2°C) and humidity (45% ± 3%) for 24 h.

Group B: Body temperature (37 ± 1°C) and humidity (90% ± 2%) for 24 h.

Group C: Distilled water at body temperature (37 ± 1°C) for 24 h.

Group D: BIM at body temperature (37 ± 1°C) for 24 h.

The greatest mean value for the DC was found in the Group D in BIM at 37°C (76.8% ± 2.1%), and it was significantly higher than mean values for Group A (63.6% ± 3.2%, $p < 0.05$), Group B (60.3% ± 3.9%, $p < 0.001$), and Group C (59.7% ± 5.7%, $p < 0.001$).

Bottom surface DC values in Group D (75.2% ± 1.7%) were also found to be significantly higher than those in Group A (54.1% ± 3.7%), Group B (54.5% ± 3.2%), and Group C (56.6% ± 9.7%) ($p < 0.001$).

Figure 3 shows spectra of uncured and cured RBC. Note the difference in 1640 cm^{-1} peak height in the cured sample due to monomer conversion. Figure 4 shows band fitted area for a cured sample.

DISCUSSION

In this study, micro-Raman spectroscopy was used to determine the DC of an RBC after different preparation conditions. Labspec 4.18 software was used to analyze data in terms of band fitting of characteristic peaks. The values for peak heights were used for calculations, because these two peaks were distinctive, relatively sharp, and had no interference from any other peaks (Figure 3). According to Shin et al. (1993), there is no *a priori* reason to expect the vibrational modes for resin-based systems to have a particular peak shape.[29] Therefore, band fitting was run to optimize the Lorentzian and Gaussian combination that would allow the best fit between the calculated curve and the real data.

Variation in methodology when preparing samples in terms of polishing may influence results and make data comparison difficult if not impossible. It has been suggested that a resin-rich layer forms on top of the RBC after polymerization due to textural features of the material, such as filler loading, size, and distribution.[33,34] In various RBCs, there is a tendency for filler particles to compress together, thus exuding resin towards the surface layer. Other authors have reported that this resin-rich layer may account for increased microleakage[35] or reduced biaxial flexure strength and microhardness[36] of RBCs.

In the present study, the DC of polished and unpolished samples of a contemporary RBC was measured by micro-Raman spectroscopy and was significantly affected by the presence of the resin-rich layer. In this study, the removal of the resin-rich layer exposed much better cured RBC material and resulted in significantly higher DC values.

Consideration was also given to whether or not sectioning of RBC samples on the Isomet influenced DC values. It was considered that sectioning procedures may alter physical properties especially deep within the RBC samples, and so, data was acquired from the middle of the sectioned samples and compared with data from the corresponding "middle" section of the "split" samples.

There is evidence that post-polymerization heating of RBCs results in weight loss of individual monomer components with a positive correlation between the loss of volatile monomer and the temperature and duration of heat.[37] According to the present study, sectioning, when performed under cooling, does not appear to be a source of material overheating, which significantly alters the DC values during sample preparation. Although theoretically, water coolant may cause the washout of soluble unreacted monomers, the present results showed no difference in DC in samples stored in water and air (45% humidity), suggesting that there was no washing out of unreacted monomers under these conditions. Therefore, it was assumed that there was,

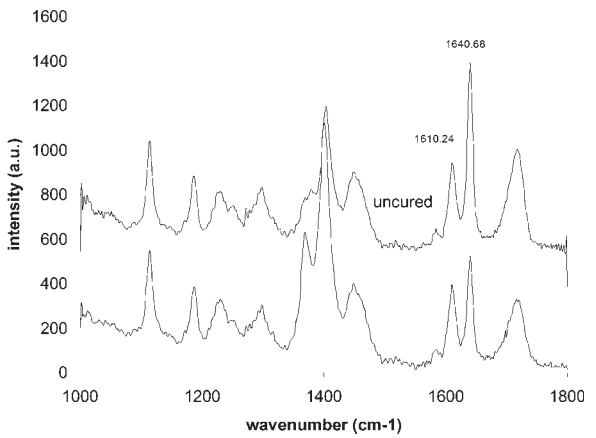

Figure 3. Micro-Raman spectra of uncured and cured Tetric EvoCeram. The characteristic peaks are distinctive, relatively sharp, and do not interfere with adjacent peaks.

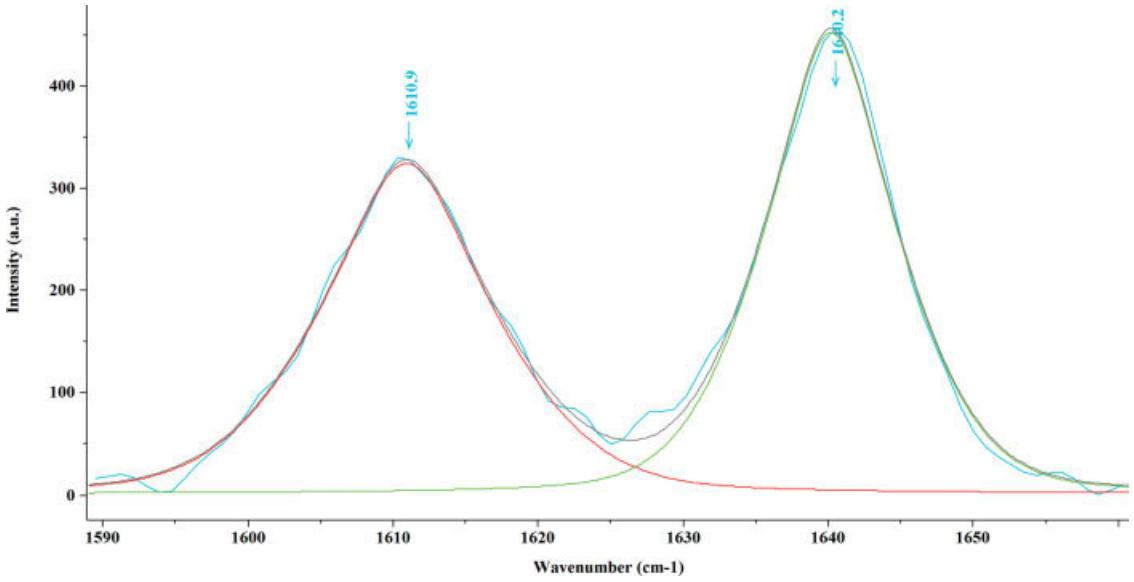

Figure 4. Band fitting of 1610 and 1640 cm^{-1} peaks of a cured sample. Area between ~1590 and 1660 cm^{-1} zoomed and extracted. Light blue curve represents raw data, while red and green curves represent fitted peaks at their exact positions. [Color figure can be viewed in the online issue, which is available at www.interscience.wiley.com.]

also, no washing out of unreacted monomers during the 10 s of sectioning with water coolant.

Most studies try to simulate conditions of the oral cavity as close as possible when storing samples for the duration of the study. The most frequently used storage temperature was 37 ± 1°C,[21–23] followed by room temperature.[7] In contrast to temperature, the range of humidity varied enormously and sometimes was not quoted.[6,7,19,23,32] Storage media was usually distilled water[21] or buffered solutions.[23]

Therefore, four different storing conditions were used in the present study. BIM similar to the one used in the present study are often referred to and marketed as "artificial saliva." Results suggested that storing material samples in BIM at 37 ± 1°C had a substantial effect on the measured DC. The DC values for both top and bottom surfaces of these samples reached 76.8 and 75.2%, respectively, being significantly higher than in samples stored in distilled water at 37 ± 1°C, 90 ± 2% humidity at 37 ± 1°C or 45 ± 3% humidity at 22 ± 2°C.

Tetric EvoCeram (TEC) is the most recent marketed material of the Tetric "family," combining the proven technology of previously developed materials and, therefore, reflects the properties of a wide range of available RBCs.

The "DC" of an RBC is the extent to which monomers change into polymers. Basically, high molecular weight dimethacrylates form a highly crosslinked polymer network through the process of free radical polymerization through the C=C double bonds in methacrylate groups. The conversion of aliphatic C=C double bonds are affected by light energy absorbed by photoinitiators, which triggers this free radical propagation, but also affecting the DC are known parameters such as resin chemistry,[38] temperature,[39] pressure,[40] and other factors. Nevertheless, there is always a certain amount of unreacted monomers in the system, which is influenced by elution into aqueous solutions or organic solvents.[41,42] Therefore, the storage medium may result in a difference between the actual and measured ratio between aliphatic C=C double bonds and the used internal standard. Because spectroscopic methods are used to determine this ratio, the term "DC" may not be fully suitable, although generally used in the literature.

The acrylic molds being a methylmethacrylate (MMA)-based material contains methacrylate groups, which, theoretically, could leach out and interact with subsequently fabricated RBC samples. The total time necessary to place the uncured RBC material, to cure it, and to remove it from the mold took less than 90 s. High performance liquid chromatography (HPLC) has been previously used to assess MMA leakage into distilled water and BIM (artificial saliva), and none could be detected after immersion for 90 s (unpublished data). It was, therefore, felt appropriate to use these molds for the experiment.

Because of UK Health and Safety policies, it is no longer possible to use human saliva for *in vitro* studies, as this could be a source of cross infection. Various BIM are often used as storage media to replicate clinical conditions as closely as possible, but there is no standard formula, and formulae are seldom given. Ongoing studies are investigating whether different formulae have the same effect as in the present study.

The DC values significantly increased when samples were stored in BIM than distilled water, and these results corroborate the findings of a previous study, which reported higher DC values in RBCs placed *in vivo* than those placed *in vitro* and stored in distilled water.[5] Authors suggested that temperature might be the cause for such a difference.

In the present study, however, micro-Raman analysis was performed after storing samples at different temperatures, and as there were no significant differences in DC, it was concluded that temperature variations during the period of storage is not the critical factor influencing the DC of RBCs. Therefore, when looking at effects of buffered incubation media, DC was calculated only for body temperature, which would be more clinically relevant.

Bisphenol-A has been detected in vivo, in human saliva after filling teeth with composite resin, suggesting that unpolymerized monomers diffuse into saliva to a certain extent.[11] Tetric EvoCeram, used in the present study, contains Bis-GMA, which is synthesized from Bisphenol-A.

Probable diffusion of monomers into BIM during the first 24 h after polymerization may result in less unreacted aliphatic C=C double bonds and, subsequently, higher values of the DC of RBC.

A possible mechanism may be hypothesized as causing the leaching out of monomers into BIM used in the current study and less into the distilled water. The monomer contains the —COOH carboxylic acid group that will dissociate to some extent as the anion $—CO^{2-}$ and H_3O^+. The solubility of this carboxylic acid will increase with increasing ionic strength, and it would be expected that the monomer to be more soluble in BIM than in deionized water, it would be leached out to a greater extent. This may not occur to the same extent with other artificial saliva formulae and indicates the need to state the composition of all storage materials in such studies.

CONCLUSION

It can be concluded that the DC of an RBC measured by micro-Raman spectroscopic analysis may be affected by differences in sample preparation and storing conditions. Water-cooled sectioning has little effect on the DC of RBCs. Significantly higher values of the DC of RBC were observed after storing samples in BIM at 37 ± 1°C for 24 h compared to distilled water or 90 ± 2% humidity at 37 ± 1°C.

REFERENCES

1. Ferracane JL, Mitchem JC, Condon JR, Todd R. Wear and marginal breakdown of composites with various degrees of cure. J Dent Res 1997;76:1508–1516.
2. Santerre JP, Shajii L, Leung BW. Relation of dental composite formulations to their degradation and the release of hydrolyzed polymeric-resin-derived products. Crit Rev Oral Biol Med 2001;12:136–151.
3. Finer Y, Santerre JP. The influence of resin chemistry on a dental composite's biodegradation. J Biomed Mater Res A 2004;69:233–246.
4. Finer Y, Santerre JP. Influence of silanated filler content on the biodegradation of bisGMA/TEGDMA dental composite resin. J Biomed Mater Res A 2007;81:75–84.
5. Lundin SA, Koch G. Cure profiles of visible-light-cured Class II composite restorations in vivo and in vitro. Dent Mater 1992;8:7–9.
6. Silva Soares LE, Rocha R, Martin AA, Pinheiro AL, Zampieri M. Monomer conversion of composite dental resins photoactivated by a halogen lamp and a LED: A FT-Raman spectroscopy study. Quim Nova 2005;28:229–232.
7. Soh MS, Yap AUJ, Yu T, Shen ZX. Analysis of the degree of conversion of LED and halogen lights using micro-Raman spectroscopy. Oper Dent 2004;29:571–577.
8. Freiberg RS, Ferracane JL. Evaluation of cure, properties and wear resistance of Artglass dental composite. Am J Dent 1998;11:214–218.
9. Lohbauer U, Rahiotis C, Krämer N, Petschelt A, Eliades G. The effect of different light-curing units on fatigue behavior and degree of conversion of a resin composite. Dent Mater 2005;2:608–615.
10. Cavalcanti BN, Rode SM, Marques MM. Cytotoxicity of substances leached or dissolved from pulp capping materials. Int Endod J 2005;38:505–509.
11. Sasaki N, Okuda K, Kato T, Kakishima H, Okuma H, Abe K, Tachino H, Tuchida K, Kubono K. Salivary bisphenol-A levels detected by ELISA after restoration with composite resin. J Mater Sci Mater Med 2005;16:297–300.
12. De Munck J, Van Landuyt K, Peumans M, Poitevin A, Lambrechts P, Braem M, Van Meerbeek B. A critical review of the durability of adhesion to tooth tissue: Methods and results. J Dent Res 2005;84:118–132.
13. Gilchrist F, Santini A, Harley K, Deery C. The use of micro-Raman spectroscopy to differentiate between sound and eroded primary enamel. Int J Paediatr Dent 2007;17:274–280.
14. Nishino M, Yamashita S, Aoba T, Okazaki M, Moriwaki Y. The laser-Raman spectroscopic studies on human enamel and precipitated carbonate containing apatite. J Dent Res 1981;60: 751–755.
15. Tsuda H, Ruben J, Arends J. Raman spectra of human dentin mineral. Eur J Oral Sci 1996;104:123–131.
16. Wentrup-Byrne E, Armstrong CA, Armstrong RS, Collins BM. Fourier transform Raman microscopic mapping of the molecular components in a human tooth. J Raman Spectrosc 1997;27:151–158.
17. Arvidsson A, Liedberg B, Moller K, Lyven B, Sellen A, Wennerberg A. Chemical and topographical analyses of dentine surfaces after Carisolv treatment. J Dent 2002;30:67–75.
18. Tramini P, Pelissier B, Valacarcel J, Bonnet B, Maury L. A Raman spectroscopic investigation of dentin and enamel structure modified by lactic acid. Caries Res 2000;34:233–240.
19. Yap AUJ, Soh MS, Han VTS, Siow KS. Influence of curing lights and modes on cross-link density of dental composites. Oper Dent 2004;29:410–415.
20. Ye Q, Wang Y, Williams K, Spencer P. Characterization of photopolymerization of dentin adhesives as a function of light source and irradiance. J Biomed Mater Res B Appl Biomater 2006;79:1–7.
21. López-Suevos F, Dickens SH. Degree of cure and fracture properties of experimental acid-resin modified composites under wet and dry conditions. Dent Mater 2007; doi:10.1016/j.dental.2007.09.006.
22. Gauthier MA, Stangel I, Ellis TH, Zhu XX. A new method for quantifying the intensity of the C=C band of dimethacrylate dental monomers in their FTIR and Raman spectra. Biomaterials 2005;26:6440–6448.
23. Spencer P, Wang Y, Bohaty B. Interfacial chemistry of moisture-aged class II composite restorations. J Biomed Mater Res B Appl Biomater 2006;77:234–240.
24. Wang Y, Spencer P. Interfacial chemistry of class II composite restorations: Structure analysis. J Biomed Mater Res 2005;75:580–587.
25. Wieliczka DM, Spencer P, Kruger MB. Raman mapping of the dentin/adhesive interface. Appl Spectrosc 1996;50:1500–1504.

26. Wieliczka DM, Kruger M, Spencer P. Raman imaging of dental adhesive diffusion. Appl Spectrosc 1997;1:1593–1596.
27. Calheiros FC, Braga RR, Kawano Y, Ballester RY. Relationship between contraction stress and degree of conversion in restorative composites. Dent Mater 2004;20:939–946.
28. Ferracane JL, Greener EH. Fourier transform infrared analysis of degree of polymerization in unfilled resins - methods comparison. J Dent Res 1984;63:1093–1095.
29. Shin WS, Li XF, Schwartz B, Wunder SL, Baran GR. Determination of the degree of cure of dental resins using Raman and FT-Raman spectroscopy. Dent Mater 1993;9:317–324.
30. Imazato S, McCabe JF, Tarumi H, Ehara A, Ebisu S. Degree of conversion of composites measured by DTA and FTIR. Dent Mater 2001;17:178–183.
31. Rueggeberg FA, Craig RG. Correlation of parameters used to estimate monomer conversion in a light-cured composite. J Dent Res 1988;67:932–937.
32. Silikas N, Kavvadia K, Eliades G, Watts D. Surface characterization of modern resin composites: A multitechnique approach. Am J Dent 2005;18:95–100.
33. Okazaki M, Douglas WH. Comparison of surface layer properties of composite resins by ESCA. SEM and X-ray diffractometry. Biomaterials 1984;5:284–288.
34. Mair LH. An investigation into the permeability of composite materials using silver nitrate. Dent Mater 1989;5:109–114.
35. Santini A, Mitchell S. Microleakage of composite restorations bonded with three new dentin bonding agents. J Esthet Dent 1998;10:296–304.
36. Gordan VV, Patel SB, Barrett AA, Shen C. Effect of surface finishing and storage media on bi-axial flexure strength and microhardness of resin-based composite. Oper Dent 2003;28:560–567.
37. Bagis YH, Rueggeberg FA. Mass loss in urethane/TEGDMA- and Bis-GMA/TEGDMA-based resin composites during post-cure heating. Dent Mater 1997;13:377–380.
38. Sideridou I, Tserki V, Papanastasiou G. Effect of chemical structure on degree of conversion in light-cured dimethacrylate-based dental resins. Biomaterials 2002;23:1819–1829.
39. Säilynoja ES, Shinya A, Koskinen MK, Salonen JI, Masuda T, Shinya A, Matsuda T, Mihara T, Koide N. Heat curing of UTMA-based hybrid resin: Effects on the degree of conversion and cytotoxicity. Odontology 2004;92:27–35.
40. Xu J, Butler IS, Gibson DF, Stangel I. High-pressure infrared and FT-Raman investigation of a dental composite. Biomaterials 1997;18:1653–1657.
41. Ferracane JL. Elution of leachable components from composites. J Oral Rehabil 1994;21:441–452.
42. Yap AU, Han VT, Soh MS, Siow KS. Elution of leachable components from composites after LED and halogen light irradiation. Oper Dent 2004;29:448–453.

Eur J Oral Sci 2008; 116: 177–183
Printed in Singapore. All rights reserved

European Journal of
Oral Sciences

Quantitative micro-Raman assessment of dentine demineralization, adhesive penetration, and degree of conversion of three dentine bonding systems

Ario Santini, Vesna Miletic

Postgraduate Dental Institute, the University of Edinburgh, Edinburgh, UK

Santini A, Miletic V. Quantitative micro-Raman assessment of dentine demineralization, adhesive penetration, and degree of conversion of three dentine bonding systems. Eur J Oral Sci 2008; 116: 177–183. © 2008 The Authors. Journal compilation © 2008 Eur J Oral Sci

Unreacted monomers in adhesive systems may cause a reduction in material properties, an increase in the long-term instability of the restoration, and pulpal irritation. The degree of dentine demineralization, adhesive penetration, and the degree of conversion (DC) across the dentine–adhesive interface of self-etch adhesives were measured using micro-Raman spectroscopy. Two-step, self-etch AdheSE, one-step self-etch AdheSE One, and etch-and-rinse Excite (control) (Ivoclar Vivadent AG, Schaan, Liechtenstein) were studied. Nine human molars were allocated to three groups and a flat dentine surface was prepared. A smear layer was produced by grinding dentine with 600-grit silicone-carbide discs under water. After application and polymerization of the adhesive, teeth were sectioned to produce four 1–mm-thick slices per tooth for micro-Raman spectroscopy. There were statistically significant differences in the depth of dentine demineralization between all adhesives. The depth and degree of demineralization decreased in the order: Excite > AdheSE > AdheSE One. The mean ± standard deviation (SD) values for DC within the adhesive layer were 85.2 ± 2.9% (Excite), 81.4 ± 4.2% (AdheSE), and 54.3 ± 10.1% (AdheSE One), and within the hybrid layer were 55.2 ± 22.5% (Excite), 65.1 ± 16.9% (AdheSE), and 42.0 ± 16.2% (AdheSE One). All systems showed a discrepancy between dentine demineralization and adhesive penetration. A significant amount of unreacted monomers were associated with all systems but particularly with the etch-and-rinse system.

Dr Ario Santini, Postgraduate Dental Institute, The University of Edinburgh, Lauriston Building, 4th floor, Lauriston Place, Edinburgh EH3 9HA, UK

Telefax: +44–131–5364971
E-mail: ariosantini@hotmail.com

Key words: adhesive systems; degree of conversion; dentine demineralization; hybrid layer; micro-Raman spectroscopy

Accepted for publication January 2008

Dentine bonding, unlike enamel bonding, has always been a clinical challenge and therefore has been extensively studied (1, 2). Numerous studies of surface characterization have employed electron microscopy [scanning electron microscopy (SEM) and transmission electron microscopy (TEM)] to investigate the thickness of the hybrid layer, the appearance, length and continuity of resin tags, the quality of hybridization within the interdiffusion zone, and the extent of resin penetration (3–14). Additionally, the dentine–adhesive interface has been studied by staining techniques (15–17).

NAKABAYASHI *et al*. (3) defined the hybrid layer as 'the structure formed in hard dental tissues by demineralization of the surface and subsurface, followed by infiltration of monomers and subsequent polymerization'. Reports on the thickness of the hybrid layer vary, with values ranging from less than 1 μm to 13 μm in sound dentine (3, 13–15), lower values in sclerotic dentine (12, 18, 19), and higher values in demineralized dentine (20, 21). Among other factors, the nature of adhesive systems and the application technique affect the extent and structure of the hybrid layer. In general, studies have shown that two-step, self-etch adhesives produce clearly defined hybrid layers and tags with more frequent lateral branching than one-step systems. However, fewer resin tags are formed with self-etch adhesives than with etch-and-rinse systems (5, 9, 14, 22–24).

With etch-and-rinse systems, the depth of demineralization is greater than the depth of penetration of adhesive (21, 25). It has been hypothesized that with self-etch adhesives the depth of demineralization should be equal to resin infiltration. Nevertheless, morphological studies have shown that even with self-etch adhesives there is a discrepancy between the demineralization and penetration zones (26, 27).

Molecular spectroscopy, such as Fourier Transform Infrared Spectroscopy (FTIR) and micro-Raman, has been found to be very useful in determining the degree of conversion (DC) of resin-based composites (28–33), of dental resins in different mixtures (34–37), and of adhesive systems (38). It is a non-destructive technique that requires minimal specimen preparation. It also allows

quantification of the degree and extent of dentine demineralization and degree of adhesive polymerization *in situ*. The use of a computer-controlled, motorized stage allows linear and spatial mapping of the highly complex dentine–adhesive interface.

The aim of this study was to quantify dentine demineralization, as well as adhesive penetration and DC of self-etch adhesives, across the dentine–adhesive interface, using micro-Raman spectroscopy, with an etch-and-rinse system as a control.

Material and methods

Nine human third molars, extracted for orthodontic reasons, were cleaned of organic debris and stored in 0.02% thymol. Informed consent was obtained from patients for the use of these teeth for research purposes. Ethical approval was granted by the Ethics Committee, Lothian NHS Board (Edinburgh, UK) to use such teeth in this study.

Each tooth was embedded in cold acrylic up to the amelo–cemental junction. The occlusal one-third was sectioned perpendicular to the long axis of the tooth using a water-cooled, low-speed diamond saw (Isomet saw; Buehler, Lake Bluff, IL, USA). A smear layer was produced by grinding the flat surface with a 600-grit silicon carbide (SiC) disc (Buehler) under water for 30 s.

The materials used in this study are listed in Table 1.

The teeth were randomly allocated to three groups: group I, Excite (control); group II, AdheSE; and group III, AdheSE One. Each material was applied in accordance with the manufacturers' instructions. In group I (control), dentine was etched with 35% phosphoric acid for 15 s, rinsed with water for 10 s, and blot-dried in accordance with the conventional wet-bonding technique. Excite was applied to the dentine surface and gently agitated for 10 s, then immediately dried by a gentle, dry stream of air for 3 s. In group II, AdheSE primer was applied to the dentine surface and brushed thoroughly for 30 s. Excess amounts were dispersed with a strong stream of air until there was no movement of the material. AdheSE bond was then applied to dentine and dispersed with a gentle air flow. In group III, AdheSE One was applied to the dentine surface and continuously brushed for 30 s. Excess amounts were dispersed with a strong stream of air until there was no movement of the material. A Mylar strip was placed on top of the uncured adhesive that was then cured using an Elipar Freelight 2, light-curing unit (LCU) (3M ESPE, St Paul, MN, USA) for 10 s. The intensity of the light was monitored via its integrated radiometer throughout the experiment and was always at maximum intensity (1,000 mW cm^{-2}).

Sections 1 mm thick were prepared using the water-cooled Isomet saw parallel to the long axis of the tooth. Samples for micro-Raman analysis were prepared by sectioning perpendicular to the long axis, 2 mm below the surface of dentine. Four samples were obtained from each tooth.

Micro-Raman spectroscopy

Micro-Raman spectroscopy was performed using LA-BRAM 300 (HORIBA Jobin Yvon, Stanmore, Middlesex, UK). The micro-Raman spectrometer was first calibrated for zero and then for coefficient values using a silicon sample. Samples were analyzed using the following micro-Raman parameters: 20 mW HeNe laser with 632.817 nm wavelength, spatial resolution $\approx$ 1.5 μm, spectral resolution $\approx$ 2.5 cm^{-1}, accumulation time 5 s with six accumulations, and magnification ×100 (Olympus UK, London, UK). Linear spectra were taken at 1-μm intervals along 20-μm lines across the dentine–adhesive interface at random sites within intertubular dentine. Six spectra were taken from each sample, giving 24 spectra from each of three teeth in each group. From these spectra, the mean ± standard deviation (SD) values were calculated for dentine demineralization, depth of adhesive penetration, and the DC of adhesives.

As previously shown (39), the quality of Raman chemical images is directly correlated with the numerical aperture of the objective and this numerical aperture is largest with a ×100 objective. To allow precise optical focusing at ×100 magnification, prior to acquiring spectra, excess water was removed from the samples by gently blow-drying with a stream of air from a dental syringe. Subsequently, spectra were acquired and at all times the samples were kept hydrated by their edges being in direct contact with water-saturated blotting paper. No thermal damage of the specimens was observed during spectral acquisition.

The demarcation line between adhesive and hybrid layers was always distinct at ×100 magnification and spectra were accumulated from a point 4 μm into the adhesive layer above this demarcation line. LABSPEC 4.18 (HORIBA Jobin Yvon) is dedicated software for data acquisition and analysis, and has been specially designed by the manufacturer of the LabRam system. Postprocessing included band fitting of characteristic peaks as a combined Gaussian/Lorentzian function with 1,000 iterations to determine the exact

Table 1

Materials

Material	Type	pH of etching agent	Composition
Excite (lot K12070)	Total etch	0.05 (35% phosphoric acid)	Phosphonic acid acrylate, HEMA, bisGMA, dimethacrylates, silica, ethanol, catalysts, stabilizers
AdheSE (lot H28512)	Two-step self-etch	1.69 (Primer)	Primer: phosphonic acid acrylate, bis-acrylamide, water, initiators, stabilizers Bond: dimethacrylates, bisGMA, HEMA, Si-dioxide, initiators, stabilizers
AdheSE One (lot K15391)	One-step self-etch	1.60	Bis-acrylamide derivatives, water, bis-methacrylamide dihydrogen phosphate, amino acid acrylamide, hydroxyl alkyl methacrylamide, highly dispersed Si-dioxide, catalysts, stabilizers

bisGMA, (2,2-Bis-[4-(2-hydroxy-3-methacryloxy-propyloxy)phenyl]propane); HEMA, 2-hydroxyethylmethacrylate; Si-dioxide, silicone dioxide.

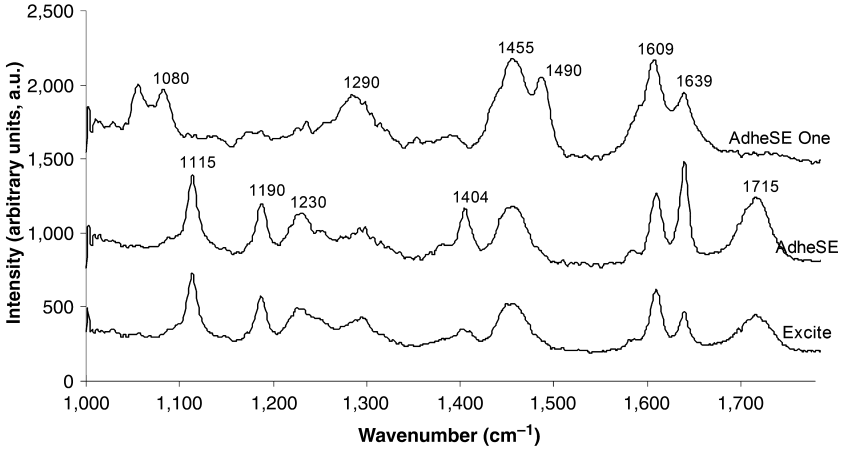

Fig. 1. Raman spectra of adhesives in the region of 1,000–1,800 cm^{-1} (a.u.).

position and peak intensities. Before band fitting, a spectrum of dentine was subtracted to eliminate the overlapping of dentine and resin peaks and to allow calculations to be made for dentine demineralization and adhesive DC. The band-fitting procedure (using the Levenberg–Marquardt method of non-linear peak fitting) provides the best fit (minimized chi-squared) over the entire peak. Low-level noise in the spectrum will not cause major deviation of the fitting routine because, by nature, it is a random effect over the peak.

The degree of dentine demineralization was calculated according to the following formula:

$$\text{Degree of demineralization} = (1 - I\ \text{demineralized}/I\ \text{mineralized}) \times 100, \quad \text{(i)}$$

where I is the intensity of the apatite peak at 960 cm^{-1} in demineralized and mineralized dentine. Each sample was its own control because linear spectra contained data from both demineralized and mineralized dentine. The intensity of the apatite peak varied in each spectrum depending on the dentine demineralization, but with each spectrum it showed a distinctive plateau at different depths within dentine. This plateau was taken as the unaffected mineralized zone, and the mean intensity of the apatite peak was calculated from three different point sources and used as the control value for mineralized dentine.

The degree of conversion of the adhesive was calculated according to the following formula:

$$\text{Degree of conversion} = (1 - R_{\text{cured}}/R_{\text{uncured}}) \times 100, \quad \text{(ii)}$$

where R is the ratio of aliphatic and aromatic peak intensities at 1,639 cm^{-1} and 1,609 cm^{-1} in cured and uncured adhesives, respectively. Calculations of the degree of demineralization and the DC were only performed using the data from linear spectra.

One-way analysis of variance (ANOVA) with Tukey's multiple comparisons method and the Kruskal–Wallis non-parametric test were used to evaluate differences in the degree of demineralization, in the depth of adhesive penetration, and in the DC among the two test groups and the control group at a 95% confidence level. The Kolmogorov–Smirnov test was performed to assess whether data followed a normal distribution, and the test for equality of variances was performed to determine if the assumption of equal variances was valid (MINITAB 15; Minitab, State College, PA,USA).

Results

Figure 1 shows micro-Raman spectra of the three groups and Table 2 lists peak assignments. Aliphatic and aromatic peaks at 1,609 cm^{-1} and 1,639 cm^{-1}, respectively, were seen in the spectra of the bisGMA-based (2,2-Bis-[4-(2-hydroxy-3-methacryloxy-propyloxy)phenyl] propane) materials Excite and AdheSE. The micro-Raman spectrum of AdheSE One confirmed the presence of aromatic bonds in its polymerized monomers. It also contained a 1,490 cm^{-1} peak that is assignable to = N-H bending (40).

Figure 2 shows the degree of dentine demineralization at 1 μm interval steps for each of the three groups. With Excite (control), dentine demineralization in excess of 90% was observed in the first 4–5 μm when dentine was etched with phosphoric acid. This value decreased but remained above 50% in the next 4 μm. Beyond 8 μm, partially demineralized dentine was left uninfiltrated by monomers in several samples. Acidic monomers in

Table 2

Peak assignments characteristic of each material

Wavenumber (cm^{-1})	Assignment	Adhesive
1,115	Phenyl, C-O-C	Excite/AdheSE
1,190	CH_3-C-CH_3	
1,230	CH-OH stretch	
1,290	$=CH_2$ rocking, C-O stretch	Excite/AdheSE/AdhSE One
1,404	CH-OH, CH_2-CO stretch	Excite/AdheSE
1,455	CH_2, CH_3 asymmetric bend	Excite/AdheSE/AdheSE One
1,609	Aromatic, C=C	
1,639	Aliphatic, C=C	
1,720	Carbonyl, C=O	
1,490	Tentative, > N-H	AdheSE One

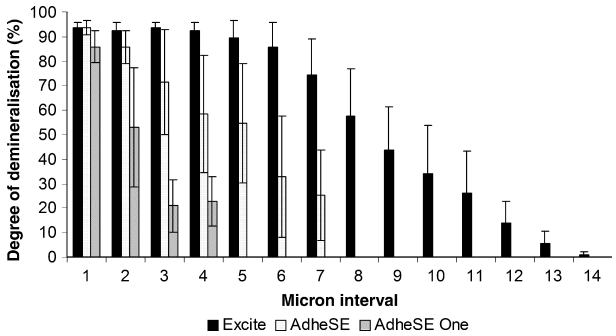

Fig. 2. Degree of dentine demineralization per μm.

AdheSE caused 90% demineralization in only the first 2 μm in dentine. The degree of dentine demineralization in this group dropped to between 55 and 70% over the next 2 μm. The least profound results, both in terms of depth and degree of dentine demineralization, were observed with AdheSE One. In the first 1 μm, more than 80% apatite was removed, and by the 3 μm level, the degree of demineralization was only around 20%.

Table 3 presents values for the mean ± SD of the depth of dentine demineralization and adhesive penetration in each group.

Figure 3 shows the DC of adhesives at 1 μm interval steps for each of the three groups. Within the adhesive layer, the results showed higher DC values with less variation for Excite and AdheSE (80–85%) compared with AdheSE One (50–60%). The DC values for Excite decreased to < 60% as soon as the adhesive came into contact with dentine, dropped to < 50% at the 3 μm level within the hybrid layer, and continued to decrease until, at the deepest point of adhesive penetration, the DC was around 30%. The DC for AdheSE decreased to 60–75% throughout the hybrid layer, whereas the DC for AdheSE One dropped to < 50% in the hybrid layer and was only 30% at the deepest point of adhesive penetration.

Table 4 gives a summary of the data for DC.

Table 3

The depth of dentine demineralization and adhesive penetration in μm

	Dentine demineralization		Adhesive penetration	
Group	Mean	SD	Mean	SD
Excite	12.5	0.8	8.0	3.0
AdheSE	6.0	1.7	5.9	1.9
AdheSE One	3.0	0.8	2.8	1.7

SD, standard deviation.

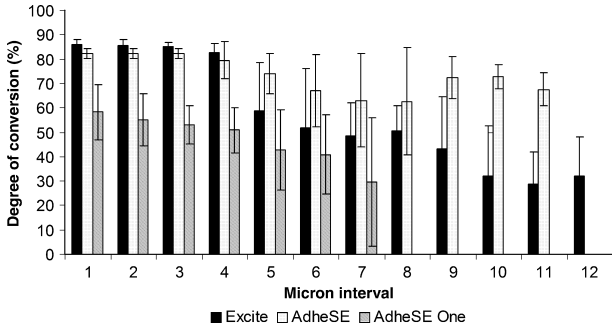

Fig. 3. Degree of conversion (DC) of adhesives per μm. The first 4 μm represent the DC values for the adhesive layer. The hybrid layer starts at 5 μm.

Dentine demineralization

The Kolmogorov–Smirnov test confirmed a normal distribution of the data ($P > 0.15$); however, Bartlett's test for equal variances showed significantly different variances among groups ($P < 0.001$), despite several transformation attempts. Therefore, the data for dentine demineralization were analyzed using the non-parametric Kruskal–Wallis test. There were statistically significant differences in the depth of dentine demineralization between all three groups of adhesives: Excite and AdheSE ($P < 0.001$), AdheSE and AdheSE One ($P < 0.001$), and Excite and AdheSE One ($P < 0.001$).

Degree of conversion within the adhesive layer

The Kolmogorov–Smirnov test showed a non-normal distribution within Excite and AdheSE groups, and, after transformation, Bartlett's test showed significantly different variances among groups ($P < 0.001$). Therefore, the data were analyzed using the non-parametric Kruskal–Wallis test. The differences between all three groups were statistically significant ($P < 0.001$).

Degree of conversion within the hybrid layer

Because the Kolmogorov–Smirnov test confirmed the normal distribution of data in all three groups and Bartlett's test showed no significant differences between variances in all three groups ($P = 0.231$), one-way ANOVA with Tukey's multiple comparisons method was performed to assess the differences in the DC between

Table 4

Degree of conversion (DC) within the adhesive layer and the hybrid layer (%)

	Adhesive layer			Hybrid layer		
	Excite	AdheSE	AdheSE One	Excite	AdheSE	AdheSE One
Mean	85.2	81.4	54.3	55.2	65.1	42.0
SD	2.9	4.2	10.1	22.5	16.9	16.2
Median	85.3	82.2	54.6	59.1	70.2	45.5
Minimum	72.3	54.4	31.4	7.4	25.5	8.3
Maximum	90.0	85.2	79.1	84.1	85.6	67.1
Lower 95% CI	84.3	80.3	52.1	44.7	58.5	36.2
Upper 95% CI	86.1	82.5	56.6	65.8	71.6	47.8

CI, confidence interval; SD, standard deviation.

the three adhesives. There was no significant difference in DC values between Excite and AdheSE ($P > 0.05$), whereas the differences between Excite and AdheSE One and between AdheSE and AdheSE One were significant ($P < 0.001$).

Discussion

Three adhesives were used in the present study. AdheSE and AdheSE One were chosen as two-step and one-step self-etch systems respectively. Excite, an etch-and-rinse adhesive, was used as the control. Manufacturers tend to have an underlying philosophy regarding adhesive chemistry. By using agents from the same manufacturer, certain chemical variations are eliminated, allowing a more controlled evaluation of the progression from etch-and-rinse through two-step to one-step agents and an assessment of any concomitant clinical advantage.

The results of the present study have shown significantly deeper demineralization with etch-and-rinse adhesives than with self-etch adhesives. This agrees with the findings of previous SEM studies (20) and micro-Raman investigations (21, 41).

Deeper demineralization was accompanied by deeper adhesive penetration with Excite compared with AdheSE and AdheSE One. The results of the present study have confirmed that adhesive penetration for etch-and-rinse systems is always less than the extent of dentine demineralization, as reported in previous studies (21, 25, 42). Up to 30% of demineralized dentine was not infiltrated by the monomers in Excite.

On the other hand, the extent of adhesive penetration with self-etch systems was almost identical to the extent of dentine demineralization, and, in most cases, less than 1 μm of demineralized dentine was unfilled with adhesive.

Differences in the degree and depth of dentine demineralization by etch-and-rinse and self-etch adhesives have been related to their different pH values (2, 26, 43). The present results indicate that the self-etch adhesives (AdheSE and AdheSE One) did not completely eliminate the problem of differential demineralization and adhesive infiltration. The degree of demineralization produced by self-etch adhesives in the present study was comparable with the degree of demineralization produced by phosphoric acid only in the first 1–2 μm. Deeper than 2 μm, there was a rapid decrease in their demineralization potential.

Apart from the problem of adhesive penetration, there is also the question of the degree of resin conversion in the resin-infiltrated zone. In previous studies, it was suggested that there was a 'pool' of unreacted monomers remaining after incomplete polymerization of the adhesive system within the hybrid layer (25, 44). However, in these studies, this conclusion was based on indirect evidence (i.e. increased microporosity within the hybrid layer after 1 yr of storage (44) or the relative comparison of peak heights in micro-Raman spectra (25). No details on either the DC values or the depth of adhesive penetration were recorded in these studies. In the present study, we were able to quantify the remaining unpolymerized monomers after determining the exact positions and intensities for aliphatic and aromatic peaks using the band-fitting method in the LABSPEC 4.18 software and by calculating the DC using the previously quoted formula (2). Furthermore, by taking the linear scans across the adhesive–dentine interface, it was possible to calculate those DC values at 1 μm intervals.

There was a significant decrease in the DC of Excite with every 1 μm in the hybrid layer until, at 6–8 μm within the hybrid layer, the lowest value of 30% was recorded. Thus, not only was demineralized dentine left uninfiltrated by the etch-and-rinse adhesive, but a substantial amount of monomers remained unpolymerized. The DC of AdheSE remained above 50% within the hybrid layer, even though this is a substantial decrease compared with its adhesive layer. The hybrid layer is created by the diffusion of adhesive monomers into the water-filled spaces created by the demineralization process and collagen exposure (3). Water, however, interferes with the polymerization process (45) and this could be the reason for the significant drop in DC values in the hybrid layer compared with the adhesive layer observed with all three adhesive systems. The decrease in DC for AdheSE may also be explained by water interference. The difference in DC between AdheSE and Excite could be related to the extent of dentine demineralization and associated interference of the polymerization process by water. Compared with Excite, AdheSE has a weaker demineralization potential, resulting in less exposure of collagen fibrils and associated water voids, and, subsequently, less water interference with the polymerization process may be expected.

With AdheSE One, there was lower DC within the adhesive layer than with Excite and AdheSE and this remained at < 50% throughout the hybrid layer. As with the etch-and-rinse adhesive, large variations in the DC of AdheSE One were noted in the hybrid layer. Despite the better demineralization/penetration ratio for AdheSE One, compared with Excite, a large amount of uncured monomer remained, as shown by lower DC values in the deepest zones.

Compared with Excite and AdheSE, AdheSE One has a substantially altered chemical composition, devoid of HEMA (2-hydroxyethylmethacrylate) and dimethacrylates. Dimethacrylate cross-linking monomers show high reactivity and the formation of a polymer network (46), whereas HEMA is associated with increased dentinal permeability and monomer diffusion (21). However, dimethacrylates and HEMA have been shown to be hydrolytically unstable in aqueous acidic solutions and degrade into diols and methacrylic acid (47, 48). In one-step self-etch adhesive systems, this problem is solved by using monomers with hydrolytically stable bonds between the polymerizable group and the strongly acidic phosphorus groups (47). However, it is unclear how these chemical alterations affect the degree of conversion. Furthermore, in certain initiator systems, an acid–base reaction between acidic monomers, and

amines and peroxides, which impairs the polymerization process, can occur (49). The newly developed photoinitiators containing acylphosphine oxides are not compatible with many newer light emitting diode [LED] LCUs (47). The manufacturer's technical data does not state which photoinitiator(s) are used in AdheSE One, and it may be that the lower DC of AdheSE One than of AdheSE and Excite relates to alterations in acidic monomers and photoinitiators in combination with LED technology.

Micro-Raman spectroscopy has certain advantages over other techniques that have been used to study the morphology of the dentine–adhesive interface. SEM and TEM require specimen preparation, as well as the use of high vacuum states, which may significantly affect the samples (6, 7, 50). In addition, TEM requires the preparation of ultrathin sections, which may not accurately mirror the characteristics of the interdiffusion zone (51).

Micro-Raman spectroscopy detects changes in the chemical composition of the dentine–adhesive complex. It is a non-destructive technique requiring minimal specimen preparation that permits the quantification of changes within the dentine–adhesive complex. Calibration curves have been generated based on the hydrogenation method developed by Rueggeberg *et al*. (52). These curves are required to relate the aliphatic : aromatic peak ratio to the DC and are generated prior to determining the DC of specimens (53). By using the aliphatic : aromatic double-bond peak ratios for uncured materials (conversion levels of 0%) and then assigning a peak ratio value of zero to a conversion level of 100%, a calibration curve can be drawn for any material. Essentially, the calibration curve indicates whether or not the aliphatic : aromatic peak ratios change linearly with the number of unreacted aliphatic groups. A linear relationship has been shown to exist between aliphatic : aromatic peak ratios and the number of unreacted aliphatic groups for bisGMA-TEGDMA (triethyleneglycol dimethacrylate) and bisGMA-HEMA systems (Y. Wang, personal communication) and we therefore assumed that a linear relationship was valid for the three current materials.

All systems showed a discrepancy between dentine demineralization and adhesive penetration. The quantitative evaluation of the DC of the three systems showed that there was a significant amount of unreacted monomers associated with all systems but particularly with the etch-and-rinse systems. Compared with Excite and AdheSE One, AdheSE showed significantly fewer unreacted monomers within the demineralized dentine. Moreover, monomer penetration virtually filled the zone of demineralization with higher monomer conversion, which was not the case with the other two systems.

In a clinical context, unreacted monomers may cause a reduction in material properties and result in the long-term instability of restorations as well as pulpal irritation. Clinically, the two-step, self-etch system, AdheSE, is superior to the other two systems with regard to these three parameters.

References

1. Swift EJ, Perdigao J, Heymann HO. Bonding to enamel and dentin: a brief history and state of the art. *Quintessence Int* 1995; **26**: 95–110.
2. De Munck J, Van Landuyt K, Peumans K, Poitevin A, Lambrechts P, Braem M, Van Meerbeek B. A critical review of the durability of adhesion to tooth tissue: methods and results. *J Dent Res* 2005; **84**: 118–132.
3. Nakabayashi N, Kojima K, Masuhara E. The promotion of adhesion by the infiltration of monomers into tooth substrates. *J Biomed Mater Res* 1982; **16**: 265–273.
4. Van Meerbeek B, Dhem A, Goret-Nicaise M, Braem M, Lambrechts P, Vanherle G. Comparative SEM and TEM examination of the ultrastructure of the resin-dentin interdiffusion zone. *J Dent Res* 1993; **72**: 495–501.
5. Shimada Y, Harnirattisai C, Inokoshi S, Burrow MF, Takatsu T. In vivo adhesive interface between resin and dentin. *Oper Dent* 1995; **20**: 204–210.
6. Carvalho RM, Yoshiyama M, Pashley EL, Pashley DH. In vitro study on the dimensional changes of human dentine after demineralization. *Arch Oral Biol* 1996; **41**: 369–377.
7. Raspanti M, Alessandrini A, Gobbi P, Ruggeri A. Collagen fibril surface: TMAFM, FEG-SEM and freeze-etching observations. *Microsc Res Tech* 1996; **35**: 87–93.
8. Cagidiaco MC, Ferrari M, Vichi A, Davidson CL. Mapping of tubule and intertubule surface areas available for bonding in Class V and Class II preparations. *J Dent* 1997; **25**: 379–389.
9. Ferrari M, Cagidiaco MC, Kugel G, Davidson CL. Dentin infiltration by three adhesive systems in clinical and laboratory conditions. *Am J Dent* 1996; **9**: 240–244.
10. Ferrari M, Mannocci F, Vichi A, Davidson CL. Effect of two etching times on the sealing ability of Clearfil Liner Bond 2 in Class V restorations. *Am J Dent* 1997; **10**: 66–70.
11. Breschi L, Perdigao J, Lopes MM, Gobbi P, Mazzotti G. Morphological study of resin-dentin bonding with TEM and in-lens FESEM. *Am J Dent* 2003; **16**: 267–274.
12. Kwong SM, Tay FR, Yip HK, Kei LH, Pashley DH. An ultrastructural study of the application of dentine adhesives to acid-conditioned sclerotic dentine. *J Dent* 2000; **28**: 515–528.
13. Van Meerbeek B, Conn LJ Jr, Duke ES, Eick JD, Robinson SJ, Guerrero D. Correlative transmission electron microscopy examination of nondemineralized and demineralized resin-dentin interfaces formed by two dentin adhesive systems. *J Dent Res* 1996; **75**: 879–888.
14. Sakoolnamarka R, Burrow MF, Tyas MJ. Interfacial micromorphology of three adhesive systems created in caries-affected dentin. *Am J Dent* 2003; **16**: 202–206.
15. Wang Y, Spencer P. Effect of acid etching time and technique on interfacial characteristics of the adhesive-dentin bond using differential staining. *Eur J Oral Sci* 2004; **112**: 293–299.
16. Wang Y, Spencer P, Hager C, Bohaty B. Comparison of interfacial characteristics of adhesive bonding to superficial versus deep dentine using SEM and staining techniques. *J Dent* 2006; **34**: 26–34.
17. Spencer P, Wang Y, Katz JL. Identification of collagen encapsulation at the dentin/adhesive interface. *J Adhes Dent* 2004; **6**: 91–95.
18. Tay FR, Pashley DH. Resin bonding to cervical sclerotic dentin: a review. *J Dent* 2004; **32**: 173–196.
19. Van Meerbeek B, Braem M, Lambrechts P, Vanherle G. Morphological characterization of the interface between resin and sclerotic dentine. *J Dent* 1994; **22**: 141–146.
20. Abu-Hanna A, Gordan VV, Mjor I. The effect of variation in etching times on dentin bonding. *Gen Dent* 2004; **52**: 28–33.
21. Wang Y, Spencer P, Walker MP. Chemical profile of adhesive/caries-affected dentin interfaces using Raman microspectroscopy. *J Biomed Mater Res A* 2007; **81**: 279–286.
22. Radovic I, Vulicevic ZR, Garcia-Godoy F. Morphological evaluation of 2- and 1-step self-etching system interfaces with dentin. *Oper Dent* 2006; **31**: 710–718.
23. Sensi LG, Marson FC, Belli R, Baratieri LN, Monteiro S. Interfacial morphology of self-etching adhesive systems in dentin. *Quintessence Int* 2007; **38**: E112–E119.

24. Abdalla AI, Garcia-Godoy F. Morphological characterization of single bottle adhesives and vital dentin interface. *Am J Dent* 2002; **15**: 31–34.
25. Hashimoto M, Ohno H, Kaga M, Sano H, Endo K, Oguchi H. The extent to which resin can infiltrate dentin by acetone-based adhesives. *J Dent Res* 2002; **81**: 74–78.
26. Wang Y, Spencer P. Physiochemical interactions at the interfaces between self-etch adhesive systems and dentine. *J Dent* 2004; **32**: 567–579.
27. Tay FR, Pashley DH, Yoshiyama M. Two modes of nanoleakage expression in single-step adhesives. *J Dent Res* 2002; **81**: 472–476.
28. Knezevic A, Tarle Z, Meniga A, Sutalo J, Pichler G, Ristic M. Degree of conversion and temperature rise during polymerization of composite resin samples with blue diodes. *J Oral Rehabil* 2001; **28**: 586–591.
29. Knezevic A, Tarle Z, Meniga A, Sutalo J, Pichler G, Ristic M. Photopolymerization of composite resins with plasma light. *J Oral Rehabil* 2002; **29**: 782–786.
30. Silva SL, Rocha R, Martin AA, Pinheiro AL, Zampieri M. Monomer conversion of composite dental resins photoactivated by a halogen lamp and a LED: a FT-Raman spectroscopy study. *Quim Nova* 2005; **28**: 229–232.
31. Soh M, Yap AU, Yu T, Shen ZX. Analysis of the degree of conversion of LED and halogen lights using micro-Raman spectroscopy. *Oper Dent* 2004; **29**: 571–577.
32. Tarle Z, Knezevic A, Demoli N, Meniga A, Sutalo J, Unterbrink G, Ristic M, Pichler G. Comparison of composite curing parameters: effects of light source and curing mode on conversion, temperature rise and polymerization shrinkage. *Oper Dent* 2006; **31**: 219–226.
33. Tarle Z, Meniga A, Knezevic A, Sutalo J, Ristic M, Pichler G. Composite conversion and temperature rise using a conventional, plasma arc, and an experimental blue LED curing unit. *J Oral Rehabil* 2002; **29**: 662–667.
34. Feilzer AJ, Dauvillier BS. Effect of TEGDMA/BisGMA ratio on stress development and viscoelastic properties of experimental two-paste composites. *J Dent Res* 2003; **82**: 824–828.
35. Ferracane J, Greener EH. Fourier transform infrared analysis of degree of polymerization in unfilled resins – methods comparison. *J Dent Res* 1984; **63**: 1093–1095.
36. Shin W, Li X, Schwartz B, Wunder SL, Baran GR. Determination of the degree of cure of dental resins using Raman and FT-Raman spectroscopy. *Dent Mater* 1993; **9**: 317–324.
37. Sideridou I, Tserki V, Papanastasiou G. Effect of chemical structure on degree of conversion in light-cured dimethacrylate-based dental resins. *Biomaterials* 2002; **23**: 1819–1829.
38. Ye Q, Wang Y, Williams K, Spencer P. Characterization of photopolymerization od dentin adhesives as a function of light source and irradiance. *J Biomed Mater Res Part B: Appl Biomater* 2006; **79**: 1–7.
39. Lee E, Adar F, Whitley A. The impact of spatial sampling density in Raman imaging. *Spectroscopy* 2006; **21**: 51.
40. Williams D, Fleming I. *Spectroscopic methods in organic chemistry*, 5th edn. Berkshire: McGraw-Hill Publishing, 1995.
41. Carvalho RM, Chersoni S, Frankenberger R, Pashley DH, Prati C, Tay FR. A challenge to the conventional wisdom that simultaneous etching and resin infiltration always occurs in self-etch adhesives. *Biomaterials* 2005; **26**: 1035–1042.
42. Sano H, Shono T, Takatsu T, Hosoda H. Microporous dentin zone beneath resin-impregnated layer. *Oper Dent* 1994; **19**: 59–64.
43. Koshiro K, Sidhu SK, Inoue S, Ikeda T, Sano H. New concept of resin-dentin interfacial adhesion: the nanointeraction zone. *J Biomed Mater Res B Appl Biomater* 2006; **77**: 401–408.
44. Sano H, Yoshikawa T, Pereira PN, Kanemura N, Morigami M, Tagami J, Pashley DH. Long-term durability of dentin bonds made with a self-etching primer, in vivo. *J Dent Res* 1999; **78**: 906–911.
45. Wang Y, Spencer P. Continuing etching of an all-in-one adhesive in wet dentin tubules. *J Dent Res* 2005; **84**: 350–354.
46. Peutzfeldt A. Resin composites in dentistry: the monomer systems. *Eur J Oral Sci* 1997; **105**: 97–116.
47. Moszner N, Salz U, Zimmermann J. Chemical aspects of self-etching enamel-dentin adhesives: a systematic review. *Dent Mater* 2005; **21**: 895–910.
48. Kazantsev O, Shirshin KV, Sivokhin AP, Tel'Nov SV, Zhiganov AE Iv, Mironycheva YL Iv. Hydrolysis of 2-hydroxyethyl methacrylate in concentrated aqueous solutions. *Russ J Appl Chem* 2003; **76**: 1296–1298.
49. Salz U, Zimmermann J, Salzer T. Self-curing, self-etching adhesive cement systems. *J Adhes Dent* 2005; **7**: 7–17.
50. Carvalho RM, Yoshiyama M, Brewer PD, Pashley DH. Dimensional changes of demineralized human dentine during preparation for scanning electron microscopy. *Arch Oral Biol* 1996; **41**: 379–386.
51. Agee KL, Pashley EL, Itthagarun A, Sano H, Tay FR, Pashley DH. Submicron hiati in acid-etched dentin are artifacts of desiccation. *Dent Mater* 2003; **19**: 60–68.
52. Rueggeberg F, Hashinger DT, Fairhurst CW. Calibration of FTIR conversion analysis of contemporary dental resin composites. *Dent Mater* 1990; **6**: 241–249.
53. Emami N, Soderholm KJ. How light irradiance and curing time affect monomer conversion in light-cured resin composites. *Eur J Oral Sci* 2003; **111**: 536–542.

JOURNAL OF DENTISTRY 36 (2008) 683–691

available at www.sciencedirect.com

ScienceDirect

journal homepage: www.intl.elsevierhealth.com/journals/jden

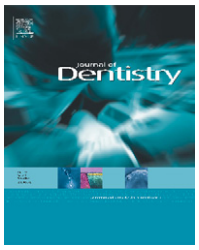

Comparison of the hybrid layer formed by Silorane adhesive, one-step self-etch and etch and rinse systems using confocal micro-Raman spectroscopy and SEM

Ario Santini *, *Vesna Miletic*

The University of Edinburgh, Postgraduate Dental Institute, Lauriston Building (4th floor), Lauriston Place, Edinburgh EH3 9HA, United Kingdom

ARTICLE INFO

Article history:
Received 22 February 2008
Received in revised form
25 April 2008
Accepted 28 April 2008

Keywords:
Confocal micro-Raman spectroscopy
SEM
Hybrid layer
Self-etch adhesives

ABSTRACT

Objectives: To determine the extent of the hybrid layer (HL) of the novel adhesive system (Silorane, 3M ESPE) compared to one-step and etch and rinse adhesive systems, using 2D confocal micro-Raman spectroscopy and SEM.

Methods: Silorane adhesive system was compared to two one-step self-etch (G Bond, GC; AdheSE One, Ivoclar Vivadent) and etch and rinse (Excite, Ivoclar Vivadent) as controls. Adhesives were applied to human dentine, cured and sections prepared perpendicular to the flat adhesive–dentine surface. Two-dimensional micro-Raman mapping was performed over 20 μm × 20 μm areas across the adhesive–dentine interface. SEM micrographs of the same specimens were obtained. One-way ANOVA (Tukey's post-test) was used to analyse the differences in HL thickness among the four adhesive systems and the paired *t*-test to compare the results obtained by micro-Raman and SEM for each adhesive.

Results: Silorane adhesive system formed a HL of comparable thickness to methacrylate-based but thicker than the acrylamide-based one-step self-etch adhesives from SEM analysis. A gradual decrease in adhesive penetration was observed in all systems. A 1-μm zone, between the cured primer and bond was identified by Raman but not visualised on SEM. Compared to SEM, HL calculated from Raman data were always greater.

Conclusions: Micro-Raman spectroscopy gives a more precise indication of dentine demineralisation and monomer infiltration and highlights the intermediate zone of ~1 μm between Silorane primer and bond, not visible with SEM at ×10,000 magnification. Giving as it does, a compilation of many linear scans it allows HL mean values to be calculated.

1. Introduction

The hybrid layer (HL) was originally defined by Nakabayashi as "the structure formed in hard dental tissues by demineralisation of the surface and subsurface, followed by infiltration of monomers and subsequent polymerisation".[1] Since this pioneering work, the morphology of the HL has been studied using scanning electron microscopy (SEM),[2–8] transmission electron microscopy (TEM)[2,9] and staining techniques[10–12] or combinations of these.[13–16] SEM and TEM require extensive chemical processing during sample preparation which can lead to a variety of artefacts.[6,8,17,18] Samples for TEM are normally embedded in epoxy resin and are often decalcified using EDTA. A limitation of these SEM and TEM preparation regimes is that they may alter or even destroy the interfacial zone.[6,19] The various staining techniques used to study the

* *Corresponding author*. Tel.: +44 131 536 4970; fax: +44 131 536 4971.
E-mail address: ariosantini@hotmail.com (A. Santini).
0300-5712/$ – see front matter
doi:10.1016/j.jdent.2008.04.016

morphology of the HL also cause sample alteration due to chemical treatment,[10,20] decalcification[11] and the non-specificity of certain dyes.[12,20]

All of these morphological techniques provide limited and indirect knowledge of the complex HL and offer only partial or no information on the interfacial chemistry. The degree of dentine demineralisation, the true extent and degree of monomer penetration and polymerisation, all of which will contribute to the durability of the bonds created by self-etching and self-priming adhesive systems, require further study.[21]

These aspects have recently been addressed by Raman spectroscopy which is a significant analytical method for studying interfacial chemistry.[22–25] Linear scans across the adhesive–dentine interface have been used to study different adhesive systems,[4,19,24,26] different dentine substrates[14,27] as well as resin-based composite–adhesive–dentine interfacial systems.[28] Acid-etching or priming with acidic monomers creates irregular demineralisation of dentine and linear scanning may not reveal the full extent of this or of adhesive penetration.

It has been hypothesized that with self-etch adhesives, the depth of demineralisation should be equal to resin infiltration.[29] Nevertheless, morphological studies have shown that even with self-etch adhesives there is a discrepancy between the demineralisation and penetration zones.[30,31]

A recently introduced low-shrinkage resin-based composite (RBC), Filtek Silorane (3M ESPE, St. Paul, MN, USA), uses a dedicated two-step self-etch adhesive system, the formulation of which is claimed by the manufacturer to specifically fit the chemistry of the RBC. To date, there have been no published studies detailing hybridization formation following the use of this adhesive system.

Using 2D confocal micro-Raman spectroscopic mapping and SEM, the objective of the present study was to analyse the adhesive–dentine interface of the Silorane adhesive system and compare it to currently available one-step self-etch adhesives as well as an etch and rinse system [controls]. The null hypothesis is that there is no difference in HL thickness between the Silorane adhesive system and controls as quantified using micro-Raman spectroscopy and SEM.

2. Materials and methods

Twelve non-carious, human third molars, extracted for orthodontic reasons were cleaned of organic debris and stored in 0.02% thymol. Informed consent was obtained from patients for the use of these teeth for research purposes. Ethical approval was granted by the Ethics Committee, Lothian NHS Board (Edinburgh, UK) to use such teeth in this study. Each tooth was embedded in cold acrylic up to the amelo-cemental junction. The occlusal one-third was sectioned perpendicular to the long axis of the tooth using a water-cooled, low-speed diamond saw (Isomet saw; Buehler, Lake Bluff, IL, USA). A smear layer was produced by grinding the flat surface with a 600-grit silicon carbide (SiC) disc (Buehler, Lake Bluff, IL, USA) under water for 30 s.

Materials used in the study are presented in Table 1.

The teeth were randomly allocated to four groups: group I, Silorane adhesive system, Group II, G Bond, group III, AdheSE One and group IV, Excite (controls).

Each material was applied in accordance with the manufacturers' instructions.

In group I, Silorane primer was applied for 15 s with an applicator brush, dispersed with a gentle air stream and cured for 10 s. Silorane bond was applied for 15 s with a new applicator and dispersed gently. In group II, G Bond was applied immediately onto the exposed surfaces with an applicator and

Table 1 – Materials used in the study

Material	Manufacturer	Type	Composition
Excite	Ivoclar Vivadent AG, Schaan, Liechtenstein	One-Bottle system (etch and rinse)	Phosphonic acid acrylate, hydroxyethyl methacrylate (HEMA), bisGMA, dimethacrylate, highly dispersed silica, ethanol, catalysts, stabilizers
G Bond	GC Corp., Tokyo, Japan	One-step self-etch (all-in-one)	4-MET (methaxcryloyloxyethyl trimellitate), UDMA, acetone, water, sillanated colloidal silica, initiator
AdheSE One	Ivoclar Vivadent, Schaan, Liechtenstein	One-step self-etch (all-in-one)	bis-Acrylamide, water, bis-methacrylamide dihydrogen phosphate, amino acid acrylamide, hydroxyl alkyl methacrylamide, highly dispersed silicon dioxide, catalysts, stabilizers
Silorane adhesive system	3M ESPE, St. Paul, MN, USA	Two-bottle self-etch	*Primer*: phosphorylated methacrylates, Vitrebond copolymer, bisGMA, HEMA, water, ethanol, silane-treated silica filler, initiators, stabilizers *Bond*: hydrophobic dimethacrylate, phosphorylated methacrylates, TEGDMA, silane-treated silica filler, initiators, stabilizers

left undisturbed for 10 s. Then, it was dried thoroughly for 5 s with a maximum air stream. In group III, AdheSE One was applied and continuously brushed for 30 s. Excess material was dispersed with a strong stream of air until there was no movement of the material. In group IV, dentine was etched with 35% phosphoric acid for 15 s, rinsed with water for 10 s, and blot-dried in accordance with the conventional wet-bonding technique. Excite was applied to the dentine surface and gently agitated for 10 s, then immediately dried by a gentle dry stream of air for 3 s.

In all groups, a Mylar strip was placed on top of the uncured adhesive that was then cured using an Elipar Freelight 2, light-curing unit (LCU) (3M ESPE, St. Paul, MN, USA) for 10 s. Light intensity was monitored via its integrated radiometer.

The bonded specimens were stored in distilled water in a light-proof container at 37 °C for 24 h. Sections 1 mm thick and 2 mm high were prepared by sectioning perpendicular to the flat adhesive–dentine surface. Four samples were obtained from each tooth.

2.1. *Confocal micro-Raman spectroscopy*

Confocal micro-Raman spectroscopy was performed using LABRAM 300 (HORIBA Jobin Yvon, Stanmore, Middlesex, UK). The micro-Raman spectrometer was first calibrated for zero and then for coefficient values using a silicon sample. Samples were analysed using the following micro-Raman parameters: 20 mW HeNe laser with 632.817 nm wavelength, lateral (*XY*) spatial resolution $< 1\ \mu m$, spectral resolution $\sim 2.5\ cm^{-1}$, and magnification $\times 100$ (numerical aperture ~ 0.95, Olympus UK, London, UK).

Two-dimensional mapping was performed over $20\ \mu m \times 20\ \mu m$ areas across the adhesive–dentine interface at $1\ \mu m$ intervals in both *X* and *Y* directions using a computerized *XY* stage. These areas covered the adhesive layer, the HL, partially demineralised and un-affected dentine and were visualised and focused at $\times 100$ magnification. Accumulation time per spectrum was 10 s and 2 spectra were taken per point. Two mappings were performed per sample at random sites. Samples were kept moist throughout the experimental procedure.

Post-processing was performed in LabSpec4.18 (HORIBA Jobin Yvon) and consisted of analysis with modelling which allowed distinguishing spectral components of the adhesive and dentine. The modelling algorithms are based on correlation fitting of known reference spectra with raw data. The reference spectra were previously taken from adhesive samples cured on glass slides and un-affected dentine samples.

2.2. *Scanning electron microscopy*

The same samples used for confocal micro-Raman imaging were afterwards prepared for SEM. Samples were polished (Beta, Buehler, Lake Bluff, IL, USA) using 600-grit and 1000-grit SiC discs under water and finished with polishing cloths with 3 μm diamond particles (TriDent, Buehler, Coventry, UK) in a colloidal silica suspension (MasterMet, Buehler, Coventry, UK). After rinsing under tap water, the samples were etched with 5M HCl for 30 s and rinsed with tap water for 5 min. They were, then, deproteinized in 1% NaOCl solution and rinsed under tap water for 5 min. The samples were critically point dried (Polaron E3000 Series II, Watford, England), mounted on aluminium stubs and gold sputter coated with 15–20 nm of gold in an Emscope SC500 (Ashford, Kent, UK) coating unit. Areas of interest were examined at appropriate magnification using a SEM (Philips XL30CP, Philips, Eindhoven, NL) at $\times 3000$, $\times 6000$, $\times 8000$ and $\times 10{,}000$ magnification.

Statistical analysis was performed using one-way ANOVA with Tukey's multiple comparisons post-test to analyse the differences in HL thickness among the four adhesive systems and the paired *t*-test to compare the results obtained by micro-Raman and SEM for each adhesive at a 95% confidence level (Minitab 15, Minitab Inc., State College, PA, USA). Kolmogorov–Smirnov test was used to determine whether data followed normal distribution and test for equal variances to assess the assumption of equal variances.

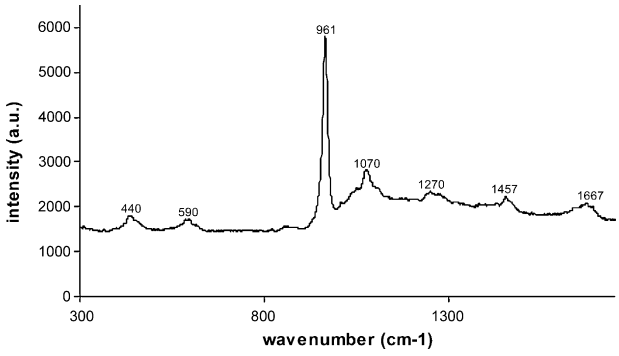

Fig. 1 – Reference spectrum for mineralised dentine with peak assignment. (a.u.–arbitrary units).

3. Results

The reference spectrum for dentine with its peak characterisation of organic and inorganic component is given in Fig. 1. Within the inorganic component, the most intense band occurred at 960 cm^{-1} (ν_1 PO symmetric stretch, associated with the phosphate group) and less intense PO bands at 440 cm^{-1} (ν_2) and 590 cm^{-1} (ν_4). The band at 1070 cm^{-1} corresponds to CO bonds of the inorganic component. Major bands associated

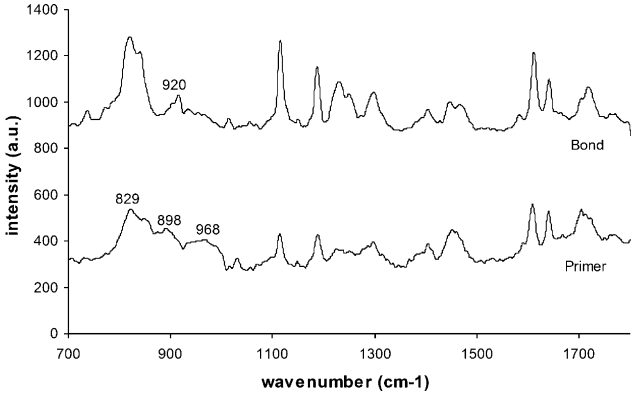

Fig. 2 – Reference spectra for Silorane primer and Silorane bond.

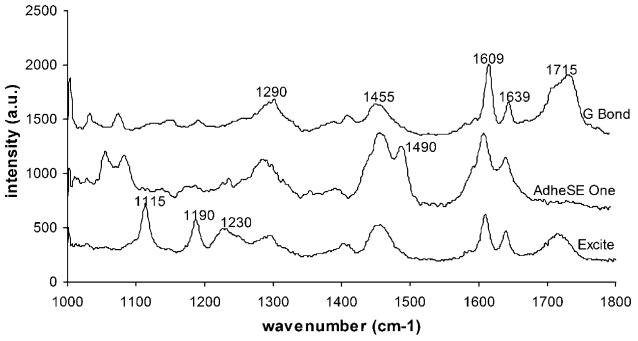

Fig. 3 – Reference spectra for control adhesive systems.

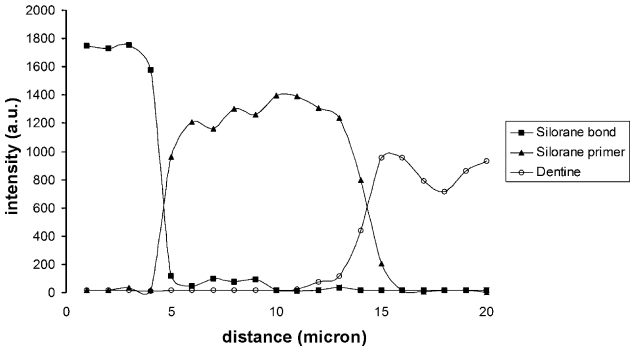

Fig. 4 – The distribution of Silorane primer and bond across the adhesive-dentine interface as a function of distance.

with the organic component occurred at 1245 cm^{-1} (amide III), 1456 cm^{-1} (amide II) and 1667 cm^{-1} (amide I).

Fig. 2 shows reference spectra for Silorane primer and bond. The bands at 1115 cm^{-1} (Phenyl, C–O–C), 1190 cm^{-1} (CH_3–C–CH_3), 1230 cm^{-1} (CH–OH stretch), 1290 cm^{-1} (=CH_2 rocking, C–O stretch), 1404 cm^{-1} (CH–OH, CH_2–CO stretch), 1455 cm^{-1} (CH_2, CH_3 asymmetric), 1609 cm^{-1} (aromatic C=C), 1639 cm^{-1} (aliphatic C=C), previously seen in methacrylate-based adhesives,[26] occurred in spectra of both components of the Silorane adhesive system. The differences in spectral features in the region of 800–1000 cm^{-1} for Silorane primer and bond were used to identify these components in micro-Raman mapping across

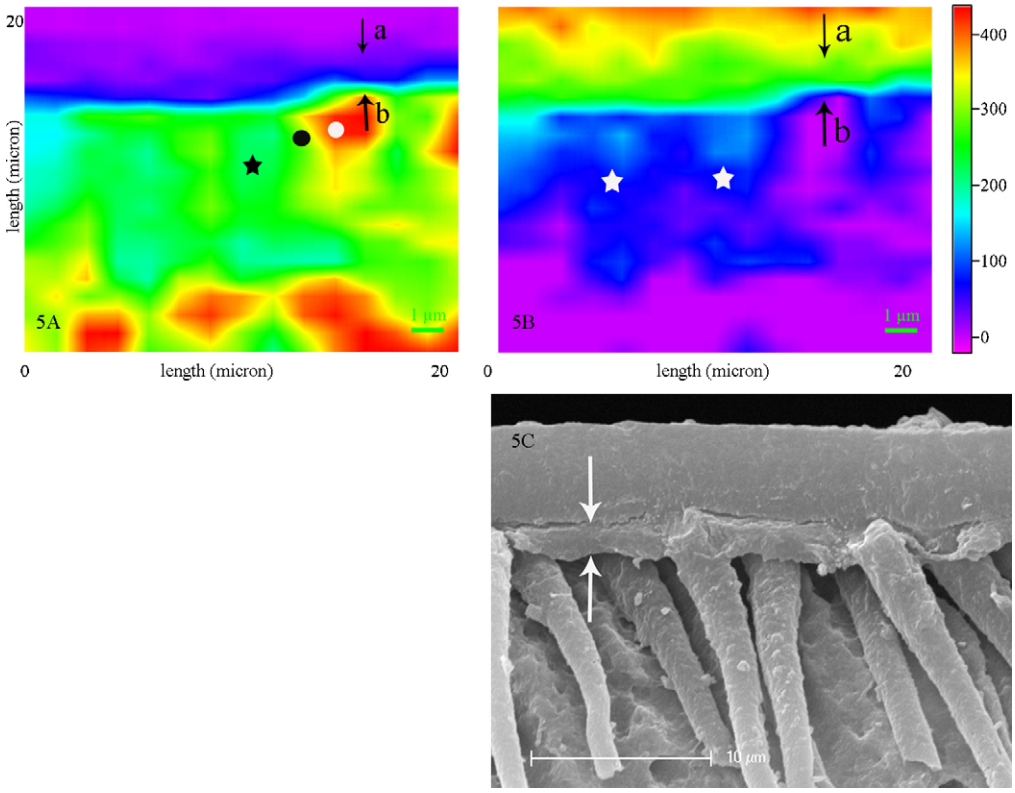

Fig. 5 – 2D micro-Raman map (20 × 20 μm) of the Silorane adhesive-dentine interface. (A) shows the range of intensity of spectral features associated with dentine, ranging from the least intense (demineralised dentine, point a, black arrow) to maximum intensity (unaffected dentine, point b, black arrow). The black star indicates a dentinal tubule, the black circle peritubular dentine and the white circle intertubular dentine. (B) shows the identical specimen area and the range of intensity of spectral features associated with adhesive starting from maximum intensity (point a, black arrow), to the minimum intensity (point b, black arrow). The white star indicates a resin tag. The colour scale shows intensity (arbitrary units). There is an inverse relationship between the spectral intensities of the dentine (left) and adhesive (right) suggesting a gradual increase in the dentine mineral content and decrease in adhesive penetration. Point "a" indicates the beginning of dentine demineralisation and is taken as the top of the HL. Point "b" indicates unaffected dentine and is considered the bottom of the HL. (C) is an SEM micrograph obtained from the same specimens used to collect micro-Raman data. The white arrows depict the HL.

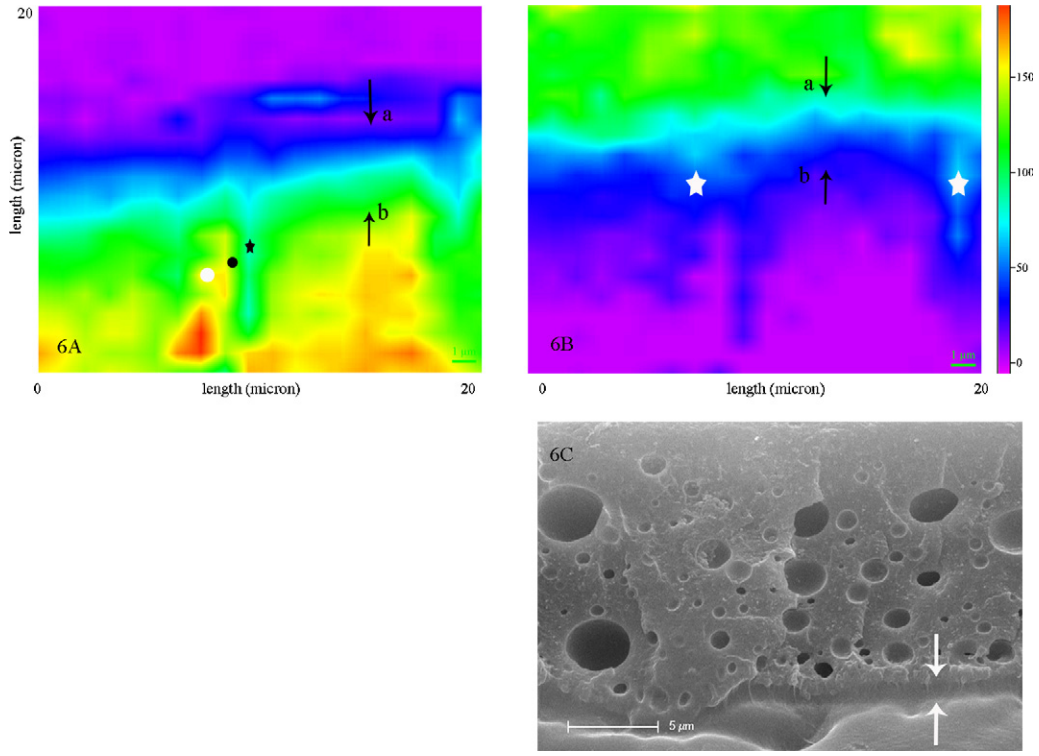

Fig. 6 – 2D micro-Raman map (20 × 20 μm) of the G Bond-dentine interface and the corresponding SEM micrograph. Explanation as in Fig. 5.

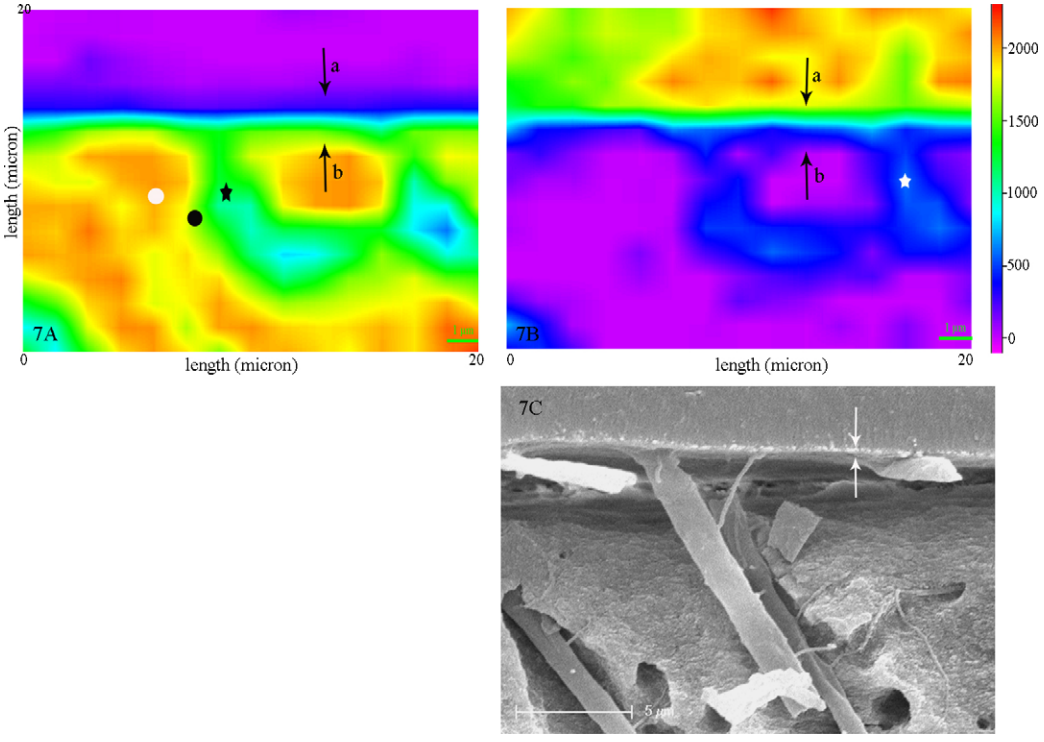

Fig. 7 – 2D micro-Raman map (20 × 20 μm) of the AdheSE One-dentine interface and the corresponding SEM micrograph. Explanation as in Fig. 5.

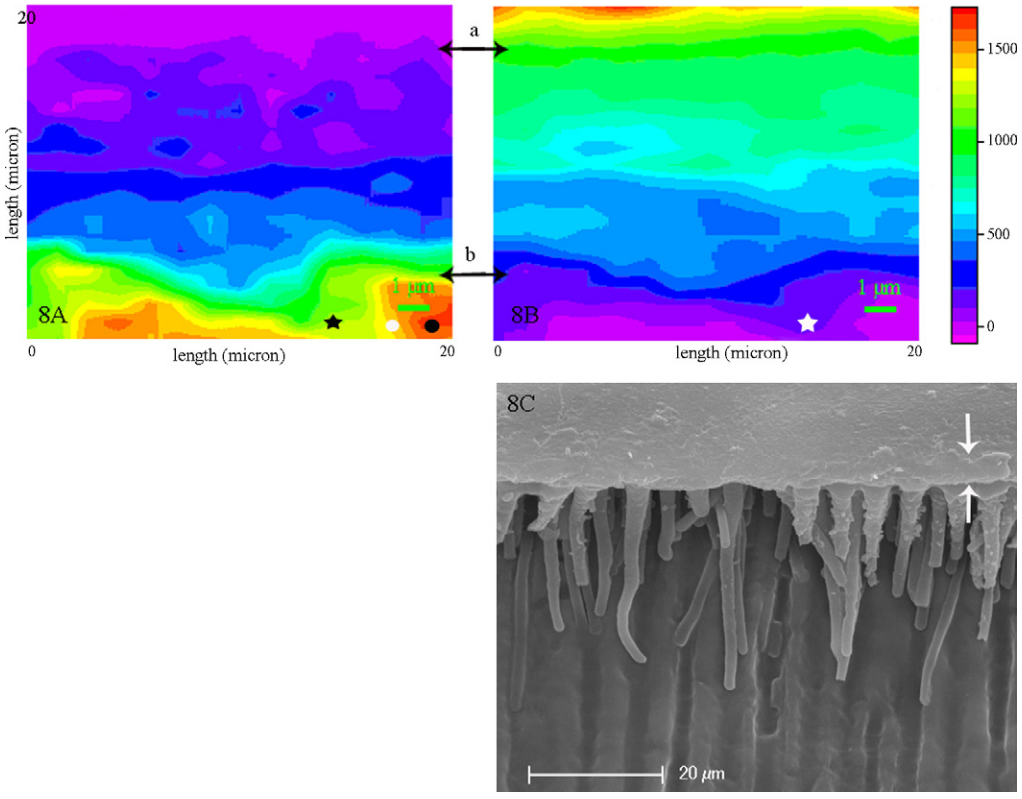

Fig. 8 – 2D micro-Raman map (20 × 20 μm) of the Excite-dentine interface and the corresponding SEM micrograph. Explanation as in Fig. 5.

the entire adhesive layer. The differences in C=O vibrations resulted in a broader 1715 cm^{-1} band in Silorane primer.

Fig. 3 shows spectra for the two self-etch and etch and rinse adhesive systems with their peak assignments. Unlike methacrylate-based adhesives, aliphatic (1639 cm^{-1}) and aromatic (1609 cm^{-1}) bands appeared broader in acrylamide-based adhesive, AdheSE One. Bands at 1115 cm^{-1} (C–O–C, Phenyl), 1190 cm^{-1} (CH_3–C–CH_3) and 1230 cm^{-1} (CH–OH) in Excite were associated with bisGMA. The band at 1715 cm^{-1} (C=O, carbonyl) occurred in methacrylate-based adhesives, but not in acrylamide-based AdheSE One, which contained a 1490 cm^{-1} band which could be assigned to >N–H group. Although, the manufacturer's data regarding the composition of G Bond suggests no methacrylates with aromatic groups, the 1609 cm^{-1} band is associated with the aromatic group in 4-MET. The bands found in all three adhesives were at 1290 cm^{-1} (=CH_2 rocking; C–O– stretch) and 1455 cm^{-1} (CH_2, CH_3 asymmetrical bending).

Fig. 4 shows the distribution of Silorane primer and bond across the adhesive–dentine interface as a function of distance. An intermediate transition zone of ~1 μm can be identified between the primer and bond, between 4 μm and 6 μm.

Representative 2D micro-Raman maps and SEM micrographs of the adhesive–dentine interface taken from the same specimens for the four materials are given in Figs. 5–8. It should be noted that the data used to calculate the HL thickness was generated directly by the software for each μm on the map and not measured arbitrarily. The HL from 2D micro-Raman maps was defined as the overlapping of spectral intensities of bands associated with aromatic and aliphatic groups representing adhesives and the phosphate group representing dentine. The thickness of the HL on SEM micrographs was measured starting from the 'electron dense edge effect' at the base of the adhesive layer to the next 'electron dense edge effect', which is usually considered the limit of the HL.

Table 2 shows the mean and standard deviation (S.D.) values for the HL thickness of examined adhesives obtained from micro-Raman data and measured on SEM micrographs. Micro-Raman data showed that HL thickness for the Silorane adhesive system was significantly lower than Excite ($p < 0.05$) but no difference was found between Silorane, AdheSE One and G Bond ($p > 0.05$). Both micro-Raman and SEM showed

Table 2 – Thickness of the HL of Silorane, the two self-etch and one etch and rinse adhesives

Method	Silorane	G Bond	AdheSE One	Excite
μRaman	3.0 (0.8)^{A,1}	3.6 (1.2)^{B,2}	2.5 (0.9)^{B,3}	7.7 (1.2)^{A,B,4}
SEM	1.9 (0.7)^{D,1}	1.6 (0.5)^{E,2}	0.9 (0.3)^{D,E,3}	5.1 (1.3)^{D,E,4}

Mean (S.D.) μm. For each row, groups with the same superscript letters are significantly different ($p < 0.05$). For each column, groups with the same superscript numerals are significantly different ($p < 0.05$).

that AdheSE One and G Bond produced significantly thinner HL than Excite ($p < 0.05$). On the other hand, SEM analysis revealed significant differences between Silorane and Excite, and also Silorane and AdheSE One ($p < 0.05$, one-way ANOVA with Tukey's post-test). In each adhesive group, HL thickness from micro-Raman was significantly greater than that from SEM analysis ($p < 0.05$, paired *t*-test).

4. Discussion

The HL is a complex structure dependant not only on the demineralisation process but also on the specific characteristics of the applied adhesive system.

The disadvantages of SEM interface preparation methods have recently been reviewed.[32] Strong acids used in preparation dissolve both the mineral within the HL that is not protected by the resin as well as the 'un-affected' dentine. The organic component of the HL is also affected by the organicolytic potential of NaOCl. Any information about the dental structure to which the adhesive was bonded is lost. The low resistance of the HL to argon ion treatment makes it easily distinguished from the adjacent adhesive and dentine,[13] though, listed drawbacks include the formation of surface granules and porosity mimicking in poorly infiltrated demineralised dentine by polishing procedure.[8] Specimen embedding into freshly mixed epoxy resin, for TEM, may cause two-directional movement of unreacted monomer molecules. Epoxy resin contains bisphenol A,[8,13] which will infiltrate any porosity in the specimen, either originally present or created during EDTA decalcification.[18] Acid dyes have been recently used to stain and identify type I collagen in the HL[10] and it remains uncertain whether these acidic dyes and acetic acid used in the staining preparation cause further dentine demineralisation and possible exposure of collagen fibrils. Alcohol, used as a drying medium in staining preparations may facilitate uncured monomer leaching or dissolution of poorly formed polymer networks resulting in artefactual dye spread.[20]

The disadvantages of all three preparation methods limit the ability to observe the true extent of altered dentine substrate hybridization.

On the other hand, micro-Raman spectroscopic specimens can be observed under normal atmospheric conditions without chemical preparation procedures that may alter the interface. Moreover, data can be acquired from moist specimens, as water is a weak Raman scatterer. 2D micro-Raman maps are a compilation of 20 μm $\times$ 20 μm scans from which data is acquired for statistical analysis.

In the present study, confocal micro-Raman spectroscopy was used to gather subsurface chemical information. Data so gathered were analysed using a computerised model function in the dedicated LabSpec software which uses a direct classical least squares (DCLS) algorithm to identify the distribution of components across a mapped area. The calculation is made on each spectrum associated with the individual pixels of the Raman map. The DCLS analysis calculates a linear combination of the pure component spectra acquired separately before the mapping analysis and provides the closest match to the original raw data spectrum. The resulting combination is of the form "$A \times \text{spectrum1} + B \times \text{spectrum2} + \cdots$", where A, B, ... are constants that are proportional to the component concentration. This results in a series of chemical images illustrating the distribution of each component across the mapped region and provides a fast and versatile method for component distribution analysis and chemical composition based on the individual Raman spectra.

The thickness of the HL obtained from micro-Raman data was significantly greater than that measured on SEM micrographs for all adhesives and this may be attributed to the previously discussed limitations of SEM. Moreover, micro-Raman spectroscopy showed a gradual decrease in adhesive penetration as a function of position for all adhesive systems suggesting that no sudden and distinct change occurs between the HL and the un-affected dentine as seen on SEM. The 2D maps showed a very heterogeneous distribution of demineralisation on the horizontal axis as well as heterogeneous penetration of monomer into this affected dentine as tended to be suggested by linear data collection.[4,19,24,26] In evaluating the adhesive–dentine interface, consideration should be given not only to the thickness of the HL but also to adhesive penetration into demineralised dentine and the resultant seal of underlying tooth tissue. The strength of the adhesive–dentine interface (bond strength) must be high enough to withstand functional stress. Total failure can lead to the loss of the restoration, but partial failure may result in sensitivity, pulpal irritation and necrosis. Few clinical consequences follow if partial failure occurs at the RBC–adhesive–interface or at the top of the hybrid layer and the adhesive layer as underlying dentine will remain sealed.[33] Failure between the bottom of the HL and the underlying dentine presents a risk of bacterial invasion, sensitivity and pulpal irritation, and this type of failure is more likely to occur when monomer penetration is less than the depth of demineralisation. The present study was not designed to show modes of failure that are liable to occur in Silorane restorations. Previous work suggested that, with the other adhesives, failure tends to occur at the top of the HL leaving the underlying dentine and pulp sealed.[34,35] Current studies are looking into failure modes, bond strength, and microleakage around Silorane restorations sealed with the Silorane adhesive system.

Because Silorane primer contains the etching monomers and is cured prior to the application of Silorane bond, it should be considered as and compared with one-step systems. For this reason, AdheSE One and G Bond, one-step systems with radically different chemical composition (Table 1), were used as comparative controls along with the etch and rinse system.

The current study showed that the thickness of the HL of Silorane adhesive system, observed by micro-Raman spectroscopy, was significantly thinner than the etch and rinse adhesive and equivalent to one-step self-etch adhesives. Similar results were obtained from SEM analysis on the same specimens, except that Silorane showed significantly thicker HL than AdheSE One. The differences in HL thickness for AdheSE One when analysed using micro-Raman spectroscopy and SEM may be explained by the fact that a significant amount of unreacted monomers remain in the HL and is removed during SEM preparation. A previous study using linear micro-Raman spectroscopy has shown that the degree of conversion of AdheSE One decreases below 50% in the first

micron of the HL with further decline to only 30% by the third micron.[26]

Silorane primer and bond were indistinguishable on SEM micrographs (Fig. 5) whereas micro-Raman showed distinctive spectra for both, indicating the separately cured layers of primer and bond. To ensure bonding with hydrated dentine, Silorane primer contains hydrophilic monomers whereas the bond has hydrophobic bi-functional monomers to match the hydrophobic Silorane resin. Though the bond is placed on the cured primer surface prior to be cured itself, Raman spectra indicate an intervening zone of circa 1 μm of mixed spectral intensities associated with both primer and bond. This may be due to an oxygen inhibition layer remaining at the cured primer surface. Further research on bond strength of the Silorane adhesive system is necessary to assess whether this intervening zone may act as a weak link in the bonding system. These features are not shown on SEM micrographs at ×10,000 and further highlight the discriminatory potential of micro-Raman at the molecular level.

In micro-Raman spectra of the cured primer, the decrease of 1609 cm^{-1} band associated with unreacted aliphatic groups suggested further saturation of these groups during the curing of Silorane bond. It was not possible to differentiate how much of this saturation was contributed by the interaction with Silorane bond aliphatic groups or remaining unreacted aliphatic groups within Silorane primer itself.

The characteristics of acidic monomers determine the ability of self-etch adhesives to etch enamel and dentine. The etching potential of self-etch adhesives is related to their pH value, though other factors including the application procedure, viscosity and solubility of the adhesives and monomer diffusion dynamics will contribute to HL thickness.[10,25] 4-MET which contains polymerizable carboxylic acid with a pH of 2.0 was one of the first developed acidic monomers and is a constituent of G Bond.[36] The lower etching potential of G Bond, compared to the Silorane adhesive system (pH 2.7; manufacturer data), may have been compensated by the longer etching time, as it is left undisturbed for 10 s prior to curing. In accord with previous TEM findings,[2] voids were consistently found throughout the G Bond adhesive layer and may be due to the lack of HEMA and phase separation. G Bond does not contain HEMA, a low viscous monomer that increases dentine wetting and solubility of other adhesive monomers that may account for short and thick resin tags. Furthermore, acetone, a co-solvent in G Bond, may induce phase separation and precipitation of adhesive components due to the changing water:acetone ratio during evaporation.[37]

Acrylamide-based AdheSE One showed thinner HLs with less numerous and slender resin tags compared to the other two self-etch adhesives, as well as the etch and rinse system. It has been stated that (di)methacrylates are hydrolytically unstable in acidic aqueous solutions of one-step self-etch adhesives, which may result in poorer cross-linking, lower bond strengths and compromised bond durability.[37] Therefore, monofunctional and cross-linking monomers have been developed, such as acrylamides, with increased hydrolytical stability.[38] These acrylamides are significantly less viscous than UDMA and bisGMA and are of exceptional high solubility, which may result in the formation of longer and thinner resin tags and a thinner HL.

5. Conclusions

2D confocal micro-Raman spectroscopy has shown to be a valuable analytical tool augmenting SEM imaging. Giving as it does, a compilation of many linear scans, it allows HL mean (S.D.) values to be calculated. Its increased discriminatory powers at a molecular level not only give a more precise indication of dentine demineralisation and monomer infiltration but also highlight the intermediate zone of circa 1 μm between Silorane primer and bond, not visible with SEM at ×10,000 magnification.

Micro-Raman spectroscopy showed that the Silorane adhesive system produced HL of comparable thickness to one-step self-etch adhesives. SEM analysis suggested that Silorane HL was of comparable thickness to methacrylate-based G Bond but significantly thicker than acrylamide-based AdheSE One. Micro-Raman spectroscopy and SEM showed that the etch and rinse adhesive system, Excite, produced thicker HL compared to Silorane, G Bond and AdheSE One.

Acknowledgement

The authors wish to express their gratitude to Dr. Simon FitzGerald (Molecular and Micro Analysis, HORIBA Jobin Yvon Ltd., Stanmore, Middlesex, UK) for his discussions on the principles of Raman spectroscopy.

REFERENCES

1. Nakabayashi N, Kojima K, Masuhara E. The promotion of adhesion by the infiltration of monomers into tooth substrates. *Journal of Biomedical Materials Research* 1982;**16**:265–73.
2. Sidhu SK, Omata Y, Tanaka T, Koshiro K, Spreafico D, Semeraro S, *et al*. Bonding characteristics of newly developed all-in-one adhesives. *Journal of Biomedical Materials Research Part B Applied Biomaterials* 2007;**80**:297–303.
3. Sunico MC, Shinkai K, Medina 3rd VO, Shirono M, Tanaka N, Katoh Y. Effect of surface conditioning and restorative material on the shear bond strength and resin-dentin interface of a new one-bottle nanofilled adhesive. *Dental Materials* 2002;**18**:535–42.
4. Sato M, Miyazaki M. Comparison of depth of dentin etching and resin infiltration with single-step adhesive systems. *Journal of Dentistry* 2005;**33**:475–84.
5. Shimada Y, Harnirattisai C, Inokoshi S, Burrow MF, Takatsu T. In vivo adhesive interface between resin and dentin. *Operative Dentistry* 1995;**20**:204–10.
6. Carvalho RM, Yoshiyama M, Brewer PD, Pashley DH. Dimensional changes of demineralized human dentine during preparation for scanning electron microscopy. *Archives of Oral Biology* 1996;**41**:379–86.
7. Ferrari M, Cagidiaco MC, Kugel G, Davidson CL. Dentin infiltration by three adhesive systems in clinical and laboratory conditions. *American Journal of Dentistry* 1996;**9**:240–4.
8. Yoshiyama M, Carvalho R, Sano H, Horner J, Brewer PD, Pashley DH. Interfacial morphology and strength of bonds made to superficial versus deep dentin. *American Journal of Dentistry* 1995;**8**:297–302.

9. Van Meerbeek B, Conn Jr LJ, Duke ES, Eick JD, Robinson SJ, Guerrero D. Correlative transmission electron microscopy examination of nondemineralized and demineralized resin-dentin interfaces formed by two dentin adhesive systems. *Journal of Dental Research* 1996;**75**:879–88.
10. Wang Y, Spencer P. Effect of acid etching time and technique on interfacial characteristics of the adhesive–dentin bond using differential staining. *European Journal of Oral Sciences* 2004;**112**:293–9.
11. Tay FR, Gwinnett AJ, Wei SH. The overwet phenomenon: an optical, micromorphological study of surface moisture in the acid-conditioned, resin–dentin interface. *American Journal of Dentistry* 1996;**9**:43–8.
12. Sundfeld RH, Valentino TA, de Alexandre RS, Briso AL, Sundefeld ML. Hybrid layer thickness and resin tag length of a self-etching adhesive bonded to sound dentin. *Journal of Dentistry* 2005;**33**:675–81.
13. Van Meerbeek B, Dhem A, Goret-Nicaise M, Braem M, Lambrechts P, VanHerle G. Comparative SEM and TEM examination of the ultrastructure of the resin–dentin interdiffusion zone. *Journal of Dental Research* 1993;**72**:495–501.
14. Wang Y, Spencer P, Hager C, Bohaty B. Comparison of interfacial characteristics of adhesive bonding to superficial versus deep dentine using SEM and staining techniques. *Journal of Dentistry* 2006;**34**:26–34.
15. Breschi L, Perdigao J, Lopes MM, Gobbi P, Mazzotti G. Morphological study of resin–dentin bonding with TEM and in-lens FESEM. *American Journal of Dentistry* 2003;**16**:267–74.
16. Kwong SM, Tay FR, Yip HK, Kei LH, Pashley DH. An ultrastructural study of the application of dentine adhesives to acid-conditioned sclerotic dentine. *Journal of Dentistry* 2000;**28**:515–28.
17. Agee KL, Pashley EL, Itthagarun A, Sano H, Tay FR, Pashley DH. Submicron hiati in acid-etched dentin are artifacts of desiccation. *Dental Materials* 2003;**19**:60–8.
18. Nakabayashi N, Pashley DH. Hybridization of dental hard tissues. Tokyo: Quintessence Publishing Co., Ltd.; 1998 p. 62.
19. Wang Y, Spencer P. Physiochemical interactions at the interfaces between self-etch adhesive systems and dentine. *Journal of Dentistry* 2004;**32**:567–79.
20. D'Alpino PH, Pereira JC, Svizero NR, Rueggeberg FA, Pashley DH. Use of fluorescent compounds in assessing bonded resin-based restorations: a literature review. *Journal of Dentistry* 2006;**34**:623–34.
21. Nakabayashi N, Pashley DH. Hybridization of dental hard tissues. Tokyo: Quintessence Publishing Co., Ltd.; 1998. pp. 106–107.
22. Hashimoto M, Ohno H, Kaga M, Sano H, Endo K, Oguchi H. The extent to which resin can infiltrate dentin by acetone-based adhesives. *Journal of Dental Research* 2002;**81**:74–8.
23. Spencer P, Wang Y, Walker MP, Wieliczka DM, Swafford JR. Interfacial chemistry of the dentin/adhesive bond. *Journal of Dental Research* 2000;**79**:1458–63.
24. Van Meerbeek B, Mohrbacher H, Celis JP, Roos JR, Braem M, Lambrechts P, *et al*. Chemical characterization of the resin–dentin interface by micro-Raman spectroscopy. *Journal of Dental Research* 1993;**72**:1423–8.
25. Wang Y, Spencer P. Quantifying adhesive penetration in adhesive/dentin interface using confocal Raman microspectroscopy. *Journal of Biomedical Materials Research* 2002;**59**:46–55.
26. Santini A, Miletic V. Quantitative micro-Raman assessment of dentine demineralization, adhesive penetration, and degree of conversion of three dentine bonding systems. *European Journal of Oral Sciences* 2008;**116**:177–83.
27. Wang Y, Spencer P, Walker MP. Chemical profile of adhesive/caries-affected dentin interfaces using Raman microspectroscopy. *Journal of Biomedical Materials Research Part A* 2007;**81**:279–86.
28. Wang Y, Spencer P. Interfacial chemistry of class II composite restorations: structure analysis. *Journal of Biomedical Materials Research Part A* 2005;**75**:580–7.
29. Nakabayashi N, Saimi Y. Bonding to intact dentin. *Journal of Dental Research* 1996;**75**:1706–15.
30. Tay FR, Pashley DH, Yoshiyama M. Two modes of nanoleakage expression in single-step adhesives. *Journal of Dental Research* 2002;**81**:472–6.
31. Carvalho RM, Chersoni S, Frankenberger R, Pashley DH, Prati C, Tay FR. A challenge to the conventional wisdom that simultaneous etching and resin infiltration always occurs in self-etch adhesives. *Biomaterials* 2005;**26**:1035–42.
32. Van Meerbeek B, Vargas M, Inoue S, Yoshida Y, Perdigao J, Lambrechts P, *et al*. Microscopy investigations. Techniques, results, limitations. *American Journal of Dentistry* 2000;**13**: 3D–18D.
33. Nakazawa Y. A study of an adhesive composite resin restoration system (Mirage-Bond System) using a NPG primer and PMDM monomer-pulp response and observation of contact area between composite resin and dental wall. *Japanese Journal of Conservative Dentistry* 1992;**35**:18–52.
34. Santini A, Plasschaert AJ, Mitchell S. Microleakage of tetric ceram/excite and Ariston pHc/Ariston liner. *American Journal of Dentistry* 2001;**14**:309–13.
35. Santini A, Plasschaert AJ, Mitchell S. Effect of composite resin placement techniques on the microleakage of two self-etching dentin-bonding agents. *American Journal of Dentistry* 2001;**14**:132–6.
36. Chang JC, Hurst TL, Hart DA, Estey AW. 4-META use in dentistry: a literature review. *Journal of Prosthetic Dentistry* 2002;**87**:216–24.
37. Moszner N, Salz U, Zimmermann J. Chemical aspects of self-etching enamel-dentin adhesives: a systematic review. *Dental Materials* 2005;**21**:895–910.
38. Moszner N, Fischer UK, Angermann J, Rheinberger V. Bis-(acrylamide)s as new cross-linkers for resin-based composite restoratives. *Dental Materials* 2006;**22**:1157–62.

available at www.sciencedirect.com

ScienceDirect

journal homepage: www.intl.elsevierhealth.com/journals/jden

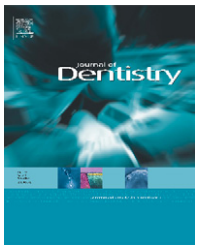

Quantification of monomer elution and carbon–carbon double bonds in dental adhesive systems using HPLC and micro-Raman spectroscopy

Vesna Miletic [a,*], *Ario Santini* [a], *Ivan Trkulja* [b]

[a] *Edinburgh Postgraduate Dental Institute, The University of Edinburgh, Lauriston Building (4th floor), Lauriston Place, Edinburgh EH3 9HA, United Kingdom*

[b] *School of Chemistry, The University of Edinburgh, West Mains Road, Edinburgh EH9 3JJ, United Kingdom*

ARTICLE INFO

Article history:
Received 22 August 2008
Received in revised form
8 November 2008
Accepted 12 November 2008

Keywords:
Adhesive
Monomer
Elution
HPLC
Degree of conversion
Raman
Dimethacrylate
Ormocer
Silorane

ABSTRACT

Objectives: To quantify monomer elution from different adhesive systems using reverse-phase high-performance liquid chromatography (HPLC) and correlate this elution with the ratio of carbon–carbon double bonds from monomer to polymer (RDB) obtained using micro-Raman spectroscopy.

Methods: Thirty dentine discs were cut from 30 human, intact, third molars and randomly allocated to five groups according to the adhesive applied: total-etch, Excite (Ivoclar Vivadent), two-bottle self-etch, Clearfil SE (Kuraray), one-bottle self-etch, Clearfil 3S (Kuraray), ormocer-based, Admira (Voco) and Filtek Silorane adhesive system (FS) (3M ESPE). Monomer elution was studied 1 h, 6 h, 24 h, 96 h and 7 days after immersion in 75% ethanol/water. The RDB was calculated immediately after light-curing and thereafter at 24 h and 7 days. The data were statistically analysed using one-way ANOVA and Pearson's correlation coefficient ($p < 0.05$).

Results: More than 90% of the whole elution occurred during the first 1 h, except for BisGMA in FS, with the highest absolute amount from Clearfil SE and the highest wt% from Admira. Initial RDB was in the ascending order FS < Admira < Excite < Clearfil SE < Clearfil 3S. In all groups, the RDB was significantly higher after 24 h and 7 days than immediately after light-curing ($p < 0.05$). Negative correlation was found only for the elution of HEMA and the RDB of Clearfil 3S.

Conclusions: Different adhesive systems showed different monomer elution kinetics. In all systems, the RDB increased after monomer elution. Overall, no direct correlation exists between the RDB of adhesives and the elution of unreacted monomers.

1. Introduction

Dental adhesives contain resin monomers similar to those found in resin-based composites (RBCs) in order to obtain a covalent bond between the adhesive and the RBC. The cured resin in the adhesive system functions as a backbone providing structural continuity and physical properties, such as strength. Monomer conversion to polymer is an important determinant of the physico-mechanical strength of the resultant polymer.[1]

Conversion is seldom complete and is generally accepted to be low in both adhesives [2,3] and RBCs.[4,5] In the literature, the

* *Corresponding author*. Tel.: +44 7748572850; fax: +44 1315364971.
E-mail address: vesna.miletic@gmail.com (V. Miletic).

0300-5712/$ – see front matter
doi:10.1016/j.jdent.2008.11.006

ratio of double-bond content of monomer to polymer is commonly defined as the degree of conversion (DC) and is conventionally calculated as the ratio of C=C double bonds in cured and uncured materials related to an internal standard. In this paper, we consider that it is more accurate to use the term ''the ratio of double-bond content of monomer to polymer (RDB)''.

Low RDB results in higher permeability[2], more water sorption[6] and more leaching of residual uncured monomers. The biocompatibility of RBCs and adhesives has been studied and it has been shown that, after curing, residual monomers may elute into the oral environment.[7] Dimethacrylates, especially, have been shown to exert cytotoxic[8,9] and endocrine disruptive effects.[10,11]

In a clinical situation, unbound components of adhesives and RBCs may diffuse through dentine into the pulp or elute from the restoration into the oral cavity. Dental adhesives may be the prime issue of concern since they consist of monomers that are more hydrophilic and of lower molecular weight than monomers typically found in RBCs.

Several studies have used high-performance liquid chromatography (HPLC) to study elution of leachable monomers from RBCs[12–16], resin mixtures[17–20] and orthodontic adhesives.[21,22] No published data have been traced on monomer elution from dental adhesives applied to dental tissues and correlated with the RDB before and after elution.

A few studies on dental adhesives used HPLC to investigate the hydrolytic stability of self-etch adhesives[23] and the correlation between retention times and partition coefficient values.[24] Kaga et al. studied the cytotoxic effect of monomers eluted from dental adhesives into the cell culture medium on L929 cells in vitro.[25]

The aim of the present study was to quantify monomer elution from different adhesive systems using reverse-phase HPLC and correlate this elution with the RDB obtained using micro-Raman spectroscopy.

The null hypothesis is: (1) that adhesives with different chemistry do not have different monomer elution kinetics (the amount of eluted monomers per time) or a different RDB and (2) that there is no correlation between these two parameters.

2. Materials and methods

2.1. *Preparation of specimens*

Thirty intact human third molars of similar size, extracted for orthodontic reasons, were cleaned of organic debris and stored in 0.02% thymol. Informed consent was obtained from patients for the use of these teeth for research purposes. Ethical approval was granted by the Ethics Committee, Lothian NHS Board, Edinburgh, Scotland, to use such teeth in this study.

Each tooth was embedded in cold acrylic up to the cemento-enamel junction and sectioned perpendicular to the long axis in the mid-coronal zone using an Isomet saw (Buehler, Lake Bluff, IL, USA) to expose flat dentine. From each tooth, one, 1-mm-thick dentine disc was prepared. A smear layer was produced by grinding the flat surface with a 600-grit silicon-carbide disc (Buehler, Lake Bluff, IL, USA) under water for 30 s.

Adhesive systems used in this study are listed in Table 1. Two of the adhesives (Excite and Admira) require dentine to be conditioned with phosphoric acid prior to application. The other three are self-etch materials.

The dentine discs were randomly allocated to five groups with six discs per group: Group I, Excite; Group II, Admira; Group III, Clearfil SE; Group IV, Filtek Silorane and Group V, Clearfil 3S.

In Groups I and II, dentine was first conditioned by etching with 35% phosphoric acid for 15 s, rinsing with water for 10 s and blot-drying in accordance with the conventional wet bonding technique. Then, prior to applying adhesives, each disc was weighed (m_0) using a METTLER TOLEDO balance (AB104; d = 0.1 mg; Mettler-Toledo Inc, Columbus, OH, USA).

In Group I, Excite was applied to the dentine surface, gently agitated for 10 s and immediately dried by a dry stream of air for 3 s. In Group II, Admira was applied to the dentine surface, left for 30 s and gently air-dried.

In groups III, IV and V pre-conditioning was not required. Dentine discs were removed from storage, blot-dried and immediately weighed (m_0).

In Group III, Clearfil SE Primer was applied to the dentine surface and left in place for 20 s. It was then dried using a mild air-stream. Clearfil SE Bond was then applied to the dentine surface and air-dried with a mild stream. In group IV, Filtek

Table 1 – Adhesive systems used in the present study.

Adhesive	Manufacturer	Type	Composition
Excite	Ivoclar Vivadent AG	1-bottle, total-etch	Phosphonic acid acrylate, HEMA, BisGMA, dimethacrylate, silica, ethanol, catalysts, stabilizers
Admira	Voco GmbH	1-bottle, total-etch	HEMA, HPMA, BisGMA, ormocers, acetone, catalysts, additives
Clearfil SE	Kuraray Europe GmbH	2-bottle, self-etch	Primer: MDP, HEMA, dimethacrylate hydrophilic, camphorquinone, N,N-diethanol p-toluidine, water. Adhesive: MDP, BisGMA, HEMA, dimethacrylate hydrophobic, camphorquinone, N,N-diethanol p-toludine, silica
Filtek Silorane	3M ESPE	2-bottle, self-etch	Primer: phosphorylated methacrylates, Vitrebond copolymer, bisGMA, HEMA, water, ethanol, silane-treated silica filler, initiators, stabilizers. Bond: hydrophobic dimethacrylate, phosphorylated methacrylates, TEGDMA, silane-treated silica filler, initiators, stabilizers
Clearfil 3S	Kuraray Europe GmbH	1-bottle, self-etch	Methacryloyoxydecyl dihydrogen phosphate (MDP), BisGMA, HEMA, initiator, stabilizer, ethanol, water, filler

Ivoclar Vivadent AG, Schaan, Liechtenstein, Kuraray Europe GmbH, Frankfurt/Main, Germany, Voco GmbH, Cuxhaven, Germany, 3M Espe, St. Paul, MN, USA.

Silorane Primer was applied for 15 s followed by gentle air-dispersion and 10 s of light-curing. Filtek Silorane Bond was applied on top of the primer and gently air-dried. In Group V, Clearfil 3S was applied to the dentine surface and left in place for 20 s. The entire surface was then air-dried with a stream of air for 10 s.

In all groups, immediately after application of adhesives to dentine discs, a Mylar strip was placed on top and the adhesive was cured for 10 s using a high-intensity LED light-curing unit (Elipar Freelight2, Ivoclar Vivadent AG, Schaan, Liechtenstein) and 1-mm-thick light guide to maintain the standardised curing distance. The intensity of the light was monitored via its integrated radiometer throughout the experiment and was always at maximum intensity of 1000 mW/cm^2. The Mylar strip was discarded immediately after light-curing and the discs were weighed (m_1). The amount of applied adhesive was calculated as $m = m_1 - m_0$.

For all adhesives, application procedure and light-curing were done in accordance with manufacturers' instructions. The whole procedure was conducted in a small fume cupboard in which the temperature and humidity were monitored throughout and remained constant at 20 ±1 °C and 50 ± 2% (USB-502, Measurement Computing, Corp, Norton, MA, USA). The procedure for each individual disc took less than 2 min. Moisture evaporation under these conditions is considered to be negligible.

2.2. Micro-Raman spectroscopy

Following light-curing, micro-Raman spectroscopy was performed using LABRAM 300 (HORIBA Jobin Yvon Ltd., Stanmore, Middlesex, UK). The micro-Raman spectrometer was first calibrated for zero and then coefficient values using a silicon sample. Samples were analyzed using the following micro-Raman parameters: 20-mW HeNe laser with 632.817 nm wavelength, spatial resolution ~1.5 μm, spectral resolution ~2.5 cm^{-1}, magnification × 100 (Olympus UK Ltd., London, UK). Three point spectra were taken on the top surface of the adhesive systems at random locations with 10 s accumulation time and six acquisitions for each point. Spectra of uncured adhesives were taken as reference. Post-processing of spectra was performed using the dedicated software LabSpec4.18 (HORIBA Jobin Yvon Ltd., Stanmore, Middlesex, UK) and included the band fitting procedure using the Levenberg–Marquardt method of non-linear peak fitting for the best fit.

The ratio of double-bond content of monomer to polymer in the adhesive was calculated according to the following formula:

$$\mathrm{RDB} = \left(1 - \frac{R_{\mathrm{cured}}}{R_{\mathrm{uncured}}}\right) \times 100$$

where R is the ratio of aliphatic and aromatic peak intensities at 1639 cm^{-1} and 1609 cm^{-1} in cured and uncured adhesives.

2.3. High-performance liquid chromatography

Immediately after micro-Raman spectroscopy, each sample was immersed in 1 ml of 75% ethanol/water solution (HPLC Gradient Grade solvents) in a glass vial and stored in a water bath at 37 °C. HPLC measurements were done 1 h, 6 h, 24 h, 96 h and 7 days after immersion. After each interval, the whole solution was taken up for analysis, following which the dentine discs were air-dried with the very mild stream of air and immersed in 1 ml of fresh ethanol/water solution.

Quantitative analysis was performed on an Agilent 1100 Series HPLC system equipped with a G1311A QuatPump, a G1313A Standard Autosampler and a G1315A DAD UV-Vis Detector. The column used was a reverse-phase Phenomenex Prodigy 5 ODS 310CA (150 mm × 4.60 mm, 5 μm particles). The mobile phase was a mixture of water (HPLC Grade, containing 0.1% trifluoroacetic acid) and acetonitrile (HPLC Grade, containing 0.04% trifluoroacetic acid) and a gradient was applied according to the following method (A: H_2O, B: CH_3CN): 90% A : 10% B–40% A: 60% B (0–7 min); 40% A: 60% B–100% B (7–10 min); 100% B (10–17.1 min); 90% A: 10% B (17.1–20 min). The flow rate was 1 mL min−1 and the injector volume was always 20 μL. UV detection was performed at 210 nm (for monitoring the elution of HEMA and TEGDMA) and 275 nm (for monitoring the elution of BisGMA). The compounds were identified by comparison of their elution times with those of the reference compounds under the same HPLC conditions. All measurements were done in triplicate.

2.4. Calibration procedure

Stock solutions of reference standards (1 mg mL^{-1}) were prepared in 75% ethanol/water solution and the solutions were stored at 4 °C. The calibration solutions were prepared from these stock solutions by dilution with 75% ethanol to obtain final concentrations of 1.0, 5.0, 10.0, 15.0, 25.0 and 50.0 ppm (μg/mL). Triple 20 μL injections were made for each standard solution, the peak area for appropriate monomers was determined and plotted versus concentration using linear regression analysis.

2.5. Statistical analysis

The data for eluted monomers and the RDB were tested for normality (Kolmogorov–Smirnov test) and for the equal variances (Bartlett's test). Both datasets showed Gaussian (normal) distribution ($p > 0.15$). However, Bartlett's test showed significant differences between variances and therefore the data were transformed so that both assumptions for the analysis of variance (ANOVA) were met. One-way ANOVA was used to test differences for either monomer elution or the RDB between the adhesives. Pearson's correlation coefficient was used to measure the degree of linear relationship between the amount of eluted monomer and the RDB for each adhesive. The significance level was set at 95% for both one-way ANOVA and Pearson's correlation coefficient.

3. Results

3.1. Calibration

Fig. 1 shows representative chromatograms for the three monomers. The regression equations were for HEMA: conc(X) = (area $Y - 94.2$)/145.2, $R^2 = 0.998$, for TEGDMA: conc(X) = (area $Y - 225.2$)/179.7, $R^2 = 0.9844$ and for BisGMA: conc(X) = (area $Y - 4.9$)/23.2, $R^2 = 0.9995$.

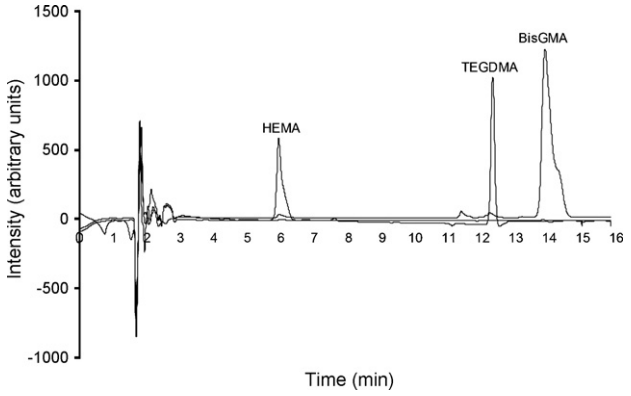

Fig. 1 – Representative chromatograms of HEMA, TEGDMA and BisGMA standard solutions.

3.2. *Monomer elution–HPLC*

Table 2 shows the amount of eluted BisGMA and HEMA from the five tested adhesive systems. More than 90% of the whole elution occurred during the first 1 h after immersion and trace amounts were detected at 24 h. In Clearfil SE and Admira less than 0.5 ppm of BisGMA was detected after 96 h whereas the concentration of BisGMA increased in Filtek Silorane from 6 h to 96 h. There was no elution of BisGMA from any of the adhesives after 7 days. The amount of eluted BisGMA was significantly different for all adhesives ($p < 0.05$), except for Excite and Clearfil 3S ($p > 0.05$).

HEMA showed similar elution kinetics to BisGMA. It eluted completely after 6 h from Clearfil 3S and after 24 h from Excite, Clearfil SE and Filtek Silorane. No HEMA was detected from Admira between 6 h and 96 h; at 96 h and 7 days, 1.1 ppm and 1.6 ppm were detected, respectively. The differences in HEMA elution between adhesives were statistically significant ($p < 0.05$), except for Excite and Admira ($p < 0.05$).

There was a statistically significant difference between the elution of BisGMA and HEMA for each adhesive (paired *t*-test; $p < 0.001$).

The total amount of eluted TEGDMA from Filtek Silorane adhesive system was detected during the first 1 h after immersion in 75% ethanol/water, the mean and standard deviation values being 8.6 ± 3.7 ppm.

Weight% of eluted BisGMA varied from 3.8 wt% (calculated from the total amount of BisGMA in uncured adhesive) for Excite to 23.1 wt% for Admira and that of HEMA from 3.9 wt% (calculated from the total amount of HEMA in uncured adhesive) for Clearfil 3S to 32.5 wt% of Admira (Table 3). There were statistically significant differences between all adhesives with respect to wt% of HEMA ($p < 0.05$). For BisGMA, the differences were statistically significant between all adhesives ($p < 0.05$), except Clearfil SE and Clearfil 3S ($p > 0.05$).

3.3. *RDB–micro-Raman spectroscopy*

Fig. 2 shows micro-Raman spectra of all adhesive systems obtained after light-curing. Similar spectra for uncured materials were used as reference to calculate the RDB.

Fig. 3 shows the RDB values for all adhesive systems immediately after light-curing and after 24 h and 7 days.

The differences were statistically significant for all adhesive systems, except for Excite and Clearfil SE, for the same time intervals ($p < 0.05$). In all groups, the RDB was significantly higher after 24 h and 7 days than the RDB calculated immediately after light-curing ($p < 0.05$). A significant difference between 24 h and 7-day intervals was observed only in the Filtek Silorane group ($p < 0.05$).

3.4. *Correlation analysis*

The linear relationship was determined between the elution of BisGMA and HEMA in Excite (Pearson's correlation coefficient: $\rho = 0.540$), Admira ($\rho = 0.698$) and Filtek Silorane ($\rho = 0.809$) ($p < 0.05$). Since the Pearson coefficient values were in the

Table 2 – Elution of BisGMA and HEMA per mg adhesive.

Time	Monomer	Adhesive system									
		Excite[1,A]		Clearfil SE[1,2,A,B]		Clearfil 3S[2,A,B]		Admira[1,2,B]		Filtek Silorane[1,2,A,B]	
		Mean (ppm)	S.D. (ppm)	Mean	S.D.	Mean	S.D.	Mean	S.D.	Mean	S.D.
1 h	BisGMA	14.2	2.1	29.2	7.9	18.9	4	8.8	2.2	2	0.7
	HEMA	25.7	7.6	49.9	7.1	13.1	2.7	26.7	6.1	2.6	1.9
6 h	BisGMA	2.5	1.4	3.2	1.9	0.5	0.1	0.6	0.2	1.9	0.5
	HEMA	0.9	0.4	1.6	0.6	0.7	0.6	0.8	0.7	0.9	0.7
24 h	BisGMA	0.2	0.3	0.5	0.4	0.1	0.2	0.5	0.3	2.6	1
	HEMA	0.4	0.3	0.3	0	0	0	0	0	0.5	0.1
96 h	BisGMA	0	0	0.2	0.3	0	0	0.3	0.4	4.9	1.5
	HEMA	0	0	0	0	0	0	1.1	0.4	0	0
7 days	BisGMA	0	0	0	0	0	0	0	0	0	0
	HEMA	0	0	0	0	0	0	1.6	0.5	0	0

The same superscript numbers indicate statistical significance in BisGMA elution (one-way ANOVA; $p < 0.05$). The same superscript letters indicate statistical significance in HEMA elution (one-way ANOVA; $p < 0.05$).

Table 3 – Elution of BisGMA and HEMA relative to the amount of either monomer in uncured adhesive (wt%) per mg adhesive (Filtek Silorane not included).

Monomer	Excite	Clearfil SE	Clearfil 3S	Admira
BisGMA				
Mean	3.8	11.9	12.0	23.1
S.D.	0.6	2.9	2.5	5.7
Significance	A,B	A	B	A,B
HEMA				
Mean	8.6	12.7	3.9	32.5
S.D.	2.5	1.8	0.9	7.9
Significance	A	A	A	A

The same letters indicate statistical significance (one-way ANOVA; $p < 0.05$).

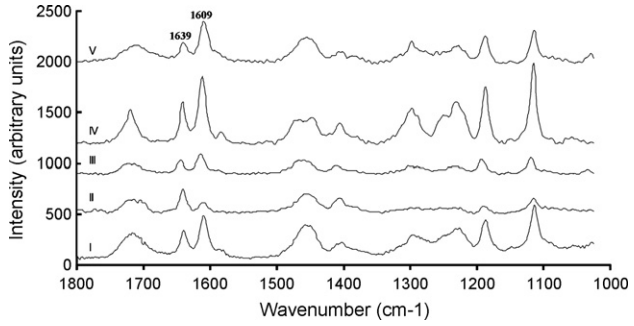

Fig. 2 – Micro-Raman spectra of cured adhesive systems. I-Excite, II-Admira, III-Clearfil SE, IV-Filtek Silorane, V-Clearfil 3S.

range $0 < \rho < 1$, the correlation was positive, i.e. the more BisGMA eluted, the more HEMA eluted from the adhesive system as well. There was no linear relationship between the elution of BisGMA and HEMA in Clearfil SE and Clearfil 3S ($p > 0.05$).

Negative correlation was found between the amount of eluted HEMA and the RDB for Clearfil 3S ($\rho = -0.758$, $p < 0.001$). It was found that Clearfil 3S samples with lower initial RDB values eluted more HEMA than samples with higher RDB.

There was no linear relationship between the amount of eluted monomers and the RDB for any other adhesive system ($p > 0.05$).

4. Discussion

In the present study monomer elution from different adhesive systems was quantified using HPLC and correlated with the RDB determined by micro-Raman spectroscopy. The adhesive systems were chosen based on the classification of total-etch, two-step self-etch and one-step self-etch systems with the addition of two adhesives based on ormocer and silorane chemistry. Another criterion for adhesive selection was that the organic component was based on BisGMA/HEMA. Although Filtek Silorane Bond contains TEGDMA, the Primer is based on BisGMA/HEMA. HEMA and BisGMA were identified by their retention times in HPLC (determined during calibration measurements). This is a standard method used for the determination of monomer elution from RBCs.[15,20] Hydrolytic products of these monomers may well elute but were not the focus of our study. The hydrolytic products of HEMA are methacrylic acid and ethylene glycol[26] which cannot be confused with HEMA as they are eluted at different retention times.

The first part of the null hypothesis was rejected because all of the materials showed different monomer elution kinetics and the RDB. The second part of the null hypothesis was also rejected because one of the materials and one of its monomers showed correlation between elution and the RDB.

In all five adhesives, virtually all HEMA was eluted by 24 h with more than 90% eluted in the first 1 h. BisGMA followed a similar pattern except in the case of Filtek Silorane where it increased up to 96 h and dropped thereafter to undetectable levels at 7 days.

Reporting on the elution of monomers from RBCs, Ferracane and Condon stated that 85–100% were eluted within 24 h.[13] It should be noted that only one material was investigated and though four of the five adhesive systems in the current study had a similar pattern, the elution of BisGMA from Filtek Silorane was very different. More recent studies using the more sensitive methodology of HPLC have shown that monomer elution extends beyond 24 h for RBCs and resin mixtures[18,19] as well as fissure sealants.[27] The current study substantiates this for dental adhesives though only trace amounts are identifiable after 24 h in most cases.

A previous study has reported that monomer elution from cured adhesives is about 1.5–2.5% of adhesive total weight.[25] In the present study, the amount of eluents relative to the total weight of adhesives was not considered appropriate for

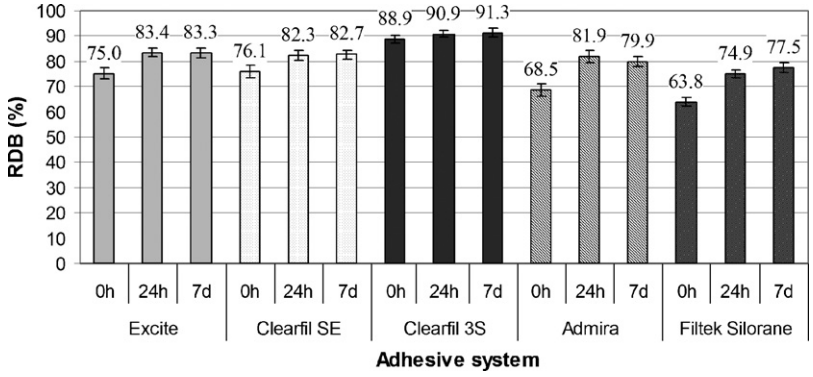

Fig. 3 – The ratio of carbon-carbon double bonds (RDB) in the adhesive systems.

material comparison due to significant qualitative and quantitative differences in monomer content in various adhesive systems. Therefore, the amount of eluted monomers relative to the total amount of monomers in uncured adhesives was calculated. Weight% for HEMA and BisGMA was calculated for Excite, Clearfil SE, Clearfil 3S and Admira but could not be calculated for Filtek Silorane because spontaneous polymerisation occurred during HPLC preparation.

Large variations were observed for both BisGMA and HEMA between the adhesives (Table 3). The highest wt% of eluted BisGMA and HEMA was associated with Admira, 23.1 wt% and 32.5 wt%, respectively. The manufacturer's data states that Admira contains monomers attached to a SiO_2 backbone as well as a pool of free monomers. The manufacturer was requested to supply ormocers contained in the adhesive system to be used as reference. As this was denied, it was impossible to determine the amount of monomers attached to the ormocer molecules and, therefore, only the free monomers were quantified. It is unclear whether the high amount of eluted monomers from Admira, found in the present study, originated solely from the pool of free monomers or from degraded unpolymerised ormocers as well.

The wt% of eluted HEMA from Excite was more than twice the value of eluted HEMA from Clearfil 3S. It has been shown that the smear layer and smear plugs retain in self-etch adhesives[28] which represent the diffusion barrier.[29] Hashimoto et al. showed that the outward fluid movement through both the smear layer and the cured adhesives was lower in self-etch than total-etch adhesives.[30] This phenomenon could account for lower HEMA elution in the one-bottle self-etch system, Clearfil 3S, than the total-etch system, Excite, in the present study.

The increased wt% of eluted HEMA from the two-bottle self-etch adhesive, Clearfil SE may be partly explained by the fact that HEMA is also contained in the bond liquid and contributes to a pool of free HEMA in the cured adhesive layer.

According to the manufacturer's data on Filtek Silorane adhesive system, the main monomers in the primer are BisGMA and HEMA and the main named constituent of the bond is TEGDMA. A previous study using two-dimensional micro-Raman spectroscopic mapping of the adhesive-dentine interface has shown the presence of two separate layers (primer and bond) in the Filtek Silorane adhesive system.[31] Elution of both HEMA and BisGMA from the primer through the overlying bond indicated the permeable nature of the bond which was not sufficient to prevent elution of HEMA and BisGMA. In a previous study, an inverse correlation was found between the ''degree of conversion'' and the permeability of dental adhesives.[2] Differences in the elution kinetics for BisGMA and HEMA occurred probably due to the larger size and greater rigidity of the bulky aromatic moieties which contribute to the lower mobility of BisGMA compared to HEMA.

TEGDMA was completely eluted from Filtek Silorane after 1 h and was not detected in the remainder of the 7-day period. TEGDMA showed faster elution than BisGMA in the other adhesives. This may be due to the differences in hydrophilicity and stereochemistry of the two dimethacrylates, the flexibility as well as the lack of bulky aromatic moieties of TEGDMA which may favour its faster release even through the highly cross-linked three-dimensional networks.

Absolute values of monomer elution are important for evaluating adverse biological effects of monomers on vital cells. Depending on the study design, these values indicate the range of monomer concentrations that the cells may be exposed to in clinical conditions. The present study design was chosen to favour maximum polymerisation of adhesives when applied to dentine as well as maximum elution of unreacted monomers into an organic solvent. When saliva and distilled water are used as solvents rather than ethanol/water, there is significantly lower elution of monomers from RBCs.[13,17,20] Moreover, the use of pure methanol as solvent enabled detection of a broad range of monomers in dental adhesives and the reliable retention prediction even of hydrophilic monomers, such as HEMA.[24] The most commonly used organic solvent for studying monomer elution from resin-based dental materials is ethanol/water solution.[12,13,19,21,27] Ethanol/water has been recommended by the US Food and Drug Administration for the use as a saliva substitute. It favours solvent penetration into the polymer matrix and enlargement of spaces between polymer chains,[19] resulting in greater elution of unreacted monomers which would otherwise remain trapped within the polymer network. Even with organic solvents, certain amounts of unreacted monomers remain because the elution process is affected not only by the solvent but also by polymer morphology and monomer distribution. It has been shown that the unreacted monomers are more likely to remain within microgels than micropores of the polymer network.[32]

Although distilled water or artificial saliva may simulate more clinically relevant conditions, it is well known that neither fully resembles the composition of human saliva. Furthermore, variations in natural salivary composition and flow rate may result in variations of monomer elution. It may, therefore, be more appropriate to create a framework of possible elution concentrations than to try and simulate every possible clinical situation.

It has been stated that residual BisGMA may be metabolised to bisphenol-A which is believed to have estrogenic activity.[33] Although reported TC50 concentrations for BisGMA[34–36], HEMA[36] and TEGDMA[34,36] vary in different studies, other studies have shown that even sub-toxic doses of monomers and extracts of dental resins may alter cellular functions such as secretion, homeostasis, dentinogenesis, or tissue repair.[35,37]

We are in the process of studying the effects of detected monomer concentrations from the present study on cellular functions and metabolism.

Positive correlation occurred between BisGMA and HEMA elution for Excite, Admira and Filtek Silorane indicating that an increase in the amount of eluted BisGMA is associated with an increased amount of eluted HEMA. This relationship was not observed in Clearfil SE and Clearfil 3S.

HEMA seems to be a good predictor of the RDB for Clearfil 3S since a direct negative correlation was found. However, the overall result of the study indicates that no direct correlation exists between the RDB of adhesives and the elution of unreacted monomers. Although it is often hypothesized that greater elution indicates lower RDB, this is not substantiated by the present study.

Both polymerisation and elution are complex processes affected by many factors. Differences in the chemical

composition and mode of application of currently available adhesive systems introduce too many variables to make their direct comparison possible. Although, the RDB indicates the differences in the ratio of carbon–carbon double bond conversion from monomer to polymer between different adhesive systems, this suggests neither the causes for these differences nor the quality of the polymer network. Furthermore, the processes such as ''dark cure'', hydrolysis within the polymer network and stereo chemical characteristics of the polymer, affect both the RDB and monomer elution, making it difficult to arrive at any definite conclusion regarding the correlation of elution and RDB.

The RDB can change depending on the elution of unreacted monomers from the surface layers of adhesive and from spaces within the polymer network or changes in the polymer chains themselves. The latter can be involved in further polymerisation, e.g. dark cure or hydrolysis. Having identified these two sources of remaining double bonds, this calls into question the often used term ''degree of conversion''.

The term ''degree of conversion'' is a process whereby the relative amount of the aliphatic C=C and aromatic C=C bonds is measured prior and following the material polymerisation. The changes should represent only the conversion of the aliphatic C=C double bonds involved in the process of polymerisation. Therefore, the term DC should not be used to describe the aliphatic C=C double bonds remaining after but not limited to the elution processes, which result in an overall reduction in these C=C double bonds. We suggest that the term ''the ratio of double-bond content of monomer to polymer (RDB)'' is more accurate.

Filtek Silorane showed lower RDB than other adhesive systems. Since the micro-Raman spectra were taken from the surface of the adhesive, the calculated RDB values corresponded to Filtek Silorane Bond. It has been shown that the reactivity of dimethacrylates in the formation of homopolymers increases with increasing distance between the methacrylate groups.[38] Therefore, it could be expected that a system containing TEGDMA shows higher RDB than found in the present study. However, the reactivity of TEGDMA could be impaired by phosphorylated methacrylates contained in the bond whose primary role is priming the dentine.[39] Their role is, however, hindered by the presence of the cured primer between the bond and dentine and could result in higher content of these phosphorylated methacrylates and lower pH of the bond. Furthermore, the nature and chemical characteristics of the hydrophobic dimethacrylate developed to match the silorane resin remains unknown and undisclosed by the manufacturer.

Significantly higher RDB of Clearfil 3S than Clearfil SE is in accordance with the previous view that primers lower the RDB of adhesives.[39] The lower RDB of Admira compared to Excite, Clearfil SE and Clearfil 3S may indicate lower reactivity of the complex ormocer molecules compared to free cross-linking monomers.

5. Conclusions

The total-etch, self-etch, ormocer-based adhesive systems and Filtek Silorane adhesive system investigated in the present study showed different monomer elution kinetics. More than 90% of the named monomers in all adhesives systems, except for BisGMA in Filtek Silorane adhesive system, eluted during the first 1 h. Both the absolute amount and wt% of eluted monomers varied in all systems. The highest absolute amount was observed for Clearfil SE whereas the highest wt% of eluted monomers was detected from Admira.

Filtek Silorane adhesive system showed the lowest and Clearfil 3S the highest RDB values both initially and after elution. In all adhesive systems, there was an increase in the RDB after monomer elution.

The overall result of the study indicates that no direct correlation exists between the RDB of adhesives and the elution of unreacted monomers although negative correlation was found for the elution of HEMA and the RDB of Clearfil 3S.

Acknowledgements

The authors would like to thank Prof. Lesley Yellowlees, Head of the School of Chemistry, the University of Edinburgh, and Prof. Mark Bradley, for allowing the use of facilities in the School of Chemistry.

REFERENCES

1. Bae JH, Cho BH, Kim JS, Kim MS, Lee IB, Son HH, *et al*. Adhesive layer properties as a determinant of dentin bond strength. *Journal of Biomedical Material Research Part B Applied Biomaterials* 2005;**74**:822–8.
2. Cadenaro M, Antoniolli F, Sauro S, Tay FR, Di Lenarda R, Prati C, *et al*. Degree of conversion and permeability of dental adhesives. *European Journal of Oral Sciences* 2005;**113**:525–30.
3. Nunes TG, Garcia FC, Osorio R, Carvalho R, Toledano M. Polymerization efficacy of simplified adhesive systems studied by NMR and MRI techniques. *Dental Materials* 2006;**22**:963–72.
4. Emami N, Soderholm KJ. How light irradiance and curing time affect monomer conversion in light-cured resin composites. *European Journal of Oral Sciences* 2003;**111**:536–42.
5. Witzel MF, Calheiros FC, Goncalves F, Kawano Y, Braga RR. Influence of photoactivation method on conversion, mechanical properties, degradation in ethanol and contraction stress of resin-based materials. *Journal of Dentistry* 2005;**33**:773–9.
6. Yap AU, Soh MS, Han TT, Siow KS. Influence of curing lights and modes on cross-link density of dental composites. *Operative Dentistry* 2004;**29**:410–5.
7. Sasaki N, Okuda K, Kato T, Kakishima H, Okuma H, Abe K, *et al*. Salivary bisphenol-A levels detected by ELISA after restoration with composite resin. *Journal of Material Science Materials in Medicine* 2005;**16**:297–300.
8. Geurtsen W, Lehmann F, Spahl W, Leyhausen G. Cytotoxicity of 35 dental resin composite monomers/additives in permanent 3T3 and three human primary fibroblast cultures. *Journal of Biomedical Material Research* 1998;**41**:474–80.
9. Geurtsen W, Spahl W, Muller K, Leyhausen G. Aqueous extracts from dentin adhesives contain cytotoxic chemicals. *Journal of Biomedical Material Research* 1999;**48**:772–7.
10. Lewis JB, Rueggeberg FA, Lapp CA, Ergle JW, Schuster GS. Identification and characterization of estrogen-like

components in commercial resin-based dental restorative materials. *Clinical Oral Investigations* 1999;**3**:107–13.
11. Nomura Y, Ishibashi H, Miyahara M, Shinohara R, Shiraishi F, Arizono K. Effects of dental resin metabolites on estrogenic activity in vitro. *Journal of Material Science Materials in Medicine* 2003;**14**:307–10.
12. Ferracane JL. Elution of leachable components from composites. *Journal of Oral Rehabilitation* 1994;**21**:441–52.
13. Ferracane JL, Condon JR. Rate of elution of leachable components from composite. *Dental Materials* 1990;**6**:282–7.
14. Michelsen VB, Lygre H, Skalevik R, Tveit AB, Solheim E. Identification of organic eluates from four polymer-based dental filling materials. *European Journal of Oral Sciences* 2003;**111**:263–71.
15. Uzunova Y, Lukanov L, Filipov I, Vladimirov S. High-performance liquid chromatographic determination of unreacted monomers and other residues contained in dental composites. *Journal of Biochemical & Biophysical Methods* 2008;**70**:883–8.
16. Yap AU, Han VT, Soh MS, Siow KS. Elution of leachable components from composites after LED and halogen light irradiation. *Operative Dentistry* 2004;**29**:448–53.
17. Kim JG, Chung CM. Elution from light-cured dental composites: comparison of trimethacrylate and dimethacrylate as base monomers. *Journal of Biomedical Material Research Part B Applied Biomaterials* 2005;**72**:328–33.
18. Munksgaard EC, Peutzfeldt A, Asmussen E. Elution of TEGDMA and BisGMA from a resin and a resin composite cured with halogen or plasma light. *European Journal of Oral Sciences* 2000;**108**:341–5.
19. Sideridou ID, Achilias DS. Elution study of unreacted Bis-GMA, TEGDMA, UDMA, and Bis-EMA from light-cured dental resins and resin composites using HPLC. *Journal of Biomedical Material Research Part B Applied Biomaterials* 2005;**74**:617–26.
20. Zhang Y, Xu J. Effect of immersion in various media on the sorption, solubility, elution of unreacted monomers, and flexural properties of two model dental composite compositions. *Journal of Material Science Materials in Medicine* 2008;**19**:2477–83.
21. Eliades T, Eliades G, Brantley WA, Johnston WM. Residual monomer leaching from chemically cured and visible light-cured orthodontic adhesives. *American Journal of Orthodontics & Dentofacial Orthopedics* 1995;**108**:316–21.
22. Eliades T, Hiskia A, Eliades G, Athanasiou AE. Assessment of bisphenol-A release from orthodontic adhesives. *American Journal of Orthodontics & Dentofacial Orthopedics* 2007;**131**:72–5.
23. Salz U, Zimmermann J, Zeuner F, Moszner N. Hydrolytic stability of self-etching adhesive systems. *Journal of Adhesive Dentistry* 2005;**7**:107–16.
24. Silikas N, Watts DC. High pressure liquid chromatography of dentin primers and bonding agents. *Dental Materials* 2000;**16**:81–8.
25. Kaga M, Noda M, Ferracane JL, Nakamura W, Oguchi H, Sano H. The in vitro cytotoxicity of eluates from dentin bonding resins and their effect on tyrosine phosphorylation of L929 cells. *Dental Materials* 2001;**17**:333–9.
26. Van Landuyt KL, Snauwaert J, De Munck J, Peumans M, Yoshida Y, Poitevin A, *et al*. Systematic review of the chemical composition of contemporary dental adhesives. *Biomaterials* 2007;**28**:3757–85.
27. Moon H-J, Lim B-S, Lee Y-K, Kim C-W. Determination of residual monomers in dental pit and fissure sealants using food/oral simulating fluids. *Bulletin of the Korean Chemical Society* 2000;**21**:1115–8.
28. Tay FR, Pashley DH. Aggressiveness of contemporary self-etching systems. I. Depth of penetration beyond dentin smear layers. *Dental Materials* 2001;**17**:296–308.
29. Wang JD, Hume WR. Diffusion of hydrogen ion and hydroxyl ion from various sources through dentine. *International Endodontic Journal* 1988;**21**:17–26.
30. Hashimoto M, Ito S, Tay FR, Svizero NR, Sano H, Kaga M, *et al*. Fluid movement across the resin–dentin interface during and after bonding. *Journal of Dental Research* 2004;**83**:843–8.
31. Santini A, Miletic V. Comparison of the hybrid layer formed by Silorane adhesive, one-step self-etch and etch and rinse systems using confocal micro-Raman spectroscopy and SEM. *Journal of Dentistry* 2008;**36**:683–91.
32. Simon G, Allen PEM, Bennett DJ, Williams DRG, Williams EH. Nature of residual unsaturation during cure of dimethacrylates examined by CPPEMAS ^{13}C NMR and simulation using a kinetic gelation model. *Macromolecules* 1989;**22**:3555–61.
33. Olea N, Pulgar R, Perez P, Olea-Serrano F, Rivas A, Novillo-Fertrell A, *et al*. Estrogenicity of resin-based composites and sealants used in dentistry. *Environmental Health Perspectives* 1996;**104**:298–305.
34. Hanks CT, Strawn SE, Wataha JC, Craig RG. Cytotoxic effects of resin components on cultured mammalian fibroblasts. *Journal of Dental Research* 1991;**70**:1450–5.
35. Kostoryz EL, Tong PY, Strautman AF, Glaros AG, Eick JD, Yourtee DM. Effects of dental resins on TNF-alpha-induced ICAM-1 expression in endothelial cells. *Journal of Dental Research* 2001;**80**:1789–92.
36. Ratanasathien S, Wataha JC, Hanks CT, Dennison JB. Cytotoxic interactive effects of dentin bonding components on mouse fibroblasts. *Journal of Dental Research* 1995;**74**:1602–6.
37. Schweikl H, Spagnuolo G, Schmalz G. Genetic and cellular toxicology of dental resin monomers. *Journal of Dental Research* 2006;**85**:870–7.
38. Peutzfeldt A. Resin composites in dentistry: the monomer systems. *European Journal of Oral Sciences* 1997;**105**:97–116.
39. Hotta M, Kondoh K, Kamemizu H. Effect of primers on bonding agent polymerization. *Journal of Oral Rehabilitation* 1998;**25**:792–9.